TU Delft

Delft University of Technology

Citation (APA)
Bouwknegt, J. (2022). *Pyrimidine and hopanoid synthesis in anaerobic yeasts*. [Dissertation (TU Delft), Delft University of Technology]. https://doi.org/10.4233/uuid:5d6357fd-5ddf-4c48-819f-6b4b6cc7e2c9

Important note
To cite this publication, please use the final published version (if applicable).
Please check the document version above.

Copyright
In case the licence states “Dutch Copyright Act (Article 25fa)”, this publication was made available Green Open Access via the TU Delft Institutional Repository pursuant to Dutch Copyright Act (Article 25fa, the Taverne amendment). This provision does not affect copyright ownership.
Unless copyright is transferred by contract or statute, it remains with the copyright holder.

Sharing and reuse
Other than for strictly personal use, it is not permitted to download, forward or distribute the text or part of it, without the consent of the author(s) and/or copyright holder(s), unless the work is under an open content license such as Creative Commons.

Takedown policy
Please contact us and provide details if you believe this document breaches copyrights.
We will remove access to the work immediately and investigate your claim.

This work is downloaded from Delft University of Technology.

Pyrimidine and hopanoid synthesis in anaerobic yeast cultures

Jonna Bouwknegt

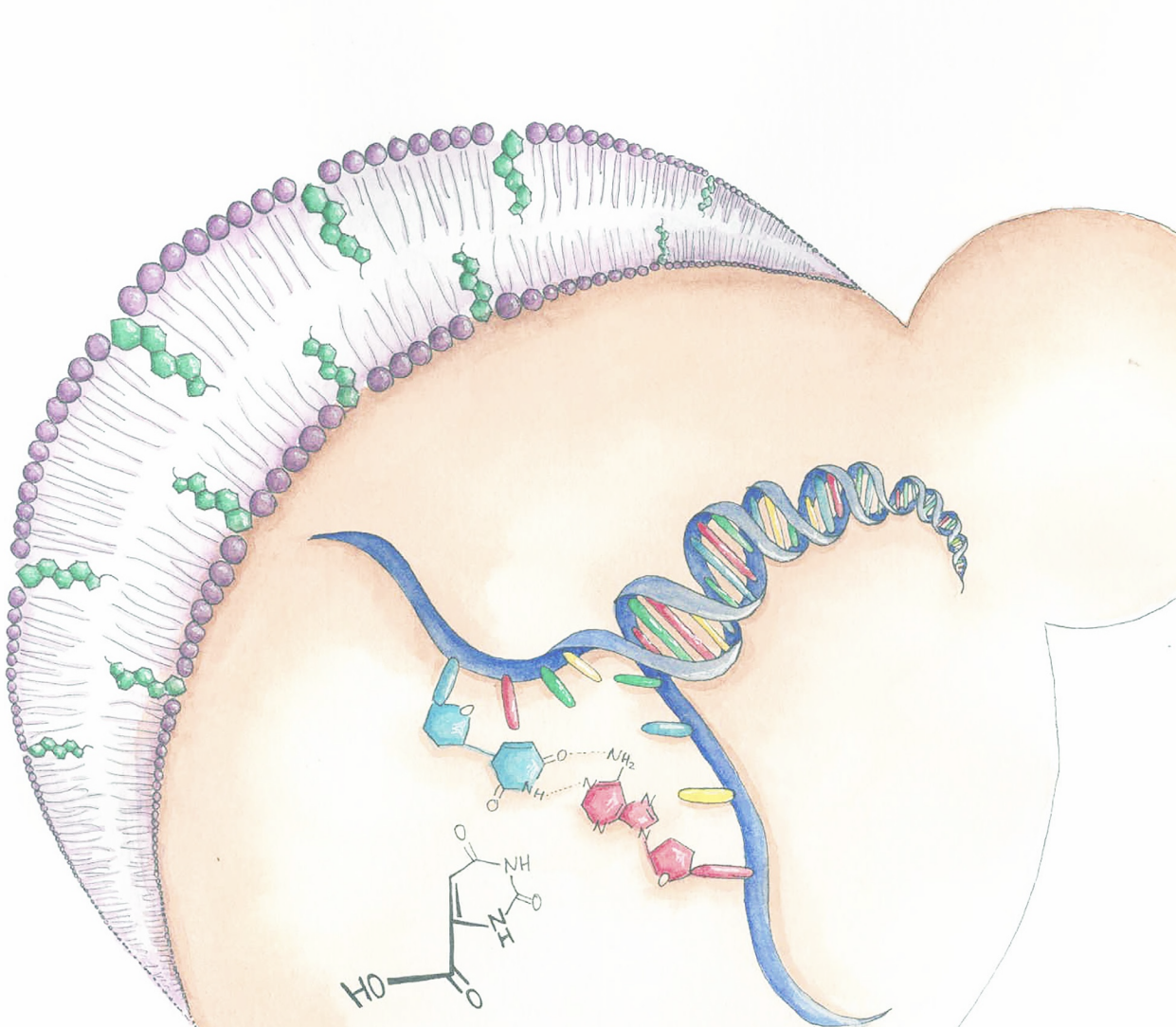

Pyrimidine and hopanoid synthesis in anaerobic yeast cultures

Proefschrift

Ter verkrijging van de graad van doctor
aan de Technische Universiteit Delft,
op gezag van de Rector Magnificus prof.dr.ir. T.H.J.J. van der Hagen
voorzitter van het College van Promoties,
in het openbaar te verdedigen op donderdag 10 maart 2022 om 12:30 uur

Door

Jonna BOUWKNEGT

Ingenieur in Life Science & Technology
Technische Universiteit Delft, Nederland

Geboren te Amsterdam, Nederland

Dit proefschrift is goedgekeurd door de promotoren Prof.dr. J.T. Pronk en Prof.dr.ir. J.G. Daran

Samenstelling promotiecommissie:

Rector magnificus	voorzitter
Prof.dr. J.T. Pronk	Technische Universiteit Delft, promotor
Prof.dr.ir. J.G. Daran	Technische Universiteit Delft, promotor

Onafhankelijke leden:

Prof.dr. S. Oliferenko	The Francis Crick Institute, Verenigd Koninkrijk
Prof.dr. B.M. Bakker	Rijksuniversiteit Groningen
Prof.dr. J.H. de Winde	Universiteit Leiden
Dr.ir. P.L. Hagedoorn	Technische Universiteit Delft
Prof.dr. P.A.S. Daran-Lapujade	Technische Universiteit Delft, reservelid

Overig lid:

Prof.dr. F. Hollmann	Technische Universiteit Delft

Tekeningen/omslag	Jonna Bouwknegt
Opmaak	Jonna Bouwknegt
Drukker	Proefschriftmaken
ISBN	978-94-6384-288-4

Om de CO_2-voetafdruk van dit proefschrift te minimaliseren 100% gerecycled papier en lettertype Century Gothic gebruikt.

Het werk dat beschreven is in dit proefschrift is uitgevoerd bij de sectie Industriële Microbiologie, afdeling biotechnologie, Factulteit Technische Natuurwetenschappen aan de Technische Universiteit Delft in Nederland. Het onderzoek werd gefinancierd door de Europese onderzoeksraad via Advanced Grant 694633.

© 2022 Jonna Bouwknegt
Alle rechten voorbehouden

Table of contents

Voor papa, mama en omi: omdat jullie altijd trots op me zijn, wat ik ook doe

Samenvatting

De mensheid maakt al meer dan 11.000 jaar gebruik van producten die afkomstig zijn van alcoholische fermentatie door micro-organismen. Brood, bio-ethanol, alcoholische dranken zoals bier en wijn, en gedestilleerde dranken zoals wodka en rum zijn allemaal producten van alcoholische fermentatie. Het meest gebruikte micro-organisme voor zulke fermentatieprocessen is bakkersgist (*Saccharomyces cerevisiae*). Een belangrijke reden hiervoor is dat bakkersgist, in tegenstelling tot veel andere gisten, de eigenschap heeft dat het kan groeien in de afwezigheid van zuurstof. Voor processen op grote schaal is het beluchten van een reactor duur, en het is moeilijk om een homogene verdeling van zuurstof in de reactor te bereiken. Tijdens de productie van ethanol komt bovendien veel CO_2 vrij, wat beluchting nog verder bemoeilijkt. In afwezigheid van zuurstof kan daarnaast ook een hogere opbrengst van dissimilatoire producten (zoals ethanol) op suiker worden behaald.

Om zonder zuurstof te kunnen groeien is in gisten een stofwisselingsroute voor fermentatie nodig. Hoewel veel gistsoorten kunnen fermenteren, zijn er echter maar weinig die ook anaeroob kunnen groeien. In gisten kunnen verschillende reacties voorkomen die essentieel zijn om te overleven, maar die direct of indirect zuurstof vereisen. Ook *S. cerevisiae* heeft zuurstof nodig voor zulke biosynthetische routes, bijvoorbeeld voor de productie van sterolen en onverzadigde vetzuren. In *S. cerevisiae* kunnen deze zuurstofbehoeften worden omzeild door de betreffende chemische verbindingen toe te voegen aan het medium. Andere gisten kunnen weer andere zuurstofbehoeften hebben die bijvoorbeeld gerelateerd kunnen zijn aan pyrimidinesynthese, synthese van bepaalde vitamines en het balanceren van redoxcofactoren. De precieze zuurstofbehoeften van veel industrieel relevante gisten zijn echter nog onbekend.

Onderzoek naar zuurstofbehoeften wordt over het algemeen op laboratoriumschaal uitgevoerd. In tegenstelling tot de situatie in industriële reactoren, is het extreem moeilijk om deze kleine systemen volledig anaeroob te krijgen. Lekkage van slechts kleine hoeveelheden zuurstof kan al voldoende zijn om in de zuurstofbehoeften voor biosynthetische routes te voorzien, die op deze manier dus snel over het hoofd worden gezien. Dit is waarschijnlijk ook de reden waarom er in de literatuur veel tegenstrijdigheden te vinden zijn over de zuurstofbehoeften van gisten. Het doel van het in dit proefschrift beschreven onderzoek was om uit te vinden hoe niet-*Saccharomyces* gisten zich hebben aangepast aan zuurstofonafhankelijke synthese van pyrimidines en aan groei in een extreem sterol-gelimiteerde anaerobe omgeving.

Om te voorkomen dat verkeerde conclusies werden getrokken door lekkage van kleine hoeveelheden zuurstof, was een stabiele en betrouwbare methode nodig om anaeroob onderzoek te doen. In **Hoofdstuk 2** staan methoden beschreven om, op laboratoriumschaal, betrouwbaar anaeroob onderzoek te kunnen

doen in anaerobe kamers en bioreactoren. Door het gebruik van controleculturen van giststammen die maar een heel klein beetje zuurstof nodig hebben om te groeien, was het mogelijk de belangrijkste oorzaken van zuurstoflekkage te identificeren en te minimaliseren. Het in dit proefschrift beschreven onderzoek was het resultaat van vier jaar onderzoek in het project ELOXY (Eliminating oxygen requirements in yeast, ofwel het elimineren van zuurstofbehoeften in gist). In deze vier jaar zijn de gebruikte kweeksystemen continu aangepast en verbeterd om zuurstoflekkage te verminderen en interpreteerbaarheid van resultaten te verbeteren. Een van de belangrijkste bevindingen hierbij was dat een anaerobe voorcultuur nodig is om intracellulaire reserves van sterolen en onverzadigde vetzuren op te maken. In anaerobe kamers bleek het openen van de voorkamer de grootste bron van zuurstoflekkage te zijn. In plaats van het frequent openen van deze voorkamer voor het analyseren van monsters buiten de kamer werd de optische dichtheid van de gistculturen daarom binnen in de anaerobe kamer gemeten. In bioreactoren lekte de meeste zuurstof naar binnen via de slangen. Het effect hiervan werd geminimaliseerd met enkele drastische aanpassingen. De beschreven methoden vormen de basis van al het anaerobe onderzoek dat is beschreven in **Hoofdstuk 3-5**.

Lang werd gedacht dat sterolen essentieel zijn voor het functioneren van membranen van eukaryoten. Om deze reden wordt aan media voor het kweken van anaerobe gistculturen altijd ergosterol, de meest voorkomende sterol in gisten, toegevoegd. Neocallimastigomycota, een groep van obligaat anaerobe schimmels, maken echter in plaats van ergosterol het sterolsurrogaat tetrahymanol. **Hoofdstuk 3** beschrijft een nieuwe adaptatie van een schimmel, de gist *Schizosaccharomyces japonicus*, die het mogelijk maakt om onder anaerobe condities te groeien in de afwezigheid van sterolen. Deze gist bleek hopanoïden te maken, stoffen die vergelijkbaar zijn met tetrahymanol en in prokaryoten ook als sterolsurrogaten werken. Door middel van gaschromatografie werd de lipide-fractie van anaeroob gekweekte culturen van *Sch. japonicus* gekarakteriseerd. Hierin bleken zich onbekende verbindingen te bevinden, terwijl ergosterol afwezig was. De onbekende lipiden werden met behulp van GC-MS geïdentificeerd als hopanoïden, waaronder diplopterol. Hoewel hopanoïden veel voorkomen in prokaryote membranen, was dit de eerste keer dat ze als sterolsurrogaten in een gist werden ontdekt.

Ergosterol wordt gemaakt vanuit squaleen, een route die in totaal 12 mol zuurstof nodig heeft voor de synthese van 1 mol ergosterol. Hopenen worden eveneens vanuit squaleen gemaakt, maar in een enkele zuurstofonafhankelijke stap die wordt gekatalyseerd door het enzym squaleen-hopeen cyclase (SHC). In het genoom van *Sch. japonicus* werd een gen aangetroffen dat sterk leek op een gen voor een SHC. De aminozuurvolgorde van het voorspelde eiwitproduct van dit gen werd vervolgens vergeleken met andere eiwitsequenties. Een fylogenetische analyse gaf hierbij een zeer sterke indicatie dat *Sch. japonicus* door horizontale gen-overdracht een *SHC* gen had verkregen van een azijnzuurbacterie. Om te onderzoeken of dit gen inderdaad voor een SHC codeerde, werd het tot expressie gebracht in bakkersgist. In de hieruit voortkomende giststam werd aanwezigheid van hopanoïden vastgesteld en bovendien kon deze genetisch gemodificeerde stam langzaam groeien onder anaerobe condities zonder dat sterolen aan het medium werden toegevoegd. Zelfs na twee keer overzetten op verse media bleef *Sch. japonicus* anaeroob groeien,

waarbij vergelijkbare groeisnelheden werden waargenomen op media met en zonder sterolen. In *S. cerevisiae* bleek het synthetiseren van hopanoïden echter niet voldoende voor snelle sterol-onafhankelijke anaerobe groei. Verder onderzoek naar de membraansamenstelling en -structuur van *Sch. japonicus* is daarom nodig om meer inzicht te verkrijgen in andere benodigdheden voor snelle sterol-onafhankelijke groei.

Net als Neocallimastigomyceten heeft *Sch. japonicus* zich aangepast voor anaerobe groei door het via horizontale gen-overdracht verkrijgen van een gen voor synthese van een sterolsurrogaat. Dat dit niet de enige vergelijkbare adaptatie voor anaerobe groei in deze organismen is, wordt beschreven in **Hoofdstuk 4**. Neocallimastigomyceten en *Sch. japonicus* zijn beide prototroof voor pyrimidines onder anaerobe condities, terwijl de meeste schimmels zuurstof nodig hebben voor pyrimidinesynthese. De vierde reactie in de stofwisselingsroute voor pyrimidinesynthese is een redoxreactie, waarin dihydroorotaat wordt omgezet in orotaat door een dihydroorotaatdehydrogenase (DHOD). De meeste schimmels hebben een quinon-afhankelijk DHOD (Ura9), dat de elektronen die vrijkomen bij deze redoxreactie afstaat aan een quinon in het mitochondriële membraan. Voor re-oxidatie van het hierbij gevormde quinol door de mitochondriële ademhaling, is uiteindelijk zuurstof nodig als elektronacceptor. Bakkersgist heeft dit probleem opgelost door via horizontale gen-overdracht een ander, zuurstofonafhankelijk DHOD (Ura1) te verkrijgen. In *Sch. japonicus* en Neocallimastigomyceten is een dergelijk gen afwezig, en in theorie zouden deze organismen dus afhankelijk zijn van zuurstof voor de synthese van pyrimidines. Eenzelfde intrigerende waarneming was eerder beschreven voor de wijn-bedervende gist *Dekkera bruxellensis*: ook deze gist kan anaeroob groeien zonder toevoeging van pyrimidines, maar heeft alleen een *URA9* gen in zijn genoom. In **Hoofdstuk 4** is onderzocht wat er met deze Ura9 eiwitten aan de hand is. Door het functioneel compenseren van een *ura1* deletie in *S. cerevisiae* met de *URA9* genen van *Sch. japonicus*, *D. bruxellensis* en de Neocallimastigomyceet *Anaeromyces robustus* werd aangetoond dat deze DHODs, in tegenstelling tot andere Ura9s, inderdaad anaeroob werken in gist.

Door de aminozuurvolgorden van de drie anaeroob werkende Ura9-varianten te vergelijken met die van DHODs van andere schimmels en bacteriën, werd gevonden dat ze onafhankelijk van elkaar geëvolueerd zijn. Door te zoeken naar overeenkomsten in ArUra9, SjUra9 en DbUra9 en verschillen met andere Ura9s, bleek dat deze drie sequenties alle drie een cysteïneresidu bevatten in het actieve centrum, terwijl typische Ura9s een serine op deze plek hebben. Bovendien had ArUra9 ook een kortere N-terminus. Het vervangen van de cysteïne door een serine veranderde niets voor een *S. cerevisiae* stam met ArUra9, terwijl deze substitutie in het *SjURA9* gen anaerobe groei volledig afhankelijk maakte van pyrimidines. De N-terminus, die in ArUra9 verkort was, zorgt er normaal gesproken voor dat de eiwitten naar het mitochondriële membraan worden gebracht en is bovendien in verband gebracht met het binden van quinon. Door het fuseren van de Ura9-eiwitten met een fluorescent eiwit (eGFP) werd bevestigd dat ArUra9 zich in tegenstelling tot andere Ura9s niet in de mitochondriën bevond, maar in het cytosol. ArUra9 bleek bovendien in staat te zijn om vrije FAD en FMN als elektronacceptoren te gebruiken.

Verrassenderwijs leidde expressie van *SjURA9* in *S. cerevisiae* tot respiratoir deficiënte giststammen die

geen meetbare hoeveelheden mitochondrieel DNA meer bevatten. Het vervolgens weer verwijderen van *SjURA9* leidde niet tot herstel van het vermogen om adem te halen. Waarom dit verschijnsel specifiek optrad met dit DHOD-gen, welke elektronacceptoren worden gebruikt door DbUra9 en SjUra9 en het exacte mechanisme van FAD/FMN-binding in ArUra9 moet nog nader worden onderzocht, maar **Hoofdstuk 4** beschrijft een nieuwe, interessante, parallelle adaptatie voor anaerobe pyrimidinesynthese.

Geïnspireerd door **Hoofdstuk 4**, werd in **Hoofdstuk 5** gezocht naar orthologen in schimmels van Ura1. In *S. cerevisiae* wordt het verkrijgen van dit van bacteriën afkomstige gen gezien als een essentiële aanpassing aan anaerobe groei. Hoewel deze aanpassing als tamelijk uniek wordt gezien, werd in **Hoofdstuk 5** een grote groep genen gevonden die homologie vertonen met *S. cerevisiae* Ura1. Vertegenwoordigers van deze groep genen uit de basidiomyceet *Schizophylum commune* en de ascomyceet *Alternaria alternata* werden in een *S. cerevisiae ura1* deletiemutant geplaatst. De hieruit voortkomende giststammen konden echter niet groeien in de afwezigheid van uracil. In plaats daarvan kon de deletie van *URA1* worden gecompenseerd door toevoeging van dihydrouracil aan de culturen. Deze waarneming suggereerde aanvankelijk dat de Ura1-orthologen geen DHODs waren maar dihydrouracil dehydrogenases (DHPDs). Deze eiwitten, die dihydrouracil in uracil omzetten en die ook de omgekeerde reactie katalyseren, lijken veel op DHODs. Anaeroob bleken deze eiwitten echter niet te werken, hetgeen suggereerde dat voor hun activiteit zuurstof nodig is. In cel-extracten van *S. cerevisiae*-stammen waarin de genen van *A. alternaria* en *Sch. commune* tot expressie waren gebracht, werd na toevoegen van dihydrouracil of dihydrothymine zowel zuurstofconsumptie als productie van waterstofperoxide gemeten. Zuurstofafhankelijke omzetting van dihydrouracil naar uracil door een dihydrouracil oxidase (DHUO) was pas eenmaal eerder beschreven in de literatuur. De vele schimmeleiwitten die bij een eerste analyse homologen vertoonden met Ura1, lijken op grond van de resultaten die in **Hoofdstuk 5** zijn beschreven waarschijnlijk allemaal dihydrouracil oxidases te zijn. De fysiologische rol van deze eiwitten is echter nog onbekend.

Het onderzoek dat in dit proefschrift wordt uiteengezet verschaft nieuwe inzichten in adaptaties van schimmels aan anaerobe groei, met de nadruk op anaerobe productie van pyrimidines en een nieuw eukaryoot sterolsurrogaat. De methoden die in dit proefschrift zijn beschreven, zijn belangrijk voor toekomstig anaeroob onderzoek aan gisten. Daarnaast is bewezen dat het gebruik van mutanten van *S. cerevisiae* om de functie van eiwitten uit lastig te kweken eukaryote organismen te onderzoeken, een zeer sterk gereedschap is voor toekomstig onderzoek in de anaerobe microbiologie.

Summary

Products resulting from alcoholic fermentation by microorganisms have been used by mankind for over 11,000 years. Alcoholic fermentation is involved in production of bread, alcoholic beverages such as wine and beer, distilled spirits such as vodka and rum, and bio-ethanol. The popularity of the most intensively used microorganism for these alcoholic-fermentation-related processes, baker's yeast (*Saccharomyces cerevisiae*), is related to its ability to grow anaerobically. In large-scale industrial bioreactors, aeration is expensive and homogenous oxygen concentrations are extremely difficult to obtain, especially during production of ethanol, which, during fermentation of hexose sugars, coincides with the production of equimolar amounts of CO_2. Moreover, to maximize the yield of dissimilation products such as ethanol on the carbohydrate feedstock, aerobic respiration should be prevented.

A fermentative pathway is a prerequisite for anaerobic growth in yeasts, but although many yeasts can ferment sugars to ethanol, only few are able to grow in the complete absence of oxygen. Yeasts that are able to grow anaerobically have specific nutritional requirements, which are needed to bypass biosynthetic reactions that either directly require molecular oxygen or are dependent on respiration. For example, synthesis of sterols and unsaturated fatty acids in *S. cerevisiae* requires oxygen. Sources of these compounds are therefore routinely included in defined media for anaerobic cultivation. Other yeast species may additionally require oxygen for other processes, including synthesis of pyrimidines, vitamins and/or redox-cofactor balancing. However, the exact oxygen requirements for industrially relevant non-*Saccharomyces* yeasts remain to be elucidated.

Oxygen requirements of yeasts are mostly investigated in laboratory-scale anaerobic cultivation systems. In contrast to the situation in industrial scale bioreactors, it is extremely difficult to achieve fully anaerobic conditions in these small set-ups. Even entry of minute amounts of oxygen may already be enough to meet minimum requirements for biosynthetic processes and thereby obscure oxygen requirements that are highly relevant at industrial scale. Moreover, this challenge in experimental design is likely to have contributed to contradicting literature regarding the oxygen requirements of yeast strains and species. The research described in this PhD thesis was aimed to obtain a deeper insight in adaptations of non-*Saccharomyces* yeasts that enable anaerobic pyrimidine synthesis and in adaptation mechanisms of such yeasts to sterol depletion under anaerobic conditions.

To avoid drawing incorrect conclusions arising from inadvertent entry of small amounts of oxygen into yeast cultures, a stable platform for anaerobic experiments was required. **Chapter 2** describes measures that can be taken to allow for meaningful experiments on oxygen requirements of yeasts in laboratory-

scale setups and, in particular, in anaerobic chambers and bioreactors. By working with control cultures that already show growth at extremely low concentrations of oxygen, key points of oxygen entry in different setups could be identified. Over a period of 4 years, the team of the ELOXY (eliminating oxygen requirements in yeasts) project of which this PhD research project was a part, continually adapted and improved cultivation systems to minimise oxygen leakage. Results of these efforts are presented and discussed in **Chapter 2**. One of the most important steps in the presented protocols was inclusion of an anaerobic pre-culture designed to deplete intracellular reserves of anaerobic growth factors such as sterols. In the anaerobic chamber, frequent use of the air lock was shown to be the main source of oxygen entry, which was minimised by measuring optical densities in the anaerobic workspace rather than repeatedly moving samples outside the chamber for analysis. Similarly, measurements were required to minimise the impact of oxygen leakage through tubing in bioreactor setups. The methods described in **Chapter 2**, form the basis for the research on biosynthetic oxygen requirements performed in **Chapters 3**-**5**.

Sterols were long thought to be essential components of eukaryotic membranes. Anaerobic cultures of *S. cerevisiae* are therefore routinely supplied with ergosterol, which is the main sterol in yeast. However, Neocallimastigomycetes, a group of deep-branching, obligately anaerobic fungi, were later shown to contain the pentacyclic triterpenoid tetrahymanol as a sterol surrogate. **Chapter 3** describes the discovery that the fission yeast *Schizosaccharomyces japonicus* grows anaerobically without supplementation of sterols, a characteristic that was not observed previously in yeasts. Investigation of the lipid composition of anaerobically grown *Sch. japonicus* by gas chromatography demonstrated the absence of ergosterol. Several initially unidentified peaks appeared on chromatograms which, by using GC-MS, were identified as hopanoids, including diplopterol. Like tetrahymanol, hopanoids were previously proposed to act as sterol surrogates, although they had not before been found in a yeast.

Whereas synthesis of ergosterol requires 12 moles of oxygen starting from squalene, hopanoids are synthesised from squalene in a single, oxygen-independent cyclisation reaction, catalysed by a squalene hopene cyclase (SHC). Based on sequence similarity, *Sch. japonicus* harboured a putative SHC gene (*SjSHC*) and phylogenetic analysis provided a strong indication that this gene had been acquired by horizontal gene transfer from an *Acetobacter* species. Membrane analysis revealed that expression of *SjSHC* in *S. cerevisiae* resulted in production of hopanoids, and moreover, supported its anaerobic growth in the absence of an exogenous sterol source. However, growth of *S. cerevisiae* strains producing hopanoids was slow. Further research into the composition and architecture of *Sch. japonicus* membranes is required to understand how this yeast achieves robust sterol-independent growth.

Horizontal gene transfer of an SHC gene represents an evolutionary adaptation of *Sch. japonicus* to an anaerobic lifestyle, similar to the acquisition of a tetrahymanol cyclase by Neocallimastigomycetes, However, as shown in **Chapter 4**, synthesis of a sterol surrogate is not the only adaptation to an anaerobic lifestyle that is shared by these phylogenetically distant eukaryotes. Neither Neocallimastigomycetes nor

Sch. japonicus require supplementation of pyrimidines under anaerobic conditions. This observation is remarkable since, in most eukaryotes, the conversion of dihydroorotate to orotate, which is the fourth step in pyrimidine synthesis, requires respiration due to the involvement of a quinone-dependent dihydroorotate dehydrogenase (DHOD), Ura9. *S. cerevisiae* has instead acquired, by horizontal gene transfer, a soluble, respiratory-independent DHOD encoded by *URA1*, which enables anaerobic pyrimidine prototrophy. Based on sequence homology, Neocallimastigomycetes and *Sch. japonicus* proteomes harboured orthologs of *URA9* genes, but did not encode a *URA1* ortholog. However, the characteristic coupling of Ura9-type DHODs to respiration would not allow them to support anaerobic pyrimidine prototrophy. A similar observation was previously made for the facultatively anaerobic yeast *Dekkera bruxellensis*. These puzzling observations were investigated in **Chapter 4**. By assaying functional complementation of a *URA1* deletion in *S. cerevisiae* with *URA9* genes from *Sch. japonicus, D. bruxellensis* and from the Neocallimastigomycete *A. robustus*, their DHODs (SjUra9, DbUra9 and ArUra9 respectively) were shown to function anaerobically. Sequence homology searches and phylogenetic analysis of fungal and bacterial Ura9 orthologs indicated that the DHODs of these three organisms had independently evolved the ability to support pyrimidine biosynthesis under anaerobic conditions. Sequence alignments of ArUra9, SjUra9 and DbUra9 with canonical quinone-dependent Ura9 protein sequences showed that their active sites contained a cysteine residue, whereas 'regular' Ura9 orthologs instead contain a strongly conserved serine in this position. In addition, an N-terminal truncation was found for ArUra9 and orthologs from other Neocallimastigomycetes. Swapping the cysteine residue of ArUra9 and SjUra9 for a serine abolished anaerobic growth of a *SjURA9*-dependent *S. cerevisiae* strain, but upon introducing the same amino-acid change in an *ArURA9*-dependent strain, anaerobic pyrimidine prototrophy was retained. The N-terminus of eukaryotic Ura9 orthologs has been implicated in their mitochondrial localisation and quinone binding. Indeed, eGFP-fused Ura9 enzymes localised to the mitochondria, with the exception of the N-terminally truncated ArUra9, which was found in the cytosol. Free FAD and FMN were shown to serve as electron acceptors for dihydroorotate oxidation by this enzyme. An unexpected phenomenon was observed in strains expressing *SjURA9*. Three independently constructed *S. cerevisiae* strains that expressed this gene had lost respiratory competence and did not show detectable mitochondrial DNA. Removing *SjURA9* did not result in a recovery of respiratory capacity. Why respiration is lost in *SjURA9* expressing *S. cerevisiae* strains, which electron acceptors are used by DbUra9 and SjUra9, and which molecular mechanism allows for use of FMN and FAD by ArUra9, remain questions that need to be answered in future research. However, the results presented in **Chapter 4** provide clear proof for an interesting parallel evolutionary adaptation to anaerobic environments in different yeasts and fungi.

In **Chapter 5**, which was inspired by the research described in **Chapter 4**, fungal proteomes were searched for possible Ura1 orthologs. Unexpectedly, this analysis revealed a large group of fungal genes that were homologous to Ura1. Previously, only few fungal species were reported to harbour such enzymes and were proposed to have acquired them by horizontal gene transfer. Apparent Ura1-orthologs of an Ascomycete, *Alternaria alternata*, and a Basidiomycete, *Schizophyllum commune*, were used to replace

URA1 in *S. cerevisiae*. The resulting strains were unable to grow without supplementation of uracil, indicating that these genes did not encode DHODs. Instead, their expression enabled uracil-auxotrophic strains of *S. cerevisiae* to grow on dihydrouracil. This result showed that the encoded enzymes were capable of converting dihydrouracil to uracil, a reaction typically catalysed by dihydropyrimidine dehydrogenases (DHPDs), which are known to be structurally similar to DHODs. Interestingly however, growth on dihydrouracil was not observed under anaerobic conditions. Experiments with cell extracts of *S. cerevisiae* strains expressing the putative DHPDs showed dihydrouracil-dependent oxygen consumption and hydrogen peroxide production. This observation implied that, instead of a reversible oxygen-independent dihydropyrimidine dehydrogenase activity, a large group of genes that initially appeared homologous to Ura1, if fact encoded dihydrouracil oxidase. This enzyme had been described in the scientific literature only once, and its physiological role remains to be elucidated.

The research described in this thesis provided new insight in evolutionary adaptations of eukaryotes to anaerobic environments and, in particular, adaptations that enable anaerobic pyrimidine synthesis and sterol-limited growth in anaerobic environments. In addition, the anaerobic cultivation methods developed as part of this project and the use of *S. cerevisiae* mutants as 'testbed' for genes from anaerobic eukaryotes that are less experimentally accessible, can be applied to study adaptations of other eukaryotes to anaerobic growth.

Chapter 1.

General Introduction

The history of alcoholic fermentation

Mankind started intentional production of alcoholic beverages, resulting from microbial fermentation, at least 11 millennia ago. Ancient beer residues were found in a cave near Haifa, Israel, in mortars dating from 11,700 to 13,700 years ago (Figure 1.1; **1**). Similarly, the earliest evidence in the archeological record for fermented grapes and other wine ingredients dates to 9000 (**2**) years ago and, recently, a 5000-year-old large-scale beer brewing facility was discovered in Egypt (Figure 1.1; **3**). *Homo sapiens* was, however, not the first species to develop a taste for alcohol-containing fermented juices. In fact, according to the "drunken monkey hypothesis", primates have been consuming fermented fruits long before humans emerged (Figure 1.1; **4**,**5**). Toxic effects of ethanol and its degradation product acetaldehyde make most animals avoid fermented fruit (**6**). However, humans, chimpanzees and gorillas were found to have an evolved alcohol dehydrogenase (ADH) with a 40-fold higher capacity for ethanol degradation than its ancestral version. The ADH of the last common ancestor of humans, chimpanzees and gorillas evolved 10 million years ago, which suggests that consumption of fermented fruits by primates goes back at least that far (**5**). This evolutionary adaptation of ADH is also found in aye-ayes (*Daubentonia madagascariensis*) and the slow loris (*Nycticebus cougang*). When these species were offered solutions with ethanol concentrations ranging from 0 to 5%, they consistently favoured the highest available alcohol content (**7**). This observation is in line with the interpretation that this evolved ADH represented an evolutionary adaptation to alcohol consumption. Our attraction to alcoholic beverages therefore appears to have a very long evolutionary history (**4**).

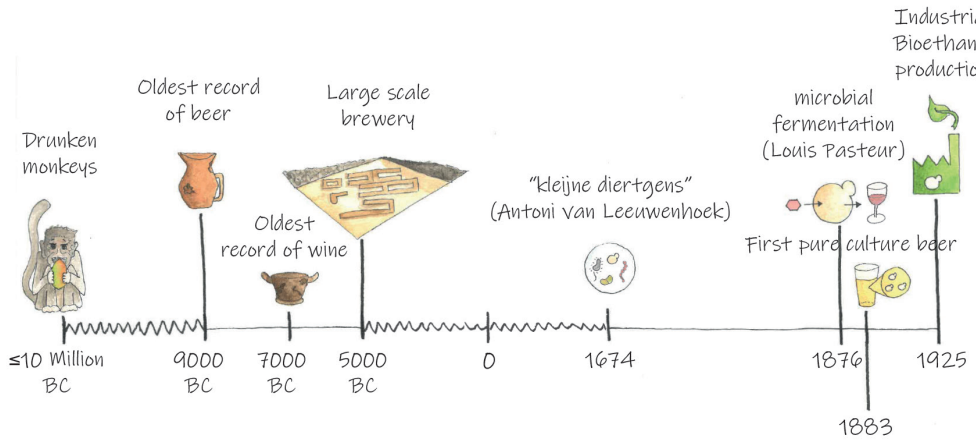

Figure 1.1. A schematic overview of the use of products of alcoholic fermentation over time.

Although fermentation processes were already widely used in prehistory, producers and consumers of alcoholic drinks long remained oblivious to the underlying mechanism. Unaware of the involvement of microorganisms, ancient producers of beer, wine and other alcoholic beverages used open fermentation vessels, into which airborne wild yeasts and bacteria could freely enter (**2**). Today, such spontaneous fermentation processes are still used to brew Lambic beers (**8**). It was not until 1674 that Antoni van Leeuwenhoek first observed microscopic organisms, which he called 'kleijne diertgens' (little animals; **Figure 1.1**; **9**). It took more than two centuries until Louis Pasteur unequivocally proved that living yeast cells ferment sugars to alcohol (**Figure 1.1**; **10**). Pasteur also showed how spoilage of beverages resulted from contamination with other microorganisms. This observation initiated drastic changes in fermentation processes and, in particular, a shift towards the closed fermentation systems, based on the pure cultures, that are predominantly used in modern fermentation processes (**Figure 1.1**; **11**).

Alcoholic fermentation pathways

Ethanol is only one of many products that can be made by microbial fermentation of glucose and other sugars. In many fermentative organisms, glucose ($C_6H_{12}O_6$) is first oxidised to two molecules of pyruvate ($C_3H_4O_3$) via the Embden-Meyerhof-Parnas variant of glycolysis. This pathway yields two molecules of ATP by substrate-level phosphorylation (2 ADP + 2 inorganic phosphate → 2 ATP), while four electrons derived from glucose are transferred to the cellular redox cofactor NAD^+ ($2\ NAD^+ + 4e^- + 2H^+ \rightarrow 2\ NADH$) (**Figure 1.2A**). Since both ADP/ATP and NAD^+/NADH are conserved moieties, continuous regeneration is required to sustain glycolytic activity and growth (**12**). ATP is a primary energy donor for biosynthesis and cellular maintenance. Regeneration of ADP is therefore intrinsically linked to these core cellular functions. In the absence of an external electron acceptor (e.g., oxygen, see below), fermentative pathways enable the re-oxidation of glycolytic NADH. Products of fermentation are in most cases derived from pyruvate and, in addition to ethanol, include compounds such as lactic acid, propionic acid, butyric acid and (iso)butanol (**13**).

In the classical yeast fermentation pathway, pyruvate derived from the Embden-Meyerhof-Parnas glycolytic pathway is first decarboxylated to acetaldehyde (C_2H_4O) in a reaction catalysed by pyruvate decarboxylase (PDC). Acetaldehyde is subsequently reduced to ethanol by NAD^+-dependent alcohol dehydrogenase, while oxidising NADH ($C_2H_4O + NADH + H^+ \rightarrow C_2H_6O + NAD^+$) (**Figure 1.2A**). Although this pathway for alcohol fermentation is often associated with yeast, it is also found in other fungi, plants and bacteria (**10**,**14**–**17**). In goldfish (*Carassius auratus*) and crucian carp (*Carassius carassius*), activity of this pathway is associated with their ability, unique among vertebrates, to survive for over 5 months under extreme oxygen limitation (**18**).

Firmicutes, Neocallimastigomycetes and some members of the Enterobacteriaceae (e.g., *Escherichia coli*), also catabolise sugars to pyruvate via the Embden-Meyerhof-Parnas pathway. However, in contrast

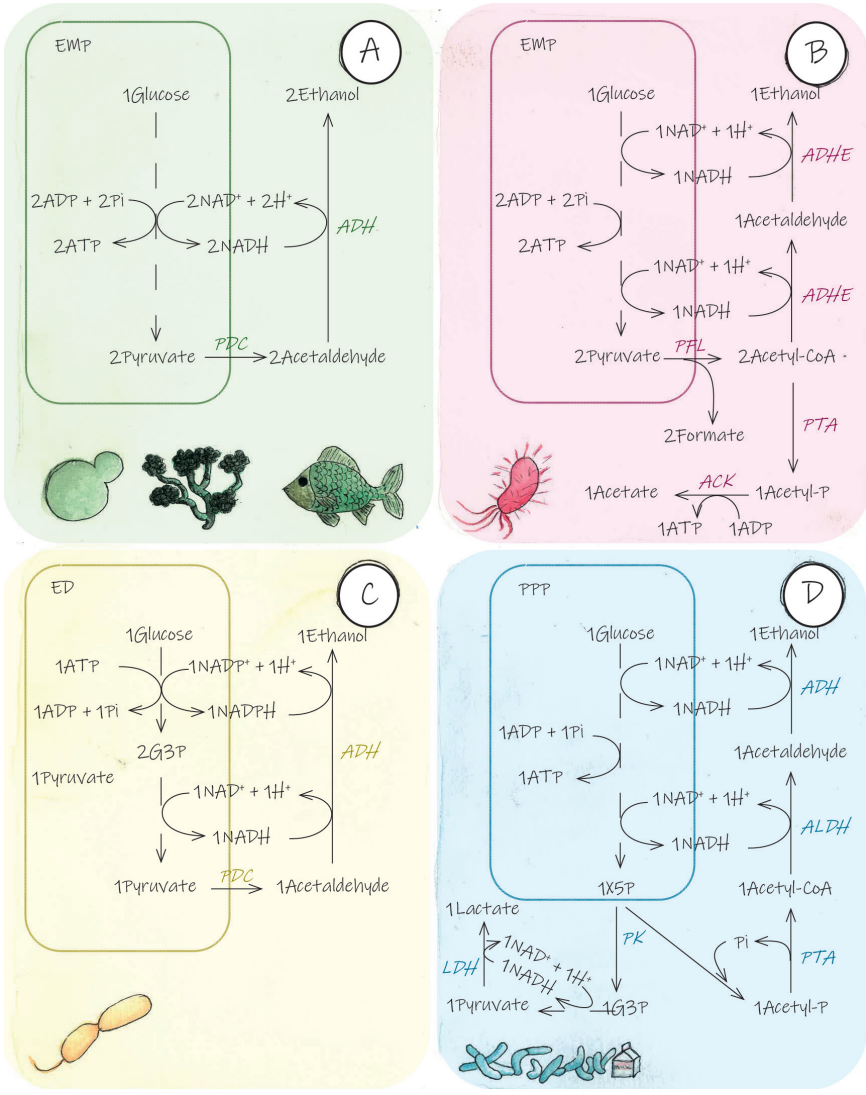

Figure 1.2. Pathways for alcoholic fermentation.

A. The classical yeast pathway; **B.** Alcoholic fermentation in *Enterobacteriaceae* species; **C.** Alcoholic fermentation in *Zymomonas mobilis*. **D.** Heterolactic fermentation.

EMP: Embden-Meyerhof-Parnas, ED: Entner-Douderoff, PKP: phosphoketolase pathway, PPP: pentosephosphate pathway, PDC: pyruvate decarboxylase, ADH: alcohol dehydrogenase, ADHE: alcohol dehydrogenase E, PFL: pyruvate formate lyase, PTA: phosphotransacetylase, PK: phosphoketolase, ACK: acetate kinase, LDH: lactate dehydrogenase, ALDH: acetylating acetaldehyde dehydrogenase, Acetyl-CoA: acetyl-Coenzyme A, G3P: glyceraldehyde-3-phosphate, X5P: xylulose-5-phosphate, Acetyl-P: acetyl-phosphate.

to the situation in yeast, ethanol formation in these organisms is initiated by conversion of pyruvate into acetyl-CoA and formate ($C_3H_4O_3^-$ + CoA → C_2H_3O-CoA + CHO_2^-) by a pyruvate formate lyase (PFL, **Figure 1.2B**; (**19**–**21**). Two electrons from NADH are transferred to acetyl-CoA, yielding acetaldehyde and CoA, after which acetaldehyde is reduced to ethanol with a second NADH. Reduction of acetyl-CoA to ethanol can be catalysed by a single enzyme, alcohol dehydrogenase E (ADHE; **22**). Conversion of a single molecule of pyruvate to ethanol via this pathway suffices to re-oxidise the NADH formed in glycolysis. This frees up one molecule of acetyl-CoA, whose conversion to acetyl-phosphate by phosphotransacetylase (PTA) enables the formation of one additional molecule of ATP by substrate-level phosphorylation in a reaction catalysed by acetate kinase (ACK).

Only one microorganism, the bacterium *Zymomonas mobilis* (**23**), is known to ferment glucose to ethanol via the Entner-Doudoroff pathway of glycolysis. The key intermediate of this pathway, 2-keto-3-deoxy-gluconate-6P, is produced from glucose at the cost of 1 ATP and with the reduction of 1 $NADP^+$ ($C_6H_{12}O_6$ + ATP + $NADP^+$ → $C_6H_{11}O_9P$ + ADP + NADPH + H^+). Subsequently, 2-keto-3-deoxy-gluconate-6P is directly converted to one molecule each of pyruvate and glyceraldehyde-3P ($C_6H_{11}O_9P$ → $C_3H_4O_3^-$ + $C_3H_7O_6P$) by a 2-keto-3-deoxy-gluconate-6P aldolase (**Figure 1.2C**; **24**). Glyceraldehyde-3P is further oxidised to a second molecule of pyruvate via reactions that also occur in the Embden-Meyerhof-Parnas glycolysis, yielding 2 ATP and 1 NADH ($C_3H_7O_6P$ + 2 ADP + P_i + NAD^+ + H^+ → $C_3H_4O_3$ + 2 ATP + NADH + H_2O). Although the Entner-Doudoroff pathway is commonly known for aerobic metabolism in, for example, *Pseudomonas* species, *Z. mobilis* anaerobically converts the pyruvate it generates to ethanol via pyruvate decarboxylase and alcohol dehydrogenase (**23**,**25**). The lower ATP yield of Entner-Doudoroff glycolysis, which potentially allows for a higher ethanol yield in growing cultures than the ATP yield of the Emden-Meyerhof-Parnas pathway, has contributed to the interest in *Z. mobilis* as a potential microbial platform for ethanol production (**26**,**27**).

Yet another metabolic pathway towards ethanol occurs in heterofermentative lactic acid bacteria. In these microorganisms, glucose is fermented via the phosphoketolase pathway (PKP) to ethanol and lactic acid (**28**). In the PKP, xylulose-5-phosphate derived from the oxidative pentose-phosphate pathway is cleaved into acetyl-phosphate and glyceraldehyde-3-phosphate ($C_5H_{10}O_8P_2^-$ + HPO_4^{2-} → $C2H_3O_5P^{2-}$ + $C_3H_7O_6P^{2-}$ + H_2O) by phosphoketolase (**Figure 1.2D**). Glyceraldehyde-3-phosphate is then metabolised to pyruvate, which is reduced to lactic acid by an NADH-dependent lactate dehydrogenase, while acetyl-phosphate is reduced to ethanol by the combined activity of phosphotransacetylase (C_2H_3OP + CoA → C_2H_3O-CoA + P_i), acetylating acetaldehyde dehydrogenase (C_2H_3O-CoA + NADH + H^+ → C_2H4O + NAD^+ + CoA) and alcohol dehydrogenase (C_2H_4O + NADH → C_2H_6O + NAD^+). During anaerobic growth on glucose, exclusive use of the phosphoketolase pathway results in the formation of equimolar amounts of ethanol and lactic acid (**Figure 1.2D**).

An energetically attractive alternative to fermentation: respiration in yeasts

A large majority of the thus far investigated yeast species are facultatively fermentative (**29**–**31**). This term implies that, depending on environmental conditions, they can either dissimilate sugars by fermentation, by respiration or via a mixed respiro-fermentative metabolism. Only a small number of yeast species are either obligately fermentative (**32**,**33**) (meaning that they are unable to respire, for example due to loss of mitochondrial DNA) or obligately respiratory (**29**,**34**).

When yeasts exhibit a respiratory glucose metabolism, the cytosolic NADH generated in glycolysis is re-oxidised via the mitochondrial respiratory chain, which uses oxygen as electron acceptor (**Figure 1.3**). Yeasts can couple oxidation of cytosolic NADH to the respiratory chain via mitochondrial 'external' NADH dehydrogenases and/or via a glycerol-3-phosphate shuttle mechanism (**35**). Translocation of electrons through the respiratory chain generates a proton motive force across the mitochondrial inner membrane, that subsequently enables synthesis of ATP via the mitochondrial F_OF_1 ATP synthetase (**Figure 1.3**). When glycolytic NADH is re-oxidised by mitochondrial respiration, pyruvate does not need to be converted to ethanol to regenerate NAD^+ and can, instead, be fully oxidised to CO_2 via the reactions catalysed by the mitochondrial pyruvate dehydrogenase complex and the enzymes of the tricarboxylic acid (TCA) cycle. For each molecule of pyruvate, these reactions yield four additional molecules of NADH and one molecule of FADH, which can again be re-oxidised by mitochondrial respiration. In addition, the TCA cycle yields one molecule of GTP (energetically equivalent to ATP) by substrate-level phosphorylation in the succinyl-CoA synthetase reaction. In total, the oxidation of 1 mole of glucose to CO_2 via glycolysis, pyruvate dehydrogenase complex and TCA-cycle yields 4 moles of ATP/GTP, 2 moles of FADH and 10 moles of NADH.

The actual ATP yield from complete respiratory dissimilation of glucose by yeasts depends on the composition of their mitochondrial respiratory chains. In yeasts such as *Saccharomyces cerevisiae*, which lack a proton-pumping Complex-I-type NADH dehydrogenase in their respiratory chains (**Figure 1.3A**), the *in vivo* P/O-ratio (ATP yield per electron pair) for oxidation of FADH and NADH is close to 1 (**36**–**38**). This low P/O ratio enables an ATP yield of 16 moles per mole of glucose. Considerably higher P/O ratios can be achieved in yeasts whose mitochondrial respiratory chains do harbour a Complex-I-type NADH dehydrogenase, such as for example *Ogataea* (previously known as *Hansenula*) *parapolymorpha* (**Figure 1.3B**; **39**).

All facultatively fermentative yeasts ferment simple sugars, such as glucose, under oxygen-limited conditions. In view of the much higher ATP yield from respiratory dissimilation, one might expect that these yeasts show a fully respiratory sugar dissimilation whenever sufficient oxygen is available. Indeed, this description fits the physiology of so-called Crabtree-negative yeasts (e.g., *Kluyveromyces marxianus* and *O. parapolymorpha*). However, Crabtree-positive yeasts such as *S. cerevisiae* exhibit a predominantly

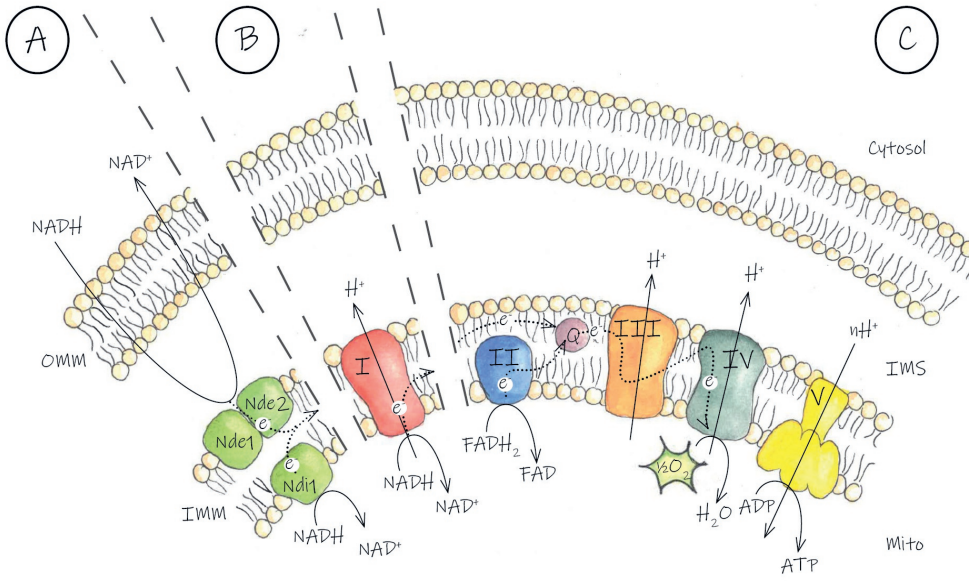

Figure 1.3. Electron transfer and ATP generation in yeast respiratory chains.

Note that the IMM is impermeable to NADH, thus requiring NADH-oxidising systems on its cytosolic and matrix sides. **A**. *S. cerevisiae* lacks a proton-translocating Complex I NADH dehydrogenase. Non-proton-translocating NADH dehydrogenases, located at the outside of the IMM (Nde1,2) or at the inside of the IMM (Ndi1) couple oxidation of NADH to the respiratory chain. **B**. Typical eukaryotic Complex I, transferring protons from the matrix to the IMS, and electrons to ubiquinone. **C**. From the NADH dehydrogenases or Complex I, electrons are transferred to the ubiquinone pool. Also, electrons derived from succinate oxidation in Complex II, are transferred to the ubiquinone pool. Electrons are transferred further through the respiratory chain, while translocating protons over the membrane, via the co-enzyme Q-cytochrome C oxidoreductase (Complex III). From Complex III, the electrons are donated to oxygen, the terminal electron acceptor of the respiratory chain, by Complex IV. Protons transferred over the mitochondrial membrane, are relocated to the matrix via an ATP synthase (Complex V).
OMM: outer mitochondrial membrane, IMS: intermembrane space, IMM: inner mitochondrial membrane, Q: ubiquinone, I, II, II, IV, V: Complex I, II, III, IV, V.

fermentative metabolism in aerobic cultures, unless sugar concentrations are kept very low (**33**,**40**). This strong tendency towards alcoholic fermentation, necessitates sugar-limited, aerobic cultivation for efficient industrial production of ATP-intensive products such as yeast biomass, proteins and complex low-molecular-weight compounds (**41**).

In most eukaryotes, respiration strictly relies on oxygen as electron acceptor, thus making anaerobic

growth dependent on fermentation. Exceptions include a few fungal species that are capable of partial denitrification (**42**,**43**), and a single fungus has been reported to use elemental sulfur (**44**). In Neocallimastigomycota, which are a group of deep-branching anaerobic fungi, hydrogenosomes instead of mitochondria are found, which also enable oxygen-independent energy conservation (**45**). In these hydrogenosomes, malate and pyruvate are converted to hydrogen, carbon dioxide and acetate, and per pyruvate one ATP is produced. Two key enzymes in these organelles are the pyruvate:ferredoxin oxidoreductase (PFOR) and hydrogenase.

Industrial relevance of anaerobic alcoholic fermentation by yeasts

1

Alcoholic fermentation by yeasts and, in particular, by *S. cerevisiae* and *Saccharomyces* hybrids, lies at the basis for several large-scale industrial activities (**46**). Beer fermentation, mostly using strains of *S. cerevisiae* (ale-type beers) or *Saccharomyces pastorianus* (hybrids of *S. cerevisiae* and *Saccharomyces eubayanus* used for brewing lager-type beers), is based on the fermentation of barley wort or other grain hydrolysates in large tanks (**47**). The same holds for the application of *Saccharomyces* strains in the fermentation of grape juice (must), apple juice and pre-fermented rice to wine, cider and sake, respectively. In addition, yeast-based anaerobic fermentation of sugar-containing hydrolysates of various agricultural feedstocks, mostly with *S. cerevisiae*, is essential for the production of a wide diversity of distilled drinks, such as vodka, gin, rum and whisky. In the production of alcoholic beverages and spirits, the yeast not only contributes to the final product by alcoholic fermentation, but also to flavour and aroma, for example by anaerobic conversion of amino acids to 'fusel' alcohols (**48**) and their esters (**49**–**51**).

In contrast to the production of alcoholic drinks, the production of fuel ethanol by *S. cerevisiae* is exclusively aimed at maximising the titer, rate and yield at which ethanol can be produced. With an estimated annual production of ca. 100 Mton, 'bio-ethanol' produced from hydrolysed corn starch (USA) or cane sugar (Brazil) is the single-largest-volume production of industrial biotechnology (**52**). Intensive academic and industrial research has, moreover, yielded engineered *S. cerevisiae* strains that can efficiently ferment the pentose sugars L-arabinose and D-xylose, which are already applied for industrial-scale fermentation of hydrolysates of agricultural residues such as corn stover (**53**). In addition, several metabolic engineering strategies have been developed to maximise ethanol yields on carbohydrate feedstocks by minimising the production of glycerol, a byproduct that in wild-type strains is essential for intracellular redox-cofactor balancing (**54**,**55**). Ethanol is not the only alcohol produced at industrial scale. Intensive metabolic engineering research and industrial strain development has yielded *S. cerevisiae* strains that, instead of ethanol, produce isobutanol (**56**,**57**).

In all applications of *Saccharomyces* yeasts that are based on alcoholic fermentation, vigorous

carbon dioxide production by the fermenting yeasts, combined with the large scale of the fermentation vessels leads to fully anaerobic conditions. In addition to their innate ethanol tolerance and high sugar fermentation rates, the ability of these yeasts to grow and ferment is therefore a key factor underlying their widespread use in these processes.

Synthetic biology opens up ever more options to engineer yeast metabolism (**58**,**59**). In the design and implementation of improved or novel-to-nature product pathways, the maximum theoretical yield is achieved when the degree of reduction of the substrate (i.e., all electrons that can be abstracted from an organic substrate when it is fully oxidised to CO_2 and water) is fully conserved in the product. In cases where such a scenario is thermodynamically feasible and a pathway can be designed and constructed that provides the micro-organism with ATP, without a need for an external electron acceptor, respiration would compete for electrons (i.e., NADH) with product formation. Ideally, such fermentation processes should therefore be operated anaerobically which, moreover, obviates the need for expensive aeration and results in lower cooling costs than for aerobic cultures (**60**,**61**). The ability to grow under anaerobic conditions may therefore become an even more important performance indicator for yeast-based production of compounds other than ethanol and isobutanol.

Not all fermentative yeasts can grow anaerobically

As mentioned above, most yeasts are facultatively fermentative and, therefore, able to conserve free energy from sugars through the combined reactions of glycolysis and alcoholic fermentation in the absence of oxygen. This observation does, however, not imply that all facultatively fermentative yeasts can also grow in the complete absence of oxygen. This apparent discrepancy is related to requirements for oxygen in processes other than energy metabolism.

Already in the 1950's, Andreasen and Stier published two foundational papers (**62**,**63**) which showed that anaerobic growth of *S. cerevisiae* requires supplementation of growth media with a source of sterols. Similarly, anaerobic growth was strongly dependent on supplementation of unsaturated fatty acids (UFAs), although a recent study showed that this requirements in *S. cerevisiae* was not absolute (**64**). These requirements can be attributed to requirements for molecular oxygen in the pathway for sterol synthesis and in the desaturation of acyl-CoA molecules, respectively (see below). Anaerobic growth experiments with *S. cerevisiae* therefore invariably involve the inclusion of sterol and UFA sources in growth media. Alternatively, anaerobic growth can be preceded by a brief, intensive aeration phase that enables cells to build intracellular sterol and UFA reserves that can be used (diluted) during a subsequent anaerobic phase of a laboratory culture or industrial process (**65**). Comparative physiological studies involving large

numbers of yeast species have shown that *Saccharomyces* species share their ability to grow fast under anaerobic conditions when supplemented with sterol and UFA sources with only very few other yeast species (but see **Chapter 3** of this thesis). As will be discussed in more detail below, the reasons for the oxygen-requirements of most non-*Saccharomyces* yeasts have not been fully resolved. This problem is not only of fundamental interest, but also has a direct bearing on industrial application.

Despite the popularity of *Saccharomyces* yeasts for anaerobic industrial applications, many other yeast species have industrially relevant characteristics that do not occur in *Saccharomyces*. For example, thermotolerant yeasts such as *K. marxianus* and *Ogataea* species, can grow up to temperatures of 50 °C (**66**,**67**), which is far above the maximum temperature of ca. 40 °C of *S. cerevisiae* (**68**). Use of thermotolerant yeasts in industrial processes could reduce cooling costs and, even more importantly, reduce the required dosage of polysaccharide-hydrolysing enzymes for hydrolysis of starch or, in second-generation bioethanol processes, of lignocellulosic compounds, to fermentable sugars. Additional advantages of non-*Saccharomyces* yeasts can involve a broader range of fermentable sugars. These advantages are exemplified by many *Kluyveromyces* yeasts that ferment lactose (**69**), the predominant sugar in whey, and *Scheffersomyces stipitis* (formerly *Pichia stipitis*) that is intensively investigated as a possible platform for ethanol production from lignocellulosic feedstocks due to its natural ability to ferment xylose (**70**). Moreover, some non-*Saccharomyces* yeasts have a very high tolerance to industrially relevant stress conditions such as low pH and/or osmotolerance (e.g. *Zygosaccharomyces* species; **71**).

The substrate range of *S. cerevisiae* has been successfully extended by genetic engineering, thus enabling anaerobic fermentation of industrially relevant sugars such as xylose, arabinose, lactose and cellobiose (**72**–**75**). However, complex traits such as thermo- and acid tolerance involve large numbers of genes (**76**,**77**) and are likely to be difficult to engineer into *S. cerevisiae*. In the case of thermotolerance, this may even require engineering of a large part of the proteome. Engineering of naturally stress-resistant yeast species could therefore provide an attractive approach. However, although these yeasts can ferment sugars to ethanol under oxygen-limited conditions, their industrial application in anaerobic fermentation processes is precluded by requirements for oxygen that are, as yet incompletely understood.

Non-dissimilatory oxygen requirements of yeasts

The ability of facultatively fermentative yeasts to conserve free energy from sugar dissimilation by alcoholic fermentation indicates that any oxygen requirements for growth are most probably linked to the direct or indirect involvement of molecular oxygen in biosynthetic processes. Laboratory studies on this subject are complicated by the fact that, in many of the species investigated, these non-dissimilatory

oxygen requirements are extremely small and easily go unnoticed in laboratory cultures, unless extensive precautions are taken to prevent unintended entry of oxygen. This technical aspect of studying oxygen requirements of yeasts is discussed in detail in **Chapter 2** of this thesis. Here, a brief overview will be presented on biochemical processes and reactions that have been implicated in the oxygen requirements of facultatively fermentative yeasts. For more in-depth information, the reader is referred to literature reviews on this subject (**78**–**80**).

Redox-cofactor balancing

During fermentative growth of yeasts, pyruvate decarboxylase and alcohol dehydrogenase enable the stoichiometric re-oxidation of the NADH formed in glycolysis to NAD^+, thus making the overall process of alcoholic fermentation redox-cofactor balanced and enabling substrate-level phosphorylation in the absence of oxygen. However, glycolytic glyceraldehyde-3-phosphate dehydrogenase reaction is not the only NADH-generating reaction in yeast metabolism. Biosynthetic processes such as protein and lipid synthesis result in a net reduction of NAD^+ to NADH during conversion of sugar and ammonia to yeast biomass (**36**,**81**). Since the NADH/NAD^+ couple is a conserved moiety, growth can only proceed by re-oxidation of this 'biosynthetic' NADH. When oxygen is available, this re-oxidation can easily be accomplished by mitochondrial respiration, but anaerobic or severely oxygen-limited conditions require an alternative 'redox sink'.

In anaerobic cultures of *S. cerevisiae*, re-oxidation of NADH is achieved by reducing the glycolytic intermediate dihydroxyacetone phosphate to glycerol-3-phosphate, in a reaction catalysed by glycerol-3-phosphate dehydrogenases (Gpd1 and Gpd2; **82**). Under anaerobic conditions *S. cerevisiae* uses the production of glycerol as a 'electron sink'. Electrons from NADH are transferred to dihydroxyacetone phosphate derived from glycolysis, resulting in the formation of glycerol-3-phosphate. Glycerol-3-phosphate is subsequently converted to glycerol by glycerol-3-phosphate phosphatase (Gpp1 or Gpp2). The importance of this reaction for anaerobic growth is evident from the inability of *S. cerevisiae* *gpd1*Δ*gpd2*Δ strains to grow anaerobically (**82**).

Facultatively fermentative yeasts such as *K. marxianus*, *Kluyveromyces lactis*, *Candida utilis* and *Zygosaccharomyces bailii* resemble *S. cerevisiae* in their ability to produce glycerol under severely oxygen-limited growth conditions (**60**,**83**,**84**). However, some facultatively fermentative yeasts, such as *Dekkera* (*Brettanomyces*) *bruxellensis*, are naturally unable to produce glycerol. This inability has been attributed to the absence of a functional glycerol-3-phosphatase and precludes anaerobic growth, unless an alternative electron acceptor such as acetoin is provided (**85**,**86**). Recently, an inability to re-oxidise biosynthetic NADH was shown to be a major contributor to the biosynthetic oxygen requirements of the thermotolerant yeast *O. parapolymorpha* (**87**).

Although the physiological role of mitochondria is often primarily associated with respiration, they also harbour key biosynthetic reactions, e.g., for synthesis of essential amino acids (e.g., L-valine, L-isoleucine).

Under anaerobic conditions, *S. cerevisiae* cannot re-oxidise mitochondrial NADH via respiration (**Figure 1.3**) and direct transport of NADH/NAD^+ across the mitochondrial inner membrane cannot contribute to mitochondrial redox cofactor balance. In *S. cerevisiae*, an ethanol-acetaldehyde shuttle resolves this redox-balancing challenge. This shuttle is based on free diffusion of acetaldehyde and ethanol across the mitochondrial membrane, and presence of isoenzymes of NAD^+-dependent alcohol dehydrogenase in the cytosol and in the mitochondrial matrix. In mutants lacking the predominant mitochondrial alcohol dehydrogenase Adh3, anaerobic growth is severely affected (**88**). This observation indicates that a mechanism for redox-cofactor shuttling between mitochondrial matrix and cytosol is also likely to be a requirement for anaerobic growth of other yeasts.

Several important redox reactions in biosynthetic processes, including oxidative protein folding (**89**) use the flavin cofactors FMN and/or FAD as electron acceptors. Under aerobic conditions, re-oxidation of $FADH_2$ and $FMNH_2$ generated in these processes can occur via respiration. In anaerobic cultures of *S. cerevisiae*, the fumarate reductases Osm1 and Frds1 can use fumarate as electron acceptor for re-oxidation of reduced flavins. The importance of this oxygen-independent re-oxidation of reduced flavins is evident from the strict requirement for oxygen of *S. cerevisiae* strains carrying a double deletion in *OSM1* and *FRDS1* (**90**).

Sterol synthesis

With the known exception of deep-branching anaerobic fungi, virtually all eukaryotes contain sterols in their membranes (but see **Chapter 3** of this thesis). These tetracyclic triterpenoids play an important role in membrane fluidity, rigidity and permeability (**95**,**96**). Membranes of vertebrates, plants and fungi contain cholesterol (**97**), phytosterols (**98**) and ergosterol (**99**) respectively, as dominant sterols. The pathways for synthesis of these different sterols largely overlap and are strongly conserved in different eukaryotic lineages (**96**). Sterol biosynthesis is a particular oxygen-intensive process, with synthesis of a single molecule of ergosterol, the major sterol in yeast, requiring 12 molecules of oxygen (**Figure 1.4**). The starting point for ergosterol biosynthesis is squalene, which is itself synthesised via the oxygen-independent mevalonate pathway that uses acetyl-CoA as a precursor (**100**). Squalene is first epoxidised to oxidosqualene, using one molecule of oxygen (**Figure 1.4**), followed by oxygen-independent conversion to lanosterol. In *S. cerevisiae*, these reactions are catalysed by the squalene monooxygenase Erg1 and the oxidosqualene cyclase (OSC) Erg7, respectively. The subsequent 12 reactions leading to ergosterol together require a further 11 oxygen molecules, which are used in demethylation and desaturation steps (**100**).

No anaerobic pathways for sterol synthesis have found in nature (**96**). *S. cerevisiae* can temporarily grow anaerobically without sterol synthesis or supplementation by mobilising intracellular stores of sterols. However, prolonged anaerobic growth is dependent on import of exogenous sterols. In *S. cerevisiae*, sterols are imported by the plasma-membrane ABC-transporters Aus1 and Pdr11 (**Figure 1.4**; **92**). Even *S. cerevisiae* strains that are deficient in sterol biosynthesis can only import sterols under anaerobic conditions, a phenomenon referred to as 'aerobic sterol exclusion' (**101**). In addition to Aus1 and Pdr11,

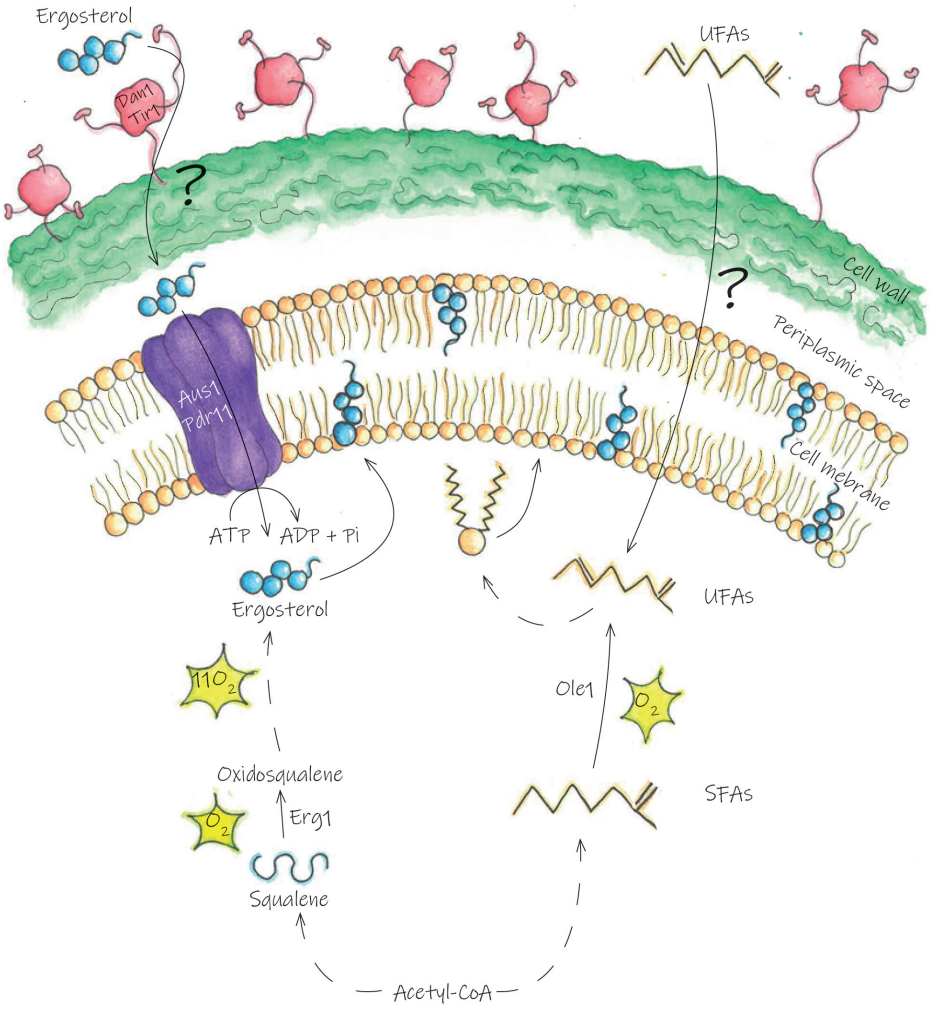

Figure 1.4. Biosynthesis and transport of ergosterol and unsaturated fatty acids (UFAs) in *S. cerevisiae*.

Biosynthesis of 1 molecule of ergosterol requires 12 molecules of oxygen, whereas synthesis of UFAs requires 1 molecule of oxygen per desaturated bond. While UFAs can freely cross the plasma membrane by diffusion (**91**), uptake of sterols requires cell wall mannoproteins (Dan1/Tir1; (**92–94**) as well as ATP-dependent transport across the plasma membrane via Aus1 or Pdr11 (**92**).

uptake of sterols by *S. cerevisiae* involves cell-wall mannoproteins belonging to the Dan and Tir families, but the mechanism by which these proteins contribute to sterol uptake remains to be elucidated (**92**–**94**). Despite the importance of sterol uptake for anaerobic growth, only few yeasts are capable of sterol import (**102**,**103**).

Obligately anaerobic fungi belonging to the Neocallimastigomycota are unable to synthetise sterols. Instead, their membranes contain tetrahymanol, a pentacyclic triterpenoid that structurally resembles ergosterol (**Figure 1.5**) and acts as a sterol surrogate. Tetrahymanol is also found in ciliates (**104**), in a fern (**105**) and in some bacteria (**106**–**108**). Just like ergosterol, it is synthesised from squalene. However, in contrast to the multistep pathway for sterol biosynthesis, tetrahymanol synthesis from squalene only requires a single, oxygen-independent cyclisation by a squalene-tetrahymanol cyclase (**109**). Recent research showed that expression of a tetrahymanol cyclase in *S. cerevisiae* promoted sterol-independent anaerobic growth (**110**), and even enabled the thermotolerant yeast *K. marxianus*, which cannot take up sterols, to grow anaerobically (**102**).

Unsaturated-fatty-acid synthesis

In addition to sterols and membrane proteins, eukaryotic plasma membranes contain sphingolipids and glycerophospholipids as major components (**111**,**112**). The relative contribution of unsaturated- and saturated fatty acids (UFAs and SFAs, respectively) in phospholipids has a strong impact on membrane fluidity (**113**) and incorporation of SFAs as well as UFAs in membranes was long thought to be essential for growth of *S. cerevisiae* (but see **Chapter 3**). In yeasts, the CoA esters of SFAs are synthesised by the Fas1/Fas2 fatty-acyl-CoA synthase complex, which uses acetyl-CoA and malonyl-CoA as precursors (**114**). CoA esters of UFAs are then synthesised from saturated acyl-CoA esters by the Ole1 Δ9-fatty acyl-CoA desaturase (**Figure 1.4**; **115**). Although anaerobic pathways for UFA synthesis occur in bacteria (**116**), yeasts depend on oxygen for UFA synthesis. Under anaerobic conditions, UFAs can freely diffuse over the plasma membrane and thus be taken up when supplied to growth media (**Figure 1.4**). Therefore, already since the 1950s (**62**,**63**), defined media for anaerobic growth of yeasts are routinely supplemented with Tween 80 (a polyoxyethylene sorbate ester of the UFA oleic acid) and ergosterol. We recently found that the requirement of *S. cerevisiae* for UFAs is not, as was long thought, absolute. When a source of UFAs was excluded from synthetic growth media, an *ole1*Δ strain of *S. cerevisiae* was shown to continue growing anaerobically through multiple serial transfers to fresh medium, albeit at a lower growth rate than observed in UFA-supplemented cultures. Analysis of the UFA-free lipid fractions of these cultures suggested that *S. cerevisiae* can compensate absence of UFAs by reducing the average chain length of SFAs (**64**).

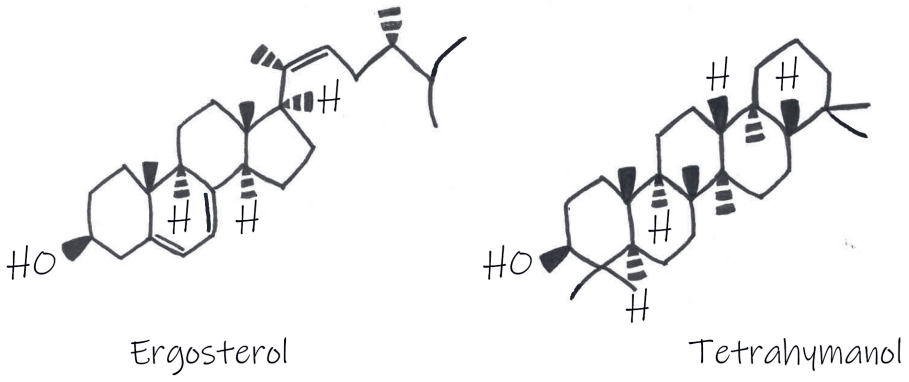

Figure 1.5. Chemical structures of the triterpenoids ergosterol and tetrahymanol.

Heme synthesis

Heme is a porphyrin molecule that is used as cofactor for hemoproteins, including the cytochromes involved in yeast mitochondrial respiration (**117**). Heme is synthesised from 5-aminolevulinate, and up until the synthesis of the intermediate coproporphyrinogen III, the pathway for heme biosynthesis is oxygen independent (**Figure 1.6**). However, the two subsequent reactions, in which a coproporphyrinogen III oxidase (1**18**) and protoporphyrinogen IX oxidase (**119**) convert coproporphyrinogen to protoporphyrin IX, together require a total of three molecules of oxygen (**Figure 1.6**). The final reaction in the pathway, in which protoporphyrin IX is converted to heme by a ferrochelatase (**120**), is again oxygen independent.

Since oxygen is essential for heme synthesis, this process is sometimes mentioned as a contributor to the biosynthetic oxygen requirements of yeasts (**78**). However, with one notable exception, hemoproteins in *S. cerevisiae* are only required for respiratory growth. This exception is sulfite reductase, which in this yeast is a heterotetramer of Met10 and Met5 that catalyses the reaction SO_3^{2-} + 3 NADPH + 3 H^+ → S^{2-} + 3 $NADP^+$ + 3 H_2O. Sulfite reductase is essential for methionine- and cysteine biosynthesis in cultures grown with sulfate as sulfur source (**121**). However, instead of a regular heme moiety, sulfite reductase contains siroheme, whose synthesis does not require oxygen (**122**). Siroheme is synthesised from the heme precursor uroporphyrinogen III, which is first converted to precorrin-2 by an S-adenosyl-l-methionine uroporphyrinogen III transmethylase (Met1 in *S. cerevisiae*). Subsequent NAD^+-dependent oxidation to sirohydrochlorin and metal incorporation to yield siroheme are both catalysed by Met8 (**Figure 1.6**; **123**,**124**). Since most fungi express a siroheme biosynthesis pathway they may, similarly to *S. cerevisiae*, not require heme supplementation for anaerobic growth (**125**).

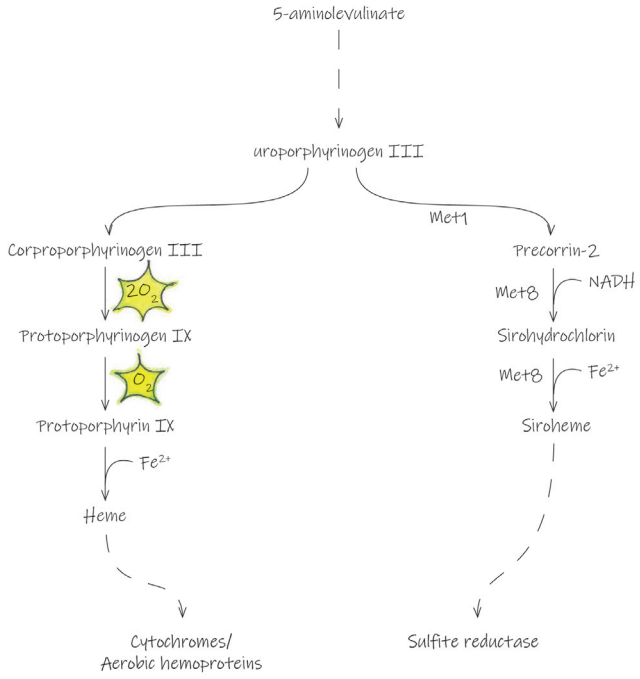

Figure 1.6. A schematic representation of heme and siroheme biosynthesis in *S. cerevisiae*.

Heme is used as cofactor in respiration-related hemoproteins in yeasts, while sulfite and nitrite reductases instead contain siroheme (**122**). The shared precursor uroporphyrinogen III is synthesised from 5-aminolevulinate via oxygen-independent reactions. In heme biosynthesis, oxidation of coproporphyrinogen III to protoporphyrinogen IX requires 2 molecules of oxygen, while an additional oxygen molecule is needed for the subsequent oxidation to protoporphyrin IX. In contrast, conversion of uroporphyrinogen III to siroheme via precorrin-2 and sirohydrochlorin, catalysed by Met1 and Met8 in *S. cerevisiae*, does not require molecular oxygen.

Vitamins

Vitamins are defined as organic compounds that are required for growth of an organism, but cannot be synthesised by the organism itself and are therefore essential nutritional ingredients. In yeast research, the term 'vitamin' is used much more loosely and in most cases refers to a group of compounds that, in

human nutrition, are classified as B-type (water-soluble) vitamins but which are not always essential for yeast growth. In particular, synthetic media for cultivation of yeasts often contain inositol, pyridoxine, p-aminobenzoic acid, biotin, nicotinic, acid, pantothenate and thiamine (**126**). Many *S. cerevisiae* strains are either auxotrophic for biotin or show extremely slow growth in biotin-free media, although biotin-prototrophic strains do occur and some near-auxotrophic strains can be evolved in the laboratory for full prototrophy (**127**,**128**). For the other 'yeast vitamins', most *S. cerevisiae* strains contain a full complement of biosynthetic genes and show significant growth rates in media from which individual 'vitamins' have been omitted (**128**,**129**). Unless yeasts lack membrane transporters that can take up these compounds from the medium, their routine inclusion in synthetic media masks the fact that several of their biosynthetic pathways in yeasts require oxygen. In natural environments and in anaerobic industrial processes that use non-defined media, nutritional complementation may not always be an option. Below, known oxygen requirements for synthesis of B-type vitamins are therefore briefly described.

Biotin

Biotin is an essential cofactor for carboxylases involved in fatty acid synthesis, amino-acid-, urea and sugar metabolism. *S. cerevisiae* contains a plasma-membrane proton symporter, Vht1 (**130**), that can transport biotin, while Bio5 (**131**) can import the biotin precursors KAPA (7-keto-8-aminopelargonic acid) and DAPA (7,8-diaminopelargonic acid). The pathway for biotin synthesis in biotin-prototrophic *S. cerevisiae* strains starts with pimeloyl-Coenzyme A, the CoA ester of the C7-dicarboxylic acid pimelic acid. Intriguingly, the mechanism by which yeasts synthesise pimeloyl-CoA remains one of few remaining white spots on their metabolic maps and involves Bio1 (**132**). Although Bio1 is often assumed to be a pimeloyl-CoA synthetase, the pimelate substrate required for such an enzyme activity is not known to be an intermediate of yeast metabolism. Conversion of pimeloyl-CoA to KAPA is catalysed by Bio6 (**Figure 1.7A**; **132**). In *S. cerevisiae* strain CEN.PK113-7D, laboratory evolution for faster growth in biotin-free media was accompanied by an increased copy number of *BIO1* and *BIO6* (**127**). Recently, expression of the *BIO1* ortholog of the biotin-prototrophic yeast *Cyberlindnera fabianii* was shown to support fast biotin-independent growth of several *S. cerevisiae* strains (**133**). However, laboratory-evolved biotin-prototrophic strains as well as prototrophic strains expressing Cf*BIO1* were unable to grow anaerobically and, sequence analysis of Sc*BIO1*, Cf*BIO1* and orthologs in other yeasts suggested that these genes instead encode oxygen-dependent oxidoreductases (**Figure 1.7A**; **133**). These results indicate that oxygen is required for biotin-auxotrophic growth of yeasts. Recently, an oxygen-independent bacterial pathway for biotin synthesis was successfully engineered into *S. cerevisiae*, thereby conferring anaerobic biotin prototrophy to laboratory and industrial strains (**134**).

Pyridine-nucleotide cofactor (NAD^+ and $NADP^+$) synthesis

Nicotinic acid is added to media as a precursor for the biosynthesis of the pyridine-nucleotide redox cofactor NAD^+, from which also $NADP^+$ can be formed (**135**). Two pathways are known in nature for NAD^+ biosynthesis; the kynurenine pathway (**136**) and synthesis from L-aspartate (**137**). Like most

other eukaryotes, *S. cerevisiae* harbours the kynurenine pathway. In this pathway, L-tryptophan is first converted to quinolinic acid. Of the five enzyme-catalysed reactions involved in this conversion, three require molecular oxygen (**Figure 1.7C**). The subsequent conversion of quinolinic acid to NAD^+, which involves nicotinic acid mononucleotide (NaMN) and nicotinic acid adenine dinucleotide (NaAD) as intermediates, does not require oxygen. The absolute requirement for oxygen of the kynurenine pathway implies that anaerobic growth of *S. cerevisiae* strictly depends on supplementation of nicotinic acid. *S. cerevisiae* takes up nicotinic acid via the Tna1 plasma-membrane transporter (**138**). Intracellular nicotinic acid is converted to the NAD^+-precursor nicotinic acid mononucleotide by the nicotinate phosphoribosyltransferase Npt1 (**Figure 1.7C**; 1**36**). Presence of a transporter for nicotinic acid and a nicotinate phosphoribosyltransferase is therefore a prerequisite for anaerobic growth of yeasts and fungi that employ the kynurenine pathway for NAD^+ synthesis.

In an alternative pathway for pyridine-nucleotide synthesis that has not been found to occur in yeasts, quinolinic acid is not generated from tryptophan but, instead, from L-aspartate. L-Aspartate is first converted into iminoaspartate by a flavoprotein L-aspartate oxidase (NadB) which can use either oxygen or fumarate as electron acceptor (**Figure 1.7C**; **139**,**140**), thereby enabling the enzyme to contribute to aerobic as well as anaerobic NAD^+ synthesis. Iminoaspartate is then converted to quinolinic acid by an quinolinic acid synthase (NadA; **141**). Although mostly found in prokaryotes, functional *nadA* and *nadB* genes were recently also identified in the Neocallimastigomycete *Piromyces finnis*. Expression of the *nadA* and *nadB* genes from this strictly anaerobic fungus in *S. cerevisiae* enabled nicotinic-acid prototrophic growth in anaerobic cultures (**142**).

Coenzyme A synthesis

Pantothenate, a precursor for Coenzyme-A synthesis and for synthesis of the acyl carrier protein, is synthesised from β-alanine and pantoate by the pantothenate synthetase Pan6 (**143**). The two-step synthesis of pantoate from α-ketoisovalerate, in *S. cerevisiae* catalysed by Ecm31 and Pan5. However, β-alanine biosynthesis in this yeast is oxygen dependent and the resulting pantothenate auxotrophy of anaerobic cultures can be nutritionally complemented by uptake of pantothenate via the Fen2 proton symporter (**144**).

In *S. cerevisiae*, β-alanine synthesis is initiated by the conversion of spermine to spermidine by the polyamine oxidase Fms1. This reaction requires one mole of oxygen per mole of spermine and, in addition to spermidine, yields equimolar amounts of hydrogen peroxide and 3-aminopropanal. The yeast aldehyde dehydrogenase Ald3 subsequently oxidises 3-aminopropanal to β-alanine (**143**). Multiple alternative pathways for β-alanine synthesis occur in nature (**Figure 1.7D**). In some yeasts and fungi, pyrimidine degradation yields β-alanine, but this pathway has been lost in *S. cerevisiae* and other Saccharomycotina (**145**). A direct formation of β-alanine by decarboxylation of L-aspartate is found in various species in all domains of life (**142**,**146**). L-Aspartate decarboxylases responsible for this reaction have been characterised from, amongst others, the red flour beetle (**147**) and *E. coli* (**148**).

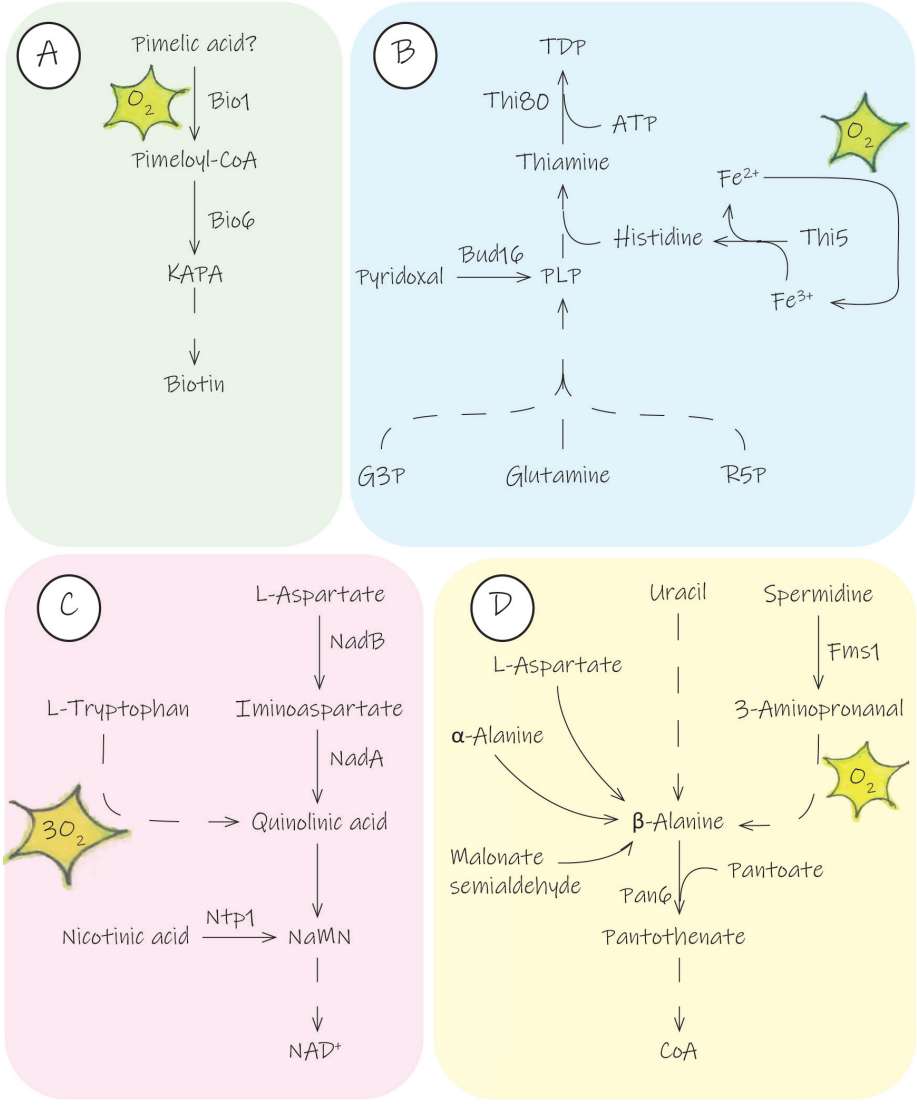

Figure 1.7. Oxygen requirements for biosynthesis of B-type vitamins.

A. Biosynthesis of biotin in *S. cerevisiae*. **B**. thiamine biosynthesis. **C**. Quinolinic acid, is synthesised from L-tryptophan in yeast, which requires the input of three molecules of oxygen. An alternative pathway via L-aspartate requires oxygen when using an L-aspartate oxidase (NadB) and quinolinate synthetase (NadA). **D**. β-alanine can be synthesised via different pathways; the reductive pathway for pyrimidine degradation (from uracil), polyamine degradation (spermidine; yeast pathway), direct conversion from L-aspartate, synthesis from α-alanine, or from malonate.

A gene encoding an L-aspartate decarboxylase (PanD) that enables the Neocallimastigomycete *Neocallimastix californiae* to grow anaerobically was recently functionally characterised and expression *panD* gene was shown to support pantothenate prototrophy in anaerobic cultures of *S. cerevisiae* (**142**).

Thiamine synthesis

Thiamine pyrophosphate (TPP) is a cofactor for various enzymes, including pyruvate decarboxylase, phenylpyruvate decarboxylase, the pyruvate-dehydrogenase and 2-oxoglutarate-dehydrogenase complexes and transketolase (**149**). In addition, thiamine has been implicated in stress tolerance of *S. cerevisiae* (**150**). Thiamine is synthesised from pyridoxal-5'-phosphate (PLP), which is itself synthesised from L-glutamine, glyceraldehyde-3-phosphate (G3P) and ribulose-5-phosphate (R5P; **Figure 1.7B**). Although none of the *S. cerevisiae* enzymes involved in thiamine synthesis are known to directly require molecular oxygen as a substrate, thiamine biosynthesis only occurs under aerobic conditions. This oxygen requirement is related to the suicide enzyme Thi5 (**151**), which provides a histidine during thiamine synthesis. Release of this histidine involves reduction of an Fe^{3+} ion to Fe^{2+}. Re-oxidation of ferrous iron to ferric iron by ferroxidases is an oxygen-dependent reaction (**Figure 1.7B**), which provides a plausible explanation for an indirect oxygen requirement for thiamine synthesis.

The anaerobic thiamine auxotrophy of *S. cerevisiae* can be nutritionally complemented by uptake of exogenous thiamine via the Thi10 plasma membrane transporter (**152**). Alternatively, pyridoxal, which is a precursor of pyridoxal-5'-phosphate can be imported via Tpn1 (**153)** and directly converted to PLP by, most likely the putative Bud16 in *S. cerevisiae* (**154**). By extrapolation, presence of either a thiamine transporter, or the combination of a pyridoxal transporter and a functional homolog of Bud16 combined is expected to be required for anaerobic, thiamine-prototrophic growth of yeasts and fungi.

DNA synthesis: ribonucleotide reductase

Reduction of ribonucleotides (NTPs), the building blocks for RNA to deoxyribonucleotides (dNTPs) is a key reaction in DNA synthesis that is catalysed by ribonucleotide reductases (RNRs; **Figure 1.8**; **155**). Three classes of RNRs have been described that differ in structure, cofactor use, metal content and, importantly, in their oxygen requirements. NTP reduction by Class I, II and III RNRs involves formation of a tyrosyl-, cysteinyl- or glycyl radical, respectively. The glycyl radical is oxygen sensitive and its formation requires binding of S-adenosyl methionine to a 4Fe-4S cluster. Class III RNRs therefore only function anaerobically. In contrast, Class-I enzymes require molecular oxygen for formation of the tyrosyl radical, while and Class-II RNRs are independent of oxygen. Most eukaryotes harbour Class-I enzymes (**156**), and some species have obtained an additional Class-II or Class-III RNR by horizontal gene transfer (**157**). This is exemplified by presence of a Class-II RNR in the facultative anaerobe *Sch. japonicus* (**157**) and a Class-III enzyme in obligately anaerobic Neocallimastigomycetes (**158**). *S. cerevisiae* only harbours a Class-I RNR, which is composed of two subunits, R1 and R2. In *S. cerevisiae* R1 is consists of either of the isoenzymes

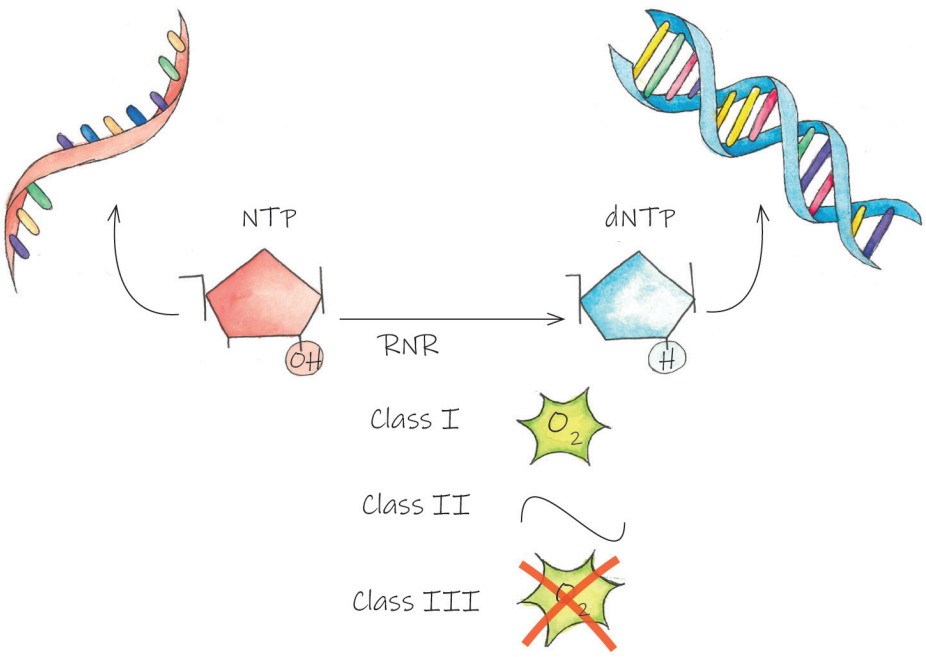

Figure 1.8. Conversion of ribonucleotides to deoxyribonucleotides by ribonucleotide reductases (RNRs).

Class-I enzymes require oxygen for the conversion, whereas Class-II enzymes do not, and Class-III RNRs are sensitive to oxygen and require an anaerobic environment for activity.
NTP; nucleoside triphosphates, dNTP; deoxy-nucleoside triphosphates.

Rnr1 or Rnr3 and R2 of enzymes Rnr2 or Rnr4. Although oxygen requirements for Class-I RNRs appear to be clear-cut, *S. cerevisiae* RNR is able to anaerobically synthesise dNTPs via an as yet unidentified mechanism.

Pyrimidine synthesis

In most yeasts and other fungi, biosynthesis of pyrimidines (i.e., uracil, thymine and cytosine), the precursors of pyrimidine ribonucleotides, requires oxygen (**159**,**160**). Pyrimidine synthesis starts from glutamine and carbamoyl phosphate, with are converted to into dihydroorotate in three consecutive

reactions (**Figure 1.9**; **156**). The first and only redox reaction in pyrimidine biosynthesis pathway is the subsequent oxidation of dihydroorotate to orotate by dihydroorotate dehydrogenase (DHOD). Electrons from dihydroorotate are donated to the prosthetic FMN group of DHOD and then transferred to an electron acceptor to re-oxidise DHOD to its active form (**162**,**163**). Three main classes of DHODs have been described, which show clear differences in amino acid sequence, electron acceptor, active site base and localisation (**164**,**165**). Class-I DHODs, mostly found in gram-positive bacteria, are soluble enzymes with a cysteine residue as active- site base (**166**). Class-I DHODs are further divided into the homodimeric type-A and heterotetrametric type-B enzymes, which use fumarate (**167**) or NAD^+ (**166**), respectively, as electron acceptor. *S. cerevisiae* and a number of closely related yeasts have a Class I-A DHOD, encoded by *URA1*. These members of the Saccharomycotina group are proposed to have obtained this gene by horizontal gene transfer (**159**,**168**). Since Ura1 uses fumarate as electron acceptor, its *in vivo* activity does not require aerobic conditions.

Instead of the Class I-A DHOD found in *S. cerevisiae*, most other eukaryotes harbour Class-II DHODs (**169**,**170**). In eukaryotes, these monomeric enzymes are associated with the outer surface of the mitochondrial inner membrane (**160**). While Class-II DHODs do not themselves require oxygen, they donate electrons to the quinone pool of the mitochondrial respiratory chain, which in yeasts uses oxygen as terminal electron acceptor. As a consequence of this indirect oxygen requirement for pyrimidine synthesis via Class-II DHODs, most yeasts cannot synthesise pyrimidines under anaerobic conditions (**159**,**171**). Media for anaerobic cultivation of yeast species that depend on oxygen for biosynthesis of pyrimidines, should therefore be supplemented with a source of pyrimidines. Although wild-type *S. cerevisiae* strains are prototrophic for pyrimidines under aerobic as well as under anaerobic conditions due to their Class-I DHOD (Ura1), they can take up exogenous uracil via the uracil permease Fur4 (**172**). Media supplementation with uracil is more common, though cytosine can in principle also be imported via the purine-cytosine permease Fcy2 (**173**), while no import system for thymine has been identified in this yeast (**174**).

Expression of *S. cerevisiae URA1*, first tested in *S. stipitis* has been proposed as a metabolic engineering strategy for eliminating oxygen requirements for pyrimidine biosynthesis (**175**). Interestingly, anaerobic synthesis of pyrimidines in yeasts may be more complicated than suggested by the previous text, as the yeast *D. bruxellensis* shows anaerobic growth without pyrimidine supplementation, while its genome only contains a *URA9* ortholog (**176**,**177**).

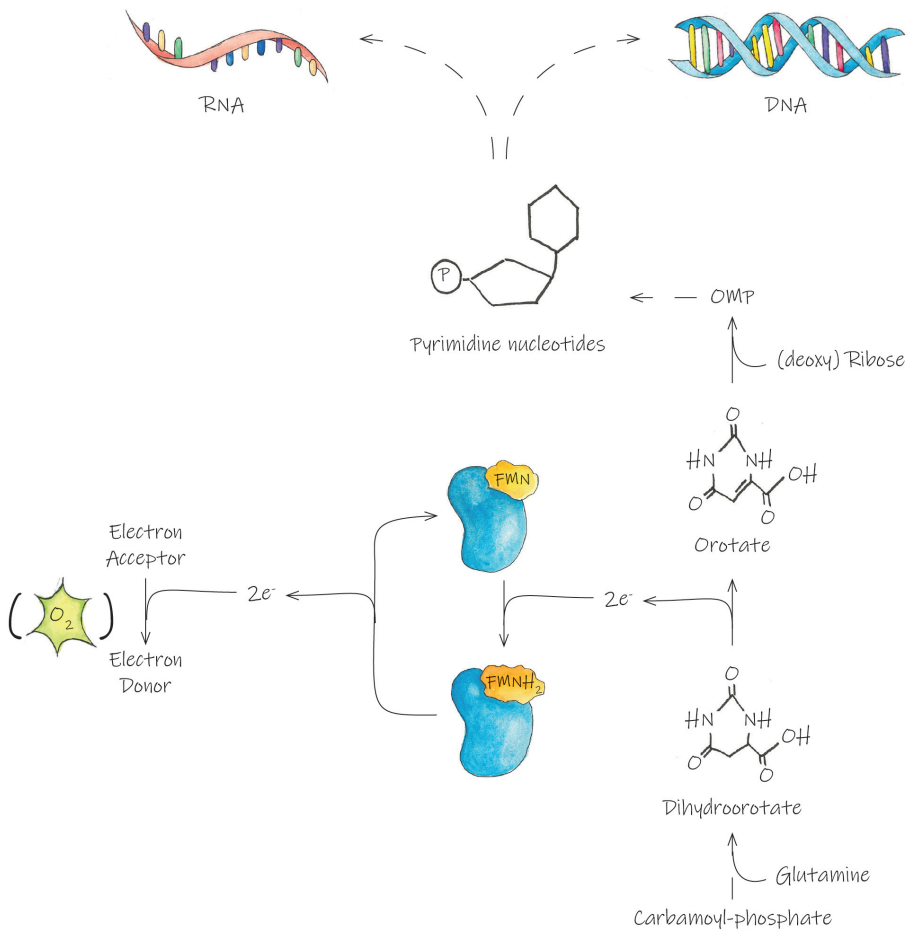

Figure 1.9. Biosynthesis of pyrimidine nucleotides from glutamine and carbamoyl phosphate.

The oxidation of dihydroorotate to orotate reduces the FMN domain in the dihydroorotate dehydrogenase, which is re-oxidised by donating electrons on an external electron acceptor. Electron acceptor couples used by different DHOD classes encompass fumarate/succinate (Class I-A), $NAD(P)^+$/NAD(P)H (Class I-B) and quinone/quinol (Class II).

DHOD; dihydroorotate dehydrogenase, OMP; orotidine monophosphate.

Scope of this thesis

Almost 70 years after the first demonstration that *S. cerevisiae* requires supplementation of sterols for anaerobic growth (**62**), we still lack a complete understanding of the inability of most other facultatively fermentative yeasts to grow anaerobically. Elucidating cellular processes that enable some yeasts to grow in the complete absence of oxygen, but are absent or incapable of supporting anaerobic growth in others, can provide a deeper insight into the adaptation of eukaryotic cells to an anaerobic lifestyle. In addition, research on this topic can be of applied significance. Only by understanding the oxygen requirements of 'non-conventional' yeasts with traits such as thermotolerance or resilience to other industrially relevant stress factors can we eventually engineer these yeasts for application in large-scale industrial processes. The goal of the research described in this thesis was therefore to contribute to the elucidation of evolutionary adaptations of non-*Saccharomyces* yeasts to anaerobic growth, with a focus on pyrimidine and sterol metabolism.

Non-dissimilatory oxygen requirements of yeasts are, in many cases, very small in comparison with the rates of oxygen uptake in respiring cultures. Minimisation of unintended entry of oxygen into cultivation systems such as shake flasks and bioreactors is therefore essential for meaningful research on this topic: even small oxygen 'leakages' can lead to incorrect conclusions. In addition, interpretation of results can be complicated by an ability of yeasts to store anaerobic growth factors and use them to temporarily continue growth in the absence of oxygen (**64**). **Chapter 2** evaluates critical steps and potential pitfalls in the design and implementation of laboratory setups for anaerobic growth studies on yeasts in anaerobic chambers and bioreactors.

At the outset of this PhD project, sterol-independent anaerobic growth of eukaryotes had only been documented for a group of deep-branching anaerobic fungi (**178**). Growth of yeasts was generally assumed to be strictly dependent on sterols, either acquired by biosynthesis or provided as nutritional supplement. **Chapter 3** describes the (re)discovery of a remarkable exception to this assumption. In line with an early publication from a famous Dutch yeast scientist (**179**), the facultatively anaerobic fission yeast *Sch. japonicus* was shown to grow anaerobically without sterol supplementation. Instead of an oxygen-independent pathway for sterol synthesis, *Sch. japonicus* was found to have acquired a unique adaptation to sterol-independent growth. This adaptation was investigated by a combination of anaerobic cultivation studies, analysis of the genome of *Sch. japonicus*, analysis of its lipid fraction of anaerobic cultures and expression of a key gene in *S. cerevisiae*.

Chapter 4 focuses on evolutionary adaptations of eukaryotes that enable them to synthesise pyrimidines, which are essential building blocks for DNA and RNA, in the absence of oxygen. In the large majority of yeasts and fungi, pyrimidine biosynthesis depends on a mitochondrial Class-II dihydroorotate dehydrogenase ('Ura9') that donates electrons to the mitochondrial respiratory chain (**160**). This coupling to mitochondrial respiration makes pyrimidine synthesis in these yeasts oxygen dependent. It has long been known that *S. cerevisiae* and a number of closely related yeasts circumvent this oxygen requirement

by instead using a soluble Class-I dihydroorotate dehydrogenase (**132**,**159**). However, alerted by earlier publications on the yeast *D. bruxellensis* (**176**,**177**), *Sch. japonicus* and even a group of strictly anaerobic fungi were found to only contain '*URA*9-type' dihydroorotate dehydrogenase genes in their genomes. To resolve whether and how these genes support anaerobic pyrimidine biosynthesis, they were expressed in *S. cerevisiae* strains from which the fumarate-dependent Ura1 enzyme was eliminated. Analysis of the physiology of these strains, enzyme-activity assays in cell extracts and localisation studies revealed an interesting case of convergent evolution.

During a search for fungal dihydroorotate dehydrogenase genes related to the research described in **Chapter 4**, a puzzling observation was made. A very large number of filamentous fungi were found to harbour genes that showed sequence similarity with the fumarate-dependent *URA1* gene of *S. cerevisiae*. However, none of these genes had been functionally analysed. Expression of two of these genes, one from an Ascomycete and one from a Basidiomycete, in *S. cerevisiae* formed the start of a functional analysis study, described in **Chapter 5**, which ultimately revealed their true identity.

Chapter 2.

Critical parameters and procedures for anaerobic cultivation of yeasts in bioreactors and anaerobic chambers

Christiaan Mooiman*
Jonna Bouwknegt*
Wijb J. C. Dekker*
Sanne J. Wiersma*
Raúl A. Ortiz-Merino
Erik de Hulster
Jack T. Pronk

* Authors have contributed equally to this work

This chapter has been published in FEMS Yeast Research

Abstract

All known facultatively fermentative yeasts require molecular oxygen for growth. Only in a small number of yeast species, these requirements can be circumvented by supplementation of known anaerobic growth factors such as nicotinate, sterols and unsaturated fatty acids. Biosynthetic oxygen requirements of yeasts are typically small and, unless extensive precautions are taken to minimise inadvertent entry of trace amounts of oxygen, easily go unnoticed in small-scale laboratory cultivation systems. This paper discusses critical points in the design of anaerobic yeast cultivation experiments in anaerobic chambers and laboratory bioreactors. Serial transfer or continuous cultivation to dilute growth factors present in anaerobically pre-grown inocula, systematic inclusion of control strains and minimizing the impact of oxygen diffusion through tubing are identified as key elements in experimental design. Basic protocols are presented for anaerobic-chamber and bioreactor experiments

Introduction

When grown under oxygen-limited conditions, the large majority of currently known yeast species at least partially ferment glucose to ethanol and carbon dioxide (**29**–**31**,**180**). The ability of these facultatively fermentative yeasts to generate ATP by substrate-level phosphorylation does not, however, imply they are all able to grow in the complete absence of oxygen. Instead, with few exceptions, even yeast species that vigorously ferment glucose under oxygen-limited conditions cannot sustain growth under strictly anaerobic conditions. This inability reflects small and often undefined oxygen requirements, which are generally attributed to a direct requirement of biosynthetic reactions for molecular oxygen and/or coupling of reactions in biosynthesis to the mitochondrial respiratory chain (**31**,**96**,**181**–**184**).

The model yeast *Saccharomyces cerevisiae* is one of few yeasts capable of fast anaerobic growth on synthetic mineral media supplemented with a fermentable sugar, a defined set of B-type vitamins, a source of sterols and unsaturated fatty acids (UFAs; **126**,**185**–**189**). The requirement of anaerobic yeast cultures for sterols and UFAs, which are frequently referred to as 'anaerobic growth factors', is due to the use of molecular oxygen in sterol biosynthesis and fatty acyl-CoA desaturation, respectively (**62**,**63**,**96**,**181**,**190**). Although the requirement of anaerobic *S. cerevisiae* cultures for UFAs is not absolute, anaerobic growth in the absence of UFA supplementation is slow (**64**). The maximum specific growth rate of *S. cerevisiae* in sterol- and UFA-supplemented, glucose-grown anaerobic batch cultures is typically only about 25 % lower than in corresponding aerobic cultures (**189**). This fast anaerobic growth of *Saccharomyces* yeasts is exceptional among yeasts (**29**,**31**) and essential for their large-scale industrial application in brewing, wine fermentation and bioethanol production (**65**,**191**–**194**). In industrial settings, large-scale fermentation processes are often preceded by an aerobic pre-cultivation phase or, alternatively, by a brief phase of intensive aeration, which enables cells to build intracellular storage of sterols and UFAs. In such set-ups, oxygen requirements for sterol and unsaturated-fatty-acid (UFA) synthesis can still negatively affect strain performance during prolonged anaerobic cultivation. For example, premature depletion of sterols and/or UFAs can cause 'stuck' brewing and wine fermentations (**195**,**196**). In addition, UFAs as well as ergosterol contribute to tolerance of *S. cerevisiae* to ethanol stress (**198**,**199**), which is an important factor for intensification of yeast-based processes for ethanol production.

The magnitude and molecular basis of the oxygen requirements of most yeasts other than *S. cerevisiae*, remain to be fully elucidated (**183**,**200**). Analysing and understanding oxygen requirements of facultatively fermentative 'non-conventional' yeasts can contribute to our comprehension of the roles of molecular oxygen in eukaryotic metabolism. In addition, such knowledge is essential for designing metabolic engineering strategies to enable application of non-conventional yeasts with industrially relevant traits, such as thermotolerance and inhibitor tolerance, in large-scale anaerobic processes (**201**–**203**).

Oxygen requirements for synthesis of key cellular components in *S. cerevisiae* can be estimated from the stoichiometry of biosynthetic reactions and reported data on biomass composition (**Table 2.1**). Although biomass composition may vary among strains and depend on cultivation conditions, such an

Table 2.1. Estimated oxygen requirements for biosynthesis of ergosterol, unsaturated fatty acids and other components of yeast biomass.

Unless otherwise indicated, data are based on reported biomass compositions of *S. cerevisiae* strains in anaerobic experiments with supplementation of Tween 80 (polyoxyethylene sorbitan monooleate), ergosterol and a selection of B-type vitamins. [a] Values are given as: Total UFA's (palmitoleate, $C_{16:1}$ /oleate, $C_{18:1}$). [b] Nicotinate is a precursor for oxygen-independent synthesis of nicotinamide adenine dinucleotides (NAD^+/$NADP^+$). [c] Oxygen-dependent reactions involved in thiamin and biotin biosynthesis by yeasts have not been fully resolved, and the indicated stoichiometries are estimates. For thiamine, the requirement of 3 moles of oxygen for the synthesis of the required NAD^+ moiety is incorporated. [d] Pantothenic acid is a precursor for oxygen-independent synthesis of Coenzyme A. [e] *S. cerevisiae* strains do not require oxygen for pyrimidine biosynthesis. Estimated oxygen requirements refer to yeasts in which pyrimidine biosynthesis depends on a respiratory-chain-coupled dihydroorotate dehydrogenase, assuming a DNA and RNA content equal to that of *S. cerevisiae*.

Biomass component Medium component	O_2 stoichiometry of biosynthesis (mol O_2 mol^{-1})	Content in *S. cerevisiae* biomass (µmol g biomass^{-1})	*S. cerevisiae* strain and growth conditions	Reference	O_2 requirement for biosynthesis (µmol g biomass^{-1})
Ergosterol *Ergosterol*	12	4.3	CBS2806, glucose-limited chemostat	(**241**)	30-52
		2.6	CEN.PK113-7D, glucose-limited chemostat	(**218**)	
		3.9	CEN.PK113-7D, batch culture	(**184**)	
UFA[a] *Tween 80*	1	21 (1.6 $C_{16:1}$, 19.4 $C_{18:1}$)	CBS2806, glucose-limited chemostat	(**241**)	21-103
		103 (44 $C_{16:1}$, 59 $C_{18:1}$)	CEN.PK113-7D, glucose-limited chemostat	(**218**)	
		58 (1.2 $C_{16:1}$, 57 $C_{18:1}$)	CEN.PK113-7D, batch culture	(**184**)	

Pyridine nucleotides *Nicotinate*[b]	3	3.8	CEN.PK113-7D, glucose limited chemostat	(**242**)	3.6-14
		4.5	Strain 210NG, aerobic ethanol-stat vitamin fed-batch	(**243**)	
		2.1-3.9	CEN.PK113-7D, glucose-limited accelerostat (NAD^+/NADH only)	(**244**)	
Biotin *Biotin*	~1[c]	0.002-0.009	Industrially produced yeast	(**245**)	~0.002 - 0.009
		0.002-0.008	Strain 1403-7A, aerobic uptake assay	(**246**)	
Coenzyme A *Pantothenate*[d]	1	0.43	Glucose limited chemostat (sum of CoA and acetyl-CoA)	(**242**)	~0.4
		~0.38	CEN.PK2-1C, aerobic shake flask (only acetyl-CoA)	(**247**)	
Thiamine *Thiamine*	~4[c]	0.025-0.22	Strain 210NG, aerobic ethanol-stat vitamin fed-batch	(**243**)	~0.0022-0.22
		0.0022-0.0029	Brewing strain #1007, static and shaken wort cultures	(**248**)	
Pyrimidines[e] *Uracil*	0.5	179	Strain 306, oxygen-limited continuous cultures	(**249**)	56-90
		111	Biomass equation in genome-scale model	(**250**)	

analysis readily identifies synthesis of sterols and UFAs as the major oxygen-requiring biosynthetic processes. However, their combined oxygen requirement of approximately 0.1 mmol O_2 (g biomass)$^{-1}$ (**Table 2.1**) requires an oxygen consumption rate of only 0.16 µmol (g biomass)$^{-1}$ min^{-1} to sustain a specific growth rate of 0.10 h^{-1} (doubling time of 6.9 h) that is used as a reference in many yeast chemostat studies (**204**–**206**).

In *S. cerevisiae*, biosynthesis of several key cofactors and their precursors requires oxygen (**Table 2.1**). In the *de novo* synthesis of the pyridine-nucleotide cofactors NAD^+ and $NADP^+$, the reactions catalysed by Bna2, Bna4 and Bna1 each require one mole of oxygen (**182**). Similarly, Fms1 catalyses an oxygen-dependent reaction in pantothenate biosynthesis (**143**), while synthesis of thiamine requires at least three moles of oxygen because NAD^+ acts as a precursor. In addition, *S. cerevisiae* has an incompletely understood oxygen requirement for synthesis of the thiamine precursor hydroxymethylpyrimidine (**207**). Recent research indicates that also the first, unresolved step of biotin biosynthesis in yeasts, catalysed by Bio1 orthologs, is oxygen dependent (**133**). Although heme biosynthesis is oxygen dependent, heme-containing proteins in *S. cerevisiae* are strongly associated with aerobic metabolism. Since, moreover, sulfite reductase contains siroheme rather than heme (**122**), anaerobic cultivation of *S. cerevisiae* does not require heme supplementation.

With the exception of pyridine-nucleotide synthesis, oxygen requirements for cofactor biosynthesis are at least two orders of magnitude lower than those for sterol and UFA biosynthesis (**Table 2.1**) and, in laboratory studies with synthetic media, they are usually masked by the routine inclusion of a mix of B-type vitamins (**128**).

In most non-*Saccharomyces* yeasts, pyrimidine metabolism depends on a mitochondrial, respiratory-chain-coupled dihydroorotate dehydrogenase (**208**,**209**) and therefore contributes a biosynthetic oxygen requirement similar in magnitude to that for sterol and UFA synthesis (**Table 2.1**). Pyrimidine biosynthesis in *S. cerevisiae* does not require oxygen, because its soluble cytosolic dihydroorotate dehydrogenase (Ura1) uses fumarate as electron acceptor (**159**,**171**).

Studies on the quantification and elucidation of oxygen requirements of yeasts, as well as physiological studies on the effects of severe oxygen limitation, require the option to reduce oxygen entry into yeast cultivation systems to extremely low levels (**31**,**64**,**79**,**184**). Here, we focus on two cultivation systems that are commonly used in such anaerobic growth studies with yeasts. Anaerobic chambers, filled with a hydrogen-containing atmosphere and equipped with a Pd catalyst to remove traces of oxygen, are often used for anaerobic batch cultivation of yeasts in shake flasks or on plates (**210**–**212**). Laboratory bioreactors are popular systems to perform controlled batch, fed-batch or continuous cultivation of yeasts under anaerobic conditions. Closed systems such as anaerobic jars for cultivation on agar plates, serum flasks and Hungate tubes will not be discussed in view of their limited applicability for quantitative analysis of growth, physiology and gene expression.

Vessels and lids of bioreactors are typically made of oxygen-impermeable materials such as glass and/or stainless steel. Their area-to-volume ratio (A/V), which is sometimes mentioned as a key factor in oxygen diffusion (**79**,**213**), is therefore not in itself a key factor in oxygen leakage. Instead, synthetic

tubing, rings and seals, as well as sensors and sampling ports, are among the key potential entry points for oxygen. Since the surface area of these sensitive points (A_s) does not scale with reactor volume, A_s/V is orders of magnitude lower in large-scale industrial bioreactors than in bench-top laboratory set-ups (**214**). When bioreactors are operated as fed-batch or chemostat cultures, additional precautions are needed to prevent oxygen entry via the medium feed (**31**).

Experimental challenges involved in preventing oxygen leakage into laboratory cultures have contributed to conflicting reports on the ability of yeast species and strains to grow anaerobically (**183**,**210**,**215**–**219**). Although these challenges are frequently mentioned in the literature (**31**,**79**,**84**), we are not aware of publications that combine a discussion of critical points in design of anaerobic yeast cultivation experiments with laboratory protocols. Based on experience in our laboratory spanning three decades (**31**,**64**,**184**,**189**), this paper aims to discuss pitfalls and challenges and share our current protocols for anaerobic cultivation of yeasts in anaerobic chambers and bioreactors.

Intracellular reserves and carry-over of anaerobic growth factors

Many yeast species accumulate lipids, including UFAs and sterols, in lipid droplets during aerobic growth on glucose (**220–222**). Toxic effects of intracellular free fatty acids and sterols are prevented by storage as nonpolar steryl esters (SE) and triacylglycerol (TAG) lipids (**223**). Lipid droplet synthesis from extracellular sources of sterols and UFAs has also been observed in heme-deficient cells (**224**,**225**) and under anaerobic conditions (**226**,**227**). Such intracellular stores of lipids can be mobilised to supply sources for membrane synthesis (**228**). Redistribution of the released UFAs and sterols over dividing yeast cells may therefore enable multiple generations upon transfer to strictly anaerobic conditions, even if sterols and UFAs are not included in growth media. This phenomenon is applied in industrial brewing, in which a brief aeration phase enables the generation of endogenous sterol and UFA reserves, which then support growth and fermentative capacity during the subsequent anaerobic fermentation process (**65**).

'Carry-over' of extracellular and/or intracellular reserves of anaerobic growth factors or their precursors may obscure biosynthetic oxygen requirements of yeasts in laboratory studies (**64**,**210**,**219**). For example, significant growth is observed upon inoculation of anaerobic shake-flask cultures of *S. cerevisiae* on glucose synthetic media without sterols or UFAs with aerobically pregrown cells (**Figure 2.1**). Increasing the glucose concentration in the anaerobic cultures can help to deplete intracellular reserves before glucose is completely consumed. In such experiments depletion of reserves is reflected by the absence of growth upon transfer of cells to a subsequent anaerobic culture on sterol- and UFA-free medium (**Figure 2.1**). The extent to which yeast strains or species grow during such a first cycle of anaerobic growth designed to deplete stores of anaerobic growth factors has no predictive value for their ability to subsequently grow in Tween 80 and sterol-supplemented medium (**Figure 2.1**). For example, *Dekkera* (*Brettanomyces*) *bruxellensis* cannot sustain anaerobic growth on intracellular reserves, but initiates growth upon addition of

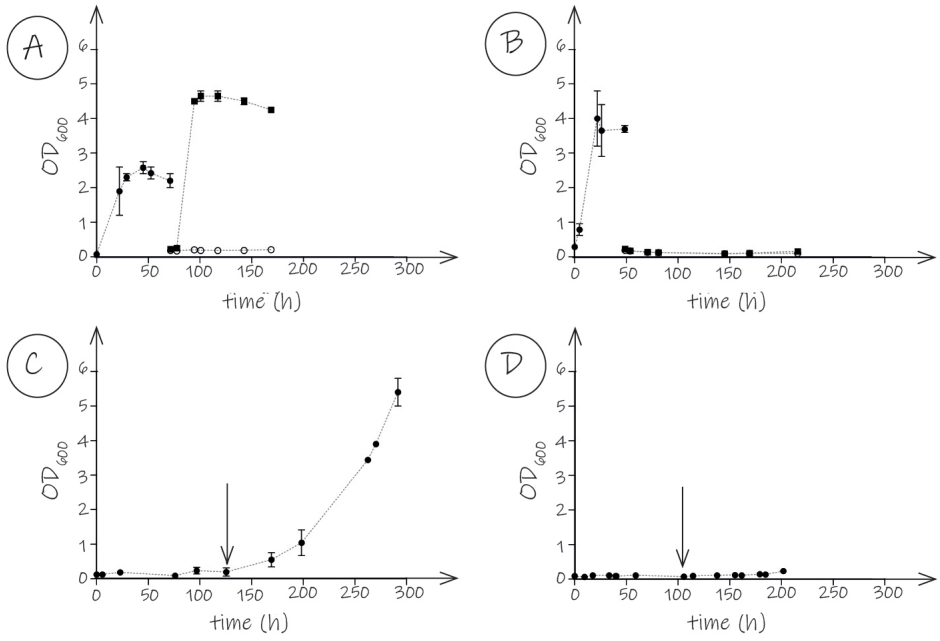

Figure 2.1. Representative growth profiles of four facultatively fermentative yeast species in standardised anaerobic chamber experiments.

Anaerobic-chamber experiments were performed as described in Protocol 1. The yeasts **A.** *S. cerevisiae*, **B.** *K. marxianus*, **C.** *D. bruxellensis* and **D.** *Tetrapisispora phaffii* were grown in 50-mL shake-flasks containing 40 mL synthetic medium with urea as nitrogen source (SMU; **232**), with supplements as indicated below. An anaerobic pre-culture (closed circles) without ergosterol or Tween 80, supplemented with 50 g L^{-1} glucose, was inoculated within the anaerobic chamber with an inoculum that had been grown aerobically on SMU with 20 g L^{-1} glucose until late exponential phase. When growth had occurred in this anaerobic pre-culture (**A** and **B**), and no further increase of the optical density was observed, aliquots were transferred to flasks with fresh SMU with 20 g L^{-1} glucose, either containing no anaerobic growth factors (open circles), or both Tween 80 and ergosterol (closed squares). When no growth was observed in the anaerobic pre-cultures for at least 100 h (**C** and **D**), a Tween 80 and ergosterol pulse was administered (indicated by arrows) and growth was further monitored. Data are represented as averages and mean deviation of two independent biological replicate cultures for each strain.

Tween 80 and ergosterol. Conversely, *Kluyveromyces marxianus* grows anaerobically in the growth-factor depletion culture, but not upon transfer to fresh medium with or without these growth factors. This pattern may reflect additional nutritional requirements for anaerobic growth and, in *K. marxianus*, has recently been attributed to absence of a functional sterol uptake system (**102**). These observations underline the necessity, irrespective of the cultivation system, to include a dedicated anaerobic pre-cultivation step to

deplete intracellular growth factors in batch-cultivation studies on anaerobic nutritional requirements of yeasts.

Monitoring anaerobicity of yeast cultures

Facultatively fermentative yeasts that cannot grow under strictly anaerobic conditions, typically show fast growth at dissolved-oxygen concentrations that are below the detection level of the polarographic oxygen probes that are commonly used in microbial cultures (**30**,**200**). Measurement of dissolved-oxygen concentrations is, therefore, not a reliable way to assess culture anaerobicity. In anaerobic chambers, indicator cultures that require small amounts of oxygen for growth can be used as a control for oxygen contamination (**183**). For example, *Kluyveromyces lactis* cannot grow on synthetic glucose medium with Tween 80 and ergosterol under strictly anaerobic conditions, but shows fast fermentative growth in oxygen-limited cultures (**200**). In our experience, cultures of a wild-type *S. cerevisiae* strain on synthetic glucose medium lacking Tween 80 and ergosterol provides an even more sensitive detection of oxygen leakage (**Figure 2.2**).

In bioreactor cultures, indicator strains cannot be in the same anaerobic compartment as the strain of interest. As outlined in several studies on anaerobic yeast cultivation, it is virtually impossible to eliminate oxygen leakage in bench-top bioreactors (**31**,**64**,**79**,**184**). In studies on oxygen-independent synthesis of (presumed) anaerobic growth factors by wild-type and engineered yeast strains, mutants in which relevant oxygen-dependent reactions have been eliminated therefore provide essential negative controls. For example, sterol-independent anaerobic growth of an *S. cerevisiae* strain expressing a eukaryotic squalene-tetrahymanol cyclase was confirmed by deleting *ERG1* (which encodes an essential enzyme in sterol synthesis; **184**).

Anaerobic chambers

Anaerobic chambers are designed to provide gas-tight, near oxygen-free interior workspaces, in which experiments can be performed by using arm-length gloves made of materials, that are resistant to oxygen diffusion, such as butyl rubber. Materials, including flasks, chemicals and inocula can be transferred to and from the anaerobic workspace via an air lock ('pass box'). A Pd catalyst, combined with a hydrogen-containing atmosphere, is generally used to remove traces of oxygen from the workspace (**229**).

Air locks are designed to remove oxygen before transfer of materials to the anaerobic workspace. However, growth experiments with *S. cerevisiae* in the presence and absence of sterol- and UFA-supplementation indicate that, even when manufacturers' protocols are strictly followed, use of the air

lock can be a significant cause of oxygen entry (**Figure 2.2**). Reducing the void volume of the air lock by inserting inert solid objects helps to reduce oxygen entry (see Protocols). Media should be pre-incubated in the anaerobic air lock and/or in the workspace before inoculation to remove traces of oxygen. Furthermore, experiments should be designed to minimise use of the air lock and, where possible, to synchronise it with catalyst replacement. This minimisation implies that routine analyses such as optical density measurements should be performed inside the anaerobic workspace rather than by regular use of the air lock for analyses on external equipment. In view of their restricted options for sampling, sample handling and long-term aseptic operation of cultures, anaerobic chambers are particularly useful for simple, parallel batch-cultivation studies in shake flasks or deep-well plates, for example to compare multiple yeast strains or cultivation conditions.

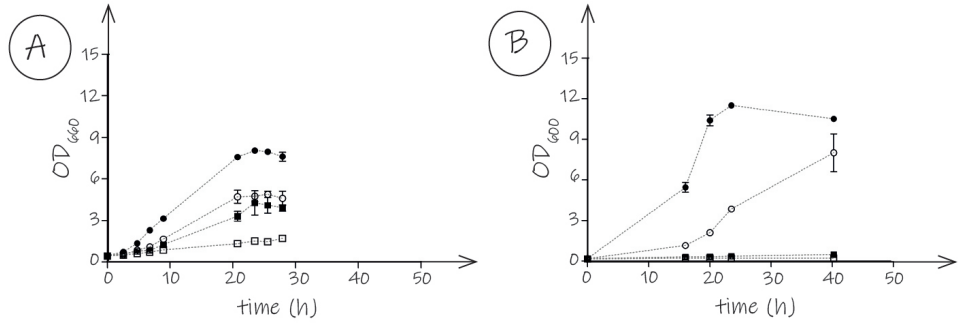

Figure 2.2. Use of the air lock of an anaerobic chamber as main source of oxygen contamination.

Anaerobic-chamber experiments were performed as described in Protocol 1. *S. cerevisiae* CEN.PK113-7D was grown in 50-mL shake-flasks containing 40 mL synthetic medium with urea as nitrogen source (SMU; **232**), with supplements as indicated below. An anaerobic pre-culture without ergosterol or Tween 80, supplemented with 50 g L^{-1} glucose, was inoculated within the anaerobic chamber with an inoculum from an exponentially growing aerobic culture on SMU with 20 g L^{-1} glucose. After the optical density increase in the pre-culture levelled off, aliquots were transferred to flasks with fresh SMU with 20 g L^{-1} glucose, supplemented with Tween 80 and ergosterol (closed circles), ergosterol only (open circles), Tween 80 only (closed squares) or SMU without these anaerobic growth factors (open squares). **A.** Optical density measurements at 660 nm were performed outside the anaerobic chamber, requiring frequent use of the air lock. **B.** Optical density was measured within the anaerobic chamber at a wavelength of 600 nm (different wavelength due to use of dedicated fixed-wavelength spectrophotometer in anaerobic chamber). This decreased the need to open the doors of the air lock. Data are represented as averages and mean deviation of two independent biological replicate cultures for each condition.

Bioreactors

Bench-top bioreactors, with working volumes ranging from 0.5 to 5 L, are widely used in quantitative microbial physiology. In contrast to the simple cultivation systems that are generally used in anaerobic chambers, they allow for simultaneous measurement and tight control of multiple process conditions, including pH, temperature, dissolved-oxygen and biomass concentration. For these reasons, laboratory-scale bioreactor cultures are also popular models for design and optimisation of large-scale industrial fermentation processes. Bioreactors can be operated in batch, fed-batch or continuous mode which are defined by the medium supply- and broth withdrawal regimes (**184**,**189**,**230**,**231**).

For anaerobic yeast cultivation in bioreactors, gas with a near zero oxygen content is continuously flushed through the cultures, in most cases in the form of high-purity nitrogen (N6) gas. However, the complexity of laboratory bioreactors makes them prone to permeation of oxygen through seals and tubing, oxygen contamination in gas and liquid flows and/or oxygen leakages through sampling ports, sensors, mass flow controllers and valves. Setting up (near-)anaerobic bioreactor cultures therefore requires great attention for experimental design.

Gas can be supplied to bioreactors either by sparging the stirred liquid phase or by leading gas through the reactor headspace. As bubble formation greatly increases the gas-liquid interface, sparging enables more efficient gas transfer than headspace aeration. In an ideal system, i.e., without any oxygen entry into the reactor, both modes of gas supply should yield the same results. When, instead, inadvertent oxygen entry occurs primarily via the inlet gas, e.g. due to oxygen contamination of high-purity nitrogen (N6) gas, supply through the headspace leads to a lower oxygen transfer to the broth, in which yeast cells maintain a vanishingly low oxygen concentration (**30**,**64**,**200**). Conversely, when oxygen predominantly enters via liquid flows or submerged sampling ports, sparging is preferable. Applying overpressure in the reactor may reduce entry of oxygen through small leaks connected to the headspace. However, at the same time, overpressure will facilitate transfer of any oxygen that enters the reactor as contaminations of the inlet gas flow, as it increases the partial pressure gradient for oxygen transfer to the broth. For our 2-L bioreactor set-ups, we have found that headspace aeration, combined with a small 0.2 bar overpressure to prevent oxygen entry during sampling, results in a lower oxygen availability than sparging (**Figure 2.3**).

Polarographic oxygen electrodes do not detect minor oxygen leaks in growing cultures and can therefore be omitted from anaerobic cultivation set-ups. Probes for pH measurement are often made of porous glass and are not sealed in a gas tight manner. In our anaerobic bioreactor set-ups, we therefore generally accept the absence of active pH control (**64**,**184**). To prevent the decrease of culture pH caused by ammonium consumption, use of urea as alternative nitrogen source is a straightforward way to avoid excessive acidification (**232**,**233**). Alternatively, a buffering compound can be included in the medium.

Bioreactors are typically connected to a significant length of synthetic tubing to enable addition of liquids and gasses. Tubes connected to the reactor are opened and closed with clamps or valves

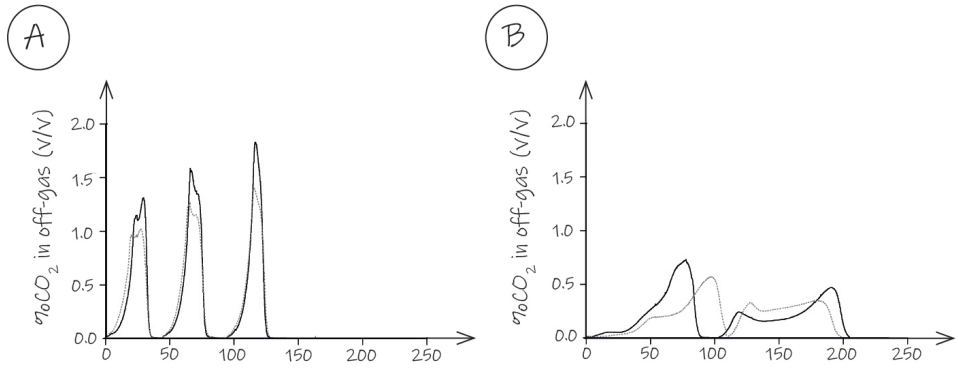

Figure 2.3. Nitrogen sparging versus headspace supply: impact on growth of *S. cerevisiae* in sequential batch reactors (SBR).

Bioreactors were assembled according to Protocol 2. Anaerobic bioreactors were operated in SBR mode, and the CO_2 content of the off-gas was used to monitor growth of *S. cerevisiae* strain IMX585 (**59**). Cultures were grown on synthetic medium with urea as nitrogen source (SMU; **232**). Nitrogen 6.0 HiQ gas (Linde AG, Schiedam, the Netherlands) was supplied to the reactor at 0.5 L min^{-1} either by **A.** sparging or **B.** through the reactor headspace. When N_2 was supplied by sparging, an initial anaerobic batch culture on SMU with 25 g L^{-1} glucose, lacking ergosterol and Tween 80 was followed by three consecutive SBR cycles on SMU with 20 g L^{-1} glucose supplemented with Tween 80 but not with ergosterol. In the cultures to which N_2 was supplied to the headspace, only two consecutive batch cultures were monitored. Data shown in the figures are from two individual biological replicates for each mode of nitrogen supply, indicated by black and grey lines.

or, alternatively, inserted in peristaltic pumps. Since permeation through tubing can be a major source of oxygen entry into reactors (**31**,**79**), choosing the right material is crucial. In selecting tubing materials, not only oxygen permeability but also factors such as tolerance to autoclaving, resistance to tearing at steel-tubing connections, and ruggedness of tubing used in peristaltic pumps need to be considered. For a long time, our group relied on Norprene A-60-G tubing for anaerobic bioreactor set-ups (**189**). For research on biosynthetic oxygen requirements, we recently changed to Fluran F-5500-A for all gas and liquid tubing, as it has a much lower oxygen permeability than Norprene A-60-G (**Table 2.2**). Masterflex C-Flex Ultra has an even lower oxygen permeability to Fluran F-5500-A but in our hands was considerably less resistant to autoclaving, which caused loss of flexibility. In addition, Fluran F-5500-A could also be used in peristaltic pumps, although this requires regular recalibration of pump rates during prolonged operation.

In bioreactors, depletion of intracellular reserves of anaerobic growth factors can be achieved

Table 2.2. Characteristics of tubing material for anaerobic bioreactor cultivation.

Silicone Peroxide and Norprene A-60-G tubing are commonly used for liquid and gas flows in aerobic and anaerobic laboratory bioreactor cultivation experiments, respectively. Oxygen permeability is expressed in Barrer (10^{-10} cm^3_{STP}·cm·cm^{-2}·s^{-1}·(cm Hg)$^{-1}$); rate of diffusion, at a given pressure, through an area of material with a specified thickness).

Tubing	O_2 Permeability (Barrer)	Autoclavability
Silicone Peroxide	4715	++
Norprene A-60-G	200	+++
Fluran F-5500-F	14	+
Nylon	5.4	+
C-Flex Ultra	1.1	---

by automated sequential batch-reactor (SBR) cultivation. In SBR set-ups, the reactor is manually or automatically emptied upon reaching a predefined biomass density or CO_2 output, leaving a small volume of culture broth to act as inoculum after automatic refilling with fresh sterile medium. Alternatively, reactors can be operated as fully continuous (chemostat) cultures. These (semi-) continuous modes of operation require that not only the bioreactors themselves, but also the medium reservoirs are gassed with nitrogen (N5.5).

In SBR cultures, medium in the tubing between the medium reservoir and the reactor is stagnant in between empty-refill cycles. We observed that slow permeation through tubing caused entry of oxygen into this stagnant medium. To prevent entry of this oxygenated medium into the bioreactor, the 'fill' phase was preceded by pumping the first 10 mL of sterile medium into a dedicated sample bottle placed between the bioreactor and the medium pump. Subsequently, the medium pump was stopped and the mild overpressure in the reactor was used to also evacuate the tubing between the bioreactor and the sample bottle (**Figure 2.4**; Supplementary file S1) before refilling the reactor.

Even when a glass medium reservoir is continuously flushed with high-purity (N6) N_2, small amounts of oxygen were found to enter bioreactors with the ingoing medium flow. This problem was most pronounced in chemostat cultures, into which medium is slowly pumped from the reservoir to the reactor and, even when using tubing with a low oxygen permeability, may become contaminated with oxygen due to permeation. Visser *et al.* (**31**) identified this mechanism as a major source of oxygen entry and placed a separate sterile, nitrogen-sparged, stirred bioreactor just in front of the actual chemostat bioreactor. We recently found that small, autoclavable membrane-contactor modules commonly used for gas exchange

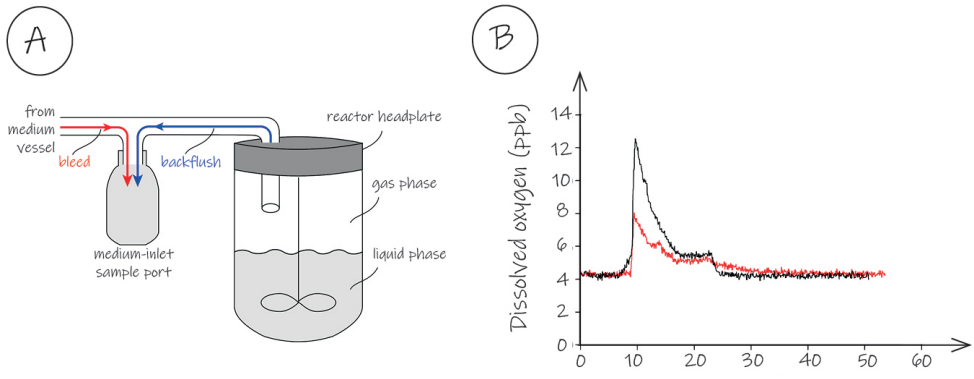

Figure 2.4. Effect of bleed and backflush of the medium inflow on dissolved oxygen concentration in anaerobic bioreactors.

A. Schematic representation of 'bleed' and 'backflush' to eliminate stagnant medium in the inlet tubing that had acquired oxygen by permeation through tubing during sequencing-batch reactor (SBR) experiments. The bleed operation disposes medium from tubing between medium reservoir and the sampling port. A separate 'backflush' operation uses overpressure in the reactor to push stagnant medium between reactor and sample point into the sample bottle. **B.** A bioreactor assembled according to Protocol 2 was filled with tap water. Dissolved oxygen in the liquid phase was measured with a sensitive Hamilton VisiTrace Optical Trace DO 225 (Hamilton, Bonaduz GR, Switzerland) sensor equipped with an optical dissolved oxygen cap (L0-80) during an empty-refill sequence of the bioreactor with bleed, without (black line) and with the backflush operation (red line). Dissolved oxygen data were recorded with Android application ArcAir (Hamilton).

(**234**–**236**) are extremely efficient, affordable and practical devices for deoxygenating the medium feed of continuous-cultivation systems (**Figure 2.5**). When a membrane-contactor module was placed near the medium entry point of bioreactors and connected to a flow of nitrogen (N5.5), *S. cerevisiae* chemostat cultures grown on glucose synthetic medium without the anaerobic growth factors ergosterol and Tween 80 completely washed out. This result marks a strong improvement on previous systems in which, under the same conditions, oxygen entry invariably led to reduced but significant steady-state biomass concentrations (**79**, **105**).

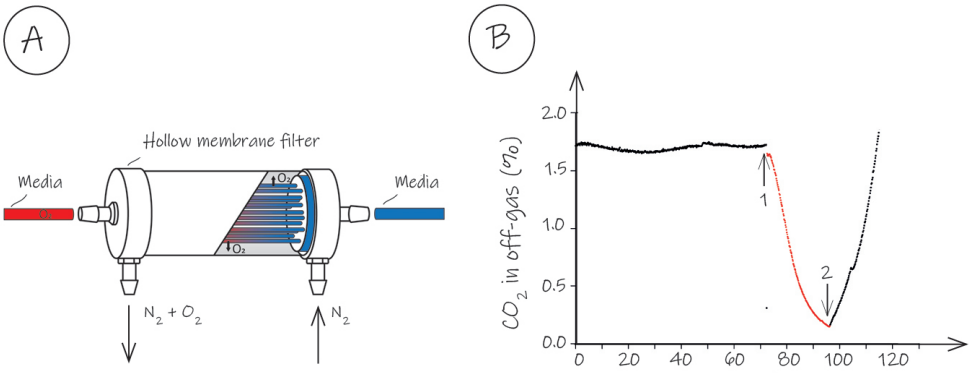

Figure 2.5. The effect of a membrane-contactor removing oxygen from the medium feed on cultures in chemostat.

A. Schematic representation of the PDMSXA-1000 membrane module (PermSelect, Ann Arbor, MI, USA). Ingoing medium contaminated with oxygen (red) due to permeation through tubing, is stripped from oxygen with 5.0 quality nitrogen gas (Linde, Schiedam, The Netherlands) and the resulting anaerobic medium (blue) enters the bioreactor. **B.** *Saccharomyces cerevisiae* CEN.PK113-7D was grown in an anaerobic chemostat culture, as described in Protocol 2. Cultures were grown at a dilution rate of 0.10 h^{-1} on synthetic medium with urea as nitrogen source (**232**) and 20 g L^{-1} glucose without supplementation of a source of either UFAs or sterols. Growth was monitored by on-line analysis of the CO_2 concentration in the off gas. After 70 h, when the steady-state residual glucose concentration was 5.0 mM (indicated by Arrow 1), the medium inlet was rerouted through the membrane module, resulting in a washout (Red line). After 96 h, when the residual glucose concentration had increased to 66 mM, the medium flow was restored to the original situation state (Arrow 2).

Conclusions and protocols

Many aspects of the anaerobic physiology of yeasts can be studied in bioreactors or shake-flasks without requiring the extreme measures discussed above. For example, energy coupling and product yields on glucose can be reliably measured in bioreactors sparged with nitrogen (N5.5) gas and equipped with Norprene tubing (**60**,**237**). Experimental design for investigations into the small oxygen requirements of yeasts for biosynthetic reactions starts with the sober realisation that complete elimination of oxygen from bench-top set-ups, and even from anaerobic chambers, is virtually impossible. Unless elaborate measures are taken, such as pure-nitrogen sparging of cultures inside an anaerobic chamber (**238**), the key challenge is to consistently and verifiably reduce oxygen entry to levels that allow for meaningful experiments. Whenever possible, inclusion of oxygen-dependent control strains and/or verification of

conclusions by genetic modification, is therefore essential.

In our research on anaerobic cultivation of yeasts, we identified carry-over of anaerobic growth factors from aerobically grown pre-cultures, frequent use of air locks in anaerobic chambers and oxygen permeation through bioreactor tubing as key points of attention. Serial transfer was found to be an essential and reliable approach to prevent misinterpretation of results caused by intracellular reserves of anaerobic growth factors. Permeation of oxygen diffusion through tubing was found to be particularly relevant for stagnant medium in tubing during SBR cultivation and during slow supply of medium during continuous operation. Use of membrane-contactor modules is a simple and promising approach to address the latter problem.

Below, two basic protocols for anaerobic cultivation of yeasts in anaerobic chambers and bioreactors are presented, along with comments that describe or explain specific points of attention. Clearly, differences in equipment, lab infrastructure and research goals may require other or additional measures. The main goal of these protocols is therefore not to provide a generally applicable manual, but to alert colleagues to potential pitfalls and possible solutions, and thereby aid them in interpreting published studies and in setting up anaerobic yeast cultivation experiments in their laboratories.

Protocol 1: Anaerobic chamber

The following step-by-step description of growth experiments in an anaerobic chamber complements the Materials and Methods section of a publication in which we used this protocol to study UFA-independent anaerobic growth of *S. cerevisiae* (**64**).

1. Place an orbital shaker platform and a small spectrophotometer, both cleaned with suitable disinfectant, in the previously cleaned workspace of the anaerobic chamber.
2. Generate an anaerobic environment in the workspace of the chamber according to manufacturer's protocol, and check its anaerobicity with a test culture (see **Note 1**).
3. Thoroughly clean all equipment and materials that will be introduced into the workspace with a suitable disinfectant (see **Note 2**).
4. Place cleaned containers/flasks containing sterile pipette tips, spectrophotometer cuvettes, demineralised water, concentrated solutions of anaerobic growth factors of interest, along with shake flasks filled with relevant sterile media, calibrated pipettes, a closable waste bin and any other required materials in the air lock of the anaerobic chamber, together with a freshly activated catalyst cartridge

(see **Note 3**). Fill up the void volume of the air lock with oxygen-impermeable materials.

5. Perform at least four vacuum/purge cycles of the air lock, including two with hydrogen-containing gas, to aid removal of oxygen by the Pd catalyst cartridge before opening the inner door of the air lock.

6. Move all required materials into the workspace of the anaerobic chamber (see **Note 4**).

7. Repeat steps 3-6 until all required materials are in the workspace. Make sure all materials are in the workspace two days before starting an experiment, to allow oxygen to be removed, especially from liquid media.

8. Grow the strains of interest and control strains (see **Note 1**) in an aerobic incubator to mid-exponential phase.

9. Prepare inocula for anaerobic experiments in small volumes (typically up to 2 % of final culture volume, to minimise introduction of dissolved oxygen into anaerobic pre-cultures via aerobically pre-grown inocula). Concentrate samples if necessary.

10. Transfer inocula into the workspace as described in steps 3-6.

11. Inoculate (see **Note 5**) the anaerobic pre-cultures at the desired optical densities.

12. Monitor optical density of the anaerobic pre-cultures over time with a spectrophotometer placed in the workspace (see **Note 6**). Next steps depend on the growth profile (see **Figure 2.2**):

    a. Growth is observed (**Figure 2.2A** and **B**; the culture uses intracellular reserves of anaerobic growth factors or can grow anaerobically in the absence of the growth factor of interest). Continue with step 13.

    b. No growth is observed (**Figure 2.2C** and **D**; the yeast cannot use intracellular reserves, has additional oxygen requirements, is unable to take up the growth factor of interest or the culture is no longer viable). Continue with step 14.

13. When the optical density no longer increases, transfer a small aliquot of the culture to separate flasks with anaerobic media, supplemented with various combinations of the anaerobic growth factor(s) of interest. Monitor growth as described above until the end of the experiment. Continue with **step 15**.

14. Add an appropriate volume of the concentrated solution of the anaerobic growth factor(s) of interest to the culture:

    a. Growth is observed (**Figure 2.2C**; the yeast grows anaerobically when provided with this anaerobic growth factor).

    b. No growth is observed (**Figure 2.2D**; the yeast has additional oxygen requirements, is unable to take up the growth factor of interest or the culture is no longer viable).

15. After terminating the anaerobic growth chamber experiment, move cultures that did not grow out of the anaerobic chamber and incubate them aerobically for a provisional indication of culture viability.

Protocol 2: Anaerobic cultivation in bioreactors

This protocol outlines key steps for anaerobic batch, sequential-batch and chemostat cultivation in bioreactors. Information on equipment and materials used in our laboratory can be found in recent publications (**64**,**102**,**239**; and see supplementary file S2).

Bioreactor batch cultivation

Steps 1–9 describe anaerobic bioreactor batch experiments. Since sequencing-batch and chemostat experiments are usually started as batch cultures, these steps also apply for those modes of cultivation.

1. Before assembling a bioreactor set-up, thoroughly check all tubing, seals, septa and O-rings for wear or damage and replace them when necessary. Minimise and standardise length of tubing for replicate bioreactors (see **Note 7**).

2. Clamp all tubing, apply an 0.4 bar overpressure and monitor pressure for at least 15 min. If a pressure drop is observed, submerge the bioreactor in water to identify the leak. Prior to autoclaving the bioreactor, remove clamps to ensure gas exchange is possible.

3. Aseptically fill the autoclaved bioreactor with sterile medium to the intended working volume minus the volume of the inoculum.

4. Activate gas analysis equipment, mass flow controllers, pressure valves and equipment used for control of process parameters (e.g. temperature, stirrer speed).

5. Sparge medium in the bioreactor and set overpressure at 0.2 bar (see **Note 8**). Continue sparging for at least 1 h with high-purity nitrogen (N6 or above) at 0.5 L N_2 (L working volume)$^{-1}$ min^{-1} (see **Note 9**).

6. Release overpressure, then stop gas flow and inoculate the bioreactor.

7. Redirect inlet nitrogen stream through bioreactor headspace, stop sparging of N_2 through culture broth, and reapply 0.2 bar overpressure

8. Clamp all tubing that is not actively used during the growth experiment as close as possible to the bioreactor (see **Note 10**).

9. Use the 0.2 bar overpressure for aseptic sampling and take a pre-sample with each sample to discard any stagnant culture from tubing.

For further operation as a sequential batch reactor experiment, continue at step 10. For further operation as a chemostat, continue until step 11 and then proceed to step 21.

10. Assemble glass medium reservoir using oxygen impermeable tubing, O-rings and include sparging equipment (e.g. air stone).

11. Aseptically connect sterile medium reservoir and effluent to bioreactor influent and effluent, respectively, via peristaltic pumps.

12. Under the chosen process conditions, aseptically adjust level sensor to the desired working volume of the subsequent batch-cultivation cycles (see **Note 11**). Connect the level sensor to influent pump, to stop pumping upon contact.

13. Leave 0.2 – 1.0 % of the working volume set in step 12 after the emptying phase. The ratio of residual over the working volume determines the number of generations in each batch-cultivation cycle (see **Note 12**).

14. Vigorously sparge medium reservoir with nitrogen (N5.5) gas for at least one hour before use and continue sparging until refilling of bioreactor is complete (see **Note 9**).

15. Empty the bioreactor by manually or automatically switching on the effluent pump (see **Note 13**).

16. Prior to refilling the bioreactor, take a sample of 10 mL from the medium inlet to discard stagnant medium from the tubing, using a sampling port close to the bioreactor lid. Use the 0.2 bar overpressure to backflush the medium in between the sampling port and the bioreactor (**Figure 2.4A**)

17. Activate the influent pump to start filling the bioreactor and switch the gas inflow from headspace to sparging to minimise oxygen entry via medium inflow.

18. Inflow of medium will automatically stop when the medium reaches the electrical level sensor. Gas inflow can be reverted to headspace (see **Note 14**).

19. Wait until the culture has depleted the limiting medium component, usually indicated by a decrease of the CO_2 concentration in the exhaust gas (see **Note 15**).

20. To initiate a subsequent empty refill cycle, repeat step 14 to 19 for another empty refill cycle.

After the anaerobic batch reactor experiment (step 1-9), connect the medium vessel (step 10-11) and continue with the next steps for an anaerobic chemostat experiment.

21. Connect the level sensor to the effluent pump, or 'pump on contact' mode (see **Note 16**).

22. Set the influent pump to a rate corresponding to the desired dilution rate of the continuous culture. Adjust level sensor if required. A culture is considered to be in a steady state when during at least five volume changes the culture parameters and physiology did not differ more than a predefined margin over three subsequent samples taken at least one volume change apart (see **Note 17**)

23. When steady-state conditions have been reached, start sampling for steady state characterisation. The experiment can be stopped, the overpressure released, and the broth weighed to determine the actual working volume.

Notes anaerobic chamber

Note 1. As controls in anaerobic growth chamber experiments, we routinely include cultures of *S. cerevisiae* CEN.PK113-7D on glucose synthetic medium with and without Tween 80 and ergosterol. If, after a first anaerobic growth cycle to deplete intracellular reserves, sustained growth is observed on glucose synthetic medium without Tween 80 and ergosterol, this is a strong indication for the presence of oxygen in the workspace. See **Figure 2.2B** for representative results of negative control cultures in which only a very slow increase of optical density is observed.

Note 2. Because no fire/Bunsen burner can be used, strict measures are needed to reduce the risk of contamination. Surfaces and equipment must be regularly disinfected with 70 % ethanol or other suitable disinfectants. Oxygen permeability of butyl rubber increases upon repeated or prolonged exposure to ethanol. Therefore, avoid spilling of ethanol on gloves while cleaning. We recommend using sterile pipette tips equipped with filters, and to clean pipettes with ethanol in between sampling of different cultures. Even when taking extensive precautions, be alert to the possibility of (cross) contamination of cultures.

Note 3. The Pd catalyst cartridge aids the removal of traces of oxygen by catalysing oxidation of hydrogen in the anaerobic gas mixture (up to 5 % H_2, 5-10 % CO_2 and N_2). Because this process generates water, the catalyst needs to be regularly reactivated by dry heating. Consult manufacturer's instructions for frequency of recycling, but be aware of trade-offs related to frequent use of the air lock. We limit use of the air lock to twice a week, despite the manufacturer's advice to re-activate the catalyst daily. This limited use of the air lock requires careful scheduling of entry and removal of materials.

Note 4. Frequent use of the air lock is a main cause of oxygen contamination in anaerobic chamber experiments (**Figure 2.2**). Preferably, materials introduced via the air lock should be accompanied by an activated catalyst cartridge and incubated in the air lock for at least 30 min to reduce oxygen entry.

Note 5. In the anaerobic pre-culture, intracellular reserves of anaerobic growth factors should be depleted. To prevent premature depletion of glucose we recommend using a high initial concentration (5 % w/v) for this pre-culture.

Note 6. Working with gloves complicates taking notes of measurements made within the anaerobic workspace. A small voice recorder attached to the anaerobic chamber facilitates recording of culture number, time and optical density.

Notes bioreactor

Note 7. To minimise oxygen entry, several modifications were made to our standard bioreactor setups. Silicone sealing rings in the headplate were replaced with less oxygen-permeable Viton rings (Eriks, Rotterdam, NL). Nylon tubing was used for non-aseptic parts of the gas supply and the length of the gas line from cylinder to bioreactor was minimized. When near-empty gas cylinders were replaced for full ones, the gas supply line was purged before reconnection. Where possible, plastic parts (e.g. tubing connectors, sterile cotton-wool filter canisters in gas lines) were replaced with stainless steel parts.

Note 8. Throughout cultivation, experimenters should be aware that the bioreactor is operated under overpressure, which pushes broth out of the bioreactor when the effluent line is opened. In addition, if the gas flow through the bioreactor is interrupted while sparging, broth can be pushed into the gas inlet. Install liquid traps to protect expensive mass flow controllers and be mindful to always release the overpressure from bioreactor before changing the gas flow.

Note 9. During sparging with nitrogen (N5.5 or above), the dissolved oxygen (DO) concentration asymptotically approaches zero. Depending on the volumetric mass-transfer coefficient (k_La), 90 % of the oxygen is usually already removed within 1 h. Sparging time prior to the experiment can be increased, but near-complete removal of oxygen may take several hours.

Note 10. Even use of highly oxygen-impermeable tubing (e.g. Fluran F-5500-A) does not completely eliminate oxygen permeation through tubing. Clamping tubes close to the bioreactor head plate helps to minimise this mode of oxygen entry.

Note 11. Adjusting the level sensor towards the top of the turbulent liquid level, while the bioreactor is operating at its mixing, gassing and temperature setpoints, ensures that a correct and constant working volume is maintained. To prevent adjustments of the level sensor from compromising aseptic conditions, 70 % ethanol can be applied to the level sensor seal.

Note 12. When biomass concentrations at the end of each batch cultivation cycle are the same, the number of generations per cycle roughly corresponds to the number of doublings of the culture volume (e.g., leaving 25 mL of broth after the emptying phase in an SBR that is subsequently refilled to a working volume of 1600 mL will result in six generations per SBR cycle).

Note 13. It is important to empty the bioreactor as fast as possible. During the majority of the emptying process the broth can still be mixed but as the liquid-gas interface drops below the impellers, the broth becomes stagnant which may lead to sedimentation of yeast to the bottom of the bioreactor. Cells at the

bottom of the bioreactor are not removed via the effluent pipe as it is not located at the absolute bottom of the bioreactor, thus selecting for fast sedimenting yeast and reducing the number of generations per cycle (**240**).

Note 14. After re-filling of the bioreactor is initiated, we recommend to sparge the broth with high-purity nitrogen (N6) to rapidly 'strip' any remaining oxygen in the medium. After filling is completed, we redirect nitrogen supply through the headspace to minimise transfer of traces of oxygen in the nitrogen gas into the liquid phase (see text and **Figure 2.3**).

Note 15. When sugar is the first nutrient to be depleted, this usually coincides with a sharp decline of the CO_2 concentration in the exhaust gas. Continuous monitoring of the CO_2 concentration in the exhaust gas is then a useful trigger mechanism for initiating a new batch. If another nutrient becomes limiting first, this may not lead to an immediate decrease of the CO_2 output, and other trigger mechanisms must be employed.

Note 16. The control loop connected to the level sensor and pump operates in opposite modes in chemostat or sequential batch reactor experiment. In chemostats, contact of the broth with the level sensor is used as a signal to start the effluent pump and thereby keep the volume of the broth constant over time. In contrast, during sequential batch reactor experiments, pumping of fresh medium is terminated upon contact when the desired working volume is reached.

Note 17. Achieving a steady state is an asymptotic process, during which adjustments to the culture introduce undesired dynamics. Adjustments of the cultivation conditions should therefore be performed directly after the batch phase or early on in the chemostat experiment. Steady state is assumed when at least 5 volume changes have occurred after the last change in growth conditions and, moreover, the biomass concentration, the concentration of the growth limiting nutrient and important biomass-specific production and consumption rates differ by less than a predefined margin (e.g. 1, 2 or 5 %, depending on the experimental goals) for a further two consecutive volume changes.

Acknowledgdements

We thank our colleagues at the Industrial Microbiology sectionfor support and stimulating discussions.

Data availability

Supplementary information can be accessed via the online version:
https://doi.org/10.1093/femsyr/foab035

Significance statement

Biosynthesis of sterols requires oxygen. This study identifies a previously unknown evolutionary adaptation in a eukaryote, which enables anaerobic growth in absence of exogenous sterols. A squalene-hopene cyclase, proposed to have been acquired by horizontal gene transfer from an acetic acid bacterium, is implicated in a unique ability of the yeast *Schizosaccharomyces japonicus* to synthesise hopanoids and grow in anaerobic, sterol-free media. Expression of this cyclase in *S. cerevisiae* confirmed that at least one of its hopanoid products acts as sterol surrogate. These observations provide new leads for research into the structure and function of eukaryotic membranes, and into the development of sterol-independent yeast cell factories for application in anaerobic processes.

Check this movie for a simplified summary of the article

Chapter 3.

A squalene-hopene cyclase in *Schizosaccharomyces japonicus* represents a eukaryotic adaptation to sterol-limited anaerobic environments

Jonna Bouwknegt*
Sanne J. Wiersma*
Raúl A. Ortiz-Merino
Eline S. R. Doornenbal
Petrik Buitenhuis
Martin Giera
Christoph Müller
Jack T. Pronk

* Authors have contributed equally to this work

This chapter has been published in Proceedings of the National Academy of Sciences

Abstract

Biosynthesis of sterols, which are key constituents of canonical eukaryotic membranes, requires molecular oxygen. Anaerobic protists and deep-branching anaerobic fungi are the only eukaryotes in which a mechanism for sterol-independent growth has been elucidated. In these organisms, tetrahymanol, formed through oxygen-independent cyclisation of squalene by a squalene-tetrahymanol cyclase, acts as a sterol surrogate. This study confirms an early report (Bulder (1971), Antonie Van Leeuwenhoek, 37, 353–358) that *Schizosaccharomyces japonicus* is exceptional among yeasts in growing anaerobically on synthetic media lacking sterols and unsaturated fatty acids. Mass spectrometry of lipid fractions of anaerobically grown *Sch. japonicus* showed the presence of hopanoids, a class of cyclic triterpenoids not previously detected in yeasts, including hop-22(29)-ene, hop-17(21)-ene, hop-21(22)-ene and hopan-22-ol. A putative gene in *Sch. japonicus* showed high similarity to bacterial squalene-hopene cyclase (SHC) genes and in particular to those of *Acetobacter* species. No orthologs of the putative *Sch. japonicus* SHC were found in other yeast species. Expression of the *Sch. japonicus* SHC gene (*Sjshc1*) in *Saccharomyces cerevisiae* enabled hopanoid synthesis and stimulated anaerobic growth in sterol-free media, thus indicating that one or more of the hopanoids produced by SjShc1 could at least partially replace sterols. Use of hopanoids as sterol surrogates represents a previously unknown adaptation of eukaryotic cells to anaerobic growth. The fast anaerobic growth of *Sch. japonicus* in sterol-free media is an interesting trait for developing robust fungal cell factories for application in anaerobic industrial processes.

Introduction

Sterols are key constituents of canonical eukaryotic membranes, in which they influence integrity, permeability and fluidity (**95**,**251**). The core pathway for sterol biosynthesis is highly conserved but the predominant final products differ for animals (cholesterol), plants (phytosterols) and fungi (ergosterol; **96**). Multiple reactions in sterol biosynthesis require molecular oxygen and no evidence for anaerobic sterol pathways has been found in living organisms or in the geological record (**96**). The first oxygen-dependent conversion in sterol synthesis is the epoxidation of squalene to oxidosqualene by squalene monooxygenase. Oxidosqualene is subsequently cyclised to lanosterol, the first tetracyclic intermediate in sterol biosynthesis, in an oxygen-independent conversion catalysed by oxidosqualene cyclase (OSC; SI Appendix, Figure S1). Molecular oxygen is also required for multiple subsequent demethylation and desaturation steps (**190**). In fungi, synthesis of a single molecule of ergosterol from squalene requires 12 molecules of oxygen.

Deep-branching fungi belonging to the Neocallimastigomycota phylum are the only eukaryotes that have been unequivocally demonstrated to naturally exhibit sterol-independent growth under strictly anaerobic conditions. These anaerobic fungi contain a squalene-tetrahymanol cyclase (STC; SI Appendix, Figure S1), which catalyses oxygen-independent cyclisation of squalene to tetrahymanol (**252**,**253**). This pentacyclic triterpenoid acts as a sterol surrogate, and acquisition of a bacterial STC gene by horizontal gene transfer is considered a key evolutionary adaptation of Neocalllimastigomycetes to the strictly anaerobic conditions of the gut of large herbivores (**254**). The reaction catalysed by STC resembles oxygen-independent conversion of squalene to hopanol and/or other hopanoids by squalene-hopene cyclases (SHC; SI Appendix, Figure S1; **109**), which are found in many bacteria (**255**,**256**). Some bacteria synthesise tetrahymanol by ring expansion of hopanol, in a reaction catalysed by tetrahymanol synthase (THS) for which the precise mechanism has not yet been resolved (**106**).

Already in the 1950s, anaerobic growth of the industrial yeast and model eukaryote *Saccharomyces cerevisiae* was shown to strictly depend on sterol supplementation (**62**) or use of intracellular stores of this anaerobic growth factor (**63**). Similarly, fast anaerobic growth of *S. cerevisiae*, which is a key factor in its large-scale application in bioethanol production, wine fermentation and brewing (**53**,**194**), requires availability of unsaturated fatty acids (UFAs). Biosynthesis of UFAs by yeasts requires an oxygen-dependent acyl-CoA desaturase (**181**) and, in anaerobic laboratory studies, the sorbitan oleate ester Tween 80 is commonly used as UFA supplement (**63**,**189**).

Per gram of yeast biomass, ergosterol and UFA synthesis require only small amounts of oxygen. Studies on these oxygen requirements therefore require extensive measures to prevent unintended oxygen entry into cultures. Even though most yeast species readily ferment sugars to ethanol under oxygen-limited conditions, only very few grow anaerobically on sterol- and UFA-supplemented media when such precautions are taken (**31**,**257**). As opposed to Neocallimastigomycetes, no evolutionary adaptations to sterol-independent anaerobic growth have hitherto been reported for yeasts, or for ascomycete and

basidiomycete fungi in general.

We recently demonstrated that expression of an STC gene from the ciliate *Tetrahymena thermophila* supported tetrahymanol synthesis and sterol-independent growth of *S. cerevisiae* (**184**). This result inspired us to re-examine a 1971 publication in which Bulder (**179**) reported sterol- and UFA-independent growth of the dimorphic fission yeast *Schizosaccharomyces japonicus*. *Sch. japonicus* was originally isolated from fermented fruit juices (**258**,**259**), and its potential for wine fermentation is being explored (**260**,**261**). It shows marked genetic and physiological differences with other fission yeasts (**262**,**263**) and has gained interest as a model for studying cell division dynamics and hyphal growth (**264–266**). *Sch. japonicus* grows well at elevated temperatures and rapidly ferments glucose to ethanol (**267**). A low sterol content, control of membrane fluidity via chain length of saturated fatty acids and respiratory deficiency may all reflect adaptations of *Sch. japonicus* to low-oxygen environments (**179**,**267–269**). However, the report by Bulder (**179**) stating that *Sch. japonicus* can grow anaerobically without sterol supplementation has not been confirmed or further investigated.

S. cerevisiae is able to synthesise sterols at nanomolar concentrations of oxygen (**238**). This high affinity for oxygen complicates experimental analysis of oxygen requirements for sterol synthesis in yeast cultures (**64**,**184**,**218**) and warranted a reassessment of the sterol requirements of *Sch. japonicus*. If confirmed, an ability of *Sch. japonicus* to grow in the absence of an exogenous supply of sterols would raise urgent questions on the molecular and evolutionary basis for this trait, which is extremely rare among eukaryotes. Based on theoretical grounds, it has been proposed that oxygen-independent sterol synthesis may be possible (**270**). Alternatively, sterol-independent growth of *Sch. japonicus* might depend on synthesis of an as yet unidentified sterol surrogate, or on membrane adaptations that involve neither sterols nor sterol surrogates. In addition to these fundamental scientific questions, independence of anaerobic growth factors is a relevant trait for large-scale industrial applications of yeasts, as exemplified by 'stuck' brewing fermentations caused by depletion of intracellular sterols and/or UFA reserves (**271**,**272**).

The goals of the present study were to reinvestigate the reported ability of *Sch. japonicus* to grow anaerobically without sterol supplementation and to elucidate its molecular basis. In view of reported challenges in avoiding oxygen contamination in laboratory cultures of yeasts (**31**,**64**,**184**,**218**), we first reassessed anaerobic growth and lipid composition of *Sch. japonicus* in the presence and absence of ergosterol. After identifying a candidate SHC gene in *Sch. japonicus*, we investigated its role in anaerobic growth by its expression in *S. cerevisiae*. In addition, we tested the hypothesis of Bulder (**186**) that *Sch. japonicus* is able to synthesise UFAs in an oxygen-independent pathway.

Results

Anaerobic growth of *Sch. japonicus* without ergosterol and UFA supplementation

To reassess conclusions from an early literature report on sterol- and UFA-independent anaerobic growth of *Sch. japonicus* (**179**), we performed serial-transfer experiments in an anaerobic chamber (**64**, Chapter 2) using phosphate-buffered synthetic medium with glucose as carbon source (SMPD), with and without supplementation of ergosterol and/or Tween 80 as source of UFAs. Parallel experiments with the *S. cerevisiae* laboratory strain CEN.PK113-7D were included to assess low-level contamination with oxygen, as reflected by residual slow growth in sterol-free media (Chapter 2).

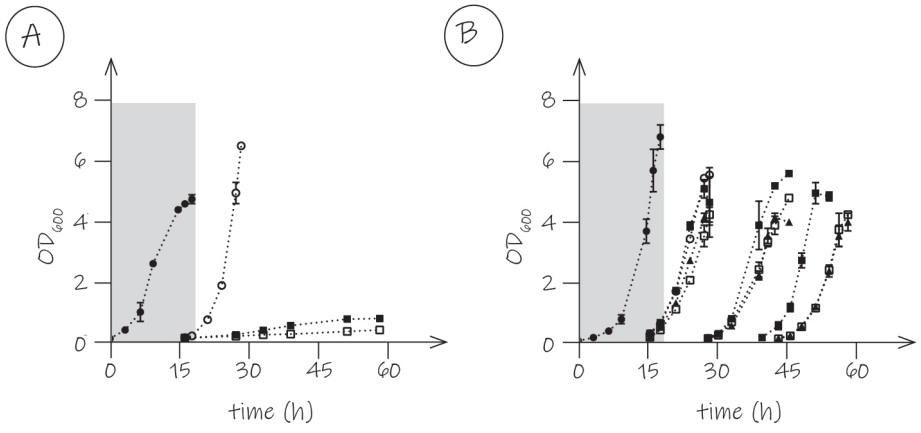

Figure 3.1. Anaerobic growth of *S. cerevisiae* CEN.PK113-7D and *Sch. japonicus* CBS5679 with different ergosterol and UFA (Tween 80) supplementation in a dark anaerobic chamber.

Anaerobic pre-cultures on SMPD on 50 g L^{-1} glucose (closed circles, grey shading) were grown until the end of the exponential phase. A. After the anaerobic pre-culture, *S. cerevisiae* was transferred to SMPD (20 g L^{-1} glucose) supplemented with either Tween 80 and ergosterol (open circles), Tween 80 only (closed squares) or neither Tween 80 nor ergosterol (open squares). B. *Sch. japonicus* was grown on the same media as *S. cerevisiae* and additionally on medium containing ergosterol but not Tween 80 (closed triangles). *Sch. japonicus* cultures supplemented with only Tween 80, only ergosterol, and those without supplements were serially transferred to fresh media with the same composition in the anaerobic chamber. Data are represented as average ± SEM of measurements on independent duplicate cultures for each combination of yeast strain and medium composition.

To deplete reserves of sterols and/or UFAs in aerobically pre-grown cells, anaerobic pre-cultures were grown on SMPD with an increased glucose concentration (50 g L^{-1}), and lacking ergosterol and Tween 80. In these pre-cultures, growth of *S. cerevisiae* CEN.PK113-7D ceased after 4.8 doublings (**Figure 3.1A**), when less than half of the glucose had been consumed (SI Appendix, Table S1). Under the same conditions, *Sch. japonicus* CBS5679 completed 6.1 doublings (**Figure 3.1B**) and, while full glucose depletion was intentionally avoided to prevent excessive flocculation and sporulation, it had consumed almost 90 % of the glucose (SI Appendix, Table S1). Samples from the anaerobic pre-cultures were transferred to SMPD (20 g L^{-1} glucose) supplemented with different combinations of ergosterol and/or Tween 80. Consistent with earlier reports (**64**), *S. cerevisiae* showed extremely slow, non-exponential growth on SMPD without ergosterol (**Figure 3.1A**), which indicated a minor entry of oxygen into the anaerobic chamber. In contrast, *Sch. japonicus* showed maximum specific growth rates of 0.26 to 0.30 h^{-1} and reached optical densities of 4 to 5 in all media tested (**Figure 3.1B**; SI Appendix, Table S2). This anaerobic growth was sustained upon two consecutive transfers in SMPD lacking either Tween 80, ergosterol, or both (**Figure 3.1B**). These results confirmed Bulder's (**179**) conclusion that *Sch. japonicus* can grow anaerobically without sterol and UFA supplementation. Remarkably, *Sch. japonicus* grew slower in aerobic cultures (0.19 h^{-1}; SI Appendix, Figure S2) than in anaerobic cultures grown on the same medium (0.24-0.26 h^{-1}; **Figure 3.1B**; SI Appendix, Table S2).

Absence of ergosterol and UFAs in anaerobically grown *Sch. japonicus*

To further investigate anaerobic growth of *Sch. japonicus* in sterol- and UFA-free media, lipid fractions were isolated from anaerobic cultures and analysed by gas chromatography with flame ionisation detection (GC-FID). UFAs were detected in aerobically grown biomass, but not in anaerobic cultures grown on SMPD without Tween 80 supplementation (**Figure 3.2**; SI Dataset S01). These results showed that fast anaerobic growth of *Sch. japonicus* on UFA-free medium did not, as suggested by Bulder (**186**), reflect oxygen-independent UFA synthesis. Total fatty-acid contents of aerobically and anaerobically grown biomass were similar, but anaerobically grown biomass showed higher contents of FA 10:0, FA 16:0 and FA 18:0 and lower contents of FA 26:0. In aerobically grown *Sch. japonicus* biomass, no FA 16:1 was detected and levels of FA 18:1 were higher than in Tween 80 supplemented anaerobic cultures (**Figure 3.2**).

S. cerevisiae biomass, grown anaerobically on SMPD with Tween 80 and ergosterol, was used as a reference for analysis of triterpenoid compounds. In addition to squalene and ergosterol, lipid samples contained small amounts of lanosterol (**Figure 3.3A**). Lipid samples from extremely slow-growing *S. cerevisiae* cultures on SMPD supplemented with only Tween 80 contained squalene and a small amount of lanosterol, but not ergosterol (SI Dataset S01). Presence of lanosterol was attributed to *de novo* synthesis, enabled by a minor entry of oxygen into the anaerobic chamber.

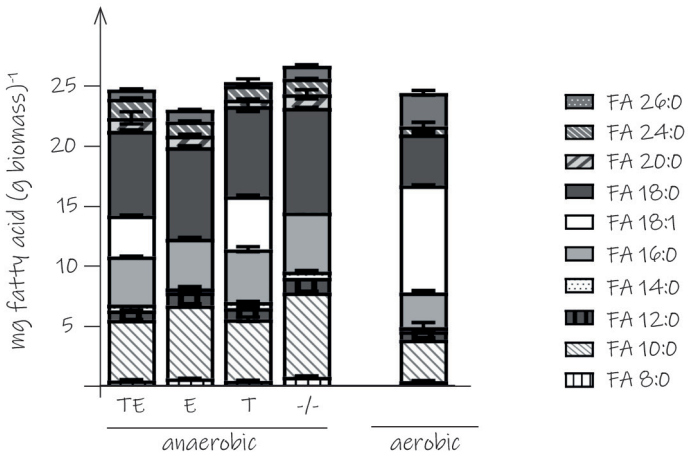

Figure 3.2. Quantification of fatty acids in *Sch. japonicus* CBS5679 biomass.

Sch. japonicus CBS5679 was grown in SMPD with 20 g L^{-1} glucose. Under anaerobic conditions, cultures were supplemented with Tween 80 and ergosterol (TE), only ergosterol (E), only Tween 80 (T) or neither of those supplements (-/-). Data are shown for the first anaerobic culture following the anaerobic pre-culture. Aerobic cultures of *Sch. japonicus* were grown in SMPD without supplements (-/-). Data are represented as average ± SEM of measurements on independent duplicate cultures for each cultivation condition. Detailed information on data presented in this figure and additional anaerobic transfers are provided in SI Dataset S01.

Similarly prepared triterpenoid fractions of anaerobic *Sch. japonicus* cultures that were supplemented with only Tween 80 did not contain detectable amounts of ergosterol or lanosterol. Instead, in addition to squalene, gas chromatography-mass spectrometry (GC-MS) revealed several compounds that were not observed in anaerobically grown *S. cerevisiae* (**Figure 3.3B**). A prominent appearance of the ions m/z 367 and 395 in mass spectra of the detected compounds was consistent with a five membered ring system with loss of either a methyl or a propyl group (**273**). We therefore hypothesised that these compounds had a pentacyclic structure. Tetrahymanol, which has not been found in wild-type yeasts but does occur in several other eukaryotes (**253**,**274**,**275**), did not match any of the detected peaks based on its relative retention time (RRT; with cholestane as reference; **184**).

Sch. japonicus synthesises hopanoids

Hopanoids are triterpenoids with a pentacyclic backbone that occur in bacteria, plants and fungi (**255**), but have not previously been found in yeasts. GC-MS analysis of biomass samples yielded eight

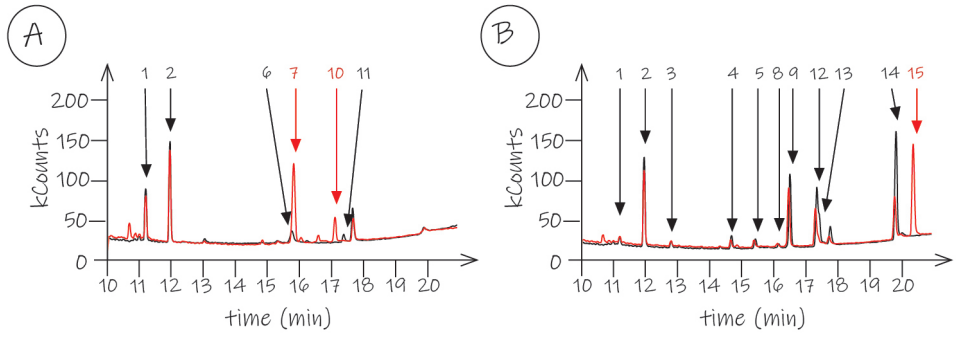

Figure 3.3. Gas chromatography-mass spectrometry (GC-MS) analysis of triterpenoid fractions of anaerobically grown yeast biomass.

Anaerobic cultures were harvested in early stationary phase. Triterpenoids were extracted for GC-MS analysis and injected immediately (black lines) or after silylation (red lines). **A.** *S. cerevisiae* CEN.PK113-7D grown anaerobically on medium supplemented with Tween 80 and ergosterol, **B.** *Sch. japonicus* CBS5679 was grown on medium supplemented with only Tween 80. Numbers indicate the following compounds: 1, squalene; 2, 5α-cholestane (internal standard); 3, squalene epoxide; 4, hop-17(22)-ene; 5, 22-Hydroxy-21aH-hopane; 6, ergosterol; 7, ergosterol-TMS-ether; 8, adian-5-ene; 9, fern-7-ene; 10, lanosterol-TMS-ether; 11, lanosterol; 12, hop-22(29)-ene (diploptene); 13, hop-21(22)-ene; 14, hopan-22-ol (diplopterol); 15, hopan-22-ol-TMS-ether.

distinct analytes that were detected in *Sch. japonicus* (Figure 3.3B) but not in *S. cerevisiae* CEN.PK113-7D (Figure 3.3A). Squalene epoxide (compound 3) was identified based on relative retention time and spectral matching with authentic standard material as previously described (**276**). Presence of squalene epoxide, but not sterols, was attributed to inadvertent entry of small amounts of oxygen into the anaerobic chamber. Hop-22(29)-ene (diploptene; compound 12) was identified based on synthetic reference material (SI Dataset S02). To investigate whether any of the remaining six unidentified components in *Sch. japonicus* (Figure 3.3B) were also hopanoids, their mass spectra (SI Dataset S02) were compared with literature data (SI Appendix Table S3; SI Dataset S02; **106**,**273**,**277**,**278**). A fragment ion with a mass-charge ratio (m/z) of 191, which frequently occurs as base peak in mass spectra of hopanoids (**273**,**277**), was detected for compounds 4, 5, 13 and 14 (SI Dataset S02). Based on comparison with published data, we tentatively identified compounds 4, 13 and 14 as hop-17(21)-ene, hop-21(22)-ene and hopan-22-ol (diplopterol), respectively(106,273,277). Mass and retention-time shifts caused by silylation (**279**) were investigated (Figure 3.3) and confirmed presence of the hydroxy group of diplopterol (Figure 3.3B; 14 and 15) in the *Sch. japonicus* biomass, as well as those of the sterols (Figure 3.3A; 6 and 7, 10 and 11) in the *S. cerevisiae* samples. A small peak at the retention time of unsilylated diplopterol was tentatively attributed to steric hindrance by the tertiary-alcohol context of its hydroxy group. In the chromatograms representing silylated

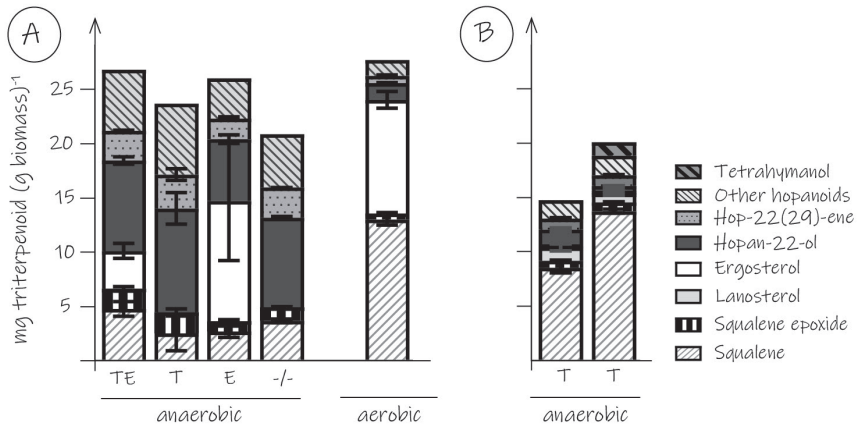

Figure 3.4. Quantification of triterpenoids in yeast biomass.

A. Triterpenoid content of cultures of *Sch. japonicus* CBS5679 grown in SMPD with 20 g L^{-1} glucose. Under anaerobic conditions, cultures were supplemented with Tween 80 and ergosterol (TE), only ergosterol (E), only Tween 80 (T) or neither of these supplements (-/-). Data are shown for the first anaerobic culture following the anaerobic pre-culture. Aerobic cultures of *Sch. japonicus* were grown in SMPD without supplements (-/-). **B.** Triterpenoid composition of anaerobic cultures of *S. cerevisiae* IMX2616 (*sga1*Δ::Sj*shc1*; left) and IMX2629 (*sga1*Δ::Sj*shc1* X-2::Ma*ths*; right) grown in SMPD with 20 g L^{-1} glucose and Tween 80 (T) supplementation. Data are represented as average ± SEM of data from two independent duplicate cultures for each cultivation condition. Detailed information on data presented in this figure and additional anaerobic transfers are provided in SI Dataset S01.

triterpenoids of *S. cerevisiae*, small additional peaks at retention times of 16.0 min and 16.6 min were attributed to ergosta-5,7,22-trien-3β-ol (also detected in the commercial ergosterol preparation used for supplementation of anaerobic growth media; SI Appendix, Figure S3) and fecosterol, an intermediate in ergosterol biosynthesis (**280**), respectively (**Figure 3.3A**).

While the base peak of compound 5 was at m/z 367, the spectrum showed the same characteristic peak of m/z 191 and a molecular ion of m/z 428. Although this observation points towards a hydroxylated structure analogous to diplopterol, compound 5 was not readily silylated. A tentative identification of compound 5 as hydroxy-21aH-hopane is consistent with its almost identical mass spectrum relative to that of diplopterol and its different retention time (**273**). Moreover, its lower signal intensity and different stereochemistry at position 21 could explain its higher resistance to silylation. For compounds 8 and 9, the ion at m/z 410 suggests an unsubstituted triterpene which is unaffected by silylation, with retention times similar to those of other identified hopenes (**Figure 3.3B**; SI Dataset S02). The corresponding base peaks of m/z 259 and 243 were previously reported for polycyclic triterpenoids with a different backbone

configuration than those of substances 4, 12 and 13 (**273**). Although compounds 8 and 9 could not be identified with a high degree of confidence, they may be adian-5-ene and fern-7-ene, respectively. These two pentacyclic triterpenoids only differ from other hopanoids by their stereochemistry and by the position of methyl groups.

The newly identified compounds were quantified by GC-FID analysis in biomass samples of anaerobic *Sch. japonicus* cultures supplemented with different combinations of Tween 80 and ergosterol. Presence of ergosterol in biomass from ergosterol-supplemented anaerobic cultures indicated that *Sch. japonicus* is able to import sterols (**Figure 3.4A**). In anaerobic cultures, the content of diplopterol, the major hopanoid detected in *Sch. japonicus*, was similar to the ergosterol content of sterol-supplemented anaerobic cultures (close to a 1:1 molar ratio; **Figure 3.4A**; SI Dataset S01).

Except for the presence and absence of ergosterol, the triterpenoid composition of anaerobically grown biomass was not markedly affected by the supplementation of ergosterol and/or Tween 80. To investigate whether hopanoid synthesis in *Sch. japonicus* is affected by oxygen availability, additional analyses were performed on aerobically grown cultures. These analyses confirmed the ability of *Sch. japonicus* strain CBS5679 to synthesise ergosterol (**Figure 3.4A**). Aerobically grown biomass showed a 3.5-fold higher squalene content than biomass grown in anaerobic cultures without Tween 80 and ergosterol, while its hopanoid content was 4-fold lower (**Figure 3.4A**; SI Dataset S01). These observations suggest that oxygen availability may regulate triterpenoid synthesis in *Sch. japonicus*.

3

Predicted *Sch. japonicus* proteins resemble bacterial squalene-hopene cyclases

In bacteria, plants and fungi, hopanoid synthesis occurs by cyclisation of squalene by squalene-hopene cyclases (SHC; **278**). To explore whether the *Sch. japonicus* genome encodes an SHC, amino acid sequences of characterised representatives of three related classes of triterpene cyclases were used as queries to search the predicted proteomes of *Sch. japonicus strains* yFS275 (**262**) and CBS5679. Specifically, sequences of an oxidosqualene cyclase (OSC) from *Sch. pombe* (SpErg7; UniProt accession Q10231; **281**), a squalene-hopene cyclase (SHC) from *Acidocaldarius alicyclobacillus* (AaShc; P33247; **282**), and a squalene-tetrahymanol cyclase (STC) from *Tetrahymena thermophila* (TtThc1; Q24FB1; **184**,**252**), were used for a HMMER (**283**) homology search. For each *Sch. japonicus* strain, this search yielded a sequence with significant homology to OSC, and another with significant homology to SHC (**Table 3.1**). Consistent with the lipid analysis results, neither strain yielded a clear STC homolog.

To explore the phylogeny of the *Sch. japonicus* OSC and SHC homologs, SpErg7, AaSHC, and TtThc1 were used as queries for HMMER searches against all eukaryotic and all bacterial protein sequences in Universal Protein Resource (UniProt) reference proteomes. A set of selected cyclase homologs (SI Dataset S03; see SI Appendix, Table S4 for detailed information) were subjected to multiple sequence alignment and used to generate a maximum-likelihood phylogenetic tree (**Figure 3.5**; SI Dataset S04). This

Table 3.1. Homology search results using amino acid sequences of characterised triterpenoid cyclases against *Sch. japonicus* proteomes.

Query coverage percentage and E-values were obtained with HMMER3 (**283**), identity percentages were calculated with Clustal (**284**).

Query	Accession of subject sequence	Query coverage (%)	E-value	Identity (%)
Subject proteome: *Sch. japonicus* yFS275				
SpErg7[a] (Q10231)	B6JW54	99.7	0.0	65.9
AaShc[b] (P33247)	B6K412	99.2	2.7×10^{-141}	38.1
Subject proteome: *Sch. japonicus* CBS5679				
SpErg7a (Q10231)	SCHJC_A005630 (SjErg7)	99.7	0.0	65.7
AaShcb (P33247)	SCHJC_C003990 (SjShc1)	98.9	2.5×10^{-139}	37.8

[a]Protein sequence of Erg7 of *Schizosaccharomyces pombe*

[b]Protein sequence of Shc of *Acidocaldarius alicyclobacillus*

phylogenetic analysis showed that the putative *Sch. japonicus* SHC sequences (SCHJC_C003990 from CBS5679, and B6K412 from yFS275) are related to bacterial SHCs, with sequences from *Acetobacter* spp. (A0A0D6N754 from *Acetobacter indonesiensis* 5H-1, and A0A0D6NG57 from *Acetobacter orientalis* 21F-2) as closest relatives (**Figure 3.5**). To check if this conclusion was biased by the selection of sequences from species of interest, the putative SHC sequence SCHJC_C003990 from *Sch. japonicus* CBS5679 was used as query for a second HMMER search of either the eukaryotic or the bacterial databases described above. The resulting E-values distribution (**Figure 3.5A**; SI Dataset S05) showed a strong overrepresentation of low E-values among bacterial sequences. Sequences of two *Acetobacter* species, A0A0D6NG57 from *A. orientalis* 21F-2 and A0A0D6N754 from *A. indonesiensis* 5H-1, showed 67.9 % and 66.9 % sequence identity, respectively, and yielded zero E-values in this search. In contrast, E-value distributions obtained with the putative OSC sequence SCHJC_A005630 from *Sch. japonicus* CBS5679 as query showed an overrepresentation of low E-values among eukaryotic sequences (**Figure 3.5B**). Horizontal gene transfer from *Acetobacter* species which, like other members of the order Rhodospirillales, are well known to synthesise hopanoids (**256**,**285**), is therefore a highly probable origin of SHC in *Sch. japonicus*. No SHC homologs were found in the predicted proteomes of Schizosaccharomycetes other than *Sch. japonicus*, nor in those of 371 Saccharomycotina yeast species included in the eukaryotic UniProt database.

In bacteria, hopanoids can be methylated or decorated with other side chains by enzymes encoded by *hpn* genes (**286**). To explore whether homologs of bacterial hopanoid-modifying enzymes occur in

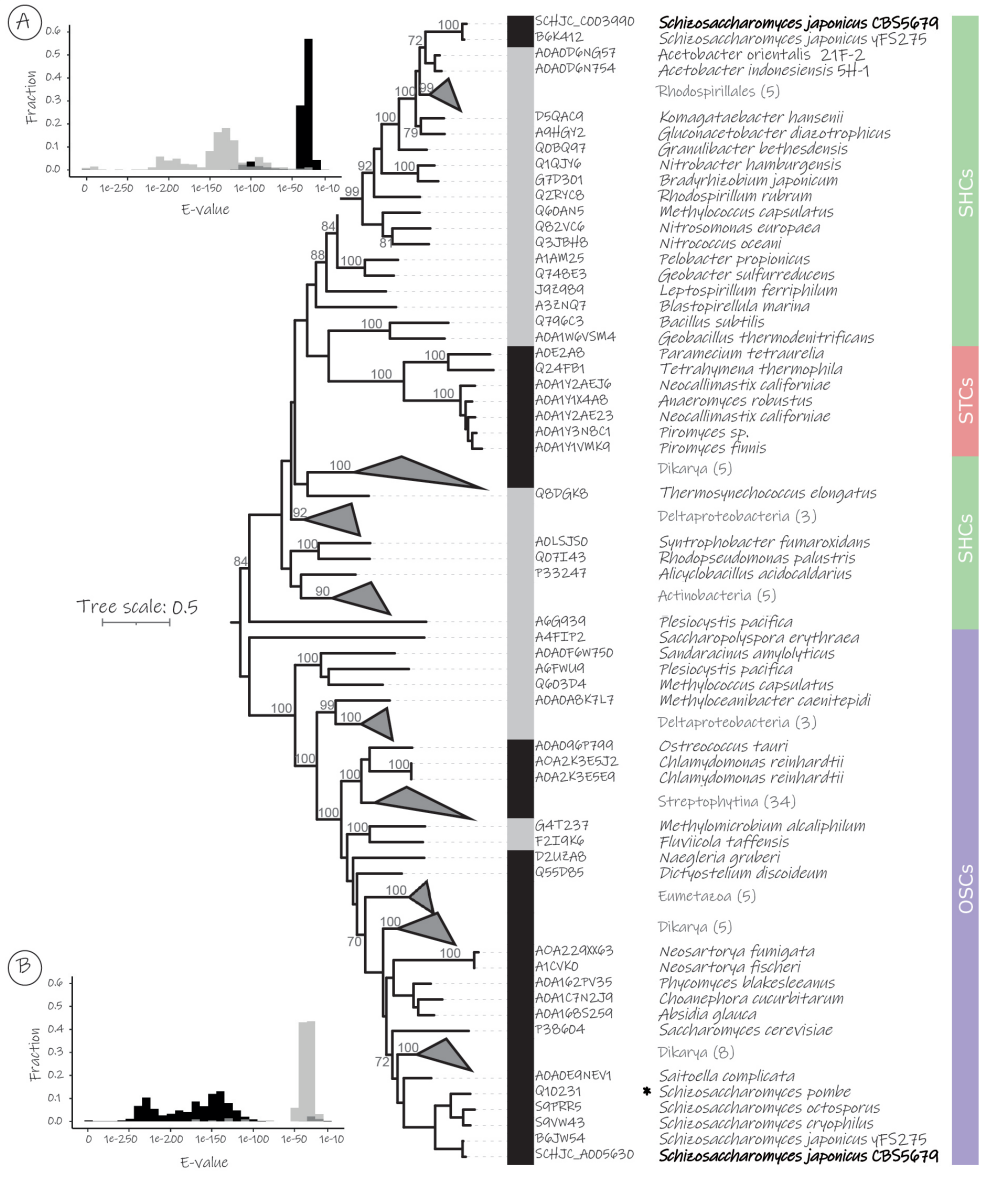

Figure 3.5. Maximum-likelihood phylogenetic tree of selected triterpenoid cyclases.

The coloured bar indicates different types of cyclases: green, squalene hopene cyclases (SHCs); red, squalene tetrahymanol cyclases (STCs); purple, oxidosqualene cyclases (OSCs). Sequences were obtained from a systematic homology search using the characterised cyclases marked with an asterisk (*Acidocaldarius*

alicyclobacillus AaShc, P33247, SHC; *Tetrahymena thermophila*, TtThc1, Q24FB1, STC; *Schizosaccharomyces pombe* SpErg7, Q10231, OSC) as queries. Eukaryotic and bacterial sequences are indicated by black and grey bars, respectively. Clades were collapsed when having three or more members from the same taxonomic division (third level below Bacteria or Eukaryota according to NCBI taxonomy) with the exception of Neocallimastogomycetes and Schizosaccharomycetes. 100 bootstrap replicates were performed, values above 70 are shown on the corresponding branches. All sequences and the final tree are provided in SI Dataset S03 and SI Dataset S04, respectively. The tree was mid-rooted, visualised and made available in iTOL (https://itol.embl.de/tree/8384480491291613138765). **A.** Distribution of HMMER E-values obtained with *Sch. japonicus SHC* (SCHJC_C003990) as query against a bacterial sequence database (grey bars) and a eukaryotic database (black bars). **B.** Distribution of HMMER E-values obtained with *Sch. japonicus* OSC (SCHJC_A005630) as query against a bacterial sequence database (grey bars) and a eukaryotic database (black bars).

Sch. japonicus, a tblastn (**287**) homology search was performed on the genome sequences of strains CBS5679 and yFS275 with amino acid sequences of HpnG, HpnH, HpnI, HpnJ, HpnK, HpnO, HpnP and HpnR from relevant bacterial species, including *A. orientalis* (SI Appendix, Table S5), as queries. Of these queries, only HpnO yielded two significant hits (alignment length of greater than 75% and E-value of lower than 1×10^{-5}). However, a tblastn search of the genome of *S. cerevisiae* CEN.PK113-7D, which does not synthesise hopanoids, with HpnO also yielded two hits. These corresponded to L-ornithine aminotransferase (Car2) and acetylornithine aminotransferase (Arg8) and showed coverages of >99%, and amino acid identities of 60% and 41%, respectively, with the two *Sch. japonicus* sequences. Homology searches therefore did not provide a clear indication for occurrence of known hopanoid-modifying enzymes in *Sch. japonicus*.

Expression of *Sch. japonicus* squalene-hopene cyclase stimulates anaerobic growth of *S. cerevisiae* in the absence of sterol supplementation

To investigate if the putative squalene-hopene-cyclase gene of *Sch. japonicus* CBS5679 (*Sjshc1*) was responsible for hopanoid synthesis, its coding sequence was codon optimised and expressed in the Cas9-expressing *S. cerevisiae* strain IMX2600. Growth and triterpenoid production of the resulting strain IMX2616 (*sga1*Δ::Sj*shc1*; SI Appendix, Table S7) was studied in anaerobic shake-flask cultures. After an anaerobic pre-culture for depletion of cellular reserves of sterols and/or hopanoids, neither the reference strain *S. cerevisiae* CEN.PK113-7D nor the strain carrying the *Sjshc1* expression cassette grew on SMPD without ergosterol and Tween 80 (**Figure 3.6**). On SMPD with only Tween 80, *S. cerevisiae* CEN.PK113-7D reached an optical density of 0.7 after 33 h (**Figure 3.6A**), at which point approximately 70 % of the initially present glucose remained unused (SI Appendix; Table S6). In contrast, *S. cerevisiae* IMX2616 (*sga1*Δ::Sj*shc1*) reached an optical density of 2.1 after the same time period (**Figure 3.6B**), at which point

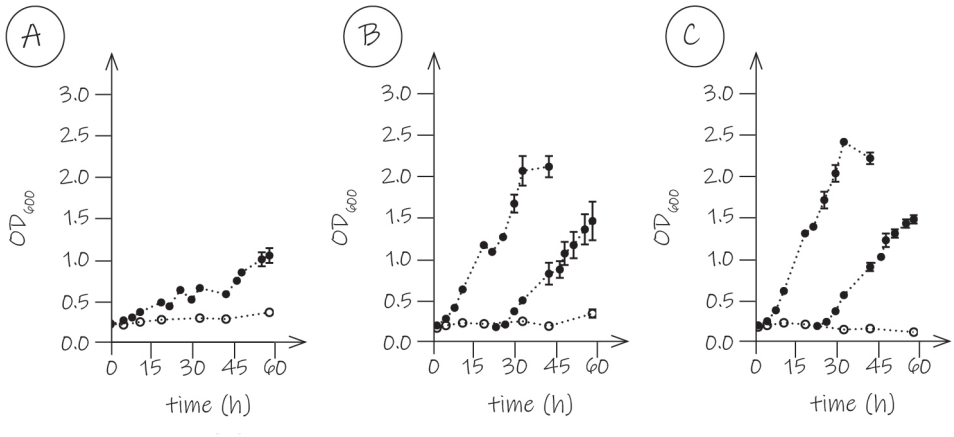

Figure 3.6. Anaerobic growth of *S. cerevisiae* strains in sterol-free media.

S. cerevisiae cultures were inoculated from an anaerobic pre-culture on SMPD (50 g L^{-1} glucose) to fresh SMPD (20 g L^{-1} glucose), either supplemented with Tween 80 (closed circles), or lacking unsaturated fatty acids and sterols (open circles). **A.** Reference strain CEN.PK113-7D. **B.** *S. cerevisiae* strain IMX2616 (*sga1*Δ::*Sjshc1*). **C.** *S. cerevisiae* strain IMX2629 (*sga1*Δ::*Sjshc1 X-2*::*Maths*). Cultures supplemented with Tween 80 represented in panel (**B**) and (**C**) were transferred to fresh medium of the same composition (closed circles) during exponential phase. Data are represented as average ± SEM of measurements on independent duplicate cultures for each yeast strain.

98 % of the initially added glucose had been consumed (SI Appendix; Table S6), and showed sustained anaerobic growth upon transfer to a second flask containing the same medium (**Figure 3.6B**). Upon termination of the experiments after 58 h, the optical density at 600 nm (OD_{600}) of the *S. cerevisiae* CEN.PK113-7D cultures had increased to 1.1.

To investigate whether *S. cerevisiae* IMX2616 (*sga1*Δ::*Sjshc1*) produced the same hopanoid compounds as *Sch. japonicus* CBS5679, biomass was harvested from anaerobic shake-flask cultures grown on SMDP with Tween 80. Analysis of the triterpenoid fraction by GC-MS and GC-FID showed the same hopanoids that were detected and identified in *Sch. japonicus* strain CBS5679 (SI Appendix; Figure S4), albeit in smaller amounts, while squalene contents were higher in the *S. cerevisiae* cultures (**Figure 3.5B**; SI Dataset S01). The only sterol identified in these samples was lanosterol (**Figure 3.5B**). Presence of this first tetracyclic intermediate of ergosterol biosynthesis and very slow, non-exponential growth of the reference strain *S. cerevisiae* CEN.PK113-7D in sterol-free medium (**Figure 3.6**), were attributed to a minor entry of oxygen into the anaerobic chamber (**184**).

In some bacteria, SHC is involved in a pathway for tetrahymanol production, in which a tetrahymanol

synthase converts hopene into tetrahymanol (**106**). To investigate whether such a two-step pathway for tetrahymanol synthesis can be engineered in *S. cerevisiae*, a codon-optimised expression cassette for the *Methylomicrobium alcaliphilum* (**106**) gene encoding THS (locus tag MEALZ_1626; referred to as *Maths*) was integrated at the X-2 locus (**288**) in strain IMX2616 (*sga1*Δ::Sj*shc1*), yielding strain IMX2629 (*sga1*Δ::Sj*shc1 X-2::Maths*; SI Appendix, Table S7). Anaerobic growth and sugar consumption rates of these two *S. cerevisiae* strains were similar (**Figures 3.6B** and **3.6C**; SI Appendix, Table S6). Tetrahymanol was detected in anaerobically grown biomass of strain IMX2629, but not of strain IMX2616 (**Figure 3.5C**; SI Appendix, Figure S5). Together, these results confirm that Sj*shc1* encodes a bona fide SHC, at least one of whose hopanoid products can act as sterol surrogate in anaerobic yeast cultures.

Discussion

The notion that sterols are indispensable components of all eukaryotic membranes was first dispelled by research on ciliates of the genus *Tetrahymena*, in which tetrahymanol acts as a sterol surrogate (**274**,**289**). Subsequent research showed that fungi belonging to the phylum Neocallimastigomycota linked their ability to maintain membrane integrity in the absence of oxygen or exogenous sterols to tetrahymanol synthesis (**253**,**275**). Acquisition of a bacterial STC-encoding DNA sequence has been proposed as a key event in their adaptation to an anaerobic lifestyle (**254**,**290**). Inspired by a half-century old, intriguing publication by Bulder (**179**) on the yeast *Sch. japonicus*, the present study uncovered hopanoid production as a similar, but different eukaryotic adaptation to minimise or eliminate oxygen requirements for sterol biosynthesis. Because efficient procedures for genetic modification of *Sch. japonicus* CBS5679 are not yet available (**291**), the role of one or more hopanoids as sterol surrogates was confirmed by expression in a heterologous host. Expression of *Sjshc1* in *S. cerevisiae* stimulated its anaerobic growth in the absence of ergosterol supplementation (**Figure 3.6**) and illustrated how the mere acquisition of an SHC gene by horizontal gene transfer may have benefited an ancestor of *Sch. japonicus* in severely oxygen-limited or anaerobic environments.

SHC enzymes and hopanoid synthesis have been found in ferns (**292**,**293**) and putative SHC proteins have been identified in several filamentous fungi (**Figure 3.5;** **294**,**295**). Although *Sch. japonicus* is therefore not unique among eukaryotes in containing an SHC, hopanoid synthesis has not previously been found in yeasts or associated with sterol-independent anaerobic growth of eukaryotes. Putative SHC genes were neither found in other *Schizosaccharomyces* species nor in more distantly related yeasts. Confinement to a single yeast species and a strong sequence similarity with putative SHC sequences from *Acetobacter* species identifies horizontal gene transfer as a highly plausible evolutionary origin of Sj*shc1* (**294**). Independent acquisition of SHC and STC genes by phylogenetically distant eukaryotes represents a

remarkable case of convergent evolution towards an anaerobic eukaryotic lifestyle.

The hopanoids identified in anaerobically grown *Sch. japonicus* CBS5679 (**Figure 3.3**; SI Appendix, Table S3) were also detected in an *Sjshc1*-expressing *S. cerevisiae* strain (**Figure 3.5**; SI Appendix, Figure S4). These results indicate that the observed product diversity originated from the Sj*Shc1* enzyme itself, rather than from additional enzyme-catalysed modifications. Formation of multiple products is consistent with reports on triterpenoid extracts of bacterial hopanoid producers and product spectra of purified bacterial SHCs (**296–298**). For example, in addition to diploptene and diplopterol, analysis of triterpenoids in *Zymomonas mobilis* biomass revealed a number of minor hopene variants, whose synthesis was attributed to deviation from the regular cyclisation process (**299**). Alternatively, minor structural variations could represent artefacts of lipid isolation and derivatisation.

In bacteria, hopanoids produced by SHC are often modified to generate side-chain extended hopanepolyols (**286)**. Molecular dynamics simulation of lipid-bilayers showed that sterols and bacteriohopanetetrol (BHT) are correctly oriented in membranes due to their polar moieties, whereas unsubstituted diploptene molecules cannot be properly inserted and instead accumulate horizontally in the hydrophobic core (**300**). In the present study, diplopterol (hopan-22-ol), the major hopanoid detected in *Sch. japonicus*, is therefore the best candidate for a role as membrane-active triterpenoid due to its hydroxyl group. It was previously demonstrated that its potential to influence order and phase-behavior of lipid bilayers resembles that of cholesterol (**301**). While the scan range of the GC-MS analyses (m/z 100-600) would have allowed for identification of methylated or double-hydroxylated hopanoids, our analyses do not exclude presence of more elaborately modified hopanoids in *Sch. japonicus*. Absence of clear homologs of bacterial genes involved in hopanoid modification (**302**,**303**) from the *Sch. japonicus* genome and the high diplopterol content of the lipid fraction of anaerobically grown biomass may, however, argue against this possibility.

The ability, unique among yeasts, of *Sch. japonicus* to grow fast in anaerobic cultures without supplementation of sterols or UFAs is likely to reflect a specialised composition of its membranes. A recent comparison of the membrane properties of *Sch. japonicus* showed remarkable differences with those of the closely related yeast species *Sch. pombe*, including a higher membrane stiffness, denser lipid packing and generally shorter and more saturated fatty acid residues (**269**). In our study, *Sch. japonicus* showed 2- to 3-fold lower squalene contents during anaerobic growth in sterol-free media than in *S. cerevisiae* strains expressing Sj*shc1* (**Figure 3.6**) or a tetrahymanol cyclase gene from *Tetrahymena thermophila* (**184**). High squalene contents have been implicated in suboptimal membrane function of *S. cerevisiae* (**304**) and may therefore at least be partially responsible for the slow anaerobic growth of these engineered *S. cerevisiae* strains (**Figure 3.5**). Cultivation of *Sch. japonicus* in UFA-free medium led to a reduction of the average chain length of saturated fatty acids (SFA; **Figure 3.2**). This change is, however, unlikely to directly affect effectiveness of hopanoids as sterol surrogates since UFA supplementation did not affect anaerobic growth rates of *Sch. japonicus* on sterol-free media (**Figure 3.1**; SI Appendix, Table S2).

Further research should resolve how hopanoids interact with other membrane components, including

squalene, acyl lipids and proteins, and thereby influence membrane functionality of *Sch. japonicus*. In bacteria, hopanoids have been implicated in tolerance to external stresses such as non-optimal temperature and pH, and the presence of antimicrobials (**305**–**307**). Elucidating how sterol surrogates interact with other membrane components, including proteins, and thereby influence membrane functionality can contribute to a deeper insight in microbial adaptation to anaerobic environments and to physicochemical stress factors. In addition, such studies will contribute to the design of membrane engineering strategies aimed at the construction of robust industrial strains of *S. cerevisiae* and other yeasts for application in anaerobic fermentation processes.

Materials and methods

Strains, media and maintenance. *Schizosaccharomyces japonicus* CBS5679 was obtained from the Westerdijk Institute (Utrecht, The Netherlands). *Saccharomyces cerevisiae* strains used and constructed in this study belonged to the CEN.PK lineage (**308**,**309**) and are listed in SI Appendix, Table S7. Yeast strains were stored at -80 °C as described previously (**184**). To avoid sexual co-flocculation (**310**) of *Sch. japonicus* CBS5679, carbon source depletion in pre-cultures was prevented and buffered synthetic media were used in all growth studies. Yeasts were grown on synthetic medium with ammonium as nitrogen source (**126**) with an increased concentration of KH_2PO_4 (14.4 g L^{-1}, SMP; **311**). Unless otherwise indicated, glucose was added from a concentrated stock solution, separately autoclaved at 110 °C, to a concentration of 20 g L^{-1} (SMPD). 800-fold concentrated stock solutions of Tween 80 (polyethylene glycol sorbitan monooleate; Merck, Darmstadt, Germany), ergosterol (≥95 %; Sigma-Aldrich, St. Louis, MO) or a combination of both were prepared with pure ethanol as solvent (**64**). Where indicated, SMPD was supplemented with Tween 80, ergosterol or both from these stock solutions to reach final concentrations of 420 mg L^{-1} and 10 mg L^{-1}, respectively. Bacto agar (BD Biosciences, 20 g L^{-1}) was added to prepare solid media. The counter-selectable amdS-marker was used as described previously (**312**). Strains with geneticin, hygromycin or nourseothricin resistance were selected by supplementing YPD with 200 mg L^{-1} geneticin (G418), 100 mg L^{-1} hygromycin B (hygB) or 100 mg L^{-1} nourseothricin (ClonNAT), respectively.

Molecular biology techniques, plasmid and strain construction. Open-reading frames of a putative squalene-hopene-cyclase gene (SHC; SCHJC_C003990) from *Sch. japonicus* CBS5679 and of a *Methylomicrobium alkaliphilum* tetrahymanol synthase gene (Genbank Accession number CCE23313) were codon-optimised for use in *S. cerevisiae* with the GeneOptimizer algorithm (GeneArt, Regensburg, Germany; **313**). A detailed description of the construction of plasmids pUDE1059 (p*TEF1*-Sj*shc1*-t*CYC1*) and pUDE1060 (p*TDH3*-Ma*ths*-t*ADH1*) is provided in SI Appendix. Plasmids and oligonucleotides are listed in SI Appendix, Tables S8 and S9, respectively. Construction of *S. cerevisiae* strains IMX2616 (*sga1*Δ::Sj*shc1*)

and IMX2629 (*sga1*Δ::*Sjshc1* X-2::*Maths*) is described in detail in SI Appendix. In brief, expression cassettes harboring *Sjshc1* or *Maths* coding sequences were amplified from plasmids pUDE1059 and pUDE1060 and used for Cas9-mediated genomic integration into a Cas9-expressing *S. cerevisiae* platform strain (**59**).

Aerobic shake-flask cultivation. Aerobic cultivation on SMPD was performed in 500-mL shake flasks with a working volume of 100 mL. A pre-culture was inoculated from a frozen stock culture and, after overnight incubation, transferred to a second pre-culture. Upon reaching mid-exponential phase, cells were transferred to fresh SMPD and optical density was monitored at 660 nm. All experiments were performed in duplicate. Light-induced flocculation of *Sch. japonicus* (**314**) was prevented by wrapping flasks in aluminum foil.

Anaerobic shake-flask cultivation. Anaerobic chamber experiments were performed as previously described (**64**), using 100-mL shake flasks containing 80 mL of medium. The anaerobic chamber was placed in a mobile darkroom that was only illuminated with red LEDs (**315**) during sampling. An aerobic pre-culture on SMPD was used to inoculate an anaerobic pre-culture on SMPD with an increased glucose concentration of 50 g L^{-1}, which was grown until the end of the exponential phase. Samples from these pre-cultures were then used to inoculate experiments on regular SMPD supplemented with either Tween 80 and ergosterol, only Tween 80 or ergosterol, or neither. Cultures of *S. cerevisiae* CEN.PK113-7D on SMPD without Tween 80 or ergosterol were included in all anaerobic chamber experiments to assess low-level oxygen contamination (**Chapter 2**). All growth experiments were performed by monitoring optical density at 600 nm in independent duplicate cultures.

Analytical methods. Extracellular metabolite concentrations were analysed by high-performance liquid chromatography (HPLC; **316**). Extraction and quantification of fatty acids, sterols and tetrahymanol by gas-chromatography with flame ionisation detection (GC-FID) was performed as previously described (**64**,**184**). A 6-point calibration of the GC-FID system with hop-22(29)-ene (Sigma Aldrich, 0.1 mg mL^{-1} in isooctane) was used for quantification of hop-22(29)-ene and other detected hopanoid compounds. Detailed methods for detection and identification of hopanoid compounds by gas-chromatography mass-spectrometry (GC-MS) are described in SI Appendix. Optical density was measured at 600 nm for anaerobic cultures with an Ultrospec 10 cell density meter (Biochrom, Harvard Biosience, Holliston, MA) placed in the anaerobic chamber. For aerobic cultures, optical density at 660 nm was measured on a Jenway 7200 spectrophotometer (Bibby Scientific, Staffordshire, UK).

Genome sequencing and assembly. The genome of *Sch. japonicus* CBS5679 was sequenced using short-read and long-read sequencing technologies. Genomic DNA was isolated with a Qiagen genomic DNA 100/G kit (Qiagen, Hilden, Germany), with minor modifications to the manufacturer's instructions. Detailed information on DNA isolation and library preparation is provided in SI Appendix. Short-read whole-genome sequencing was performed on a MiSeq platform (Illumina). Long-read sequencing was performed using the MinION platform (Oxford Nanopore Technologies). Base-calling was performed using Guppy v2.1.3 (Oxford Nanopore Technologies) using dna_r9.4.1_450bps_flipflop.cfg. Genome assembly was performed using Flye v2.7.1-b167359(317). Flye contigs were polished using Pilon v1.18 (**318**).

The polished assembly was annotated with Funannotate v1.7.1 (**319**) using RNAseq data from bioprojects PRJNA53947 and PRJEB30918 as evidence of transcription, adding functional information with Interproscan v5.25-64.0 (**320**).

Sequence homology search and phylogenetic analyses. Eukaryotic and bacterial amino acid sequence databases were built from UniProtKB reference proteomes (Release 2019_02) using the taxonomic divisions (taxids) shared with databases from the National Center for Biotechnology Information (NCBI). Only amino acid sequences from reference or representative organisms having genome assemblies at chromosome or scaffold level according to the NCBI genomes database (Release 2019_03) were included. Amino acid sequences of an oxidosqualene cyclase (OSC) from *Sch. pombe* (SpErg7; UniProt accession Q10231; **281**), a squalene-hopene cyclase (SHC) from *Acidocaldarius alicyclobacillus* (AaShc; P33247; **282**), and a squalene-tetrahymanol cyclase (STC) from *Tetrahymena thermophila* (TtThc1; Q24FB1; **184**,**252**) were used as queries for a HMMER3 (**283**) homology search. HMMER hits with an E-value below 1×10^{-5} and a total alignment length (query coverage) exceeding 75 % of the query sequence were considered significant. A total number of 128 selected sequences (see SI Appendix, Table S4 and SI Dataset S06 for detailed information) were subjected to multiple sequence alignment using MAFFT v7.402 (**321**) in "einsi" mode. Alignments were trimmed using trimAl v1.2 (**322**) in "gappyout" mode, and used to build a phylogenetic tree with RAxML-NG v0.8.1 (**323**) using 10 random and 10 parsimony starting trees, 100 Felsestein Bootstrap replicates, and PROTGTR+FO model. The final, midr-ooted tree provided in SI Dataset S04 was visualized using iTOL (**324**).

Data availability

Whole-genome sequencing data for *Sch. japonicus* CBS5679 have been deposited under the BioProject accession PRJNA698797 in NCBI.

Supplementary information can be accessed via the online version: https://doi.org/10.1101/2021.03.17.435848

Acknowledgements

This work was funded by an Advanced Grant of the European Research Council to JTP (grant 694633). We gratefully acknowledge Jasmijn Hassing for constructing strain IMX2600, and Nicolò Baldi for the construction of plasmid pUDR538. We thank our colleagues in the Industrial Microbiology group of Delft University of Technology for stimulating discussions.

Chapter 4.

Class-II dihydroorotate dehydrogenases from three phylogenetically distant fungi support anaerobic pyrimidine biosynthesis

Jonna Bouwknegt
Charlotte C. Koster
Aurin M. Vos
Raúl A. Ortiz-Merino
Mats Wassink
Marijke A.H. Luttik
Marcel van den Broek
Peter L. Hagedoorn
Jack T. Pronk

A revised version of this chapter was published in Fungal Biology and Biotechnology

Abstract

Background. In most fungi, quinone-dependent Class-II dihydroorotate dehydrogenases (DHODs) are essential for pyrimidine biosynthesis. Coupling of these Class-II DHODHs to mitochondrial respiration makes their *in vivo* activity dependent on oxygen availability. *Saccharomyces cerevisiae* and closely related yeast species harbour a cytosolic Class-I DHOD (Ura1) that uses fumarate as electron acceptor and thereby enables anaerobic pyrimidine synthesis. Here, we investigate DHODs from three fungi (the Neocallimastigomycete *Anaeromyces robustus* and the yeasts *Schizosaccharomyces japonicus* and *Dekkera bruxellensis*) that can grow anaerobically but, based on genome analysis, only harbour a Class-II DHOD.

Results. Heterologous expression of putative Class-II DHOD-encoding genes from fungi capable of anaerobic, pyrimidine-prototrophic growth (Ar*ura9*, Sj*URA9*, Db*URA9*) in an *S. cerevisiae ura1*Δ strain supported aerobic as well as anaerobic pyrimidine prototrophy. GFP-tagged SjUra9 and DbUra9 were localised to *S. cerevisiae* mitochondria, while ArUra9, whose sequence lacked a mitochondrial targeting sequence, was localised to the yeast cytosol. Experiments with cell extracts showed that ArUra9 used free FAD and FMN as electron acceptors. A strain expressing Db*URA9* initially grew slowly without pyrimidine supplementation. Adapted faster growing Db*URA9*-expressing strains showed mutations in *FUM1*, which encodes fumarase. Expression of Sj*URA9* in *S. cerevisiae* reproducibly led to loss of respiratory competence and mitochondrial DNA, which coincided with the natural respiratory deficiency of *Sch. japonicus*. A cysteine residue (C265 in SjUra9), which is found in the active sites of all three anaerobically active Ura9 orthologs, was shown to be essential for anaerobic activity of SjUra9 but not of ArUra9.

Conclusions. Activity of fungal Class-II DHODs was long thought to be dependent on an active respiratory chain, which in most fungi requires the presence of oxygen. By heterologous expression experiments in *S. cerevisiae*, this study shows that phylogenetically distant fungi independently evolved Class-II dihydroorotate dehydrogenases that enable anaerobic pyrimidine biosynthesis. Further structure-function studies are required to understand the mechanistic basis for the anaerobic activity of Class-II DHODs and an observed loss of respiratory competence in *S. cerevisiae* strains expressing an anaerobically active DHOD from *Sch. japonicus*.

Background

Oxidation of dihydroorotate to orotate, an essential reaction for pyrimidine biosynthesis in all domains of life, is catalysed by the flavoprotein dihydroorotate dehydrogenase (DHOD) (**162**,**163**). Depending on the type of DHOD, different electron acceptors are used for re-oxidation of the flavin cofactor. Soluble Class-I DHODs include homodimeric fumarate-dependent type I-A enzymes and heterotetrameric NAD^+-dependent type I-B enzymes (**166**,**324**), while membrane-bound Class-II DHODs are quinone-dependent and coupled to respiration (**160**). Protein sequence identity between Class-I and Class-II DHODs is only approximately 20 % (**164**,**171**,**325**).

Class I-A and Class-II DHODs contain a single FMN cofactor per subunit. In heterotetrameric Class I-B enzymes, two subunits also each contain an FMN cofactor, while the other two both contain an FAD cofactor and an [2Fe-2S] cluster (**166**). Class-I DHODs contain an active-site cysteine residue involved in deprotonation of C5 of dihydroorotate, while Class-II enzymes have a serine in the same position acting as the catalytic base (**326–330**).

Most eukaryotes harbour a monomeric Class-II DHOD that donates electrons to the quinone pool of the mitochondrial respiratory chain (**165**,**169–171**). Bacterial Class-II DHODs have an N-terminal sequence that localises them to the inside of the cytoplasmic membrane, whereas eukaryotic enzymes are targeted to the outside of the mitochondrial inner membrane (**160**). This mitochondrial targeting also applies to fungal Class-II DHODs, which include the Ura9 orthologs of yeasts such as *Lachancea kluyveri* and *Schizosaccharomyces pombe* (**176**). Since respiration in yeasts requires oxygen as electron acceptor, reliance on these respiration-coupled enzymes precludes pyrimidine-prototrophic anaerobic growth (**171**).

Class-I DHODs predominantly occur in gram-positive bacteria and archaea (**331**) but are also found in a small number of yeasts, including *Saccharomyces cerevisiae* and closely related species (**159**,**168**). *S. cerevisiae* is among the few yeast species that are able to grow under strictly anaerobic conditions (**31**). ScUra1, a Class-IA, fumarate-coupled DHOD, enables *S. cerevisiae* to synthesise pyrimidines in the absence of oxygen (**159**,**168**). A small number of other Saccharomycetes, including *Kluyveromyces lactis* and *L. kluyveri*, harbour Ura1 as well as Ura9 orthologs (**159**,**208**,**332**). Based on sequence similarity of yeast Sc*URA1* orthologs with *Lactococcus* genes, they are assumed to have been acquired by horizontal gene transfer (**159**,**169**).

In line with a proposed essentiality of Sc*URA1* orthologs for anaerobic pyrimidine synthesis by yeasts (**159**,**333**), replacement of Sc*URA1* by a Class-II DHOD gene from *L. kluyveri* (Lk*URA9*) or *Sch. pombe* (*SpURA3*) yielded strains that were only pyrimidine prototrophic under aerobic conditions (**159**,**171**). Conversely, replacement of Sc*URA1* by Lk*URA1* supported aerobic as well as anaerobic pyrimidine prototrophy (**159**). Introduction of Sc*URA1* in *URA9*-dependent yeasts was proposed as a metabolic engineering strategy for enabling anaerobic, pyrimidine-prototrophic growth of yeasts lacking a native

Sc*URA1* ortholog (**175**).

The long-held assumption that expression of a Class-I DHOD is required for anaerobic pyrimidine biosynthesis in eukaryotes was first challenged when *Dekkera bruxellensis*, which only harbours a *URA9* ortholog, was shown to grow anaerobically in pyrimidine-free media (**334**). A hypothesis that DbUra9 is able to use a non-quinone electron acceptor (**176,177**) was, however, not experimentally tested.

We recently observed that *D. bruxellensis* may not be the only eukaryote in which anaerobic pyrimidine synthesis involves a Class-II DHOD. Inspection of the genome of the fission yeast *Sch. japonicus*, which shows fast anaerobic growth in synthetic media without uracil (**179**, and see **Chapter 3**), suggested that it only contains a *URA9* ortholog. Moreover, genomes of Neocallimastigomycetes, a group of deep-branching, obligately anaerobic fungi that lack mitochondria and instead harbor hydrogenosomes (**21,45**), also appeared to lack orthologs of soluble Class-I DHOD.

The goals of the present study were to investigate whether *URA9* orthologs in eukaryotes capable of anaerobic growth indeed support anaerobic pyrimidine biosynthesis, and to gain more insight into underlying mechanisms and trade-offs. To this end, we expressed putative Class-II DHOD genes from the obligately anaerobic Neocallimastigomycete *Anaeromyces robustus* (Ar*ura9*), the facultative anaerobes *Sch. japonicus* (Sj*URA9*) and *D. bruxellensis* (Db*URA9*), as well as from the oxygen-requiring yeasts *Ogataea parapolymorpha* (Op*URA9*) and *Kluyveromyces marxianus* (Km*URA9*), in an *S. cerevisiae ura1*Δ background. After studying aerobic and anaerobic growth of the resulting strains in uracil-supplemented and uracil-free synthetic media, we analysed subcellular localisation of Ura9-eGFP fusion proteins in *S. cerevisiae* and assessed the impact of a conserved amino-acid substitution in anaerobically functional Ura9 orthologs. To identify possible natural electron acceptors, we performed enzyme assays in cell extracts of an *S. cerevisiae* strain expressing ArUra9 and re-sequenced the genomes of laboratory-evolved *S. cerevisiae* strains whose anaerobic growth depended on expression of Db*URA9*. We found that instead of quinone, ArUra9 uses free flavins as electron acceptors and that expression of Sj*URA9* in *S. cerevisiae* results in loss of respiration.

Results

Obligately anaerobic Neocallimastigomycetes and facultatively anaerobic yeasts harbour putative Class-II DHODs

A preliminary exploration of the occurrence of Class-I and Class-II DHODs in selected fungal proteomes was based on sequence comparisons with the Class-I and Class-II enzymes of *L. kluyveri* (LkUra1 and

LkUra9, respectively; **159**; Table 4.1). Consistent with earlier studies, the *S. cerevisiae* proteome only showed a sequence with strong similarity to LkUra1 (ScUra1; **159,208,327**). Similarly, proteomes of the yeasts *O. parapolymorpha* and *K. marxianus*, which both require oxygen for growth (**87,102**) yielded previously described Class-II DHOD sequences with strong homology to LkUra9 (OpUra9 and KmUra9, respectively; **69,208**). As previously described, *K. marxianus* also showed a sequence with high sequence similarity to LkUra1 (KmUra1; **332**) while the facultatively anaerobic yeast *D. bruxellensis* only showed a sequence with high similarity to LkUra9 (DbUra9; **176,177,208**). Sequence comparison with LkUra1 provided no indication for the presence of a Class-I DHOD in the obligately anaerobic Neocallimastigomycetes *Piromyces finnis*, *Neocallimastix californiae* and *Anaeromyces robustus*. Instead, single predicted protein sequences with high similarity to the Class-II DHOD LkUra9 were identified in these species (Table 4.1) and tentatively called PfUra9, NcUra9 and ArUra9, respectively. A similar result was obtained for the facultatively anaerobic fission yeast *Sch. japonicus* (**179**, and see Chapter 3), whose putative Class-II DHOD was tentatively named SjUra9 (Table 4.1).

To study the phylogeny of fungal Ura9 orthologs, the amino-acid sequence of LkUra9 was used as query for a sequence analysis using a hidden Markov model method (HMMER; **282**) against all fungal proteomes in Uniprot (**335**), and best hits were used for orthology prediction (see Methods). A similar strategy was performed to obtain all possible bacterial LkUra9 orthologs. The resulting 331 fungal and 73 bacterial Ura9 orthologs were then used to build a phylogenetic tree (Figure 4.1, Additional files 1-3). This phylogenetic analysis revealed that LkUra9 orthologs from obligate anaerobic fungi and from the facultative anaerobic yeasts *Sch. japonicus* and *D. bruxellensis* do not share a common ancestor. Furthermore, bacterial Ura9 orthologs were clearly separated from fungal Ura9 orthologs. These results indicated that, if Ura9 orthologs of Neocallimastigomycetes, *D. bruxellensis* and *Sch. japonicus* have properties that enable anaerobic pyrimidine synthesis, these are likely to have evolved independently, and without involvement of horizontal gene transfer (HGT).

Dependence of anaerobic, pyrimidine-prototrophic growth of phylogenetically distant fungi on a Class-II DHOD ('Ura9') is remarkable in view of the reported coupling of eukaryotic Class-II DHODs to mitochondrial aerobic respiration. The origins of these particular Class-II DHODs differ from the proposed acquisition by HGT of respiration-independent Class-I DHODs by an ancestor of *S. cerevisiae* (**159,168**) and from proposed HGT-driven adaptations of *Sch. japonicus* (**157**, and see Chapter 3) and Neocallimastigomycetes (**158,178**) to anaerobic growth.

Heterologous *URA9* genes complement aerobic pyrimidine auxotrophy of *ura1Δ S. cerevisiae*

To assess and compare functionality of putative Class-II DHOD genes of the Neocallimastigomycete *A. robustus* and of the facultatively anaerobic yeasts *Sch. japonicus* and *D. bruxellensis*, the *ScURA1*

Table 4.1. *Lanchancea kluyveri* LkUra1 and LkUra9 sequence homology results using selected fungal proteomes.

Proteomes of the Neocallimastigomycetes *A. robustus* (NCBI taxid 1754192), *P. finnis* (1754191), *N. californiae* (1754190), and the yeasts *Sch. japonicus* (402676), *D. bruxellensis* (5007), *K. marxianus* (1003335), *O. parapolymorpha* (871575) and *S. cerevisiae* (559292) were subjected to blastp searches using LkUra1 (DHOD Class I-A, UniProt KB accession number Q7Z892) and LkUra9 (DHOD Class II, accession number Q6V3W9) amino acid sequences as queries.

Subject proteome	Resulting GenBank accession	Query coverage (%)		E-value		Identity (%)		Interpretation	
		LkUra1	LkUra9	Ura1	Ura9	LkUra1	LkUra9	Ura1	Ura9
D. bruxellensis	XP_041139490.1	95	90	5·10-17	$4{\cdot}10^{-145}$	24.5	50.9	No	Yes
A. robustus	ORX87218.1	56	77	3·10-9	$2{\cdot}10^{-85}$	27.0	44.6	No	Yes
P. finnis	ORX52621.1	56	77	5·10-9	$7{\cdot}10^{-86}$	24.9	44.9	No	Yes
N. californiae	ORY72481.1	54	74	2·10-8	$5{\cdot}10^{-82}$	27.7	44.9	No	Yes
Sch. japonicus	XP_002171492.1	63	97	2·10-13	$1{\cdot}10^{-113}$	30.6	44.3	No	Yes
S. cerevisiae	NP_012706.1	100	71	0.0	$4{\cdot}10^{-9}$	80.3	23.8	Yes	No
K. marxianus	XP_022674337.1	100	73	0.0	$2{\cdot}10^{-12}$	77.1	25.1	Yes	No
	XP_022675611.1	94	95	$6{\cdot}10^{-11}$	0.0	24.0	73.7	No	Yes
O. parapolymorpha	XP_013936870.1	95	91	$1{\cdot}10^{-9}$	0.0	23.0	63.4	No	Yes

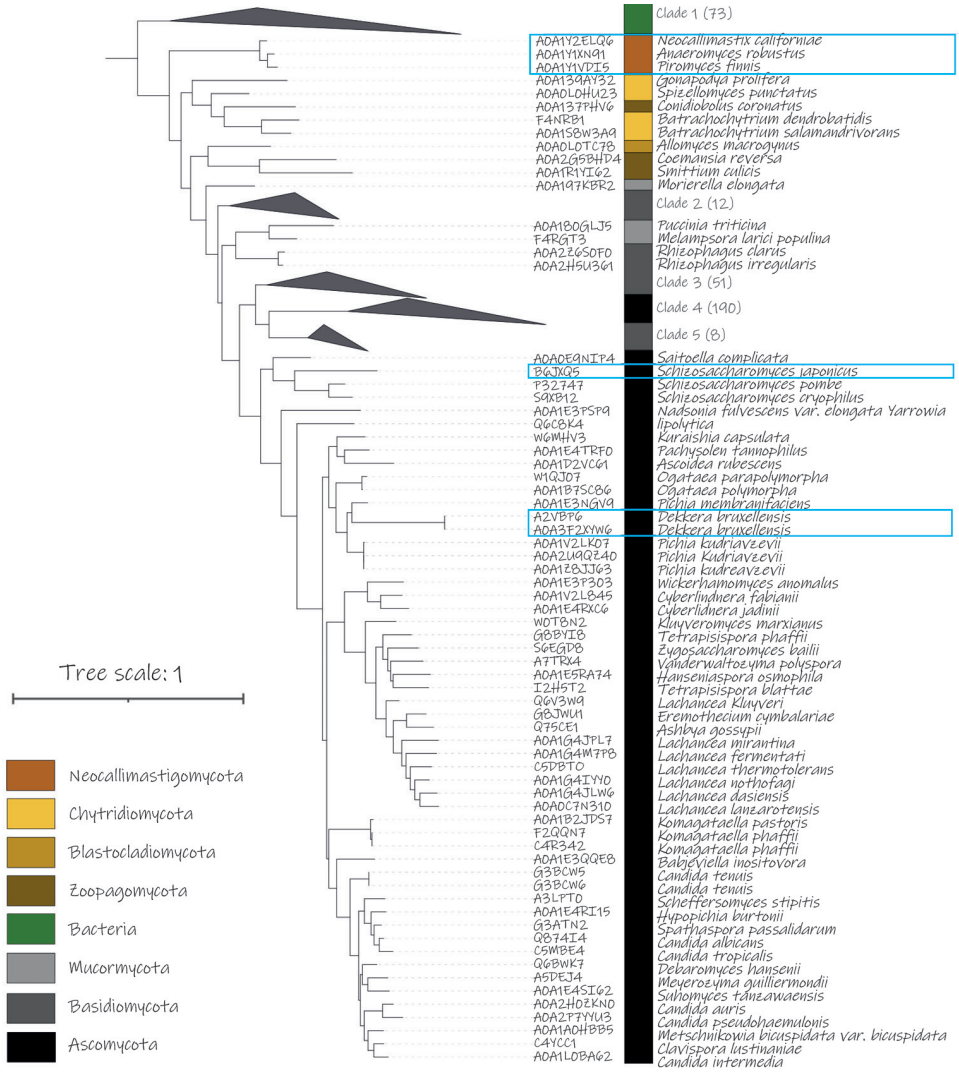

Figure 4.1. Phylogenetic tree of fungal Ura9 orthologs.

An orthology search using *L. kluyveri* Class-II dihydroorotate dehydrogenase (LkUra9; UniProt KB accession number: Q6V3W9) as query yielded 331 fungal and 73 bacterial Ura9 orthologs (Additional file 1). These Ura9 orthologs were used to calculate a maximum-likelihood phylogenetic tree which was rooted using the bacterial clade as outgroup, and for which only bootstrap values above 75 are shown. Blue boxes indicate species capable of pyrimidine-prototrophic anaerobic growth. Numbers of sequences in collapsed clades are indicated and include Bacteria (clade 1), Basidiomycota (clade 2, 3 and 5) and Ascomycota (clade 4). The raw phylogenetic tree in phyml format is provided in Additional file 3, and interactive visualisation is provided in iTOL (https://itol.embl.de/export/193190253145445116327490 60).

open-reading frame of *S. cerevisiae* was replaced by expression cassettes for codon-optimised Ar*ura9*, Sj*URA9* or Db*URA9* coding sequences (Additional file 4). As a reference, Sc*URA1* was replaced by expression cassettes for *URA9* coding sequences of the aerobic yeasts *K. marxianus* and *O. parapolymorpha*. The *S. cerevisiae* reference strain CEN.PK113-7D (*ScURA1*) showed fast aerobic growth (0.36 h^{-1}) on glucose-containing synthetic media with and without uracil (SMUD+ura and SMUD, respectively). As anticipated, the congenic *ura1*Δ strain IMK824 grew on SMUD+ura (0.30 h^{-1}) but not on SMUD (**Figure 4.2**; Additional file 5; Table S1). A lower specific growth rate of strain IMK824 on SMUD+ura than observed for CEN.PK113-7D probably reflected a growth-limiting rate of uracil uptake by uracil-auxotrophic *S. cerevisiae* (**336**).

S. cerevisiae strains in which expression cassettes for Ar*ura9,* Db*URA9,* Km*URA9* or Op*URA9* replaced Sc*URA1*, all grew aerobically on SMUD+ura as well as on SMUD, at specific growth rates (0.34 h^{-1} to 0.35 h^{-1}) that were similar to those of the strain CEN.PK113-7D (Sc*URA1*). An *S. cerevisiae* strain in which Sj*URA9* replaced Sc*URA1* also grew aerobically on SMUD and SMUD+ura but on both media showed an almost two-fold lower specific growth rate (0.19 h^{-1}) than the other strains (**Figure 4.2**; Additional file 5; Table S1).

These results show that ArUra9, SjUra9 and DbUra9 are functional DHODs that, under aerobic conditions, complement a *ura1*Δ mutation in *S. cerevisiae*. Complementation of *S. cerevisiae ura1* null mutants was previously demonstrated for Class-II DHODs of the oxygen-requiring yeasts *L. kluyveri* (LkUra9; **159**) and *Sch. pombe* (SpUra3; **171**).

When expression cassettes for the heterologous *URA9* genes were introduced in an *S. cerevisiae ura1*Δ strain on a multi-copy vector, specific growth rates of the resulting strains on SMUD as well as on SMUD+ura were lower (11-44%) than those of strains carrying a single integrated copy of the expression cassette (Additional file 5; Table S1).

4

Class II-DHODs of *A. robustus*, *D. bruxellensis* and *Sch. japonicus* support anaerobic growth of an *S. cerevisiae ura1Δ* strain

A. robustus, *D. bruxellensis* and *Sch. japonicus* have been reported to grow anaerobically in synthetic media without pyrimidine supplementation (**179**,**334**,**337**). To test whether expression of ArUra9, DbUra9 and SjUra9 supports anaerobic, pyrimidine-prototrophic growth of *S. cerevisiae*, strains in which their structural genes replaced Sc*URA1* were grown anaerobically on SMUD and SMUD+ura.

The reference strain *S. cerevisiae* CEN.PK113-7D, which expresses the native fumarate-dependent Class I-A DHOD ScUra1, grew anaerobically at similar growth rates on SMUD and SMUD+ura (0.24-0.25 h^{-1}), while strain IMK824 (*ura1*Δ) only grew anaerobically (0.26 h^{-1}) on SMUD+ura (**Figure 4.2**, Additional file 5; Table S1). Also strains IMI446 and IMI447, in which Sc*URA1* was replaced by *URA9* genes of the aerobic yeasts *K. marxianus* and *O. parapolymorpha*, did not show anaerobic growth unless media were supplemented with uracil (**Figure 4.2**, Additional file 5; Table S1). These results are in line with the coupling of canonical eukaryotic Class-II DHODs to the quinone pool of the mitochondrial respiratory chain

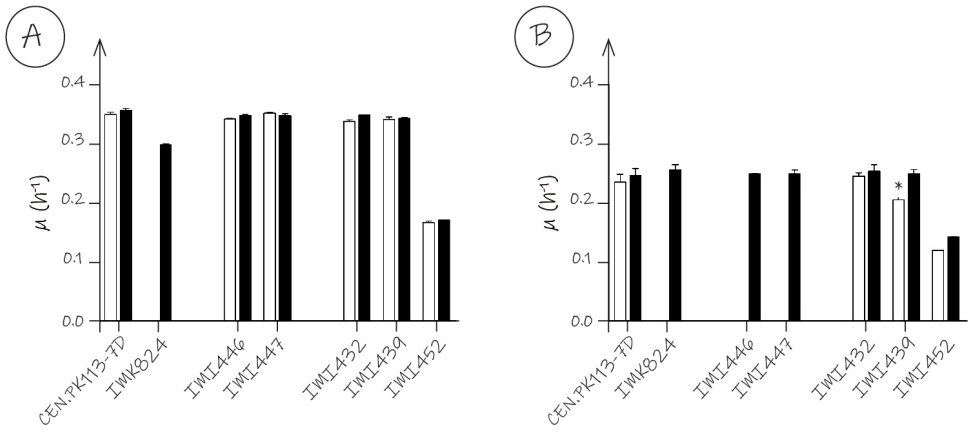

Figure 4.2. Complementation of uracil auxotrophy of *S. cerevisiae ura1*Δ strains by expression of heterologous *URA9* orthologs.

The native Sc*URA1* gene of *S. cerevisiae* was replaced by *URA9* orthologs from *K. marxianus* (Km), *O. parapolymorpha* (Op), *A. robustus* (Ar), *D. bruxellensis* (Db) or *Sch. japonicus* (Sj). **A.** aerobic cultures, **B.** anaerobic cultures. Open bars indicate specific growth rates (μ) on synthetic medium without uracil (SMUD), closed bars indicate μ in uracil-supplemented synthetic medium (SMUD+ura). Relevant genotypes of *S. cerevisiae strains*: CEN.PK113-7D, *ScURA1* reference strain; IMK824, *ura1*Δ reference strain; IMI446, *ura1*Δ::Km*URA9*; IMI447, *ura1*Δ::Op*URA9*; IMI432, *ura1*Δ::Ar*ura9*; IMI439, *ura1*Δ::Db*URA9*; IMI452, *ura1*Δ::Sj*URA9*. *Since strain IMI439 (*ura1*Δ::Db*URA9*) showed delayed growth in initial anaerobic cultures on SMUD, its specific growth rate on SMUD was measured after transfer to a second culture. Data represent the average from biological duplicates and mean deviation (Additional file 5; Table S1).

(**159,160,171,338,339**), and with previous results of Gojković *et al.* (**159**) and Nagy *et al.* (**171**).

In contrast to expression of *URA9* orthologs from aerobic yeasts, expression of Ar*ura9* in *S. cerevisiae* supported fast anaerobic growth (0.25 h^{-1}) without uracil supplementation (**Figure 4.2**, Additional file 5; Table S1). An *S. cerevisiae* strain in which Sc*URA1* was replaced by an Sj*URA9* expression cassette, also showed anaerobic growth on both SMUD and SMUD+ura, but at approximately two-fold lower specific growth rates (**Figure 4.2**, Additional file 5; Table S1). These results demonstrate that ArUra9 and SjUra9 function in *S. cerevisiae* under anaerobic conditions.

Strain IMI439, in which Db*URA9* replaced Sc*URA1*, did not show anaerobic growth on SMUD during the first 30 h of incubation (Additional file 5; Figure S1). After 68 h, when OD_{600} had increased to 2.9, the strain was transferred to fresh SMUD, which resulted in immediate anaerobic growth. In a parallel experiment with strain IMI447, which expressed Km*URA9*, no growth was observed upon transfer to fresh SMUD.

These results indicated that not only the Class-II DHOD from *D. bruxellensis* (**176,177**), but also those from

the Neocallimastigomycete *A. robustus* and from the facultatively anaerobic yeast *Sch. japonicus* support pyrimidine synthesis under anaerobic conditions. The delayed anaerobic growth of an *S. cerevisiae* strain in which Db*URA9* replaced Sc*URA1* suggested that anaerobic functionality of DbUra9 in *S. cerevisiae* may require physiological or genetic adaptations.

A cysteine residue in the active site of SjUra9 is required for activity under anaerobic conditions

In an attempt to identify potential biologically relevant differences in the amino acid sequences of Ura9 orthologs from oxygen-requiring yeast strains and the anaerobically functioning Ura9 enzymes, sequences of ArUra9, SjUra9, DbUra9, KmUra9 and OpUra9 were subjected to a multiple sequence alignment, along with those of the characterised Class II DHODs of *L. kluyveri* (LkUra9), *Sch. pombe* (SpUra3), and DHOD sequences of the Neocallimastigomycetes *N. californiae* (NcUra9) and *P. finnis* (PfUra9; Additional file 5; Figure S2). In comparison with the yeast Ura9 sequences, those of the three Neocallimastigomycetes showed a 76-81 amino-acid truncation at their N-termini. In canonical fungal Ura9 enzymes, the N-terminus contains a mitochondrial targeting sequence (**160**,**339**) and is proposed to be involved in quinone binding (**340**,**341**).

The Neocallimastigomycete Ura9 sequences as well as those of the two facultatively anaerobic yeasts (DbUra9 and SjUra9) contained a cysteine residue instead of the conserved serine that acts as catalytic base in canonical Class-II DHODs (**328**,**329**,**342**). Of 331 fungal Ura9 orthologs (Additional file 1) only three additional proteins (from *Coemansia reversa, Smittium culisis* and *Gonapodya prolifera*) harboured a cysteine at this position, but did not show an N-terminal truncation (Additional file 1 and Additional file 5; Figure S2).

Since soluble fumarate- and NAD^+-dependent Class-I DHODs also use a cysteine as catalytic base (**329**,**330**), we investigated the relevance this residue for *in vivo* activity of ArUra9 and SjUra9 in *S. cerevisiae*. To this end, we introduced point mutations in Ar*ura9* (C168S) and Sj*URA9* (C265S) to change the cysteine codon for a serine, yielding strains IMG007 (*ura1*Δ::Ar*ura9*^{C168S}) and IMG008 (*ura1*Δ::Sj*URA9*^{C265S}). In addition, a point mutation in the corresponding serine codon of Km*URA9* was introduced to change it to a cysteine, yielding strain IMG005 (*ura1*Δ::*KmURA9*^{S263C}).

Changing the active-site serine residue (S263) of KmUra9 to a cysteine did not affect aerobic growth of *S. cerevisiae* IMG005 (*ura1*Δ::Km*URA9*^{S263C}) relative to that of its parental strain IMI446 (*ura1*Δ::Km*URA9*) (**Figure 4.3**, Additional file 5; Table S1). This result indicated that, at least in KmUra9, the serine catalytic base that is strongly conserved in canonical Class-II DHODs, is not essential for activity under aerobic conditions. However, strain IMG005 did not grow anaerobically without uracil supplementation (**Figure 4.3**, Additional file 5; Table S1), indicating that replacement of the catalytic-base serine residue by a cysteine is not sufficient to enable anaerobic functionality of KmUra9.

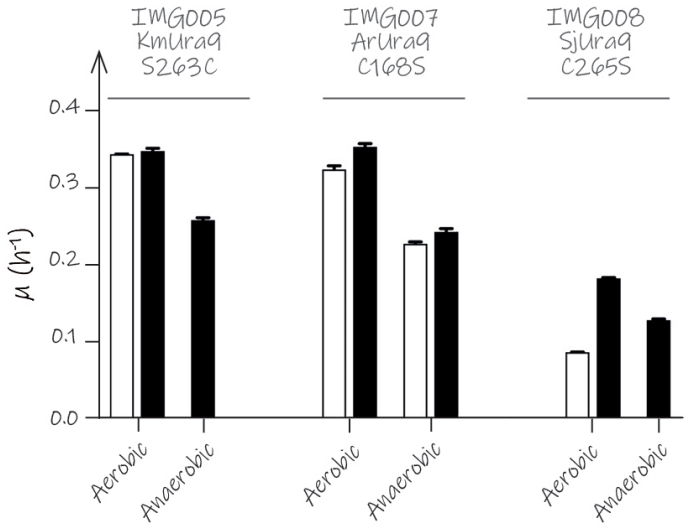

Figure 4.3. Complementation of uracil auxotrophy of *S. cerevisiae ura1*Δ strains by expressing mutated heterologous *URA9* orthologs.

The native Sc*URA1* gene of *S. cerevisiae* was replaced by *URA9* orthologs from *K. marxianus* (Km), *A. robustus* (Ar) or *Sch. japonicus* (Sj) with single-nucleotide mutations affecting a specific serine or cysteine residue. Open bars indicate specific growth rates (μ) on synthetic medium without uracil (SMUD), closed bars indicate μ in uracil-supplemented synthetic medium (SMUD+ura). Cultures were grown aerobically or anaerobically as indicated in the Figure. Relevant genotypes of *S. cerevisiae* strains: IMG005; *ura1*Δ::Km*URA9*^{S263C}, IMG007; *ura1*Δ::Ar*ura9*^{C168S}, IMG008; *ura1*Δ::Sj*URA9*^{C265S}. Data represent the average from biological duplicates and mean deviation (Additional file 5; Table S1).

Replacing the active-site cysteine residue in ArUra9 by a serine did not affect aerobic or anaerobic growth on SMUD of strain IMG007 (*ura1*Δ::Ar*ura9*^{C168S}) relative to its parental strain, indicating that both variants were active under aerobic as well as anaerobic conditions (**Figure 4.3**, Additional file 5; Table S1). This result demonstrated that the active-site cysteine residue in ArUra9 is not required for its functionality in anaerobic *S. cerevisiae* culture. A strikingly different result was obtained upon changing the cysteine residue in the active site of SjUra9 to a serine. Under aerobic conditions, exponential growth of strain IMG008 (*ura1*Δ::Sj*URA9*^{C265S}) on SMUD was nearly two-fold slower than that of its parental strain IMI452 (*ura1*Δ::Sj*URA9*). In contrast, strain IMG008 (*ura1*Δ::Sj*URA9*^{C265S}) failed to grow on SMUD under anaerobic conditions. These results indicated that the active-site cysteine residue in SjUra9, but not in ArUra9, is required for DHOD activity under anaerobic conditions.

Subcellular localisation of heterologous Ura9 orthologs expressed in *S. cerevisiae*

To investigate subcellular localisation of Ura9 orthologs, eGFP fusions of anaerobically active ArUra9, DbUra9 and SjUra9, as well as OpUra9 were expressed from multicopy (mc) plasmids in an *S. cerevisiae ura1*Δ strain, followed by fluorescence-microscopy analysis of the resulting strains (**Figure 3.4**). A co-expressed mRuby2 fluorescent protein fused to the pre*COX4* mitochondrial targeting sequence (**343**) was used as marker for mitochondrial localisation.

In *S. cerevisiae* strains IME600 (*ura1*Δ mcAr*ura9-eGFP*), IME601 (*ura1*Δ mcDb*URA9-eGFP*) and IME604 (*ura1*Δ mcOp*URA9-eGFP*), mRuby2 fluorescence showed multiple small mitochondria, a pattern that is representative for respiring cells (**344**). Consistent with the localisation of canonical eukaryotic Class-II DHODs (**160**), OpUra9-eGFP fluorescence overlapped with that of pre*COX4*-MTS-mRuby2 (**Figure 3.4A**). A similar co-localisation of DbUra9-eGFP and mRuby in strain IME601 indicated that, despite its activity under anaerobic conditions, DbUra9 was targeted to mitochondria (**Figure 4.4B**). In contrast, ArUra9-eGFP revealed a clear cytosolic localisation (**Figure 4.4C**), consistent with its N-terminal truncation, but representing a striking difference with canonical eukaryotic Class-II DHODs.

In strain IME602 (*ura1*Δ mcSj*URA9-eGFP*), mRuby2 fluorescence did not reveal the punctuate mitochondrial structures seen in the other strains. Instead, eGFP fluorescence was associated with tubular structures, that partially overlapped with a less defined mRuby2 fluorescence (**Figure 4.4D**). Although elongated mitochondrial morphologies occur in fermenting *S. cerevisiae* cells (**344**), the diffuse mRuby2 fluorescence in strain IME602 did not allow for clear localisation of SjUra9-eGFP. This strain was therefore also stained with the mitochondrial-membrane-potential dependent dye MitoTracker Deep Red. This approach only yielded vague tube-like structures or no fluorescence at all (**Figure 4.4E**). Since the mRuby2-fused pre*COX4*-mitochondrial targeting sequence is also dependent on the mitochondrial membrane potential (**343**), we hypothesised that expression of Sj*URA9* reduces or abolishes mitochondrial membrane potential, possibly as a consequence of a loss of respiratory capacity (**345**).

Expression of Sj*URA9* in *S. cerevisiae* causes loss of respiratory capacity and mitochondrial DNA

To investigate whether Sj*URA9* causes loss of respiratory capacity, Sj*URA9*-expressing *S. cerevisiae* strains were tested for their ability to grow on non-fermentable carbon sources. In addition, presence of mitochondrial DNA was assessed by staining with the DNA-specific dye 4',6-diamidino-2-phenylindole (DAPI, **346**) and by whole-genome sequencing. In contrast to the reference strain *S. cerevisiae* CEN.PK113-7D (**Figure 3.5B**), three independently constructed strains expressing Sj*URA9* (IMI452, IMI462

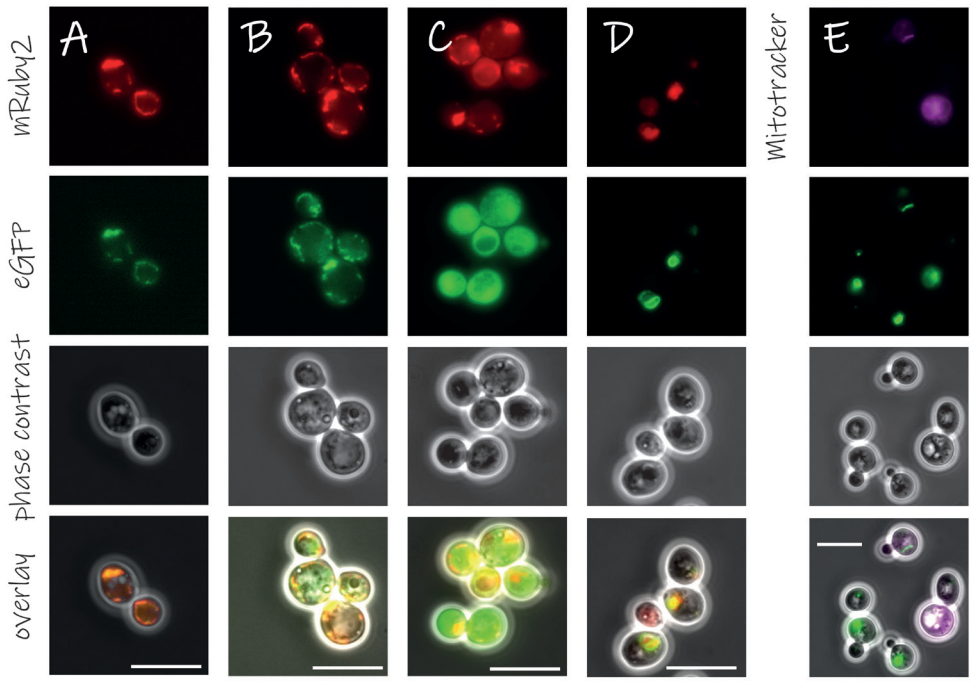

Figure 4.4. Fluorescence microscopy images of *S. cerevisiae* strains expressing mitochondrially targeted mRuby2 together with different Ura9 orthologs fused to eGFP.

Cells were grown on SMUD for at least two duplications and fluorescence of eGFP, mRuby and MitoTracker Deep Rep FM was detected by fluorescence microscopy. For each strain, from top to bottom: mRuby2/MitoTracker Deep Red FM fluorescence specifically localised to mitochondria, indicating localisation of mitochondrial mass; eGFP fluorescence, tagged to different Ura9 orthologs, indicating subcellular Ura9 localisation; phase-contrast image; and an overlay of all channels. From left to right; **A.** IME604, expressing Op*URA9-eGFP*, **B.** IME601 (Db*URA9-eGFP*), **C.** IME600 (Ar*ura9-eGFP*), **D.** IME602, (Sj*URA9-eGFP*) and **E.** IME602 stained with MitoTracker Deep Red FM. Scale bars are equivalent to 10 µm. Pictures are a representation of the full culture.

and IME571; Additional file 5; Table S4) failed to grow on synthetic medium supplemented with ethanol and glycerol (SMEG, **Figure 3.5E, F, G, H**, respectively). Removal of the Sj*URA9* expression plasmid from strain IME571, yielding strain IMS1206, did not recover growth on these non-fermentable carbon sources (**Figure 3.5I**). The inability of Sj*URA9*-expressing strains to grow on SMEG resembled that of the respiratory-deficient strain IMK242 (**347**). In contrast, strain IME603, which expressed Sc*URA1* from a multicopy plasmid, as well as all other *URA9*-expressing *ura1*Δ strains did grow on SMEG, (Additional file 5; Figure S2).

Sch. japonicus strains are naturally respiratory deficient but do have a mitochondrial genome (**348**).

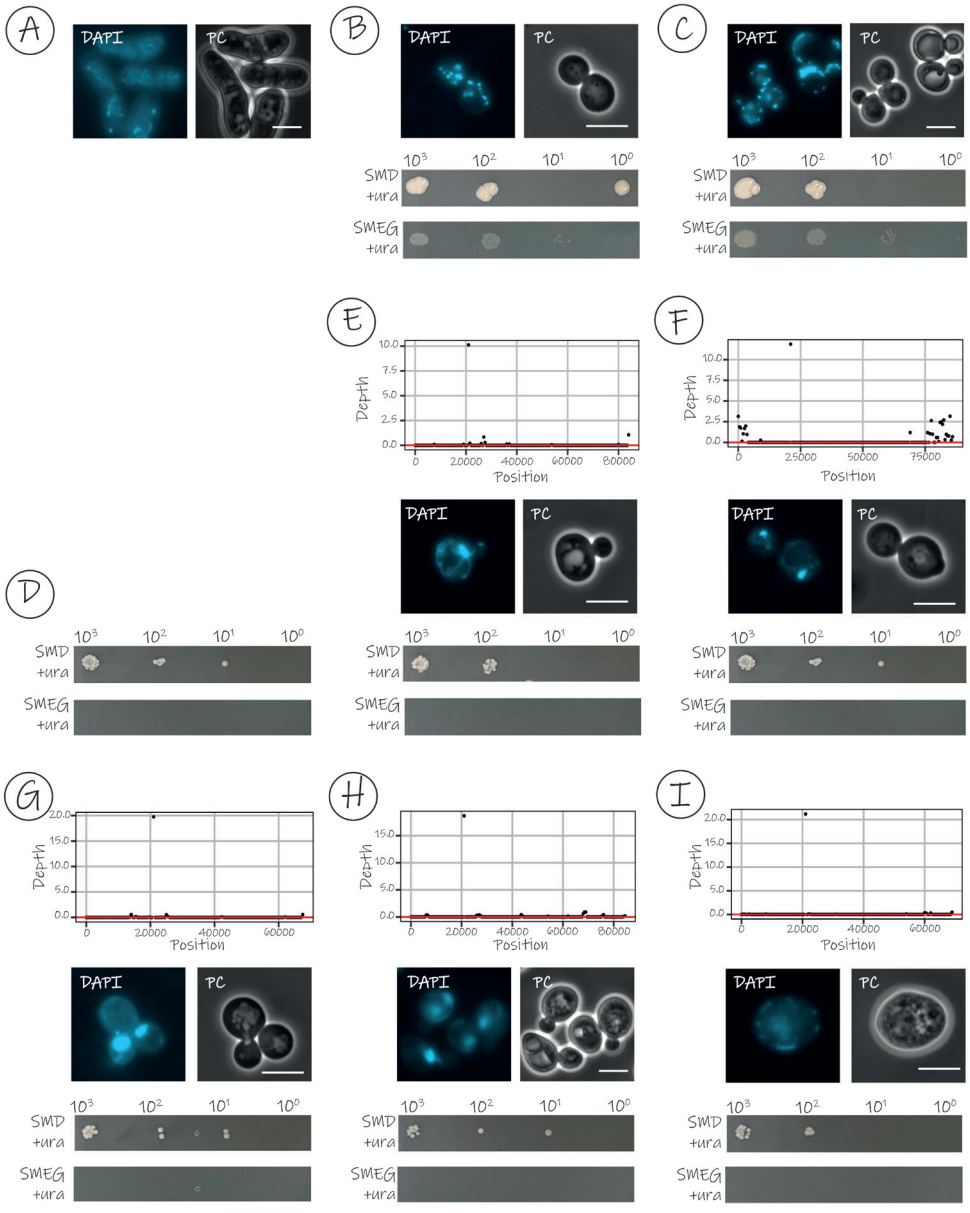

Figure 4.5. Mitochondrial DNA integrity and respiratory capacity of strains expressing Sj*URA9*.

Top: sequencing coverage depth (average of non-overlapping 500 bp sliding window of the mitochondrial genome) obtained by short-read sequencing of mitochondrial DNA relative to the reference strain CEN.PK113-7D. Middle: phase contrast (PC) microscopy and fluorescence of nuclei and mitochondrial nucleoids of yeast cells stained with the DNA-specific fluorescent dye DAPI; scale bars represent 5 µm. Bottom: spot plate assays on

glucose-containing synthetic medium with uracil (SMUD+ura) and ethanol-glycerol containing synthetic medium with uracil (SMEG+ura). SMUD+ura and SMEG+ura plates were incubated at 30 °C for 3 and 10 days respectively. Panels show data for the following yeast strains: **A.** *Sch. japonicus* CBS5679, **B.** *S. cerevisiae* CENPK.113-7D (reference), **C.** *S. cerevisiae* IME603 (multicopy Sc*URA1*), **D.** *S. cerevisiae* IMK242 (*rip1*Δ::*kanMX*), **E.** *S. cerevisiae* IMI452 (*ura1*Δ::Sj*URA9*, from IMX585), **F.** *S. cerevisiae* IMI462 (*ura1*Δ::Sj*URA9*, from IMX2600), **G.** *S. cerevisiae* IMG008 (*ura1*Δ::Sj*URA9*^{C265S}), **H.** *S. cerevisiae* IME571 (multicopy *SjURA9*) and, **I.** *S. cerevisiae* IMS1206 (IME571 cured from its Sj*URA9* expression plasmid).

Extranuclear DAPI staining of *Sch. japonicus* cultures revealed tubular structures which probably represent mitochondria (**Figure 4.5A**). In contrast, reference *S. cerevisiae* strain CEN.PK113-7D (**Figure 4.5B**) and an *S. cerevisiae* strain expressing Sc*URA1* from a multicopy plasmid (IME603; **Figure 4.5C**), showed punctuated extranuclear DAPI staining. Three of the four *SjURA9*-expressing *S. cerevisiae* strains only clearly showed fluorescent nuclei, while strain IMI452 (*ura1*Δ::Sj*URA9*) showing vague DAPI-stained tubular structures. Whole-genome sequencing of the *SjURA9*-expressing *S. cerevisiae* strains IMI452, IMI462, IMG008 and IME571 indicated absence of mitochondrial DNA in all four strains (**Figure 4.5**). Consistent with this observation, respiratory capacity was not restored when the Sj*URA9*-expressing plasmid was removed from strain IME571 (**Figure 4.5**).

ArUra9 can use free FAD and FMN as electron acceptors

The cytosolic localisation of ArUra9 and the absence of mitochondria in Neocallimastigomycetes implied that its activity in *S. cerevisiae* was unlikely to involve components of the mitochondrial respiratory chain. To identify possible natural electron acceptors of ArUra9, enzyme-activity assays were performed in cell extracts of strain IME569 (*ura1*Δ mcA*rura9*). Cell extracts of strains IME603 (mcSc*URA1*) and IMK824 (*ura1*Δ) were included as references.

Consistent with literature reports (**349**), cell extracts that only contained the Class-I DHOD ScUra1 (strain IME603) showed dihydroorotate oxidation with fumarate as electron acceptor (0.11 µmol·mg protein^{-1}.min^{-1}), while a similar activity was observed with the artificial electron acceptor phenazine methosulfate (PMS, **Table 4.2**). ScUra1-containing cell extracts also showed dihydroorotate oxidation without addition of electron acceptor (**Table 3.2**), which was attributed to a previously reported ability of DHODs to use molecular oxygen as electron acceptor (**167**,**350–352**).

A high rate of PMS-dependent dihydroorotate oxidation (0.13 µmol·mg protein^{-1}·min^{-1}) confirmed DHODase activity in cell extracts of the ArUra9-expressing strain IME569. A low activity in the absence of an added electron acceptor (**Table 4.2**) suggested that, like other DHODs, ArUra9 can use molecular oxygen as electron acceptor. Assays in which fumarate, NAD^+, $NADP^+$ or decylubiquinone were

Table 4.2. Dihydroorotate-dehydrogenase activities in cell extracts of *S. cerevisiae* strains expressing different DHODs, measured with different electron acceptors.

Activities were measured in *S. cerevisiae* strains IMK824 (*ura1*Δ), IME603 (expressing Sc*URA1* from a multicopy plasmid) and in the strain IME569 (expressing Ar*ura9* from a multicopy plasmid). Activities were measured without addition of electron acceptor (none), 0.1 mM phenazine methosulfate (PMS), 1 mM fumarate, 1 mM nicotinamine adenine dinucleotide (NAD^+), 1 mM nicotinamide adenine dinucleotide phosphate ($NADP^+$), 0.1 mM decylubiquinone (QD), 20 µM flavin mononucleotide (FMN) or 20 µM flavin adenine dinucleotide (FAD). Activities are represented as the average ± mean deviation of activities measured with two independently prepared cell extracts.

Electron acceptor	DHOD activity (µmol·mg protein^{-1}·min^{-1})		
	S. cerevisiae IMK824 *ura1*Δ	*S. cerevisiae* IME603 mc*URA1*	*S. cerevisiae* IME569 *ura1*Δ mcAr*ura9*
-	<0.005	0.010±0.001	0.008±0.001
PMS	<0.005	0.111±0.007	0.132±0.029
Fumarate	<0.005	0.110±0.020	0.006±0.000
NAD^+	<0.005	<0.005	<0.005
$NADP^+$	<0.005	<0.005	<0.005
Q_D	<0.005	0.033±0.022	0.009±0.003
FMN	<0.005	0.037±0.002	0.126±0.012
FAD	<0.005	0.011±0.002	0.148±0.032

added to reaction mixtures did not increase activities beyond this basal level. Other compounds with a standard redox potential above or close to that of DHOD-bound FMN cofactors (-242 to -310 mV; **352–354**) were therefore tested. Addition of flavin adenine mononucleotide (FAD; E'^0 = -219 mV; **355**), flavin mononucleotide (FMN; E'^0 = -219 mV; **355**) strongly promoted dihydroorotate oxidation by cell extracts of the ArUra9-expressing strain IME569, with DHOD activities of 0.15 µmol·mg protein^{-1}·min^{-1} and 0.13 µmol·mg protein^{-1}·min^{-1}, respectively. Supplementation of dihydroxyacetone phosphate (DHAP), acetaldehyde, pyruvate or oxaloacetate as electron acceptor did not increase enzyme activity.

Table 4.3. Mutations in Db*URA9* expressing strains, evolved for anaerobic pyrimidine prototrophy.

Two cultures of IMI439 (*ura1*Δ::Db*URA9*) were independently evolved under anaerobic conditions on SMUD (Figure S1). Two single colony isolates from each flask were subjected to whole-genome resequencing and predicted amino-acid substitutions were only found in Vps1 and Fum1.

Evolution line	Strain	Mutations	
		Vps1	Fum1
1	IMS1167	I401L	M432I
	IMS1128	I401L	M432I
2	IMS1169	-	A294V
	IMS1170	-	I218M

Fast anaerobic growth of Db*Ura9*-dependent *S. cerevisiae* strains correlates with mutations in *FUM1*

Attempts to identify electron acceptors of the mitochondrial DbUra9 and SjUra9 enzymes by experiments with cell extracts and isolated mitochondria were unsuccessful. We therefore investigated whether the adaptation of *S. cerevisiae* IMI439 (*ura1*Δ::Db*URA9*) to fast anaerobic, pyrimidine-prototrophic growth (Additional file 5; Figure S1) could provide insight into its *in vivo* cofactor use. Two independent cultures of this strain on SMUD were incubated anaerobically until growth occurred and then transferred to fresh medium, in which they instantaneously grew (Additional file 5; Figure S1). Upon reaching stationary phase, two single colonies were isolated from each culture, yielding isolates IMS1167, IMS1168, IMS1169 and IMS1170. To check whether these isolates had acquired stable mutations that enabled anaerobic growth, they were first grown aerobically on SMUD+ura and then transferred to anaerobic medium with a reduced uracil content (SMUD+ura0.1). Upon reaching late-exponential phase, the resulting anaerobic, pyrimidine-limited pre-cultures were used to inoculate anaerobic cultures on SMUD and SMUD+ura, in which all four isolates showed instantaneous anaerobic growth (Additional file 5; Table S1). To identify possible causal mutation(s) involved in this acquired phenotype, the genomes of the four strains were sequenced and compared with that of their parental strain IMI439 (*ura1*Δ::Db*URA9*). Strains IMS1167 and IMS1168, which originated from the same anaerobically adapted culture, both harboured the same two mutations (resulting in the amino-acid changes Vps^{I401L} and Fum1^{M432I}; **Table 4.3**). Strains IMS1169 and IMS1170, which were isolated from the second anaerobically adapted cultures, each harboured

a different mutation in *FUM1* (resulting in the amino-acid changes Fum1^{A294V} and Fum1^{T218M}, respectively; Table 4.3). The occurrence of three different mutations in *FUM1*, which encodes fumarase, suggests that the intracellular fumarate concentration may be important for the activity of DbUra9 in anaerobic *S. cerevisiae* cultures.

Discussion

Fumarate-dependent Class-IA DHODs in *S. cerevisiae* (ScUra1) and closely related yeasts circumvent the oxygen requirement of respiration-dependent pyrimidine synthesis via the mitochondrial Class-II DHODs that occur in most other fungi (**159,168,332**). The assumption that presence of a Class-IA DHOD is required for anaerobic pyrimidine prototrophy in fungi was first called into question when analysis of the genome of *D. bruxellensis* showed absence of a Class-IA DHOD gene and, instead, revealed a sequence (Db*URA*9) with similarity to Class-II DHOD genes (**176,177,208**). We identified similar situations in obligately anaerobic Neocallimastigomycetes and in the facultatively anaerobic fission yeast *Sch. japonicus* (Table 4.1, Figure 4.1). Heterologous expression studies in *ura1*Δ *S. cerevisiae* showed that DbUra9, as well as orthologs from the Neocallimastigomycete *A. robustus* (ArUra9) and *Sch. japonicus* (SjUra9), supported anaerobic pyrimidine prototrophy. This phenotype was not observed for *ura1*Δ strains expressing *URA*9 genes from the aerobic yeasts *K. marxianus* and *O. parapolymorpha* (Figure 4.2) nor in similar experiments involving *URA*9 genes from other aerobic yeasts (**159,171,175**).

A cysteine as catalytic base is considered a hallmark of Class-I DHODs (**167**) while, with few reported exceptions, Class-II enzymes have a serine in this position (**170**). Instead, the three anaerobically active Ura9 orthologs investigated in this study had a Cys in the catalytic-base position and shared this feature with only 3 of 331 other predicted fungal Ura9 orthologs. The latter three sequences originated from *Coemansia reversa*, *Smittium culicis* and *Gonapodya prolifera* (Figure 4.1), which were all originally isolated from microaerobic or anoxic environments (dung (**356**), insect guts (**357**) and submerged fruits (**358**), respectively). A Cys-to-Ser change in the active site of *Sch. japonicus* SjUra9 specifically abolished its ability to support anaerobic pyrimidine prototrophy of *S. cerevisiae* (Figure 4.3). While this result suggested that a Cys as catalytic base can be relevant for anaerobic functionality, changes at the same position of *K. marxianus* KmUra9 (Ser to Cys) and *A. robustus* ArUra9 (Cys to Ser) showed it is neither sufficient nor absolutely required for anaerobic activity of Class-II DHODs (Figure 4.3).

Consistent with the N-terminal truncation of Ura9 orthologs from Neocallimastigomycetes (Additional file 5; Figure S2), an ArUra9-eGFP fusion expressed in *S. cerevisiae* was localised to the cytosol (Figure 4.4). Enzyme assays in cell extracts showed that ArUra9 can use free FAD and FMN as electron acceptors (Table 4.2), which was not previously observed for DHODs. Biochemical standard redox

potentials of the non-enzyme-bound $FADH_2$/FAD and $FMNH_2$/FMN redox couples ($E^{0'}$ = -219 mV; **359**) and those of DHOD-bound $FMNH_2$/FMN (-242 to -330 mV; **352–354**) are compatible with either of these flavin cofactors acting as physiological electron acceptor of ArUra9. In anaerobic chemostat cultures of *S. cerevisiae*, intracellular FAD and FMN contents of 0.17 and 0.09 µmol (g biomass)$^{-1}$ were reported (**242**). While use of free flavins in cellular redox reactions is relatively rare, the *S. cerevisiae* fumarate-reductase Osm1 can re-oxidise free $FADH_2$ (**360**). Since combined deletion of *OSM1* and its paralog *FRD1* abolishes anaerobic growth of *S. cerevisiae* (**361**), we could not experimentally verify their involvement in the *in vivo* anaerobic activity of ArUra9. Sequences with strong homology to *S. cerevisiae* Frd1 and/or Osm1 were found in Neocallimastigomycetes, *Sch. japonicus* and *D. bruxellensis* (Additional file 5; Table S3). *In silico* prediction of subcellular localisation indicated that these putative fumarate reductases were mitochondrial in *Sch. japonicus* and *D. bruxellensis*. Consistent with the inferred cytosolic localisation of ArUra9, they were predicted to occur in the cytosol of Neocallimastigomycetes (Additional file 5; Table S3).

Previous studies implicated the N-terminal domains of Class II DHODs in quinone binding (**340**,**362**). Based on analysis of 1500 Class II DHOD sequences and structural alignments, Sousa *et al.* (**170**) proposed conserved residues involved in quinone binding, stabilising and pocket entry (Additional file 5; Figure S2). Ura9 sequences from Neocallimastigomycetes lacked several residues proposed to be involved in quinone binding due to their N-terminal truncation, while for another, a positively-charged residue was replaced by a hydrophobic one (Additional file 5; Figure S2). Although quinones have been found in Neocallimastigomycetes (**289**), these observations and the absence of quinone-dependent DHOD activity in cell extracts containing ArUra9 (**Table 4.2**) indicate that quinones are unlikely to be involved in pyrimidine synthesis.

Sch. japonicus and *D. bruxellensis* Ura9 orthologs retained an N-terminal mitochondrial targeting sequence, as well as conserved residues proposed to be involved quinone binding (Additional file 5; Figure S2). The only difference in quinone-associated residues was a Tyr-to-Phe change in SjUra9 (Y137), which may not have affected functionality (Additional file 5; Figure S2). We were unable to measure activities of DbUra9 and SjUra9 in cell extracts with the artificial electron acceptor PMS or other potential electron acceptors.

DbUra9-expressing *ura1*Δ isolates of *S. cerevisiae* evolved for fast anaerobic pyrimidine-prototrophy revealed three different mutations in the *FUM1* fumarase gene. Mutations in the human fumarase gene (*FH*) have been implicated with different types of cancer due to increased fumarate concentrations (**363**). Thr218 and Ala294 of DbUra9 correspond to Val197 and Ala274, respectively, in FH and are both located in highly conserved regions (**364**,**365**), while Ala274 resides in the active site (**366**). Mutation of Ala274 to a valine in human fumarate hydratase was implicated in ovarian mucinous cystadenoma (**367**), and resulted in a 50% decreased activity of the enzyme (**365**). By analogy, it seems probably that the $Fum1^{A294V}$ change in strain IMS1169 also led to a reduced fumarase activity. Corresponding amino acids in human *FH* of Thr218 and Met432 are located in the core helix, and accumulated fumarate resulting from mutations

in this helix have been associated with different types of cancer (**366**). Higher intracellular fumarate concentrations due to a reduced activity or affinity of Fum1 variants might favour *in vivo* use of fumarate as electron acceptor, as in Class I-A enzymes (**167**). Alternatively, they could stimulate re-oxidation of $FADH_2$ via fumarate reductases.

Anaerobic pyrimidine synthesis, combined with acquisition by horizontal gene transfer of genes enabling sterol-independent anaerobic growth (squalene hopene cyclase; see **Chapter 3**) and anaerobic deoxynucleotide synthesis (Class-I ribonucleotide reductase; **157**), indicates that *Sch. japonicus* is remarkably well adapted to anaerobic growth. The observation that independently constructed SjUra9-expressing *S. cerevisiae* strains all showing loss of respiratory capacity and loss of mitochondrial DNA (**Figure 4.5**) revealed a trade-off between anaerobic pyrimidine synthesis and respiratory competence. Quinone-dependent DHODs are known to react with oxygen, leading to formation of hydrogen peroxide and superoxide (**350**). In *S. cerevisiae*, these reactive oxygen species have been implicated in loss of respiratory capacity (**368**). Despite presence of respiratory proteins, including low levels of all cytochromes (**369**), *Sch. japonicus* strains are naturally respiratory deficient (**32**,**266**,**370**). Based on our results, this phenotype may either have provided a driving force for evolution of a respiration-independent DHOD or, alternatively, be a consequence of the adaptation of SjUra9 for anaerobic functionality.

Conclusions

Our results show that, in addition to the well-established acquisition of a Class-I DHOD by *S. cerevisiae* and closely related yeasts, at least three separate events in fungal evolution enabled anaerobic pyrimidine synthesis by variants of Class-II DHODs that do not depend on aerobic respiration. These anaerobically active variants were shown to have a cysteine instead of a conserved serine residue in their catalytic sites. Their *in vivo* activities were not dependent on aerobic respiration, and, in Neocallimastigomycetes, they were not membrane associated and could use free FAD or FMN as electron acceptor. These remarkable differences with canonical Class-II DHODs underline the plasticity of fungal genomes and genes under selective pressure and extend our knowledge on eukaryotic adaptation to anoxic environments. We hope this study will stimulate further research to elucidate the mechanism(s) by which the reduced flavin cofactor of the membrane-associated Class-II DHODs from *D. bruxellensis* and *Sch. japonicus* is re-oxidised under anaerobic conditions and the trade-off between anaerobic functionality and loss of respiratory capacity in the case of SjUra9.

Methods

Yeast strains, media and strain maintenance. *S. cerevisiae* strains were derived from the CEN.PK lineage (Additional file 5; Table S4; **307,371**). *O. parapolymorpha* CBS11895, *K. marxianus* CBS6556 and *Sch. japonicus* CBS5679 were obtained from the Westerdijk Institute (Utrecht, The Netherlands). Synthetic media with ammonium as nitrogen source (SM) and with urea as nitrogen source (SMU), containing vitamins and trace elements, were prepared and sterilised as described previously (**126,232**). A separately autoclaved (30 min, 110 °C) D-glucose solution (50 % w/v) was added to sterile SMU or SM at a concentration of 20 g L^{-1}, yielding SMUD and SMD, respectively. SM with ethanol and glycerol (SMEG) and complex yeast extract-peptone-glucose medium (YPD) were prepared as described previously (**237**). Where indicated, YPD was supplemented with 200 mg L^{-1} filter-sterilised geneticin (G418; Thermo Fisher Scientific, Waltham, MA) or hygromycin B (HygB; Thermo Fisher Scientific). Synthetic media for anaerobic growth experiments were supplemented with Tween 80 and ergosterol (**126**). Uracil-auxotrophic strains were routinely grown on SMUD supplemented with 150 mg L^{-1} uracil (SMD+ura) or, to obtain uracil-limited pre-cultures, with 15 mg L^{-1} uracil (SMUD+ura0.1). Solid synthetic and complex media were prepared by adding 20 g L^{-1} Bacto agar (Difco laboratories Inc, Detroit, MI) prior to autoclaving. *Escherichia coli* strains were grown on Lysogeny Broth (LB; **372**), supplemented with 100 mg L^{-1} filter-sterilised ampicillin (Sigma Aldrich, St. Louis, MO) or chloramphenicol (Sigma Aldrich) as indicated (LB-amp and LB-cam, respectively). Frozen stock cultures of yeast strains were prepared as described previously (**59**) after growth to mid-exponential phase at 30 °C on YPD (strains CENPK.113-5D, CEN.PK113-7D, IMX585, IMX2600, CBS6556 and CBS11895), on SMUD+ura (strain IMK824) or on SMUD (other strains). *E. coli* strains were grown at 37 °C on LB-amp or LB-cam and frozen stock cultures were prepared as described by Mans *et al.* (**59**).

Molecular biology techniques. Phusion High Fidelity DNA Polymerase (Thermo Fisher Scientific) and PAGE-purified oligonucleotide primers (Additional file 5; Table S5, Sigma Aldrich) were used in polymerase chain reactions (PCRs) for cloning and sequencing. Diagnostic PCRs were performed with desalted oligonucleotides (Additional file 5; Table S5, Sigma Aldrich) and DreamTag Mastermix 2X (Thermo Fisher Scientific). Genomic DNA as template for PCRs was isolated using a YeaStar Genomic DNA kit (Zymo Research, Irvine, CA). PCR products were purified with a GeneElute PCR Clean-Up kit (Sigma Aldrich) or from 1% agarose gels using a Zymoclean Gel DNA Recovery Kit (Zymo Research). Gibson Assembly of purified DNA fragments with 20 bp sequence overlaps was performed with the NEBuilder HiFi DNA Assembly Mastermix (New England Biolabs, Ipswich, MA). Golden-Gate assembly was performed according to Lee *et al.* (**373**). *E. coli* XL1-Blue (Agilent Technologies, Santa Clara, CA) was chemically transformed following manufacturer's instructions and plated on selective media. Correct plasmid assembly was verified by diagnostic PCRs on *E. coli* transformants (**59**). Cas9-mediated genome

editing in *S. cerevisiae* was performed according to Mans *et al.* (**59**). The LiAc/SS-DNA/PEG method (**374**) was used for yeast transformation with plasmids (at least 1 µg DNA per transformation) or linear DNA fragments (0.5-1 µg per transformation). Single-colony isolates of randomly picked transformants were obtained by three re-streaks on selective media. Integrations and deletions were verified by diagnostic PCRs with genomic DNA as a template. Construction of plasmids and yeast strains is described in detail in Additional file 6.

Whole-genome DNA sequencing. Genomic DNA of yeast strains was isolated from overnight cultures on YPD, except for strain IME571 that was grown on SMUD, using the Qiagen Genomic DNA 100/G kit (Qiagen, Hilden, Germany) with the Proteinase-K step extended to 3 h. DNA concentrations were measured on a Qubit Fluorometer (Invitrogen, Carlsbad, CA, USA) with the QuBit BR dsDNA Assay kit (Invitrogen). Whole-genome sequencing on an Illumina MiSeq platform (Illumina Novoseq 6000, Illumina Inc., San Diego, CA, USA) was performed by Novogene Europe (Cambridge, UK; strains IMI439, IMS1167, IMS1168, IMS1169 and IMS1170), Macrogen Europe BV (Amsterdam, The Netherlands; strains IMG008, IME571 and IMS1206) or in-house (strains IMI452 and IMI462). For in-house sequencing, the Nextera DNA Flex 509 Library Prep kit (Illumina) was used for paired-end library preparation. Genome sequences were deposited at GenBank (BioProject accession number PRJNA745202).

Whole-genome sequence analysis. Sequencing data were processed as described previously (**142**). For sequence analysis of the evolved strains IMS1167-IMS1170, their parental strain IMI439 was used as reference to obtain sequence differences. For IMI452/IMI462/IMG008 or IME571/IMS1206 IMI452 and IME571 were used as reference, respectively. Identified SNP's were individually checked with the Integrated Genomics Viewer (IGV; **375**). Mitochondrial DNA coverage plots were generated by calculating the average of non-overlapping 500 bp sliding windows (R version 3.6.0).

Protein sequence homology search and phylogenetic analysis. Proteomes of *A. robustus* (NCBI taxid 1754192), *P. finnis* (taxid 1754191), *N.californiae* (taxid 1754190), *Sch. japonicus* (taxid 402676), *D. bruxellensis* (5007; **376**), *K. marxianus* (1003335) and *O. parapolymorpha* (871575) were subjected to protein blast search in NCBI (**377**), using LkUra1 (UniProt KB accession number Q7Z892) and LkUra9 (Q6V3W9) as queries and applying default settings. Similarly, the proteomes of *A. robustus, P. finnis, N. californiae, Sch. japonicus* and that of *D. bruxellensis* were subjected to a protein blast using ScFrd1 (GenBank accession number EIW10990.1) or Osm1 (EIW09573.1) as query, default settings were applied.

To predict the localisation of putative fumarate reductases in *A. robustus, N. californiae, P. finnis, D. bruxellensis* and *Sch. japonicus*, protein sequences were compared to known fungal sorting signals and motifs using the online computational tool WoLF PSORT (**378**). The highest scoring cellular component for fungal settings was retrieved.

Bacterial and fungal amino acid sequences available from UniProt reference proteomes release 2019_02 (**379**) were systematically searched for Class-II dihydroorotate dehydrogenase orthologs. The database of fungal reference proteomes (taxid 4751) was supplemented with sequences available from the UniProt trembl division for the following organisms: *D. bruxellensis* (taxid 5007), *Komagataella*

phaffii (taxid 981350), *Komagataella pseudopastoris* (taxid 169507), *Komagataella pastoris* (taxid 4922), *Ogataea polymorpha* (taxid 460523), *Pichia membranifaciens* (taxid 763406), *Pichia kudriavzevii* (taxid 4909), *N. californiae* (taxid 1754190), *P. finnis* (taxid 1754191), *A. robustus* (taxid 1754192) and *Piromyces* sp. E2 (taxid 73868). Then, a Class-II DHOD of *L. kluyveri* CBS3082 (Q6V3W9; LkUra9; **159**) was used as query for a HMMER search (**282**), using cutoff values of 1e-5 and requiring hits to correspond to at least 75 % of the query sequence length resulting in 724 fungal and 1595 bacterial Ura9 homologs. The sets of Ura9 homologs were further used to select a set of orthologs. For this purpose, the database of fungal proteomes was used to calculate all possible co-ortholog sets with proteinortho v6.0.25 (**380**) running diamond v2.0.8 (**381**), obtaining 331 Ura9 orthologs (Additional file 1). Similarly, the search for bacterial Ura9 orthologs resulted in 73 sequences (Additional file 1). Ura9-orthologous amino-acid sequences were then subjected to multiple sequence alignment using MAFFT v7.40286 (**320**) in "einsi" mode. Alignments were trimmed using trimAl v1.287 (**321**) in "gappyout" mode, and used to build a phylogenetic tree with RAxML-NG v0.8.188 (**322**) using 10 random and 10 parsimony starting trees, 100 Felsestein Bootstrap replicates, and LG model. The resulting phylogenetic tree was visualized using iTOL (Interactive Tree Of Life) tool v6 (**323**).

Multiple sequence alignment of selected Ura9-orthologs was performed in Clustal Omega (**382**) with default settings. Protein sequences of Ura9 orthologs were retrieved from the Uniprot database for *Sch. pombe* (SpUra3; Uniprot KB accession number P32747); *L. kluyveri* (LkUra9; Q6V3W9), *O. parapolymorpha* (OpUra9; W1QJ07), *K. marxianus* (KmUra9; Q6SZS6), *E. coli* (EcUra9; P0A7E1), *D. bruxellensis* (DbUra9; I2JUI3), *Sch. japonicus* (SjUra9; B6JXQ5), *A. robustus* (ArUra9; A0A1Y1XN91), *N. californiae* (NcUra9; A0A1Y2ELQ6) and *P. finnis* (PfUra9; A0A1Y1VDI5) and *C. reversa* (CmUra9; A0A2G5BHD4), *Sm. culicis* (ScuUra9; A0A1R1YI62) and *G. prolifera* (GpUra9; A0A139AY32).

Cultivation of yeast strains. Aerobic shake-flask cultures were grown in an Innova Incubator (New Brunswick Scientific, Edison, NJ) at 30 °C and 200 rpm. Pre-cultures in 100-mL shake flasks with a working volume of 40 mL were inoculated with frozen stock cultures. Primary pre-cultures of yeast strains expressing plasmid-borne DHOD genes were grown on SMUD and those of other yeast strains on SMUD+ura, and were used to inoculate a secondary pre-culture on SMUD (for plasmid expressing strains) or SMUD+ura0.1. Upon reaching late exponential phase, cultures were centrifuged (5 min at 3000 *g*) and washed twice with demineralised water. Washed cell suspensions were used to inoculate 500-mL shake flasks containing 100 mL of SMUD+ura or SMUD, at an initial optical density at 660 nm (OD_{660}) of 0.2.

Anaerobic cultures were grown in 100-mL shake flasks with a working volume of 80 mL. Pre-cultures were grown aerobically on SMUD+ura as described above, until stationary phase, washed twice with sterile demineralised water and transferred to an anaerobic pre-culture on SMUD+ura0.1, supplemented with Tween80 and ergosterol. Flasks were incubated on an IKA KS 260 orbital shaker (240 rpm; Dijkstra Verenigde BV, Lelystad, The Netherlands) placed in a Shel Lab Bactron 300 anaerobic workstation (Sheldon Manufacturing Inc, Cornelius, OR) at 30 °C. The gas mixture supplied to the anaerobic workstation contained 10 % CO_2, 5 % H_2 and 85 % N_2. Measures to minimise inadvertent oxygen entry were

implemented as described in Chapter 2. When anaerobic pre-cultures reached stationary phase, they were used to inoculate cultures on SMUD and SMUD+ura supplemented with Tween 80 and ergosterol.

For spot-plate experiments, yeast strains were pre-grown on 20 mL SMUD in 100-mL shake flasks, centrifuged (5 min, 3000 *g*) and washed twice with demineralised water. Washed cultures were used for cell counts with a Z2 Coulter particle count and size analyzer (Beckman Coulter, Brea, CA) set at particle size 2.5-7.5 µm. Cells were diluted to a final concentration of 2.5·105 cells mL^{-1}, and subsequently diluted to $2.5 \cdot 10^4$ cells mL^{-1}, $2.5 \cdot 10^3$ cells mL^{-1} and $2.5 \cdot 10^2$ cells mL^{-1}. From these four dilutions, 4 µL of each strain and dilution was transferred to SMD, SMD+ura, SMEG and SMEG+ura plates. All strains were pre-grown and plated in duplicate.

Analytical methods. Extracellular metabolite concentrations were measured by high performance liquid chromatography as described by Verhoeven *et al.* (**315**) Optical density at 660 nm of aerobic cultures was measured using an Jenway 7200 spectrophotometer (Bibby Scientific, Staffordshire, UK) after accurate dilution to an OD_{660} between 0.1 and 0.3. Anaerobic cultures were first diluted to an optical density at 600 nm (OD_{600}) between 0.15 and 0.35, followed by optical densities measurements at 600 nm on an Ultrospec 10 cell density meter (Biochrom, Harvard Biosience, Holliston, MA) that was placed in the anaerobic workstation (see Chapter 2).

Microscopy analysis and staining. MitoTracker Deep Red FM (Invitrogen) staining was performed on early exponential phase aerobic cultures by adding 250 nM MitoTracker Deep Red FM to a 1-mL culture sample and subsequent incubation in the dark at 37 °C for 15 min. DNA staining was performed on 1-mL samples of early exponential phase, aerobic cultures on 10 mL SMUD in 50-mL vented Greiner tubes (Greiner Bio-One, Kremsmünster, Austria). Cultures were supplemented with 300 nM 4',6-diamidino-2-phenylindole (DAPI) dihydrochloride (Sigma Aldrich) and incubated in the dark for 10-15 min at 20 °C. Phase-contrast microscopy was performed using a Zeiss Axio Imager Z1 (Carl Zeiss AG, Oberkochen, Germany) that was equipped with a HAL 100 Halogen illuminator, HBO 100 illuminating system and AxioCam HRm Rev3 detector (60N-C 1'' 1.0x) (Carl Zeiss AG). The lateral magnification objective 100x/1.3 oil was used with Immersol 518F type F immersion oil (Carls Zeiss AG). Fluoresence of eGFP was detected using filter set 10 (Carl Zeiss AG; excitation bandpass (BP) 470/20, emission 540/25). MitoTracker Deep Red and mRuby2 were imaged with filterset 14 (excitation BP 535/25, emission longpass (LP: 590) and 50 (excitation BP 640/30, emission BP 690/50) respectively (Carls Zeiss AG). For analysis of DAPI dihydrochloride fluorescence, filterset 49 (excitation Short Pass (SP) 380, emission BP 445/50) was used (Carl Zeiss AG). Results were analysed using the Fiji package of ImageJ (**383**).

Preparation of cell extracts. Strains carrying multi-copy plasmids expressing dihydroorotate dehydrogenases, were grown to mid-exponential phase in 100-mL shake flask cultures on SMUD. After centrifugation at 3000 *g* and at 0 °C, biomass was resuspended in 4 mL ice-cold 10 mM potassium phosphate buffer (pH 7.5) with 2 mM EDTA and stored at -20 °C. Samples were thawed on ice, centrifuged at 3000 *g* and at 4 °C, washed with 10 mL ice-cold sonication buffer (100 mM potassium phosphate buffer, pH 7.5 with 2 mM $MgCl_2$) and resuspended in 4 mL sonication buffer containing 1 tablet of cOmplete Mini protease inhibitor (Sigma Aldrich) per 10 mL buffer. Cell extracts were prepared by sonication

and centrifugation as described previously (**384**). Bovine serum albumin (Sigma Aldrich) was used as a reference for analysis of protein concentrations in cell extracts (**385**).

Dihydroorotate dehydrogenase activity assays in cell extracts. Dihydroorotate dehydrogenase assays were performed at 30 °C in potassium phosphate buffer, (100 mM, pH 7.5) using a Hitachi U-3010 UV/Visible spectrophotometer (Chiyoda, Tokyo, Japan). Formation of orotate or reduction of $NAD(P)^+$ was monitored by measuring absorbance at 300 nm (ε = 3.05 mM^{-1} cm^{-1}; **165**) or 340 nm (ε = 6.22 mM^{-1} cm^{-1}; **386**) respectively, upon addition of 1 mM dihydroorotate to a temperature-equilibrated reaction mixture containing buffer, cell extract and/or either of the electron acceptors fumarate (1 mM), decylubiquinone (Q_D, 0.1 mM, dissolved in dimethylsulfoxide), nicotinamide adenine dinucleotide (NAD^+, 1 mM), nicotinamine adenine dinucleotide phosphate ($NADP^+$, 1 mM), flavine adenine dinucleotide (FAD, 20 µM), flavin mononucleotide (FMN, 20 µM) or the artificial electron acceptor phenazine methosulfate (PMS, 0.1 mM). Enzyme assays were performed on two separately prepared cell extracts. Reduction potentials of tested electron acceptors mentioned in the text are relative to the standard hydrogen electrode.

Data availability

Figure 4.1 was made available online: https://itol.embl.de/export/193190253145446711626368835

Whole-genome sequencing data from strains IMS1167, IMS1168, IMS1169, IMS1170, IMI452, IMI462, IMG008, IME571 and IMS1206 was deposited at NCBI (BioProject accession number PRJNA745202)

Supplemental information is available via the online article: https://doi.org/10.21203/rs.3.rs-762539/v1

Acknowledgements

We gratefully thank Göktuğ Aba for construction of pUDC286 and Siem Eerden for construction of pUDE672 and pUDE677, Robert Stella for pUD538 and Petrik Buitenhuis for construction of pUDE815. We acknowledge Jisk van der Meer for constructing pUDR386, pUDE765, pUDE809, IMK839, IMI446, IMI447 and IMI452 and Magdalena Kaminska for construction of IMX2165, IMX2203, IMX2209, IMG005 and IMG007. We thank Marc Strampraad for the help with the enzyme assays and Sanne Wiersma and Nicole Bennis for their help with the aerobic growth study. We also thank Sanne Wiersma for critically reading the manuscript.

4

Chapter 5.

Identification of fungal dihydrouracil oxidase genes by expression in *Saccharomyces cerevisiae*

Jonna Bouwknegt*
Aurin M. Vos*
Raúl A. Ortiz-Merino
Daphne C. van Cuylenburg
Marijke A.H. Luttik
Jack T. Pronk

* Authors have contributed equally to this work

An updated version of this manuscript has been submitted for publication in Antonie van Leeuwenhoek

Abstract

Analysis of fungal proteome sequences revealed a large gene family with sequence similarity to the *S. cerevisiae* Class-I dihydroorotate dehydrogenase Ura1. Expression of codon-optimised representatives from the ascomycete *Alternaria alternata* and the basidiomycete *Schizophyllum commune* only complemented the uracil auxotrophy of an *S. cerevisiae ura1*Δ mutant when aerobic cultures were supplemented with dihydrouracil. A hypothesis that these genes encode $NAD(P)^+$-dependent dihydrouracil dehydrogenases (EC 1.3.1.1 or 1.3.1.2) was, however, not consistent with an observed absence of complementation in anaerobic cultures. Uracil- and thymine-dependent oxygen consumption and hydrogen-peroxide production by cell extracts of *S. cerevisiae* strains expressing the *A. alternata* and *S. commune* genes showed that they encode active dihydrouracil oxidases (DHUO, EC1.3.3.7). Activity of dihydrouracil oxidase (DHUO, EC1.3.3.7), which catalyses the reaction dihydrouracil + O_2 → uracil + H_2O_2, was only reported in a single organism, *Rhodotorula glutinis*, and structural genes for this enzyme were hitherto not identified. A potential applicability of fungal DHUO genes a counter-selectable marker genes for genetic modification of *S. cerevisiae* was demonstrated by the observation that DHUO-expressing strains were highly sensitive to 5-fluoro-dihydrouracil (5F-dhu) and that plasmids bearing DHUO expression cassettes were readily lost during growth 5F-dhu-containing media. Further research should explore the physiological significance of the apparent widespread occurrence of DHUO in fungi.

Introduction

Cellular contents of the pyrimidines cytidine, thymine and uracil are the net result of uptake, *de novo* synthesis, salvage pathways and degradation (**387,388**). Whereas pyrimidine biosynthesis is highly conserved across all domains of life (**387**), pyrimidine degradation can occur via at least four different pathways (**389–392**).

The conserved pyrimidine biosynthesis pathway and the reductive pathway for pyrimidine degradation that occurs in most eukaryotes (**389,393**) involve similar, reversible redox reactions (**161**). In pyrimidine biosynthesis, dihydroorotate dehydrogenase (DHOD) oxidises dihydroorotate to orotate (**Figure 5.1A**), while the reductive pyrimidine degradation pathway starts with reduction of uracil to dihydrouracil (**Figure 5.1B**) by $NAD(P)^+$-dependent dihydropyrimidine dehydrogenases (DHPD), whose protein sequences show similarity to those of DHODs (**325,394**). Genetic defects in human pyrimidine catabolism have been implicated in neurological disorders and mainly affect DHPD (**395,396**). Furthermore, human DHPD plays a key role in resistance to the anticancer drug 5-fluorouracil (5-FU) by reducing it to the less toxic 5-fluorodihydroxyuracil (**396–399**).

Eukaryotic DHPDs, encoded by mammalian *DPYD* orthologs and plant *PYD1* orthologs, have been isolated and characterised (**400–402**). They are homodimers containing one FAD, one FMN and four [4Fe-4S] clusters (**401,403**). After reduction of the FAD cofactor with NADPH, electrons are transferred to FMN via the [4Fe-4S] clusters, after which $FMNH_2$ reduces the pyrimidine substrate. With uracil as the substrate, this reaction yields dihydrouracil (**404**).

DHPDs active in pyrimidine degradation as well as DHODs active in pyrimidine synthesis are flavoproteins. Most fungi harbour homodimeric Class-II DHODs, which are localised to the outside of the inner mitochondrial membrane (**160**). These enzymes are orthologs of Ura9 in yeasts such as *Lachancea kluyveri* and *Ogataea parapolymorpha*, and donate electrons on the quinone pool of the mitochondrial respiratory chain (**69,159,208**). As a consequence, pyrimidine synthesis is, in the large majority of fungi, dependent on the availability of oxygen (**171**). *Saccharomyces* yeasts and a small number of closely related species instead harbour Class I-A DHODs (Ura1 in *S. cerevisiae*), which are soluble homodimers with one FMN domain per subunit that use fumarate as electron acceptor (**352**). Presence of Ura1 orthologs, which are proposed to have been acquired by horizontal gene transfer (HGT) from lactic acid bacteria (**159**), was long considered essential for anaerobic pyrimidine prototrophy of fungi (**168**). This notion was first questioned when the facultative anaerobic yeast *Dekkera bruxellensis* was shown to only contain a DHOD gene with sequence similarity to yeast Class-II DHOD genes (**145,177**). It was recently shown that expression of an Class-II DHOD gene from *D. bruxellensis*, obligately anaerobic Neocallimastigomycetes, or from the facultatively anaerobic fission yeast *Schizosaccharomyces japonicus*, supported anaerobic growth of *S. cerevisiae ura1*Δ strains without pyrimidine supplementation (see **Chapter 4**).

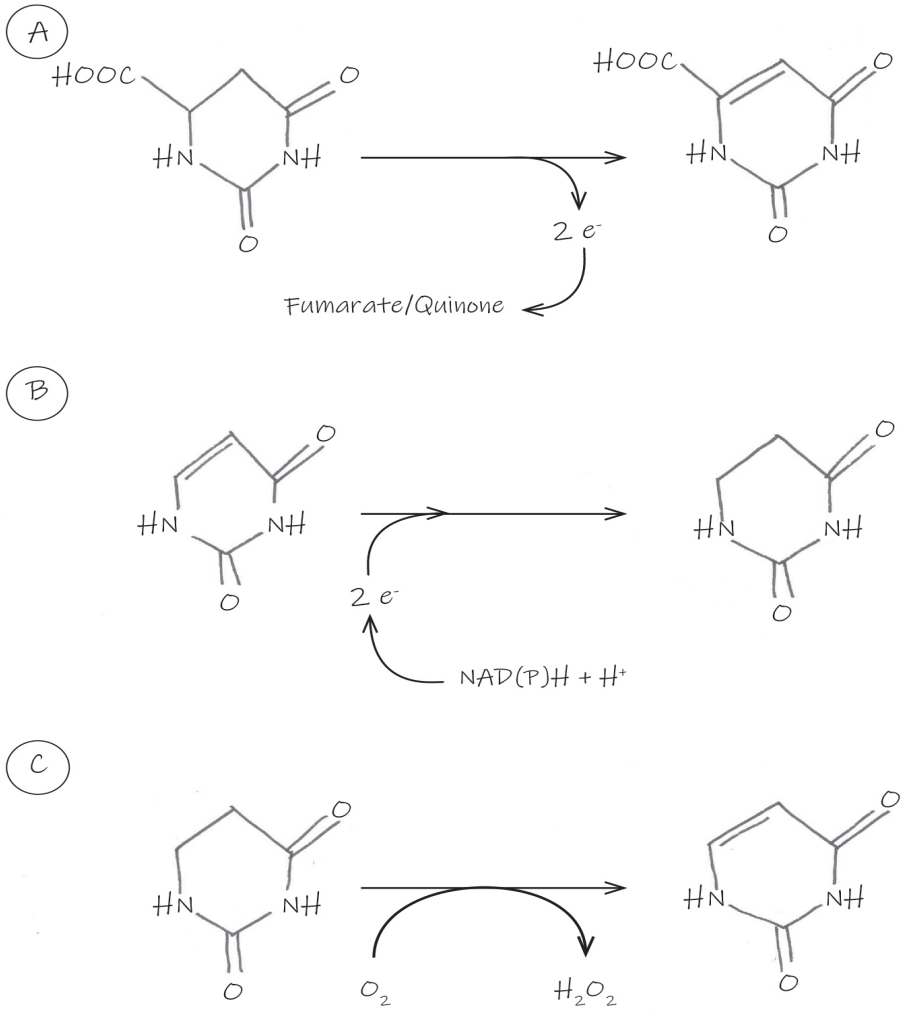

Figure 5.1. Reactions catalysed by dihydroorotate dehydrogenase, dihydropyrimidine dehydrogenase and dihydrouracil oxidase.

A. In pyrimidine biosynthesis, fungal dihydroorotate dehydrogenase catalyses the oxidation of dihydroorotate orotate and donates electrons to the quinone pool of the respiratory chain (Class-II DHOD; but see **Chapter 4**) or to fumarate (Class-I DHOD). **B.** In the reductive pathway for pyrimidine degradation, dihydropyrimidine dehydrogenases (DPHD) catalyse the reduction of uracil to dihydrouracil, using NAD(P)H as electron donor. **C.** Dihydrouracil oxidase, which has only been described in *Rhodotorula glutinis* (**405,406**), catalyses the oxidation of dihydrouracil with molecular oxygen and forms hydrogen peroxide.

When searching fungal proteomes for Ura1 homologs, we encountered a large number of putative proteins in ascomycetes and basidiomycetes that showed sequence similarity to Class-I DHOD genes. Widespread occurrence of these sequences in fungi was unexpected in view of the previously reported connection of Class-I DHOD genes to anaerobic growth and the proposed role of HGT in their acquisition. To explore the biochemical function of the proteins encoded by this unexplored gene family, we expressed representatives from the ascomycete *Alternaria alternata* and the basidiomycete *Schizophyllum commune* in a *ura1*Δ strain of *Saccharomyces cerevisiae*. Since *S. cerevisiae* and other post-whole-genome-duplication Saccharomycotina yeast species lost the ability to degrade pyrimidines (**407**), expression in the *ura1*Δ genetic background enabled us to test DHOD as well as DHPD activity of the encoded proteins. In addition, the ability of *S. cerevisiae* to grow anaerobically enabled an assessment as to whether activity depended on the presence of oxygen. Growth experiments and enzyme activity assays in cell extracts showed that the *A. alternata* and *Sch. commune* genes encoded dihydrouracil oxidases (DHUO) that catalyse oxygen-dependent oxidation of dihydrouracil to uracil (**Figure 5.1C**) and also showed activity with dihydrothymine. Based on the reported ability of human DHPD to convert 5-fluorodihydrouracil to the toxic compound 5-fluorouracil (**397**), we tested whether fungal DHUO genes can be applied as counter-selectable marker for genetic engineering of *S. cerevisiae*.

Results

A large cluster of uncharacterised fungal protein sequences show similarity with yeast Ura1

The amino-acid sequence of the Class-I-A DHOD LkUra1 from *L. kluyveri* was used as query for a HMMER search against fungal proteomes available from Uniprot. Selection of the best hit for each proteome yielded 203 putative Ura1 orthologs (**Figure 5.2**, Dataset S01, S02). Phylogenetic analysis showed that sequences of eight of these proteins originating from Mucormycotina were more closely related to the well-known Class-I-A DHODs from *S. cerevisiae, L. kluyveri* and closely related Saccharomycotina yeasts than to the other sequences (**Figure 5.2**). This observation coincided with the reported ability of dimorphic Mucor species to grow anaerobically without pyrimidine supplementation (**408**,**409**). A large group of additional putative orthologs of LkUra1 in Ascomycota and Basidiomycota (**Figure 5.2**) was unexpected, since the only known fungal Class-I-A DHODs are proposed to have been obtained by horizontal gene transfer (**159**). Most of the proteomes in which these sequences were found originated from aerobic fungi that harbour Class-II dihydroorotate dehydrogenases (see **Chapter 4**) which does not indicate a clear evolutionary advantage of additionally harbouring a Class I-A DHOD. We therefore hypothesised that,

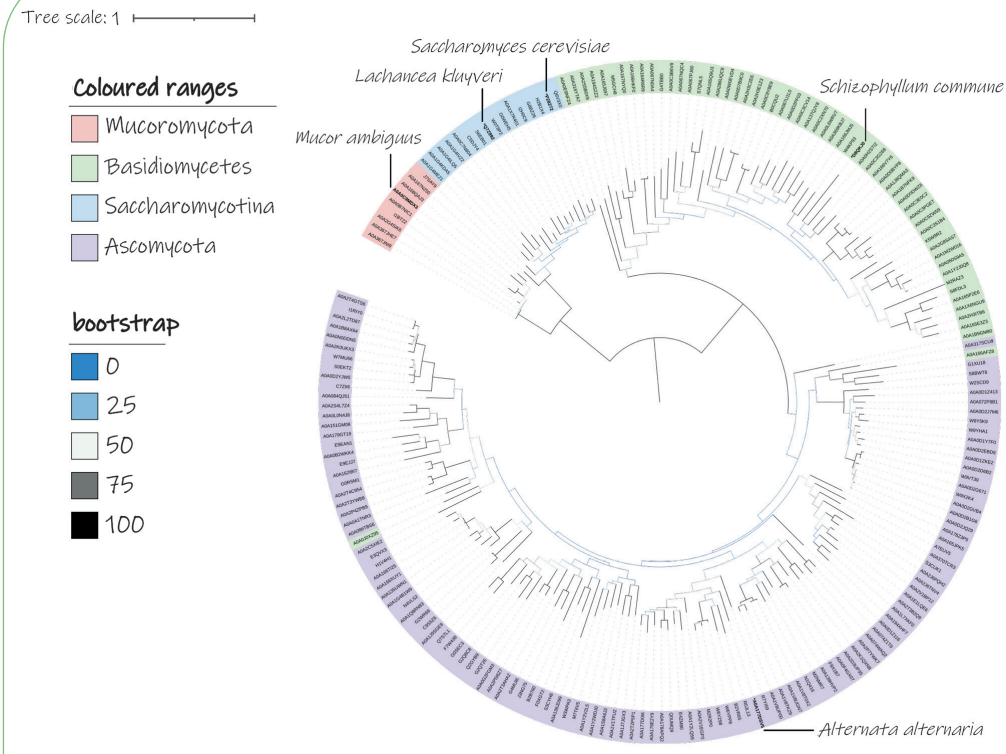

Figure 5.2. Maximum likelihood phylogenetic tree of fungal proteins homologous to dihydroorotate dehydrogenase from *L. kluyveri* (LkUra1).

A search for orthologs or Class I-A dihydroorotate dehydrogenases using *L. kluyveri* LkUra1 (UniProt KB accession number: Q7Z892) as query resulted in 203 proteins (Dataset S01). Clusters corresponding to the phyla Basidiomycota, Ascomycota and Mucormycota are indicated in colour. Sequences that were functionally analysed in this study, as well as the the characterised Ura1 proteins of *L. kluyveri* (**159**), and *S. cerevisiae* (**352**) are indicated with the corresponding species name. The tree was mid-point rooted, and the raw phylogenetic tree is provided in Dataset S02. Bootstrap values and species can be accessed from: https://itol.embl.de/tree/838448010495161822549 3.

rather than DHODs, this group of protein sequences with homology to LkUra1 might comprise proteins with a related function, such as DHPDs (**394**). The group of putative Ura1-orthologs showed two large clusters, which almost exclusively consisted of sequences from either ascomycetes or basidiomycetes. Only two sequences from basidiomycetes (*Exidia glandulosa*; A0A166AFZ8 and *Cutaneotrichonsporon oleaginosum*; A0A0J0XZ95) clustered with those from ascomycetes (**Figure 5.2**).

Table 5.1. Complementation by uracil (ura) or dihydrouracil (dhu) of uracil-auxotrophic *S. cerevisiae* strains expressing fungal proteins with homology to Ura1.

Specific growth rates were measured in duplicate shake-flask cultures for each combination of strain and medium composition, data are represented as average ± mean deviation. SMD, synthetic medium with glucose; SMD+ura, SMD supplemented with 1.5 g L^{-1} uracil; SMD+dhu, SMD supplemented with 2.5 g L^{-1} dihydrouracil. When no exponential growth was observed, growth rates were indicated by not applicable (n.a.).

Strain	Relevant genotype	SMD	SMD+ura	SMD+dhu
IMX585	*URA1*	0.37±0.00	0.37±0.00	0.37±0.01
IMK824	*ura1*Δ	n.a.	0.35±0.00	n.a.
IMI433	*ura1*Δ::Aa*dho*	n.a.	0.37±0.00	0.34±0.00
IMI434	*ura1*Δ::Sc*dho*	n.a.	0.35±0.00	0.34±0.01

Putative Ura1-orthologs from *A. alternata* and *Sch. commune* are not DHODs

To investigate the biochemical activity of the group of fungal proteins with sequence similarity to yeast Ura1, a representative from an ascomycete (*A. alternata*; Aa; A0A177DSV5) and a basidiomycete (*Sch. commune*; Sc; D8QKJ0) were selected (**Figure 5.2**). An alignment of these sequences with those of Ura1 orthologs from *L. kluyveri* and *S. cerevisiae* confirmed the strong similarity inferred from the phylogenetic analyses. Conserved amino-acid residues involved in flavin cofactor binding, as well as an active-site cysteine residue that is strongly conserved in Class-I-A DHODs occurred in all four sequences (SI Figure S1). Codon-optimised coding regions of the corresponding genes, which will be referred to as A*adho* and Sc*dho* (see below), respectively, were expressed in the uracil-auxotrophic *S. cerevisiae* strain IMK824 (*ura1*Δ), which lacks DHOD activity and whose growth on synthetic medium with glucose (SMD) should therefore require supplementation with uracil (SMD+ura; **168**). Since the *S. cerevisiae* genome does not encode a DHPD (**407**), *in vivo* DHOD activity of the heterologous proteins should complement the *ura1*Δ mutation on SMD, while *in vivo* DHPD activity should only do so upon supplementation of media with dihydrouracil (SMD+dhu). As anticipated, the reference *S. cerevisiae* strain IMX585 (*URA1*) showed the same specific growth rate (0.37 h^{-1}) on all three media, while strain IMK824 (*ura1*Δ) only grew on SMD+ura supplemented with uracil (**Table 5.1**). The latter, IMK824, grew slightly slower on SMD+ura than the reference strain (**Table 5.1**), probably reflecting a limitation in uracil import (**336**). Strains IMI433 (*ura1*Δ::Aa*dho*) and IMI434 (*ura1*Δ::Sc*dho*) did not show growth on SMD (**Table 5.1**), indicating that the heterologous fungal genes were either not functionally expressed in *S. cerevisiae* or did not encode functional DHODs. The subsequent observation that both strains showed a specific growth rate

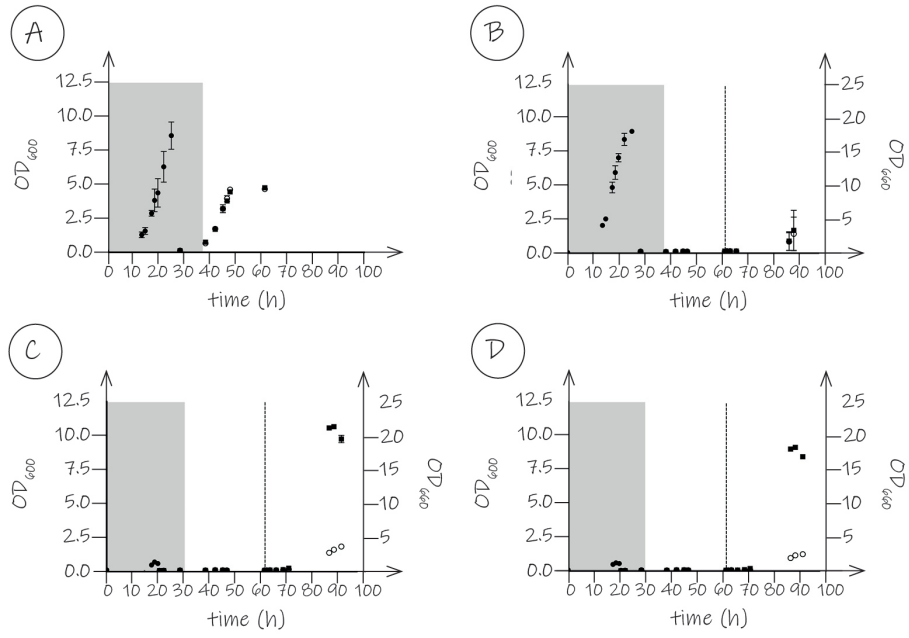

Figure 5.3. Anaerobic growth curves of *S. cerevisiae* strains expressing genes encoding putative Ura1 orthologs from *A. alternata* (A*adho*) and *Sch. commune* (S*cdho*).

Strains were pre-grown anaerobically (●) on medium with a limiting amount of uracil (strain IMK824 (*ura1*Δ)) or dihydrouracil (strains IMX585 (*URA1*), IMI433 (*ura1*Δ::A*adho*) and IMI434 (*ura1*Δ::S*cdho*) to deplete intracellular pyrimidine reserves (grey boxes; **Chapter 2**. Strains were then transferred to fresh media with dihydrouracil (SMD+dhu; ■) or without dihydrouracil (SMD; ○). After 70 h, strains IMI433 and IMI434 were transferred to aerobic conditions. **A.** *S. cerevisiae* IMX585 (*URA1*), **B.** strain IMK824 (*ura1*Δ), **C.** strain IMI433 (*ura1*Δ::A*adho*), **D.** strain IMI434 (*ura1*Δ::S*cdho*). Data represent the average and mean deviation of duplicate cultures.

of 0.34 h^{-1} on SMD+dhu, which did not support growth of the *ura1*Δ strain IMK824 (**Table 5.1**), led us to hypothesise that A*adho* and S*cdho* both encode fungal DHPDs.

Absence of dihydrouracil oxidation in anaerobic cultures of *S. cerevisiae* strains expressing A*adho* or S*cdho*

To test whether dihydrouracil oxidation by strains IMI433 (*ura1*Δ::A*adho*) and IMI434 (*ura1*Δ::S*cdho*)

required oxygen, their anaerobic growth was compared with that of the reference strains IMX585 and IMK824 (*ura1*Δ). After aerobic pre-cultivation on permissive synthetic media, washed cell suspensions were transferred to second-stage, anaerobic precultures on SMUD with a limiting amount of uracil (SMUD+ura0.1) or dihydrouracil (SMUD+dhu0.1). Upon a subsequent transfer, strain IMK824 (*ura1*Δ) did not grow on SMUD unless uracil was supplemented (**Figure 5.3**), showing that the pre-cultivation procedure had successfully depleted any intracellular reserves of pyrimidines. When the *S. cerevisiae* strains expressing either A*adho* or S*cdho* were similarly transferred to an anaerobic culture, no growth on SMUD or SMUD+dhu was observed (**Figure 5.3**). However, upon transfer of anaerobic cultures of these strains on SMD+dhu to an aerobic environment, instantaneous growth occurred (**Figure 5.3**). These results show that oxygen is required for *in vivo* oxidation of dihydrouracil by by ScDho and AaDho.

A*adho* and S*cdho* encode dihydrouracil oxidases

The oxygen requirement for dihydrouracil oxidation of *S. cerevisiae* strains expressing A*adho* or S*cdho* raised the possibility that these genes might encode dihydrouracil oxidases (DHUO; **405**). To test this hypothesis, expression cassettes were introduced in an *S. cerevisiae ura1*Δ background on multicopy (mc) plasmids. Cell extracts of the resulting strains IME664 (*ura1*Δ mcA*adho*) and IME665 (*ura1*Δ mcS*cdho*) were then used for enzyme activity assays, with extracts of the congenic *S. cerevisiae* strains CEN.PK113-7D (*URA1*) and IMK824 (*ura1*Δ) as references. Extracts of strains IME664 and IME665 showed dihydrouracil-dependent oxygen uptake (**Table 5.2**; 48 ± 2 and 171 ± 6 nmol (mg protein)$^{-1}$ min^{-1}, respectively) and dihydrothymine-dependent oxygen uptake. (88 ± 8 and 228 ± 4 nmol (mg protein)$^{-1}$ min^{-1}). No significant rates of oxygen uptake were observed upon addition of dihydrouracil or dihydrothymine to cell extracts of strains CEN.PK113-7D or IMK824 (**Table 5.2**). When catalase, which catalyses the reaction 2 $H_2O_2 \rightarrow O_2 + 2\ H_2O$, was added during oxidation of dihydrouracil by cell extracts of strains IME664 or IME665, the oxygen concentration in the reaction mixture immediately increased (**Figure 5.4**). This increase corresponded to about 40 % of the initially consumed oxygen, which suggests that some catalase was already present in the cell extracts. These results supported the hypothesis that A*adho* and S*cdho* are structural genes encoding active fungal dihydrouracil oxidases.

Dihydrouracil oxidase activity was previously only reported in two studies on *Rhodotorula glutinis* (**405,406**). Since the proteome of *R. glutinis* is not available from Uniprot, no Ura1-ortholog was found in our phylogenetic analysis. However, homologous proteins were found in *R. taiwanensis* (A0A2S5B0X9) and *R. graminis* (A0A194S2Z2). Although the early studies on *R. glutinis* and the present study indicate activity with dihydrouracil as well as dihydrothymine, this enzyme activity is classified as a dihydrouracil oxidase (EC1.3.3.7). We therefore propose the gene names *dho* (for dihydrouracil oxidase) for the genes encoding A0A177DSV5 from *A. alternata* and D8QKJ0 from *Sch. commune*.

Table 5.2. Dihydropyrimidine oxidase activities in cell extracts of *S. cerevisiae* strains expressing Aa*dho* or Sc*dho*.

Activities were determined in cell extracts by monitoring oxygen upon addition of 0,2 mM dihydrouracil (dhu) or dihydrothymine (dht). Experiments were performed in a Clark electrode, in a 4-mL reaction chamber kept at 30°C and containing 0.1 M potassium phosphate buffer (pH 7.5) with 2 mM $MgCl_2$. Activities are presented as average and mean deviation of measurements on two independently prepared cell. No detectable oxygen consumption was indicated by n.d.

Strain	Relevant genotype	Activity (nmol·mg protein^{-1}·min^{-1})	
		dhu	dht
CEN.PK113-7D	*URA1*	n.d.	n.d.
IMK824	*ura1*Δ	n.d.	n.d.
IME664	*ura1*Δ mcA*adho*	6.6 ± 0.3	12.3 ± 1.1
IME665	*ura1*Δ mcS*cdho*	23.8 ± 0.8	31.7 ± 0.5

5-fluorodihydrouracil is toxic for strains expressing A*adho*

Since expression of fungal dho genes enabled uracil-auxotrophic mutants of *S. cerevisiae* to grow on SMD+dhu, they can be used as dominant selectable marker genes in such strains. To explore their possible use as counter-selectable markers in this yeast, we investigated whether the DHUOs encoded by A*adho* and S*cdho* convert 5-fluorodihydrouracil (5F-dhu) into the toxic compound 5-fluorouracil (5-FU), as has been described for mammalian DHPDs (**397**,**410**). The two DHUO-expressing strains *S. cerevisiae* IMI433 and IMI434, the uracil-auxotrophic strains IMX581 (*ura3*Δ) and IMK824 (*ura1*Δ) and the reference strain IMX585 (*URA1*) were plated on SMD+ura and on SMD with 5F-dhu and uracil. Growth of the reference strain IMX585 was not substantially affected by 5F-dhu (**Figure 5.5**). In contrast, 5F-dhu strongly inhibited growth of the DHUO-expressing strains and even completely blocked growth of strain IMI433 (*ura1*Δ::A*adho*). Growth of the *ura1* and *ura3* null mutants IMK824 and IMX581 on SMD+ura was also inhibited by 5F-dhu, to similar extent as the inhibition observed for strain IMI434 (*ura1*Δ::S*cdho*). This observation suggests that 5F-dhu inhibits uracil uptake via the *S. cerevisiae* Fur4 transporter (**172**). The much stronger growth inhibition by 5F-dhu observed for strain IMI433 indicates that AaDho has activity towards this substrate while, based on the growth assays on plates, no conclusion could be drawn on whether the same holds for ScDho.

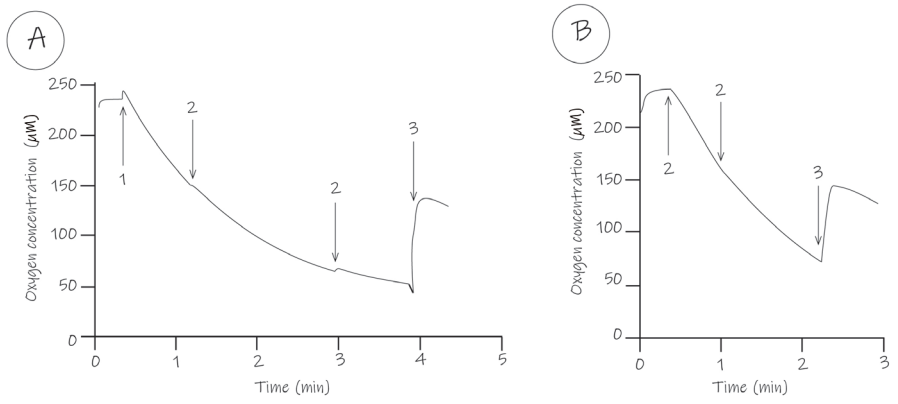

Figure 5.4. Dihydrouracil-dependent oxygen consumption and catalase-dependent oxygen formation during oxidation of dihydrouracil by cell extracts of *S. cerevisiae* strains expressing fungal dihydrouracil oxidases.

Reaction volumes of 4 mL contained cell extracts of **A.** *S. cerevisiae* IME664 (A*adho*), **B.** strain IME665 (S*cdho*). Oxygen concentration was monitored with a Clark-type electrode. Arrows indicate the following additions: 1; 0.125 mM dihydrouracil, 2; 0.25 mM dihydrouracil, 3; approximately 500 U catalase.

A*adho* can be used as counter-selectable marker gene

To test counter-select ability, A*adho* and S*cdho* were expressed in a *ura3* null mutant of *S. cerevisiae* from a plasmid that also carried a *URA3* marker gene. These strains were then tested for plasmid loss and viability after growth on SMD+ura with and without 5F-dhu. The reference strain IME426, which contained the *URA3*-carrying empty plasmid, showed the same viability after growth on SMD+ura with and without 5F-dhu (**Table 5.3**). The fraction of viable cells of this strain that had lost the plasmid after growth on SMD+ura with 5F-dhu was lower than after growth on SMD+ura (50 % versus 67 %; **Table 5.3**). This observation was consistent with the hypothesis that 5F-dhu inhibits uracil uptake.

In contrast to the empty-plasmid control strain, *S. cerevisiae* strains harbouring plasmid-borne expression cassettes for A*adho* (IME410) or S*cdho* (IME414) showed a 2.1-fold and 1.6-fold lower fraction of viable cells, respectively, after growth on SMD+ura with 5F-dhu than after growth on SMD+ura. This indication that 5F-dhu was toxic for both strains was even more strongly supported by the observation that, after growth on SMD+ura with 5F-dhu, strains IME414 (expressing A*adho*), IME410 (expressing S*cdho*) showed plasmid losses of 99.4 % and 93 %, respectively. This difference was consistent with results from

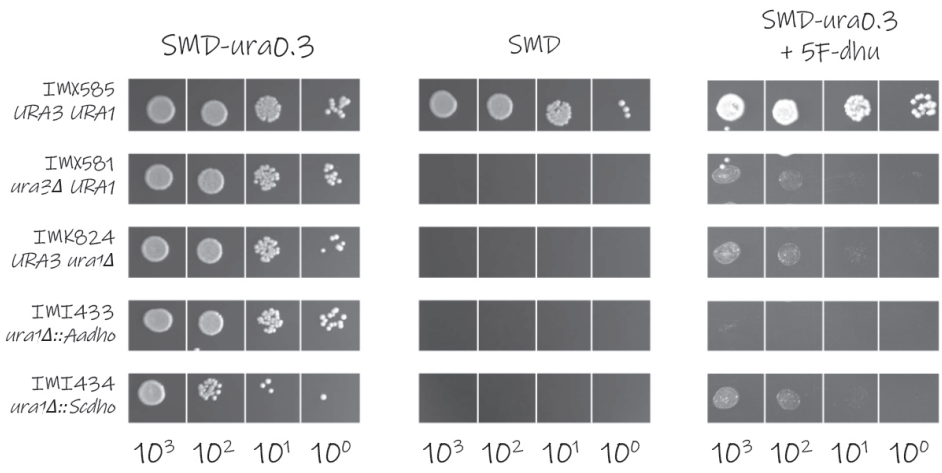

Figure 5.5. Effect of 5-fluorodihydrouracil on growth of *S. cerevisiae* strains expressing fungal dihydrouracil oxidases.

Strains IMX585 (*URA1*), IMK824 (*ura1*) and IMX581 (*ura3* null mutant), IMI433 (*URA1* multi-copy A*adho*) and IMI434 (multi-copy Sc*dho*) were plated on synthetic medium with 20 g L^{-1} glucose (SMD; left), medium supplied with 150 mg L^{-1} uracil (SMD+ura; middle) and SMD supplied with 50 mg L^{-1} dihydrouracil and 2.5 g L^{-1} of 5-fluorodihydrouracil (SMD+ura0.3+5F-dhu; right) and incubated aerobically at 30°C for 2 d. Duplicate experiments yielded the same results.

growth experiments with strains expressing a single copy of the *dho* genes, in which strain IMI433 showed a stronger growth inhibition by 5F-dhu than strain IME434 (**Figure 5.5**). In contrast, DHUO activities were higher in cell extracts of *S. cerevisiae* IME665, which expressed ScDho, than in the AaDho-expressing strain IME664 (**Table 5.2**). These results indicate that *Aadho* can be effectively selected against by growth of *S. cerevisiae* strains in non-selective medium supplemented with 5F-dhu.

Table 5.3. Effect of 5-fluoro-dihydrouracil on viability and plasmid loss of *S. cerevisiae* strains expressing the fungal dihydrouracil oxidase genes Aa*dho* and Sc*dho*.

Yeast strains were grown to late-exponential phase on either SMD with 1.5 g L^{-1} uracil (SMD+ura) or on SMD supplemented with both 0.15 g L^{-1} uracil (SMD+ura0.1) and 2.5 g L^{-1} 5F-dhu. Viability was calculated as the percentage of 768 cells plated on SMD+ura that formed colonies. Plasmid loss was calculated from the ratio of cell counts after plating on SMD and SMD+ura. Results are presented as the average ± mean deviation of data obtained with duplicate cultures for each strain.

Strain	Relevant genotype	CFU (%)		Plasmid loss (%)	
		SMD+ura	SMD+ura0.1 +5F-dhu	SMD+ura	SMD+ura0.1 +5F-dhu
IME426	ura3-52 pUD63 (*URA3*)	84 ± 2	87 ± 1	67 ± 2	50 ± 1
IME410	ura3-52 pUDE737 (*URA3* Aa*dho*)	92 ± 2	44 ± 6	61 ± 3	99 ± 0
IME414	ura3-52 pUDE736 (*URA3* Sc*dho*)	91 ± 0	57 ± 5	60 ± 2	94 ± 1

Discussion

While searching fungal proteomes for indications of horizontal gene transfer (HGT) of genes encoding Class-I DHODs, we serendipitously found a large cluster of fungal orthologs of the Class-I DHOD of the yeast *L. kluyveri*. Two fungal genes encoding representatives from this cluster, one from an ascomycete and one from a basidiomycete, were found to encode dihydrouracil oxidases (DHUO, EC1.3.3.7). Based on a phylogenetic analysis, it is highly probable that such dho genes occur in a wide range of ascomycetes and basidiomycetes (**Figure 5.1**). Hitherto, DHUO activity had only been reported in two studies on the yeast *R. glutinis* (**405**,**406**) and no structural gene for DHUO had been identified. Despite their extensive sequence similarity with Class-I-dihydroorotate dehydrogenases (DHOD) from the yeasts *L. kluyveri* and *S. cerevisiae* (SI Figure S1), heterologous expression of the two *dho* genes in an *S. cerevisiae ura1*Δ strain did not complement its uracil prototrophy unless dihydrouracil was included in growth media (**Table 5.1**), and complementation was oxygen dependent (**Figure 5.3**).

In addition to the large cluster of putative fungal Dho sequences, a small group of LkUra1 orthologs was found in *Mucor* species, which showed stronger similarity with LkUra1 and Ura1 orthologs from other Saccharomycotina yeasts than with the putative Dho family. Together with a brief mention

in the literature that *Mucor* DHOD resembles Class I-A enzymes (**411**), this observation suggested that, similar to some Saccharomycotina yeasts, these dimorphic fungi have acquired a Class-I-A DHOD by horizontal gene transfer. Consistent with this interpretation, a protein Blast search showed that all eight Mucormycete Ura1-orthologs showed high sequence similarity to Class-I DHODs from Neisseriacaea (Table S2). Further research should verify if these proteins indeed encode Class I-A DHODs, for example by heterologous expression of a putative *Mucor ura1* gene in an *S. cerevisiae ura1*Δ strain, and investigate a possible relation with the reported pyrimidine-prototrophic anaerobic growth of *Mucor* species (**408**).

Dihydrouracil and dihydrothymine, the substrates of DHUO, are intermediates of the reductive pathway for pyrimidine degradation, which also provides β-alanine for pantothenate synthesis (**389**,**412**). Ultraviolet radiation induces conversion of pyrimidines in DNA into dihydrouracil, dihydrothymine and dihydrocytosine (**413**,**414**). Subsequent base- or nucleotide excision repair can lead to direct or indirect release of dihydropyrimidines in cells (**415**). Recent studies on cancer cells and on *in vitro* DNA replication in *Xenopus* egg extracts showed that dihydropyrimidines cause DNA-protein crosslinking, interfere with DNA replication and cause transcriptional stress (**416**). In mammalian cells, the zinc metalloprotein dihydropyrimidinase is a key enzyme for dihydropyrimidine detoxification (**417**,**418**). Dihydropyrimidinase in the yeast *L. kluyveri* was also shown to be zinc protein (**419**) and, based on sequence similarity, this enzyme probably occurs in many other fungi (Dataset_S03). However, DHUO may still play a role in dihydropyrimidine detoxification during disbalances in pyrimidine metabolism, for example when zinc limitation prevents optimal activity of dihydropyrimidinase.

Sequences of fungal DHUOs showed a very strong sequence similarity with Class-I-A DHOD sequences, with conserved residues for flavin binding and in putative catalytic site (Figure S1), while no indications were found for binding of the four [4Fe-4S] clusters that occur in homodimeric mammalian dihydropyrimidine dehydrogenases. The reactions catalysed by DHOD and DHUO, a flavin-mediated reduction of fumarate and an oxidase reaction, respectively, appear remarkably different in view of their strong sequence similarity. However, Class-I DHODs as well as quinone-dependent Class-II DHOD show a low rate of oxygen-dependent dihydroorotate oxidation (**167**,**350–352**). The evolutionary plasticity of cofactor used by these enzymes is also evident from the recent finding that Class-II DHODs in obligately anaerobic fungi evolved to alter their cofactor specificity, thereby acquiring the ability to support pyrimidine synthesis in the absence of mitochondrial respiration (see **Chapter 4**). Detailed structure-function analysis is required to resolve the structural factors that determine the different electron donor and electron acceptor specificities of Class-I DHODs and DHUOs, and to dissect the evolutionary histories of these enzymes in fungi. Pyrimidine degradation routes have been hypothesised to derive from neofunctionalisation of biosynthesis proteins (**420**). It will be interesting to explore whether additional neo- or retrofunctionalisation events have occurred, or can be made to occur in the lab (**421**), that change DHUOs into either dihydroorotate oxidases or dihydrouracil dehydrogenases or vice versa.

Methods

Growth media. Synthetic medium with 20 g L^{-1} D-glucose (SMD) for growth of *S. cerevisiae* was prepared and sterilised as described previously (**126**). Anaerobic cultures were grown on synthetic medium with urea as nitrogen source (SMUD), supplemented with the anaerobic growth factors Tween 80 and ergosterol (**232**). Uracil was added to media as an autoclaved (121 °C, 20 min) 3.75 g L^{-1} uracil solution, to final concentrations of either 0.15 g L^{-1} (SM(U)D+ura), 50 mg L^{-1} (SM(U)D+ura0.3) or 15 mg L^{-1} (SM(U)D+ura0.1) as indicated. When indicated, dihydrouracil (Sigma-Aldrich, St. Louis, Missouri, USA) was added to media prior to sterilisation, to a concentration of 0.15 g L^{-1}. Similarly, a filter-sterilised stock solution of 5-fluorodihydrouracil (5F-dhu; abcr GmbH, Karlsruhe, Germany) was added to sterile medium to a concentration of 2.5 g L^{-1} where indicated. Complex yeast extract-peptone-dextrose medium (YPD) was prepared as described previously. For selection of strains harbouring the *kanMX* marker gene, 200 mg L^{-1} of Geneticin (G418) was added to YPD. *Escherichia coli* cultures were grown on Lysogeny Broth (LB; **372**) autoclaved at 121 °C for 20 min and supplemented with 100 mg L^{-1} ampicillin (LB-amp). Solid media were prepared by adding 20 g L^{-1} Bacto Agar (BD Biosciences).

Strains and maintenance. *S. cerevisiae* strains used in this study (**Table 5.4**) were derived from the CEN.PK lineage (**422**). For preparation of frozen stock cultures, yeast strains were pre-grown on SMD+ura (**126**). Plasmid-containing *E. coli* XLI-blue (Agilent Technologies, Santa Clara, CA, USA) strains were pre-grown at 37 °C and *S. cerevisiae* strains at 30 °C in an Innova incubator shaker (New Brunswick Scientific, Edison, NJ, USA) set at 200 rpm. Cultures were harvested in stationary phase, supplemented with 30 % (w/v) glycerol and stored at -80 °C.

Molecular Biology Techniques. PCR amplification was performed with Phusion High-Fidelity Polymerase (Thermo Fischer Scientific, Waltham, MA, USA) or DreamTaq (Thermo Fisher Scientific) for cloning and diagnostic purposes, respectively, according to manufacturers' protocols. Oligonucleotide primers (SI Table S1) were purchased from Sigma-Aldrich. PCR products amplified from plasmid templates were digested with FastDigest DpnI (Thermo Fischer Scientific) to avoid contamination with template DNA. Fragment sizes were analysed by electrophoresis on 1 % (w/v) agarose gels. PCR products were purified with the GeneElute PCR Clean-Up Kit (Sigma-Aldrich) or the Zymoclean Gel DNA Recovery Kit (Zymo Research, Irvine, CA, USA) following manufacturers' protocols. Plasmids were purified using the GeneElute Plasmid Miniprep Kit (Sigma-Aldrich).

Plasmid construction. Coding regions of DHUO genes from *A. alternata* (A0A177DSV5) and *Sch. commune* (D8QKJ0), referred to as A*adho* and Sc*dho*, respectively, were derived from the UniProt Database (**379**). Plasmids pUD709 (Sc*dho*) and pUD708 (A*adho*), carrying versions of these sequences that were codon optimised for expression in *S. cerevisiae* using the online GeneOptimizer tool (**312**), were obtained from GeneArt (GeneArt, Regensburg, Germany; **Table 5.5**). Coding regions were PCR amplified from these plasmids using primer pairs 12365/12366 and 12363/12364, respectively. A pUDE63 backbone, containing a *TDH3* promoter and an *AHD1* terminator, was PCR amplified with primer

Table 5.4. *S. cerevisiae* strains used in this study.

Strain	Relevant genotype	Reference
CEN.PK 113-5D	*MATa HIS3 LEU2 TRP1 ura3-52*	(**422**)
CEN.PK 113-7D	*MATa HIS3 LEU2 TRP1 URA3*	(**422**)
IMX581	*MATa HIS3 LEU2 TRP1 ura3-52 can1Δ::cas9-natNT2*	(**59**)
IMX585	*MATa HIS3 LEU2 TRP1 URA3 can1Δ::cas9-natNT2*	(**59**)
IMK824	*MATa HIS3 LEU2 TRP1 URA3 can1Δ::cas9-natNT2 ura1Δ*	This study
IMI433	*MATa HIS3 LEU2 TRP1 URA3 can1Δ::cas9-natNT2 ura1Δ::Aadho*	This study
IMI434	*MATa HIS3 LEU2 TRP1 URA3 can1Δ::cas9-natNT2 ura1Δ::Scdho*	This study
IME410	*MATa HIS3 LEU2 TRP1 ura3-52* pUDE737	This study
IME414	*MATa HIS3 LEU2 TRP1 ura3-52* pUDE736	This study
IME426	*MATa HIS3 LEU2 TRP1 ura3-52* pUD63	This study
IME664	*MATa HIS3 LEU2 TRP1 URA3 can1Δ::cas9-natNT2 ura1Δ* pUDE737	This study
IME665	*MATa HIS3 LEU2 TRP1 URA3 can1Δ::cas9-natNT2 ura1Δ* pUDE736	This study

pair 7823/7998, followed by Gibson Assembly (New England Biolabs, Ipswich, MA, USA; (**423**) with the A*adho* and S*cdho* coding regions. The resulting plasmids pUDE736 (*TDH3*p-A*adho-ADH1*t) and pUDE737 (*TDH3*p-S*cdho-ADH1*t) carried yeast expression cassettes for the two putative dho genes. pUDR348, which carries an expression cassette for a guide RNA targeting the *URA1* locus of *S. cerevisiae* IMX585 (*can1Δ::cas9-natNT2*) was constructed by Gibson assembly of a pMEL13 backbone and 2µm fragment as described previously (**59**). The pMEL13 backbone was amplified with PCR primer 6005 and the 2µm fragment with primer pair 11334/11335 (SI Table S1). *E. coli* XLI-Blue was transformed with the constructed plasmids and incubated for 5 min on ice, followed by 1 h incubation at 37 °C prior to plating on LB with ampicillin.

Strain construction. *S. cerevisiae* strains were transformed with the LiAc/SS-DNA/PEG-method (**374**), using 1-2 µg plasmid DNA. *S. cerevisiae* strains IME410, IME414 and IME426 were constructed by transformation of CEN.PK 113-5D (*ura3-52*) with plasmids pUDE737 (A*adho*), pUDE736 (S*cdho*) and pUD63 (empty vector), respectively, followed by selection on SMD plates and diagnostic PCR. Similarly, IME664 (*ura1Δ* mcA*adho*) and IME665 (*ura1Δ* mcS*cdho*) were constructed by transforming the *S. cerevisiae ura1* null mutant IMK824 with pUDE737 (A*adho*) and pUDE736 (S*cdho*). For Cas9-mediated deletion or integration of genes in the Cas9-expressing reference strain *S. cerevisiae* IMX585 (*can1Δ::cas9-natNT2*; **59**), a published CRISPR/Cas9 protocol was used (**58**). The *URA1* locus was targeted using the guide-RNA

Table 5.5. Plasmids used in this study.

Strain	Relevant charcateristic	Reference
pUD63	2µm *ampR URA3 TDH3*p-*ADH1*t	(**424**)
pUD708	*ampR Scdho*	GeneArt
pUD709	*ampR* A*adho*	GeneArt
pMEL13	2µm *ampR kanMX* gRNA-*CAN1*	(**59**)
pUDE63	2µm *ampR URA3 TDH3*p-*pgmB-ADH1*t	(**424**)
pUDE736	2µm *ampR URA3 TDH3*p-*Scdho-ADH1*t	This study
pUDE737	2µm *ampR URA3 TDH3*p-A*adho-ADH1t*	This study
pUDR348	2µm *ampR kanMX* gRNA-*URA1*	This study

plasmid pUDR348. For construction of the *ura1* deletion strain IMK824, strain IMX58 was co-transformed with a repair oligonucleotide obtained by annealing oligonucleotides 11336 and 11337 (SI Table S1) and pUDR348. For integration of expression cassettes of the putative *dho* genes from *A. alternata* and *Sch. commune*, repair fragments containing these genes with upstream and downstream flanking *URA1* sequences, were amplified from pUDE736 and pUDE737, respectively, with primers 12479 and 12480. Integration of these fragments at the *URA1* locus yielded strains IMI433 (*ura1*Δ::A*adho*) and IMI434 (*ura1*Δ::*Scdho*), respectively.

Phylogeny of putative LkUra1 orthologs. For a systematic search for Ura1 orthologs, fungal reference proteomes (taxid 4751) available from UniProt reference proteomes release 2019_02 (**379**) were supplemented with sequences available from the UniProt trembl division for the following organisms: *D. bruxellensis* (taxid 5007), *Komagataella phaffii* (taxid 981350), *Komagataella pseudopastoris* (taxid 169507), *Komagataella pastoris* (taxid 4922), *Ogataea polymorpha* (taxid 460523), *Pichia membranifaciens* (taxid 763406), *Pichia kudriavzevii* (taxid 4909), *Neocallimastix californiae* (taxid 1754190), *Piromyces finnis* (taxid 1754191), *Anaeromyces robustus* (taxid 1754192) and *Piromyces* sp. E2 (taxid 73868). The sequence of Ura1 of *L. kluyveri* CBS3082 (LkUra1, Q7Z892; **159**) was used as query for a HMMER search of these sequences (**282**). Cutoff values of 1e-5 were used, and hits were required to correspond to at least 75 % of the query sequence length. From the resulting sequence, Ura1 orthologs were identified by calculating all possible co-ortholog sets with proteinortho v6.0.25 (**380**) running diamond v2.0.8 (**381**). The resulting 203 fungal Ura1 orthologs (Dataset_S01) were subjected to a multiple sequence alignment using MAFFT v7.40286 (**320**) in "einsi" mode. Alignments were trimmed using trimAl v1.287 (**321**) in "gappyout" mode, and used to build a phylogenetic tree with RAxML-NG v0.8.188 (**322**) using 10 random and 10 parsimony starting trees, 100 Felsestein Bootstrap replicates, and LG model. The resulting phylogenetic tree (Dataset_S02) was visualised using iTOL (Interactive Tree Of Life) tool v6 (**323**). To search for fungal

homologs of dihydropryimidinases (DHP), a protein search (blastp; **425**) was performed on fungal proteomes (taxid: 4751) with the DHP protein of *L. kluyveri* (Uniprot KB accession: Q9P903) as query. All proteins scores with an E-value below 1e-50 are provided in Dataset_S03.

Aerobic growth experiments. Shake-flask cultures were grown in 500-mL flasks containing 100 mL of medium. A frozen stock culture was used to inoculate a pre-culture on SMD+ura. Upon reaching stationary phase, a 1-mL sample of this pre-culture was transferred to a second pre-culture on SMD+ura0.1. This second pre-culture was grown until late exponential phase, centrifuged (5 min at 3000 *g*), washed twice with sterile demineralised water and used as inoculum for either plate or shake-flask growth experiments. Shake flasks were incubated in an Innova incubator (New Brunswick Scientific), operated at 30°C and at 200 rpm. Agar plates were incubated for 2 d at 30 °C. For cell sorting experiments, SMD was used for the first pre-culture, while the second culture was grown on either 1 mL SMD+ura0.1 supplemented with 5F-dhu and or on 1 mL SMD+ura in a sterile 1.5 mL Eppendorf tube (Eppendorf Corporate, Hamburg, Germany).

Anaerobic cultivation. Anaerobic cultures were grown in a Bactron 300-2 anaerobic workstation (Sheldon Manufacturing Inc, Cornelius, OR, USA) with equipped with a Pd-catalyst and filled with a mixed gas atmosphere (85 % N_2, 10 % CO_2, 5 % H_2). To minimise oxygen entry, the protocols described by Chapter 2 for cultivation in anaerobic chambers were followed. Flasks were placed on an IKA KS 260 basic orbital shaker (IKA-Werke, Staufen im Breisgau, Germany) at 240 rpm and temperature in the workspace was maintained at 30 °C. Strains were pre-grown aerobically, centrifuged (3000 *g*, 5 min), washed with sterile demineralised water and used to inoculate medium in the anaerobic workspace. The initial optical density at 600 nm of anaerobic pre-cultures, which were grown on SMUD+dhu0.1 or SMUD+ura0.1 was 0.2. Stationary-phase pre-cultures were used to start subsequent anaerobic growth experiments on SMUD or SMUD+dhu. All anaerobic (pre)cultures were supplemented with Tween 80 and ergosterol.

Analytical methods and calculation. Optical density of aerobic cultures was measured at 660 nm (OD_{660}) with a Jenway 7200 Spectrophotometer (Bibby Scientific, Staffordshire, UK). Maximum specific growth rates were calculated from the slope of ln OD_{660} versus time during the exponential phase, taking into account at least six time points. Optical density measurements in anaerobic cultures were performed at 600 nm with an Ultrospec 10 cell density meter (Biochrom, Harvard Biosience, Holliston, MA, USA) placed in the anaerobic workstation. For spot-plate experiments, cell counts in late-exponential-phase shake-flask cultures were first determined using a Z2 Coulter Counter Analyzer (Beckman Coulter Life Sciences, Indianapolis, IN, USA) following the manufacturer's protocol. Prior to analysis, cultures were diluted one hundred-fold with Isoton II (Beckman Coulter, Brea, CA, USA), followed by five replicate cell counts on each sample.

Cell extract preparation and enzyme assays. Cell extracts were prepared by sonication and centrifugation (**384**) of cells grown aerobically on SMUD+dhu. Protein concentrations in cell extracts were determined with the Lowry method (**385**) and with bovine serum albumin as reference. Oxygen consumption was measured with a Clark-type electrode at 30 °C in 0.1 M potassium phosphate buffer (pH 7.5) with 2 mM $MgCl_2$ as described previously (**344**), using two independently prepared cell extracts

for each yeast strain,. Air-saturated buffer (236 µM) was used to calibrate the oxygen electrode. Assays were performed in a reaction volume of 4 mL and started by addition of dihydrothymine or dihydrouracil (final concentration 0.1 mM). Production of H_2O_2 was tested by addition of 2 or 5 µL catalase suspension from bovine liver (200,000 U mL^{-1}; Sigma Aldrich) during the reaction.

Viability and plasmid loss assays. Single cells were sorted with a BD FACSAria II SORP cell sorter (BD Biosciences) as described previously (**426**), with the modification that cells were sorted based on forward scatter (FSC) and side scatter (SSC) instead of fluorescence. Late-exponential-phase cultures grown on either SMD+ura+5F-dhu or on SMD were diluted ten-fold in sterile Isoton II (Beckman Coulter) and >105 events were analysed. The FSC of analysed events was plotted against the SSC to set the sorting region such that bias for cell morphology was avoided. Unless indicated differently, 4 x 384 single cells were sorted from each culture using the single-cell sorting mask (0/32/16), and placed on two SMD and two SMD+ura plates.

Availability data and material

All data generated or analysed in this study have been made available online: https://figshare.com/s/9ec9590f4662f640b72a

Supplemental information is available via the preprint: https://doi.org/10.21203/rs.3.rs-762539/v1

5

Acknowledgements

We thank Charlotte Koster for help with the FACS analyses and our colleagues at the Industrial Microbiology group of TU Delft for inspiring discussions.

Outlook

The research described in this thesis addresses a long-standing question in fundamental and applied yeast research: why are so many yeast species that are able to ferment sugars to ethanol, unable to grow in the absence of oxygen?

From a fundamental point of view, this research question can be translated in the question which evolutionary adaptations enabled a small minority of eukaryotic species to acquire the ability to grow in strictly anoxic requirements. Before this question could be experimentally tackled, a technical problem needed to be surmounted. The amounts of oxygen required by some yeast species are so small that even minute oxygen leakages in cultivation systems can easily lead to erroneous conclusions on the ability to grow anaerobically. Therefore, the research team of the ERC project 'ELOXY' (Elimination Oxygen Requirements in Yeasts) of which this PhD project was a part, invested much time and effort in minimising oxygen entry into bioreactor cultures and into anaerobic chambers. By sharing pitfalls and key experimental design criteria with colleagues (**Chapter 2**, also published in a specialised yeast research journal) it is intended to help avoid confusing reports on anaerobic growth capabilities of yeasts due to uncertainty about the impact of inadvertent oxygen entry into cultivation systems. Some of the relevant discoveries on experimental design, such as the implementation of membrane contactors for removing traces of oxygen from the inlet medium of bioreactors, came too late to have an impact on this project, but will undoubtedly facilitate further research on anaerobic microbiology at the TU Delft and elsewhere.

The need for extensive measures to minimise oxygen entry, with the goal to rule out misinterpretation of results due to oxygen leakage, made the experiments described in this thesis quite laborious. To extend the research described in this thesis to a larger number of yeasts and fungi and to test hypotheses by genetic modification, high-throughput methods for cultivation under strictly anaerobic conditions should be developed and tested. In view of the importance of pre-cultivation steps and serial transfer for interpretation of anaerobic growth experiments outlined in **Chapter 2**, such experiments may require the design and implementation of anaerobic workstations with internal robotics to inoculate, monitor and transfer cultures. Since anaerobic pre-cultures play an elemental role in the cultivation setup, high-throughput set-ups might, for example, include 24-well plate shakers and a pipetting robot installed in an anaerobic workspace.

One of the priority targets for this research project was the synthesis of pyrimidines which, in the large majority of eukaryotes, is coupled to mitochondrial respiration and therefore requires oxygen. According to the literature available at the start of the project, the ability of eukaryotic cells to grow anaerobically without supplementation of pyrimidines was coupled to the presence, in only a small number of yeasts and fungi, of a soluble Class I-A dihydroorotate dehydrogenase. *Saccharomyces cerevisiae* and a small number

of related yeasts, acquired a gene encoding such an enzyme by horizontal gene transfer from lactic acid bacteria. The research described in **Chapter 4**, shows that a completely different adaptation to anaerobic pyrimidine biosynthesis occurred independently at least three times in the evolution of yeast and fungal lineages. This adaptation enabled the 'canonical' respiration-linked Class-II dihydroorotate dehydrogenases to function in anaerobic cells. For Neocallimastigomycetes, a group of deep-branching, strictly anaerobic fungi, we showed that the evolved anaerobically active enzyme not only used soluble FAD and FMN, instead of quinone, as electron acceptors, but was also no longer membrane associated. This observation did, however, not address all questions on this remarkable evolutionary adaptation. In particular, it would be highly interesting to understand which structural changes in the protein are needed for the observed cofactor specificity. The demonstration, in **Chapter 4**, that the responsible gene can be functionally expressed in yeast will facilitate such studies, as Neocallimastigomycetes themselves are difficult to grow and are not yet accessible for genome editing techniques.

Also the yeasts *Schizosaccharomyces japonicus* and, in line with earlier reports, *Dekkera bruxellensis*, were shown to harbour anaerobically functional Class II dihydroorotate dehydrogenases, which coincided with their ability to grow anaerobically without supplementation of pyrimidines. We still do not fully understand how these enzymes, SjUra9 and DbUra9, evolved to support anaerobic pyrimidine synthesis. Both enzymes retained their quinone binding sites, suggesting quinone might still be involved in their activity. We were, however, unable to detect activities of these mitochondrial targeted enzymes in cell extracts or isolated mitochondria. Identification of their cofactor specificity may therefore require protein purification and/or expression in a prokaryotic host. In addition, it would be interesting to test if quinones play a role in their anaerobic activity by expressing them in *ura1*Δ yeast strains in which quinone synthesis has been disabled.

A particularly enigmatic aspect of the anaerobically active Class II dihydroorotate dehydrogenases is related to a shared cysteine residue in their active sites, which sets them apart from almost all other Class II enzymes from yeasts and fungi, which instead have a serine in this position. In fact, although not expressly stated in **Chapter 3**, it was this cysteine residue that first attracted my attention to *Sch. japonicus*, which formed the basis for a very interesting new line of research. It would be highly interesting to also test anaerobic activity of three putative Class-II enzymes from three little studied fungal species that shared this peculiar characteristic, as well as the anaerobic growth characteristics of these species. More importantly, structure-function analysis should resolve what role, if any, this cysteine residue plays in the acquisition of anaerobic functionality and electron acceptor use. This question may be addressed studied with heterologously expressed and purified enzymes in which this residue has been changed for other amino acids. Based on a recent publication (**179**) that describes the diversity of Class II enzymes, also a number of bacterial enzymes with a cysteine in their active sites could be included in such studies.

A final aspect of the research on dihydroorotate dehydrogenases that merits further research is the apparent trade-off between anaerobic functionality and induction of loss of respiratory competence in *S. cerevisiae* strains expressing SjUra9. Transcriptome analysis as well as measurements of reactive oxygen species in strains of *S. cerevisiae* (over)expressing SjUra9 are likely to shed more light on this intriguing

observation.

In **Chapter 3** we showed another remarkable adaptation of *Sch. japonicus* to an anaerobic lifestyle that effectively eliminated the 70-year old dogma in yeast physiology that anaerobic growth of yeasts requires a source of sterols. The fast anaerobic growth of this peculiar yeast in the absence of both sterols and unsaturated fatty acids has not been observed for any other yeast. The research described in this thesis shows that its ability, also unique among yeasts, to produce hopanoids contributes to its sterol-independent anaerobic growth. However, while expression of the responsible gene in *S. cerevisiae* indeed led to hopanoid production, anaerobic growth of the resulting strain in anaerobic, sterol-free medium was much slower than that of sterol-supplemented cultures. This observation indicates that, in addition to hopanoids, membranes of *Sch. japonicus* have other characteristics that contribute to fast, sterol-dependent anaerobic growth. Detailed analysis of the membrane composition and architecture of *Sch. japonicus* membranes and reconstruction of key characteristics in *S. cerevisiae* will contribute to a deeper insight into a unique eukaryotic adaptation to anaerobic environments. In addition, development of sterol-independent, robust yeast strains can be extremely relevant for the development of anaerobic yeast 'cell factories' that can be applied for processing of feedstocks, without a need for aeration to prevent sterol depletion and 'stuck' fermentations.

Chapter 5 was a spin-off of the research on dihydroorotate dehydrogenases described in **Chapter 3**. Identification of structural genes for fungal dihydropyrimidine oxidase, an enzyme activity that had only been reported once before in the literature, raises the tantalising question what the physiological role of these enzymes is. Genome-wide expression studies in strains lacking or overexpressing these enzymes, coupled with hypothesis-driven research (e.g. on a possible link with DNA excision repair mechanisms) provide logical first steps for follow-up research on this topic.

References

1. Liu L, Wang J, Rosenberg D, Zhao H, Lengyel G, Nadel D. Fermented beverage and food storage in 13,000 y-old stone mortars at Raqefet Cave, Israel: Investigating Natufian ritual feasting. J Archaeol Sci Reports. Elsevier; 2018;21:783–93.

2. McGovern PE, Zhang J, Tang J, Zhang Z, Hall GR, Moreau RA, Nuñez A, Butrym ED, Richards MP, Wang CS, Cheng G, Zhao Z, Wang C. Fermented beverages of pre- and proto-historic China. Proc Natl Acad Sci U S A. 2004;101:17593–8.

3. Shawkat A. 5,000-year-old "industrial-scale" brewery unearthed in Egypt [Internet]. CBS News. 2021 [cited 2021 Jun 28]. Available from: https://www.cbsnews.com/news/egypt-5000-year-old-industrial-scale-brewery-unearthed

4. Dudley R. Evolutionary origins of human alcoholism in primate frugivory. Q Rev Biol. 2000;75:3–15.

5. Carrigan MA, Uryasev O, Frye CB, Eckman BL, Myers CR, Hurley TD, Benner SA. Hominids adapted to metabolize ethanol long before human-directed fermentation. Proc Natl Acad Sci U S A. 2015;112:458–63.

6. Levey DJ. The evolutionary ecology of ethanol production and alcoholism. Integr Comp Biol. 2004;44:284–9.

7. Gochman SR, Brown MB, Dominy NJ. Alcohol discrimination and preferences in two species of nectar-feeding primate. R Soc Open Sci. 2016;3.

8. Bossaert S, Crauwels S, Lievens B, De Rouck G. The power of sour - A review: Old traditions, new opportunities. BrewingScience. 2019;72:78–88.

9. van Leeuwenhoek A. Alle de brieven. Amsterdam: Swets & Zeitlinger; 1939.

10. Pasteur L. Études sur la bière. Paris: Gauthier-Villars; 1876.

11. Hansen EC. Recherches sur la physiologie et la morphologie des ferments alcooliques V. Methodes pour obtenir des cultures pures de *Saccharomyces* et de mikroorganismes analogues. C. R. Trav. Lab. Carlsberg 2. 1883.

12. Reich JG, Sel'kov EE. Energy metabolism of the cell: a theoretical treatise. London: Academic Press; 1981.

13. Huang W, Tang I. Chapter 8. Bacterial and Yeast Cultures – Process Characteristics, Products, and Applications. In: Yang S-T, editor. Bioprocessing for Value-Added Products from Renewable Resources: New Technologies and Applications. Ohio: Elsevier B.V.; 2007. p. 185–223.

14. Smith AM, ap Rees T. Pathways of carbohydrate fermentation in the roots of marsh plants. Planta. 1979;146:327–34.

15. Skory CD, Freer SN, Bothast RJ. Screening for ethanol-producing filamentous fungi. Biotechnol Lett.

1997;19:203–6.

16. Chandra Raj K, Ingram LO, Maupin-Furlow JA. Pyruvate decarboxylase: A key enzyme for the oxidative metabolism of lactic acid by *Acetobacter pasteurianus*. Arch Microbiol. 2001;176:443–51.

17. Van Zyl LJ, Schubert WD, Tuffin MI, Cowan DA. Structure and functional characterization of pyruvate decarboxylase from *Gluconacetobacter diazotrophicus*. BMC Struct Biol. 2014;14:1–13.

18. Fagernes CE, Stensløkken KO, Røhr ÅK, Berenbrink M, Ellefsen S, Nilsson GE. Extreme anoxia tolerance in crucian carp and goldfish through neofunctionalization of duplicated genes creating a new ethanol-producing pyruvate decarboxylase pathway. Sci Rep. 2017;7:1–11.

19. Thauer RK, Kirchniawy FH, Jungermann KA. Properties and function of the Pyruvate formate lyase reaction in *Clostridiae*. Eur J Biochem. 1972;27:282–90.

20. Knappe J, Schnacht J, Möckel W, Höpner T, Vetter H, Edenharder R. Pyruvate Formate-Lyase Reaction in *Escherichia coli*. Eur J Biochem. 1969;11:316–27.

21. Akhmanova A, Voncken FGJ, Hosea KM, Harhangi H, Keltjens JT, Op Den Camp HJM, Vogels GD, Hackstein JHP. A hydrogenosome with pyruvate formate-lyase: Anaerobic chytrid fungi use an alternative route for pyruvate catabolism. Mol Microbiol. 1999;32:1103–14.

22. Clark DP. The fermentation pathways of *Escherichia coli*. FEMS Microbiol Lett. 1989;63:223–34.

23. Dawes EA, Ribbons DW, Large PJ. The route of ethanol formation in *Zymomonas mobilis*. Biochem J. 1966;98:795–803.

24. Entner N, Douderoff M. Glucose and gluconic acid oxidation of *Pseudomonas saccharophila*. J Biol Chem. American Society for Biochemistry and Molecular Biology.; 1952;196:853–62.

25. Conway T. The Entner-Doudoroff pathway: history, physiology and molecular biology. FEMS Microbiol Rev. 1992;103:1–28.

26. Rogers PI, Jeon YJ, Lee KJ, Lawford HG. *Zymomonas mobilis* for fuel ethanol and higher value products. Adv Biochem Eng Biotechnol. 2007;108:263–88.

27. Doelle HW, Kirk L, Crittenden R, Toh H, Doelle MB. *Zymomonas mobilis* - Science and industrial application. Crit Rev Biotechnol Biotechnol. 1993;13:57–98.

28. DeMoss RD, Bard BC, Gunsalus IC. The mechanism of the heterolactic fermentation: A new route for ethanol formation. J Bacteriol. 1951;62:499–511.

29. Merico A, Sulo P, Piškur J, Compagno C. Fermentative lifestyle in yeasts belonging to the *Saccharomyces* complex. FEBS J. 2007;274:976–89.

30. van Dijken JP, van den Bosch E, Hermans JJ, de Miranda LR, Scheffers WA. Alcoholic fermentation by 'non-fermentative' yeasts. Yeast. 1986;2:123–7.

31. Visser W, Scheffers WA, Batenburg-Van der Vegte WH, Van Dijken JP. Oxygen requirements of yeasts. Appl Environ Microbiol. 1990;56:3785–92.

32. Bulder CJEA, Weijers C. Absence of cyanide-insenstive respiration in *Schizosaccharomyces japonicus*. FEMS Microbiol Lett. 1982;15:145–7.

33. De Deken RH. The Crabtree effect: a regulatory system in yeast. J Gen Microbiol. 1966;44:149–56.

34. Gutiérrez A, Boekhout T, Gojkovic Z, Katz M. Evaluation of non-*Saccharomyces* yeasts in the

fermentation of wine, beer and cider for the development of new beverages. J Inst Brew. 2018;124:389–402.

35. Rønnow B, Kielland-Brandt MC. *GUT2*, a gene for mitochondrial glycerol 3-phosphate dehydrogenase of *Saccharomyces cerevisiae*. Yeast. 1993;9:1121–30.

36. Bakker BM, Overkamp KM, van Maris AJA, Kötter P, Luttik MAH, van Dijken JP, Pronk JT. Stoichiometry and compartmentation of NADH metabolism in *Saccharomyces cerevisiae*. FEMS Microbiol Rev. The Oxford University Press; 2001;25:15–37.

37. van Gulik WM, Heijnen JJ. A metabolic network stoichiometry analysis of microbial growth and product formation. Biotechnol Bioeng. 1995;48:681–98.

38. Verduyn C, Stouthamer AH, Scheffers WA, van Dijken JP. A theoretical evaluation of growth yields of yeasts. Antonie Van Leeuwenhoek. 1991;59:49–63.

39. Juergens H, Hakkaart XDV, Bras JE, Vente A, Wu L, Benjamin KR, Pronk JT, Daran-Lapujade P, Mans R. Contribution of complex I NADH dehydrogenase to respiratory energy coupling in glucose-grown cultures of *Ogataea parapolymorpha*. Appl Environ Microbiol. 2020;86:1–18.

40. Postma E, Verduyn C, Scheffers WA, Van Dijken JP. Enzymic analysis of the crabtree effect in glucose-limited chemostat cultures of *Saccharomyces cerevisiae*. Appl Environ Microbiol. 1989;55:468–77.

41. Weusthuis RA, Pronk JT, Van Den Broek PJA, Van Dijken JP. Chemostat cultivation as a tool for studies on sugar transport in yeasts. Microbiol Rev. 1994;58:616–30.

42. Shoun H, Tanimoto T. Denitrification by the fungus *Fusarium oxysporum* and involvement of cytochrome P-450 in the respiratory nitrite reduction. J Biol Chem. 1991;266:11078–82.

43. Shoun H, Kim DH, Uchiyama H, Sugiyama J. Denitrification by fungi. FEMS Microbiol Lett. 1992;94:277–81.

44. Abe T, Hoshino T, Nakamura A, Takaya N. Anaerobic elemental sulfur reduction by fungus *Fusarium oxysporum*. Biosci Biotechnol Biochem. 2007;71:2402–7.

45. Yarlett N, Orpin CG, Munn EA, Greenwood CA. Hydrogenosomes in the rumen fungus *Neocallimastix patriciarum*. Biochem J. 1986;236:729–39.

46. Walker G, Stewart G. *Saccharomyces cerevisiae* in the production of fermented beverages. Beverages. 2016;2:30.

47. Gorter De Vries AR, Pronk JT, Daran JMG. Lager-brewing yeasts in the era of modern genetics. FEMS Yeast Res. 2019;19:1–17.

48. Hazelwood LA, Daran JM, Van Maris AJA, Pronk JT, Dickinson JR. The Ehrlich pathway for fusel alcohol production: A century of research on *Saccharomyces cerevisiae* metabolism. Appl Environ Microbiol. 2008;74:2259–66.

49. Engan S. Wort composition and beer flavour - the influence of some amino acids on the formation of higher aliphatic alcohols and esters. J Inst Brew. 1969;76:254–61.

50. Hilary A, Peddie B. Ester formation in brewery fermentations. J Inst Brew. 1990;96:327–31.

51. Suomalainen H. Yeast esterases and aroma esters in alcoholic beverages. J Inst Brew. 1981;87:296–

300.

52. Gombert AK, van Maris AJA. Improving conversion yield of fermentable sugars into fuel ethanol in 1st generation yeast-based production processes. Curr Opin Biotechnol. Elsevier Ltd.; 2015;33:81–6.

53. Jansen MLA, Bracher JM, Papapetridis I, Verhoeven MD, de Bruijn H, de Waal PP, van Maris AJA, Klaassen P, Pronk JT. *Saccharomyces cerevisiae* strains for second-generation ethanol production: from academic exploration to industrial implementation. FEMS Yeast Res. 2017;17:1–20.

54. Papapetridis I, Van Dijk M, Van Maris AJA, Pronk JT. Metabolic engineering strategies for optimizing acetate reduction, ethanol yield and osmotolerance in *Saccharomyces cerevisiae*. Biotechnol Biofuels. BioMed Central; 2017;10:1–14.

55. Papapetridis I, Goudriaan M, Vázquez Vitali M, De Keijzer NA, Van Den Broek M, Van Maris AJA, Pronk JT. Optimizing anaerobic growth rate and fermentation kinetics in *Saccharomyces cerevisiae* strains expressing Calvin-cycle enzymes for improved ethanol yield. Biotechnol Biofuels. BioMed Central; 2018;11:1–17.

56. Milne N, Wahl SA, van Maris AJA, Pronk JT, Daran JM. Excessive by-product formation: A key contributor to low isobutanol yields of engineered *Saccharomyces cerevisiae* strains. Metab Eng Commun. Elsevier; 2016;3:39–51.

57. Wess J, Brinek M, Boles E. Improving isobutanol production with the yeast *Saccharomyces cerevisiae* by successively blocking competing metabolic pathways as well as ethanol and glycerol formation. Biotechnol Biofuels. BioMed Central; 2019;12:1–15.

58. Dicarlo JE, Norville JE, Mali P, Rios X, Aach J, Church GM. Genome engineering in *Saccharomyces cerevisiae* using CRISPR-Cas systems. Nucleic Acids Res. 2013;41:4336–43.

59. Mans R, van Rossum HM, Wijsman M, Backx A, Kuijpers NGA, van den Broek M, Daran-Lapujade P, Pronk JT, van Maris AJA, Daran J-MG. CRISPR/Cas9: a molecular Swiss army knife for simultaneous introduction of multiple genetic modifications in *Saccharomyces cerevisiae*. FEMS Yeast Res. 2015;15:fov004.

60. Weusthuis RA, Visser W, Pronk JT, Scheffers WA, Van Dijken JP. Effects of oxygen limitation on sugar metabolism in yeasts: A continuous-culture study of the Kluyver effect. Microbiology. 1994;140:703–15.

61. Heijnen JJ, Roels JA. A macroscopic model describing yield and maintenance relationships in aerobic fermentation processes. Biotechnol Bioeng. 1981;23:739–63.

62. Andreasen AA, Stier TJB. Anaerobic nutrition of *Saccharomyces cerevisiae* I. Ergosterol requirement for growth in a defined medium. J Cell Comp Physiol. 1953;41:23–36.

63. Andreasen AA, Stier TJB. Anaerobic nutrition of *Saccharomyces cerevisiae* II. Unsaturated fatty acid requirement for growth in defined medium. J Cell Comp Physiol. 1954;43:271–81.

64. Dekker WJC, Wiersma SJ, Bouwknegt J, Mooiman C, Pronk JT. Anaerobic growth of *Saccharomyces cerevisiae* CEN.PK113-7D does not depend on synthesis or supplementation of unsaturated fatty acids. FEMS Yeast Res. 2019;19.

65. Casey GP, Magnus CA, Ingledew WM. High-gravity brewing: Effects of nutrition on yeast composition, fermentative ability, and alcohol production. Appl Environ Microbiol. 1984;48:639–46.

66. Hong J, Wang Y, Kumagai H, Tamaki H. Construction of thermotolerant yeast expressing thermostable cellulase genes. J Biotechnol. 2007;130:114–23.

67. Cabeca-Silva, C Madeira-Lopes A. Temperature relations of yields, growth and thermal death in the yeast *Hansenula polymorpha*. Z Allg Mikrobiol. 1984;24:129–32.

68. Walsh RM, Martin PA. Growth of *Saccharomyces cerevisiae* and *Saccharomyces uvarum* in a Temperature gradient incubator. J Inst Brew. 1977;83:169–72.

69. Fonseca GG, Heinzle E, Wittmann C, Gombert AK. The yeast *Kluyveromyces marxianus* and its biotechnological potential. Appl Microbiol Biotechnol. 2008;79:339–54.

70. Slininger PJ, Bothast RJ, Okos MR, Ladisch MR. Comparative evaluation of ethanol production by xylose-fermenting yeasts presented high xylose concentrations. Biotechnol Biofuels. 1985;7:431–6.

71. Li GJ, Hyde KD, Zhao RL, Hongsanan S, Abdel-Aziz FA, Abdel-Wahab MA, et al. Fungal diversity notes 253–366: taxonomic and phylogenetic contributions to fungal taxa. Fungal Divers. 2016;78:1–237.

72. Kuyper M, Harhangi HR, Stave AK, Winkler AA, Jetten MSM, de Laat WTAM, den Ridder JJJ, op den Camp HJM, van Dijken JP, Pronk JT. High-level functional expression of a fungal xylose isomerase: The key to efficient ethanolic fermentation of xylose by *Saccharomyces cerevisiae*. FEMS Yeast Res. 2003;4:69–78.

73. Wisselink HW, Toirkens MJ, del Rosario Franco Berriel M, Winkler AA, van Dijken JP, Pronk JT, van Maris AJA. Engineering of *Saccharomyces cerevisiae* for efficient anaerobic alcoholic fermentation of L-arabinose. Appl Environ Microbiol. 2007;73:4881–91.

74. Rubio-Texeira M, Arévalo-Rodríguez M, Luis Lequerica J, Polaina J. Lactose utilization by *Saccharomyces cerevisiae* strains expressing *Kluyveromyces lactis LAC* genes. J Biotechnol. 2000;84:97–106.

75. Ha SJ, Galazka JM, Kim SR, Choi JH, Yang X, Seo JH, Glass NL, Cate JHD, Jin YS. Engineered *Saccharomyces cerevisiae* capable of simultaneous cellobiose and xylose fermentation. Proc Natl Acad Sci U S A. 2011;108:504–9.

76. Meijnen JP, Randazzo P, Foulquié-Moreno MR, Van Den Brink J, Vandecruys P, Stojiljkovic M, Dumortier F, Zalar P, Boekhout T, Gunde-Cimerman N, Kokošar J, Štajdohar M, Curk T, Petrovič U, Thevelein JM. Polygenic analysis and targeted improvement of the complex trait of high acetic acid tolerance in the yeast *Saccharomyces cerevisiae*. Biotechnol Biofuels. BioMed Central; 2016;9:1–18.

77. Lindberg L, Santos AXS, Riezman H, Olsson L, Bettiga M. Lipidomic profiling of *Saccharomyces cerevisiae* and *Zygosaccharomyces bailii* reveals critical changes in lipid composition in response to acetic acid stress. PLoS One. 2013;8:1–12.

78. Snoek ISI, Steensma HY. Factors involved in anaerobic growth of *Saccharomyces cerevisiae*. Yeast. 2007;24:1–10.

79. da Costa BLV, Basso TO, Raghavendran V, Gombert AK. Anaerobiosis revisited: growth of *Saccharomyces cerevisiae* under extremely low oxygen availability. Appl Microbiol Biotechnol. Applied Microbiology and Biotechnology; 2018;102:2101–16.

80. Dashko S, Zhou N, Compagno C, Piškur J. Why, when, and how did yeast evolve alcoholic

fermentation? FEMS Yeast Res. 2014;14:826–32.

81. van Dijken JP, Scheffers WA. Redox balances in the metabolism of sugars by yeasts. FEMS Microbiol Lett. 1986;32:199–224.

82. Björkqvist S, Ansell R, Adler L, Lidén G. Physiological response to anaerobicity of glycerol-3-phosphate dehydrogenase mutants of *Saccharomyces cerevisiae*. Appl Environ Microbiol. 1997;63:128–32.

83. Kiers J, Zeeman AM, Luttik M, Thiele C, Castrillo JI, Steensma HY, Van Dijken JP, Pronk JT. Regulation of alcoholic fermentation in batch and chemostat cultures of *Kluyveromyces lactis* CBS 2359. Yeast. 1998;14:459–69.

84. Rodrigues F, Côrte-Real M, Leao C, Van Dijken JP, Pronk JT. Oxygen requirements of the food spoilage yeast *Zygosaccharomyces bailii* in synthetic and complex media. Appl Environ Microbiol. 2001;67:2123–8.

85. Scheffers WA. Stimulation of fermentation in yeast by acteoin and oxygen. Nature. 1966;210:533–4.

86. Wijsman MR, van Dijken JP, van Kleeff BHA, Scheffers WA. Inhibition of fermentation and growth in batch cultures of the yeast *Brettanomyces intermedius* upon a shift from aerobic to anaerobic conditions (Custers effect). Antonie Van Leeuwenhoek. 1984;50:183–92.

87. Dekker WJC, Juergens H, Ortiz-Merino RA, Mooiman C, van den Berg R, Mans R, Pronk JT. Re-oxidation of cytosolic NADH is a major contributor to the high oxygen requirements of the thermotolerant yeast *Ogataea parapolymorpha* in oxygen-limited cultures. BioRXiv [preprint]. 2021; Available from: https://doi.org/10.1101/2021.04.30.442227

88. Bakker BM, Bro C, Kotter P, Luttik MAH, Van Dijken JP, Pronk JT. The mitochondrial alcohol dehydrogenase Adh3p is involved in a redox shuttle in *Saccharomyces cerevisiae*. Journal Bacteriol. 2000;182:4730–7.

89. Tu BP, Weissman JS. Oxidative protein folding in eukaryotes: Mechanisms and consequences. J Cell Biol. 2004;164:341–6.

90. Camarasa C, Faucet V, Dequin S. Role in anaerobiosis of the isoenzymes for *Saccharomyces cerevisiae* fumarate reductase encoded by *OSM1* and *FRDS1*. Yeast. 2007;24:391–401.

91. Hamilton JA, Kamp F. How are free fatty acids transported in Membranes? Is It by proteins or by free diffusion through the lipids? Diabetes [Internet]. 1999;48:2255–69. Available from: http://diabetes.diabetesjournals.org/content/diabetes/48/12/2255.full.pdf

92. Wilcox LJ, Balderes DA, Wharton B, Tinkelenberg AH, Rao G, Sturley SL. Transcriptional profiling identifies two members of the ATP-binding cassette transporter superfamily required for sterol uptake in yeast. J Biol Chem. 2002;277:32466–72.

93. Alimardani P, Régnacq M, Moreau-Vauzelle C, Ferreira T, Rossignol T, Blondin B, Bergès T. *SUT1*-promoted sterol uptake involves the ABC transporter Aus1 and the mannoprotein Dan1 whose synergistic action is sufficient for this process. Biochem J. 2004;381:195–202.

94. Abramova N, Sertil O, Mehta S, Lowry C V. Reciprocal regulation of anaerobic and aerobic cell wall mannoprotein gene expression in *Saccharomyces cerevisiae*. J Bacteriol. 2001;183:2881–7.

95. Parks LW, Smith SJ, Crowley JH. Biochemical and physiological effects of sterol alterations in yeast - A review. Lipids. 1995;30:227–30.

96. Summons RE, Bradley AS, Jahnke LL, Waldbauer JR. Steroids, triterpenoids and molecular oxygen. Philos Trans R Soc B Biol Sci. 2006;361:951–68.

97. Maxfield R, Mondal M. Sterol and lipid trafficking in mammalian cells. Biochem Soc Trans. 2006;34:335–9.

98. Tarkowská D, Strnad M. Plant ecdysteroids: plant sterols with intriguing distributions, biological effects and relations to plant hormones. Planta. 2016;244:545–55.

99. Prasad R, Shah AH, Rawal MK. Antifungals: mechanism of action and drug resistance. In: Ramos J, Sychrová H, Kschischo M, editors. Yeast Membrane Transport. Cham: Springer International Publishing; 2016. p. 327–49.

100. Hu Z, He B, Ma L, Sun Y, Niu Y, Zeng B. Recent advances in ergosterol biosynthesis and regulation mechanisms in *Saccharomyces cerevisiae*. Indian J Microbiol. Springer India; 2017;57:270–7.

101. Lorenz RT, Parks LW. Regulation of ergosterol biosynthesis and sterol uptake in a sterol-auxotrophic yeast. J Bacteriol. 1987;169:3707–11.

102. Dekker WJC, Ortiz-Merino RA, Kaljouw A, Battjes J, Wiering FW, Mooiman C, de la Torre P. Engineering the thermotolerant industrial yeast *Kluyveromyces marxianus* for anaerobic growth. Metab Eng. 2021;67:347–64

103. Tesnière C, Pradal M, Legras JL. Sterol uptake analysis in *Saccharomyces* and non-*Saccharomyces* wine yeast species. FEMS Yeast Res. 2021;21:1–13.

104. Harvey HR, Mcmanus GB. Marine ciliates as a widespread source of tetrahymanol and hopan-3β-ol in sediments. Geochim Cosmochim Acta. 1991;55:3387–90.

105. Zander JM, Caspi E, Pandey GN, Mitra CR. The presence of tetrahymanol in *Oleandra wallichii*. Phytochemistry. 1969;8:2265–7.

106. Banta AB, Wei JH, Welander P V. A distinct pathway for tetrahymanol synthesis in bacteria. Proc Natl Acad Sci. 2015;112:13478–83.

107. Kleemann G, Poralla K, Englert G, Kjosen H, Liaaen-Jensen S, Neunlist S, Rohmer M. Tetrahymanol from the phototrophic bacterium *Rhodopseudomonas palustris*: first report of a gammacerane triterpene from a prokaryote. J Gen Microbiol. 1990;136:2551–3.

108. Bravo JM, Perzl M, Härtner T, Kannenberg EL, Rohmer M. Novel methylated triterpenoids of the gammacerane series from the nitrogen-fixing bacterium *Bradyrhizobium japonicum* USDA 110. Eur J Biochem. 2001;268:1323–31.

109. Abe I. Enzymatic synthesis of cyclic triterpenes. Nat Prod Rep. 2007;24:1311–31.

110. Wiersma SJ, Mooiman C, Giera M, Pronk JT. Squalene-tetrahymanol cyclase expression enables sterol-independent growth of *Saccharomyces cerevisiae*. Appl Environ Microbiol. 2020;86:1–15.

111. Van Meer G, Voelker DR, Feigenson GW. Membrane lipids: Where they are and how they behave. Nat Rev Mol Cell Biol. 2008;9:112–24.

112. van der Rest ME, Kamminga AH, Nakano A, Anraku Y, Poolman B, Konings WN. The plasma membrane of *Saccharomyces cerevisiae*: Structure, function, and biogenesis. Microbiol Rev. 1995;59:304–22.

113. de Kroon AIPM, Rijken PJ, de Smet CH. Checks and balances in membrane phospholipid class and acyl chain homeostasis, the yeast perspective. Prog Lipid Res. 2013;52:374–94.

114. Tehlivets O, Scheuringer K, Kohlwein SD. Fatty acid synthesis and elongation in yeast. Biochim Biophys Acta - Mol Cell Biol Lipids. 2007;1771:255–70.

115. Stukey JE, McDonough VM, Martin CE. Isolation and characterization of *OLE1*, a gene affecting fatty acid desaturation from *Saccharomyces cerevisiae*. J Biol Chem. 1989;264:16537–44.

116. White SW, Zheng J, Zhang YM, Rock CO. The structural biology of type II fatty acid biosynthesis. Annu Rev Biochem. 2005;74:791–831.

117. Moraes CT, Diaz F, Barrientos A. Defects in the biosynthesis of mitochondrial heme c and heme a in yeast and mammals. Biochim Biophys Acta - Bioenerg. 2004;1659:153–9.

118. Zagorec M, Buhler JM, Treich I, Keng T, Guarente L, Labbe-Bois R. Isolation, sequence, and regulation by oxygen of the yeast *HEM13* gene coding for coproporphyrinogen oxidase. J Biol Chem. 1988;263:9718–24.

119. Camadro JM, Thome F, Brouillet N, Labbe P. Purification and properties of protoporphyrinogen oxidase from the yeast *Saccharomyces cerevisiae*. Mitochondrial location and evidence for a precursor form of the protein. J Biol Chem. 1994;269:32085–91.

120. Labbe-Bois R. The ferrochelatase from *Saccharomyces cerevisiae*. Sequence, disruption, and expression of its structural gene *HEM15*. J Biol Chem. 1990;265:7278–83.

121. Thomas D, Surdin-Kerjan Y. Metabolism of sulfur amino acids in *Saccharomyces cerevisiae*. Microbiol Mol Biol Rev. 1997;61:503–32.

122. Tripathy BC, Sherameti I, Oelmüller R. Siroheme: An essential component for life on earth. Plant Signal Behav. 2010;5:14–20.

123. Raux E, McVeigh T, Peters SE, Leustek T, Warren MJ. The role of *Saccharomyces cerevisiae* Met1p and Met8p in sirohaem and cobalamin biosynthesis. Biochem J. 1999;338:701–8.

124. Hansen J, Muldbjerg M, Chérest H, Surdin-Kerjan Y. Siroheme biosynthesis in *Saccharomyces cerevisiae* requires the products of both the *MET1* and *MET8* genes. FEBS Lett. 1997;401:20–4.

125. Barrera A, Alastruey-Izquierdo A, Martín MJ, Cuesta I, Vizcaíno JA. Analysis of the protein domain and domain architecture content in fungi and its application in the search of new antifungal targets. PLoS Comput Biol. 2014;10:e1003733.

126. Verduyn C, Postma E, Scheffers WA, van Dijken JP. Effect of benzoic acid on metabolic fluxes in yeasts: A continuous-culture study on the regulation of respiration and alcoholic fermentation. Yeast. 1992;8:501–17.

127. Bracher JM, de Hulster E, Koster CC, van den Broek M, Daran JMG, van Maris AJA, Pronk JT. Laboratory evolution of a biotin-requiring *Saccharomyces cerevisiae* strain for full biotin prototrophy and identification of causal mutations. Appl Environ Microbiol. 2017;83:1–16.

128. Perli T, Wronska AK, Ortiz-Merino RA, Pronk JT, Daran JM. Vitamin requirements and biosynthesis in *Saccharomyces cerevisiae*. Yeast. 2020;37:283–304.

129. Perli T, Moonen DPI, Broek M van den, Pronk JT, Daran J-M. Adaptive laboratory evolution and reverse engineering of single- vitamin prototrophies in *Saccharomyces cerevisiae*. Appl Environ Microbiol. 2020;86:e00388-20

130. Stolz J, Hoja U, Meier S, Sauer N, Schweizer E. Identification of the plasma membrane H^+-biotin symporter of *Saccharomyces cerevisiae* by rescue of a fatty acid-auxotrophic mutant. J Biol Chem. 1999;274:18741–6.

131. Phalip V, Kuhn I, Lemoine Y, Jeltsch JM. Characterization of the biotin biosynthesis pathway in *Saccharomyces cerevisiae* and evidence for a cluster containing *Bl05*, a novel gene involved in vitamer uptake. Gene. 1999;232:43–51.

132. Hall C, Dietrich FS. The reacquisition of biotin prototrophy in *Saccharomyces cerevisiae* involved horizontal gene transfer, gene duplication and gene clustering. Genetics. 2007;177:2293–307.

133. Wronska AK, Haak MP, Geraats E, Bruins Slot E, van den Broek M, Pronk JT, Daran J-M. Exploiting the diversity of Saccharomycotina yeasts to engineer biotin-independent growth of *Saccharomyces cerevisiae*. Appl Environ Microbiol. 2020;1–21.

134. Wronska AK, van den Broek M, Perli T, de Hulster E, Pronk JT, Daran JM. Engineering oxygen-independent biotin biosynthesis in *Saccharomyces cerevisiae*. Metab Eng. 2021;67:88–103.

135. Kawai S, Suzuki S, Mori S, Murata K. Molecular cloning and identification of *UTR1* of a yeast *Saccharomyces cerevisiae* as a gene encoding an NAD kinase. FEMS Microbiol Lett. 2001;200:181–4.

136. Panozzo C, Nawara M, Suski C, Kucharczyka R, Skoneczny M, Bécam A-M, Rytka J, Herbert CJ. Aerobic and anaerobic NAD^+ metabolism in *Saccharomyces cerevisiae*. FEBS Lett. 2002;517:97–102.

137. Begley TP, Kinsland C, Mehl RA, Osterman A, Dorrestein P. The biosynthesis of nicotinamide adenine dinucleotides in bacteria. Vitam Horm. 2001;61:103–19.

138. Llorente B, Dujon B. Transcriptional regulation of the *Saccharomyces cerevisiae DAL5* gene family and identification of the high affinity nicotinic acid permease *TNA1* (YGR260w). FEBS Lett. 2000;475:237–41.

139. Nasu S, Wicks FD, Gholson RK. L-Aspartate oxidase, a newly discovered enzyme of *Escherichia coli*, is the B protein of quinolinate synthetase. J Biol Chem. 1982;257:626–32.

140. Korshunov S, Imlay JA. Two sources of endogenous hydrogen peroxide in *Escherichia coli*. Mol Microbiol. 2010;75:1389–401.

141. Ceciliani F, Caramori T, Ronchi S, Tedeschi G, Mortarino M, Galizzi A. Cloning, overexpression, and purification of *Escherichia coli* quinolinate synthetase. Protein Expr Purif. 2000;18:64–70.

142. Perli T, Vos AM, Bouwknegt J, Dekker WJC, Wiersma SJ, Mooiman C, Ortiz-Merino RA, Daran J-M, Pronk JT. Identification of oxygen-independent pathways for pyridine nucleotide and Coenzyme A synthesis in anaerobic fungi by expression of candidate genes in yeast. MBio. 2021;12:e00967-21.

143. White WH, Gunyuzlu PL, Toyn JH. *Saccharomyces cerevisiae* is capable of *de novo* pantothenic acid biosynthesis involving a novel pathway of β-alanine production from spermine. J Biol Chem.

2001;276:10794–800.

144. Stolz J, Sauer N. The fenpropimorph resistance gene *FEN2* from *Saccharomyces cerevisiae* encodes a plasma membrane H^+-pantothenate symporter. J Biol Chem. 1999;274:18747–52.

145. Piškur J, Schnackerz KD, Andersen G, Björnberg O. Comparative genomics reveals novel biochemical pathways. Trends Genet. 2007;23:369–72.

146. Tomita H, Yokooji Y, Ishibashi T, Imanaka T, Atomia H. An archaeal glutamate decarboxylase homolog functions as an aspartate decarboxylase and is involved in β-Alanine and coenzyme a biosynthesis. J Bacteriol. 2014;196:1222–30.

147. Borodina I, Kildegaard KR, Jensen NB, Blicher TH, Maury J, Sherstyk S, Schneider K, Lamosa P, Herrgård MJ, Rosenstand I, Öberg F, Forster J, Nielsen J. Establishing a synthetic pathway for high-level production of 3-hydroxypropionic acid in *Saccharomyces cerevisiae* via β-alanine. Metab Eng. Elsevier; 2015;27:57–64.

148. Ramjee MK, Genschel U, Abell C, Smith AG. *Escherichia coli* L-aspartate-a-decarboxylase: Preprotein processing and observation of reaction intermediates by electrospray mass spectrometry. Biochem J. 1997;323:661–9.

149. Hohmann S, Meacock PA. Thiamin metabolism and thiamin diphosphate-dependent enzymes in the yeast *Saccharomyces cerevisiae*: genetic regulation. Biochim Biophys Acta - Protein Struct Mol Enzymol. 1998;1385:201–19.

150. Wolak N, Kowalska E, Kozik A, Rapala-Kozik M. Thiamine increases the resistance of baker's yeast *Saccharomyces cerevisiae* against oxidative, osmotic and thermal stress, through mechanisms partly independent of thiamine diphosphate-bound enzymes. FEMS Yeast Res. 2014;14:1249–62.

151. Lai R-Y, Huang S, Fenwick MK, Hazra A, Zhang Y, Rajashankar K, Philmus B, Kinsland C, Sanders JM, Ealick SE, Begley TP. Thiamin pyrimidine biosynthesis in *Candida albicans*: a remarkable reaction between histidine and pyridoxal phosphate. J Am Chem Soc. 2012;134:9157–9.

152. Enjo F, Nosaka K, Ogata M, Iwashima A, Nishimura H. Isolation and characterization of a thiamin transport gene, *THI10*, from *Saccharomyces cerevisiae*. J Biol Chem. 1997;272:19165–70.

153. Stolz J, Vielreicher M. Tpn1p, the plasma membrane vitamin B6 transporter of *Saccharomyces cerevisiae*. J Biol Chem. 2003;278:18990–6.

154. Kanellis P, Gagliardi M, Banath JP, Szilard RK, Nakada S, Galicia S, Sweeney FD, Cabelof DC, Olive PL, Durocher D. A screen for suppressors of gross chromosomal rearrangements identifies a conserved role for PLP in preventing DNA lesions. PLoS Genet. 2007;3:1438–53.

155. Henderson JF, Paterson ARP. Enzymatic reduction of ribonucleotides. In: Henderson JF, Paterson ARP, editors. Nucleotide Metabolism. Academic Press; 1973. p. 244–63.

156. Lundin D, Torrents E, Poole AM, Sjöberg BM. RNRdb, a curated database of the universal enzyme family ribonucleotide reductase, reveals a high level of misannotation in sequences deposited to Genbank. BMC Genomics. 2009;10:1–8.

157. Lundin D, Gribaldo S, Torrents E, Sjöberg BM, Poole AM. Ribonucleotide reduction - Horizontal transfer of a required function spans all three domains. BMC Evol Biol. 2010;10.

158. Murphy CL, Youssef NH, Hanafy RA, Couger MB, Stajich JE, Wang Y, Baker K, Dagar SS, Griffith GW, Farag IF, Callaghan TM, Elshahed MS. Horizontal gene transfer as an indispensable driver for evolution of Neocallimastigomycota into a distinct gut dwelling fungal lineage. Appl Environ Microbiol. 2019;85:e00988-19.

159. Gojković Z, Knecht W, Zameitat E, Warneboldt J, Coutelis JB, Pynyaha Y, Neuveglise C, Møller K, Löffler M, Piškur J. Horizontal gene transfer promoted evolution of the ability to propagate under anaerobic conditions in yeasts. Mol Genet Genomics. 2004;271:387–93.

160. Rawls J, Knecht W, Diekert K, Lill R, Löffler M. Requirements for the mitochondrial import and localization of dihydroorotate dehydrogenase. Eur J Biochem. 2000;267:2079–87.

161. Moffatt B, Ashihara H. Purine and pyrimidine nucleotide synthesis and metabolism. Arab B. 2002;1:e0018.

162. Larsen JN, Jensen KF. Nucleotide sequence of the *pyrD* gene of *Escherichia coli* and characterization of the flavoprotein dihydroorotate dehydrogenase. Eur J Biochem. 1985;151:59–65.

163. Kerr CT, Miller RW. Dihydroorotate-ubiquinone reductase complex of *Escherichia coli B*. J Biol Chem. 1968;243:2963–8.

164. Reis RAG, Calil FA, Feliciano PR, Pinheiro MP, Nonato MC. The dihydroorotate dehydrogenases: Past and present. Arch Biochem Biophys. 2017;632:175–91.

165. Nørager S, Jensen KF, Björnberg O, Larsen S. *E. coli* dihydroorotate dehydrogenase reveals structural and functional distinctions between different classes of dihydroorotate dehydrogenases. Structure. 2002;10:1211–23.

166. Rowland P, Nørager S, Jensen KF, Larsen S. Structure of dihydroorotate dehydrogenase B: Electron transfer between two flavin groups bridged by an iron-sulphur cluster. Structure. 2000;8:1227–38.

167. Björnberg O, Rowland P, Larsen S, Jensen KF. Active site of dihydroorotate dehydrogenase A from *Lactococcus lactis* investigated by chemical modification and mutagenesis. Biochemistry. 1997;36:16197–205.

168. Hall C, Brachat S, Dietrich FS. Contribution of horizontal gene transfer to the evolution of *Saccharomyces cerevisiae*. Eukaryot Cell. 2005;4:1102–15.

169. Nara T, Hshimoto T, Aoki T. Evolutionary implications of the mosaic pyrimidine-biosynthetic pathway in eukaryotes. Gene. 2000;257:209–22.

170. Sousa FM, Refojo PN, Pereira MM. Investigating the amino acid sequences of membrane bound dihydroorotate:quinone oxidoreductases (DHOQOs): Structural and functional implications. Biochim Biophys Acta - Bioenerg. 2021;1862:148321.

171. Nagy M, Lacroute F, Thomas D. Divergent evolution of pyrimidine biosynthesis between anaerobic and aerobic yeasts. Proc Natl Acad Sci U S A. 1992;89:8966–70.

172. Jund R, Weber E, Chevallier M R. Primary structure of the uracil transport protein of *Saccharomyces cerevisiae*. Eur J Biochem. 1988;171:417–24.

173. Weber E, Rodriguez C, Chevallier MR, Jund R. The purine-cytosine permease gene of

Saccharomyces cerevisiae: primary structure and deduced protein sequence of the *FCY2* gene product. Mol Microbiol. 1990;4:585–96.

174. Grenson M. The utilization of exogenous pyrimidines and the recycling of uridine-5'-phosphate derivatives in *Saccharomyces cerevisiae*, as studied by means of mutants affected in pyrimidine uptake and metabolism. Eur J Biochem. 1969;11:249–60.

175. Shi NQ, Jeffries TW. Anaerobic growth and improved fermentation of *Pichia stipitis* bearing a *URA1* gene from *Saccharomyces cerevisiae*. Appl Microbiol Biotechnol. 1998;50:339–45.

176. Piškur J, Ling Z, Marcet-Houben M, Ishchuk OP, Aerts A, LaButti K, Copeland A, Lindquist E, Barry K, Compagno C, Bisson L, Grigoriev I V., Gabaldón T, Phister T. The genome of wine yeast *Dekkera bruxellensis* provides a tool to explore its food-related properties. Int J Food Microbiol. 2012;157:202–9.

177. Woolfit M, Rozpdowska E, Piškur J, Wolfe KH. Genome survey sequencing of the wine spoilage yeast *Dekkera (Brettanomyces) bruxellensis*. Eukaryot Cell. 2007;6:721–33.

178. Takishita K, Chikaraishi Y, Leger MM, Kim E, Yabuki A, Ohkouchi N, Roger AJ. Lateral transfer of tetrahymanol-synthesizing genes has allowed multiple diverse eukaryote lineages to independently adapt to environments without oxygen. Biology Direct. 2012.

179. Bulder CJEA. Anaerobic growth, ergosterol content and sensitivity to a polyene antibiotic, of the yeast *Schizosaccharomyces japonicus*. Antonie Van Leeuwenhoek. 1971;37:353–8.

180. Barnett JA, Payne RW, Yarrow D. Yeasts: Characteristics and identification. Cambridge University Press; 1979.

181. Martin CE, Oh C-S, Jiang Y. Regulation of long chain unsaturated fatty acid synthesis in yeast. Biochim Biophys Acta - Mol Cell Biol Lipids. Elsevier; 2007;1771:271–85.

182. Panozzo C, Nawara M, Suski C, Kucharczyka R, Rytka J, Herbert CJ, Skoneczny M, Be A. Aerobic and anaerobic NAD^+ metabolism in *Saccharomyces cerevisiae*. FEBS Lett. 2002;517:97–102.

183. Snoek II, Steensma YH. Why does *Kluyveromyces lactis* not grow under anaerobic conditions? Comparison of essential anaerobic genes of *Saccharomyces cerevisiae* with the *Kluyveromyces lactis* genome. FEMS Yeast Res. 2006;6:393–403.

184. Wiersma SJ, Mooiman C, Giera M, Pronk J. Squalene-tetrahymanol cyclase expression enables sterol- independent growth of *Saccharomyces cerevisiae*. Appl Env Microbiol. 2020;86:1–15.

185. Wheeler GE, Rose AH. Location and properties of an esterase activity in *Saccharomyces cerevisiae*. J Gen Microbiol. 1973;74:189–92.

186. Bulder CJEA, Reinik M. Unsaturated fatty acid composition of wild type and respiratory deficient yeasts after aerobic and anaerobic growth. Antonie Van Leeuwenhoek. 1974;40:445–55.

187. Fekete S, Ganzler K, Fekete J. Fast and sensitive determination of polysorbate 80 in solutions containing proteins. J Pharm Biomed Anal. Elsevier; 2010;52:672–9.

188. Perli T, Moonen DPI, van den Broek M, Pronk JT, Daran J-M. Adaptive laboratory evolution and reverse engineering of single-vitamin prototrophies in *Saccharomyces cerevisiae*. Appl Env Microbiol. 2020;86:1–23.

189. Verduyn C, Postma E, Scheffers WA, Van Dijken JP. Physiology of *Saccharomyces cerevisiae* in

anaerobic glucose-limited chemostat cultures. J Gen Microbiol. 1990;136:395–403.

190. Liu JF, Xia JJ, Nie KL, Wang F, Deng L. Outline of the biosynthesis and regulation of ergosterol in yeast. World J Microbiol Biotechnol. Springer Netherlands; 2019;35:1–8.

191. Parapouli M, Vasileiadis A, Afendra AS, Hatziloukas E. *Saccharomyces cerevisiae* and its industrial applications. AIMS Microbiol. 2020;6:1–31.

192. Depraetere SA, Delvaux F, Schutter D De, Williams IS, Winderickx J, Delvaux FR. The influence of wort aeration and yeast preoxygenation on beer staling processes. Food Chem. 2008;107:242–9.

193. Mauricio JC, Millán C, Ortega JM. Influence of oxygen on the biosynthesis of cellular fatty acids, sterols and phospholipids during alcoholic fermentation by *Saccharomyces cerevisiae* and *Torulaspora delbrueckii*. World J Microbiol Biotechnol. 1998;14:405–10.

194. Holm Hansen E, Nissen P, Sommer P, Nielsen JC, Arneborg N. The effect of oxygen on the survival of non-*Saccharomyces* yeasts during mixed culture fermentations of grape juice with *Saccharomyces cerevisiae*. J Appl Microbiol. 2001;91:541–7.

195. Bisson LF. Stuck and sluggish fermentations. Am J Enol Vitic. 1999;107–19.

196. Munoz E, Ingledew WM. Effect of yeast hulls on stuck and sluggish wine fermentations: importance of the lipid component. Appl Environ Microbiol. 1989;55:1560–4.

197. Aries V, Kirsop BH. Sterol synthesis in relation to growth and fermentation by brewing yeasts inoculated at different concentrations. J Inst Brew. 1977;83:220–3.

198. Vanegas JM, Contreras MF, Faller R, Longo ML. Role of unsaturated lipid and ergosterol in ethanol tolerance of model yeast biomembranes. Biophys J. Biophysical Society; 2012;102:507–16.

199. Johnston EJ, Moses T, Rosser SJ. The wide-ranging phenotypes of ergosterol biosynthesis mutants, and implications for microbial cell factories. Yeast. 2020;37:27–44.

200. Merico A, Galafassi S, Piškur J, Compagno C. The oxygen level determines the fermentation pattern in *Kluyveromyces lactis*. FEMS Yeast Res. 2009;9:749–56.

201. Sun L, Alper HS. Non-conventional hosts for the production of fuels and chemicals. Curr Opin Chem Biol. Elsevier Ltd; 2020;59:15–22.

202. Thorwall S, Schwartz C, Chartron JW, Wheeldon I. Stress-tolerant non-conventional microbes enable next-generation chemical biosynthesis. Nat Chem Biol. Springer US; 2020;16:113–21.

203. Lacerda MP, Oh EJ, Eckert C. The model system *Saccharomyces cerevisiae* versus emerging non-model yeasts for the production of biofuels. Life. 2020;10:1–20.

204. Tai SL, Boer VM, Daran-Lapujade P, Walsh MC, de Winde JH, Daran JM, Pronk JT. Two-dimensional transcriptome analysis in chemostat cultures: Combinatorial effects of oxygen availability and macronutrient limitation in *Saccharomyces cerevisiae*. J Biol Chem. 2005;280:437–47.

205. van Eunen K, Bouwman J, Daran-Lapujade P, Postmus J, Canelas AB, Mensonides FIC, *et al.* Measuring enzyme activities under standardized *in vivo*-like conditions for systems biology. FEBS J. 2010;277:749–60.

206. Papini M, Nookaew I, Uhlén M, Nielsen J. *Scheffersomyces stipitis:* A comparative systems biology

study with the Crabtree positive yeast *Saccharomyces cerevisiae*. Microb Cell Fact. 2012;11:1–16.

207. Wightman R, Meacock PA. The THI5 gene family of *Saccharomyces cerevisiae:* Distribution of homologues among the hemiascomycetes and functional redundancy in the aerobic biosynthesis of thiamin from pyridoxine. Microbiology. 2003;149:1447–60.

208. Riley R, Haridas S, Wolfe KH, Lopes MR, Hittinger CT, Göker M, et al. Comparative genomics of biotechnologically important yeasts. Proc Natl Acad Sci U S A. 2016;113:9882–7.

209. Wolfe KH. Comparative genomics and genome evolution in yeasts. Philos Trans R Soc B Biol Sci. 2006;361:403–12.

210. Thomas KC, Hynes SH, Ingledew WM. Initiation of anaerobic growth of *Saccharomyces cerevisiae* by amino acids or nucleic acid bases: ergosterol and unsaturated fatty acids cannot replace oxygen in minimal media. J Ind Microbiol Biotechnol. 1998;21:247–53.

211. Madeira-Jr JV, Gombert AK. Towards high-temperature fuel ethanol production using *Kluyveromyces marxianus*: On the search for plug-in strains for the Brazilian sugarcane-based biorefinery. Biomass and Bioenergy. 2018;119:217–28.

212. Kozak BU, van Rossum HM, Benjamin KR, Wu L, Daran JMG, Pronk JT, Van Maris AJA. Replacement of the *Saccharomyces cerevisiae* acetyl-CoA synthetases by alternative pathways for cytosolic acetyl-CoA synthesis. Metab Eng. 2014;21:46–59.

213. Simpson R, Sastry SK. Scale-up in chemical and bioprocess engineering.In: Chemical and bioprocess engineering. Springer New York, New York, NY, 2013; pp 261–275.

214. Ju L, Chase GG. Bioprocess engineering improved scale-up strategies of bioreactors. Bioprocess Eng. 1992;8:49–53.

215. Wilkins MR, Mueller M, Eichling S, Banat IM. Fermentation of xylose by the thermotolerant yeast strains *Kluyveromyces marxianus IMB2, IMB4,* and *IMB5* under anaerobic conditions. Process Biochem. 2008;43:346–50.

216. Hughes SR, Bang SS, Cox EJ, Schoepke A, Ochwat K, Pinkelman R, et al. Automated UV-C Mutagenesis of *Kluyveromyces marxianus* NRRL Y-1109 and selection for microaerophilic growth and ethanol production at elevated temperature on biomass sugars. J Lab Autom. 2013;18:276–90.

217. Møller K, Olsson L, Piškur J. Ability for anaerobic growth is not sufficient for development of the petite phenotype in *Saccharomyces kluyveri*. J Bacteriol. 2001;183:2485–9.

218. da Costa BLV, Raghavendran V, Franco LFM, Chaves Filho ADB, Yoshinaga MY, Miyamoto S, Basso TO, Gombert AK. Forever panting and forever growing: physiology of *Saccharomyces cerevisiae* at extremely low oxygen availability in the absence of ergosterol and unsaturated fatty acids. FEMS Yeast Res. 2019;19:1–14.

219. Macy JM, Miller MW. Anaerobic growth of *Saccharomyces cerevisiae* in the absence of oleic acid and ergosterol? Arch Microbiol. 1983;80:64–7.

220. Clausen MK, Christiansen K, Jensen PK, Behnke O. Isolation of lipid particles from baker's yeast. FEBS Lett. 1974;43:176–9.

221. Kohlwein SD. Triacylglycerol homeostasis: Insights from yeast. J Biol Chem. 2010;285:15663–7.

222. Rajakumari S, Grillitsch K, Daum G. Synthesis and turnover of non-polar lipids in yeast. Prog Lipid Res. 2008;47:157–71.

223. Eisenberg T, Büttner S. Lipids and cell death in yeast. FEMS Yeast Res. Oxford University Press; 2014;14:179–97.

224. Spanova M, Czabany T, Zellnig GN, Leitner E, Hapala I, Daum GN. Effect of lipid particle biogenesis on the subcellular distribution of squalene in the yeast *Saccharomyces cerevisiae*. J Biol Chem. 2010;285:6127–33.

225. Spanova M, Zweytick D, Lohner K, Klug L, Leitner E, Hermetter A, Daum G. Influence of squalene on lipid particle/droplet and membrane organization in the yeast *Saccharomyces cerevisiae*. Biochim Biophys Acta - Mol Cell Biol Lipids. 2012;1821:647–53.

226. Valachovič M, Hronská L, Hapala I. Anaerobiosis induces complex changes in sterol esterification pattern in the yeast *Saccharomyces cerevisiae*. FEMS Microbiol Lett. 2001;197:41–5.

227. Boender LGM, van Maris AJA, de Hulster EAF, Almering MJH, van der Klei IJ, Veenhuis M, de Winde JH, Pronk JT, Daran-Lapujade P. Cellular responses of *Saccharomyces cerevisiae* at near-zero growth rates: Transcriptome analysis of anaerobic retentostat cultures. FEMS Yeast Res. 2011;11:603–20.

228. Meyers A, Weiskittel TM, Dalhaimer P. Lipid droplets: Formation to breakdown. Lipids. Springer Berlin Heidelberg; 2017;52:465–75.

229. Speers AM, Cologgi DL, Reguera G. Anaerobic cell culture. Curr Protoc Microbiol. 2009;1–16.

230. Lee J, Lee SY, Park S, Middelberg APJ. Control of fed-batch fermentations. Biotechnol Adv. 1999;17:29–48.

231. Kallscheuer N, Menezes R, Foito A, da Silva MH, Braga A, Dekker W, *et a*l. Identification and microbial production of the raspberry phenol salidroside that is active against Huntington's disease. Plant Physiol. 2019;179:969–85.

232. Luttik MAH, Kötter P, Salomons FA, van der Klei IJ, van Dijken JP, Pronk JT. The *Saccharomyces cerevisiae ICL2* gene encodes a mitochondrial 2-methylisocitrate lyase involved in propionyl-coenzyme a metabolism. J Bacteriol. 2000;182:7007–13.

233. Hensing MCM, Bangma KA, Raadonk LM, de Hulster E, van Dijken JP, Pronk JT. Effects of cultivation conditions on the production of heterologous a-galactosidase by *Kluyveromyces lactis*. Appl Microbiol Biotechnol. 1995;43:58–64.

234. Engler AJ, Le A V., Baevova P, Niklason LE. Controlled gas exchange in whole lung bioreactors. J Tissue Eng Regen Med. 2018;12:e119–29.

235. Bakonyi P, Nemestóthy N, Lankó J, Rivera I, Buitrón G, Bélafi-Bakó K. Simultaneous biohydrogen production and purification in a double-membrane bioreactor system. Int J Hydrogen Energy. 2015;40:1690–7.

236. Orgill JJ, Atiyeh HK, Devarapalli M, Phillips JR, Lewis RS, Huhnke RL. A comparison of mass transfer coefficients between trickle-bed, Hollow fiber membrane and stirred tank reactors. Bioresour Technol. Elsevier Ltd; 2013;133:340–6.

237. Mans R, Hassing EJ, Wijsman M, Giezekamp A, Pronk JT, Daran JM, van Maris AJA. A CRISPR/Cas9-based exploration into the elusive mechanism for lactate export in *Saccharomyces cerevisiae*. FEMS Yeast Res. 2017;17:1–12.

238. Waldbauer JR, Newman DK, Summons RE. Microaerobic steroid biosynthesis and the molecular fossil record of Archean life. Proc Natl Acad Sci U S A. 2011;108:13409–14.

239. Juergens H, Niemeijer M, Jennings-Antipov LD, Mans R, Morel J, van Maris AJA, Pronk JT, Gardner TS. Evaluation of a novel cloud-based software platform for structured experiment design and linked data analytics. Sci Data. 2018;5:1–12.

240. Oud B, Guadalupe-Medina V, Nijkamp JF, De Ridder D, Pronk JT, Van Maris AJA, Daran JM. Genome duplication and mutations in *ACE2* cause multicellular, fast-sedimenting phenotypes in evolved *Saccharomyces cerevisiae*. Proc Natl Acad Sci U S A. 2013;110.

241. Arneborg N, Høy C E, Jørgensen OB. The effect of ethanol and specific growth rate on the lipid content and composition of *Saccharomyces cerevisiae* grown anaerobically in a chemostat. Yeast. 1995;11:953–9.

242. Seifar RM, Ras C, Deshmukh AT, Bekers KM, Suarez-Mendez C, da Cruz ALB, van Gulik WM, Heijnen JJ. Quantitative analysis of intracellular coenzymes in *Saccharomyces cerevisiae* using ion pair reversed phase ultra high performance liquid chromatography tandem mass spectrometry. J Chromatogr A. 2013;1311:115–20.

243. Paalme T, Kevvai K, Vilbaste A, Hälvin K, Nisamedtinov I. Uptake and accumulation of B-group vitamers in *Saccharomyces cerevisiae* in ethanol-stat fed-batch culture. World J Microbiol Biotechnol. 2014;30:2351–9.

244. Bekers KM, Heijnen JJ, Gulik WM. Determination of the *in vivo* NAD:NADH ratio in *Saccharomyces cerevisiae* under anaerobic conditions, using alcohol dehydrogenase as sensor reaction. Yeast. 2015;32:541–57.

245. Suomalainen H, Keränen AJA. The effect of biotin deficiency on the synthesis of fatty acids by yeast. 1963;70.

246. Kosugi A, Koizumi Y, Yanagida F, Udaka S. A permease exhibiting a dual role for lysine and biotin uptake in *Saccharomyces cerevisiae*. J Biosci Bioeng. 2000;89:90–3.

247. Liu W, Zhang B, Jiang R. Improving acetyl-CoA biosynthesis in *Saccharomyces cerevisiae* via the overexpression of pantothenate kinase and PDH bypass. Biotechnol Biofuels. BioMed Central; 2017;10:1–9.

248. Hucker B, Wakeling L, Vriesekoop F. Vitamins in brewing: Presence and influence of thiamine and riboflavin on wort fermentation. J Inst Brew. 2016;122:126–37.

249. Oura E. The effect of aeration on the growth energetics and biochemical composition of baker's yeast. University of Helsiniki, Finland; 1972.

250. Förster J, Famili I, Fu P, Palsson B, Nielsen J. Genome-scale reconstruction of the *Saccharomyces cerevisiae* metabolic network. Genome Res. 2003;13:244–53.

251. Lingwood D, Simons K. Lipid rafts as a membrane organizing principle. Science (80-). 2010;327:46–50.

252. Saar J, Kader JC, Poralla K, Ourisson G. Purification and some properties of the squalene-tetrahymanol cyclase from *Tetrahymena thermophila*. BBA - Gen Subj. 1991;1075:93–101.

253. Kemp P, Lander DJ, Orpin CG. The lipids of the rumen fungus *Piromonas communis*. J Gen Microbiol. 1984;130:27–37.

254. Ourisson G, Neurochimie C De, Pascal B, Rohmer M, Nationale E, Chimie S De, Werner A, I IB, Tiibingen U, Morgenstelle A Der. Prokaryotic hopanoids and other polyterpenoid sterol surrogates. Annu Rev Microbiol. 1987;41:301–33.

255. Rohmer M, Bouvier-Nave P, Ourisson G. Distribution of hopanoid triterpenes in prokaryotes. J Gen Microbiol. 1984;130:1137–50.

256. Barnett JA, Payne RW, Yarrow D. A guide to identifying and classifying yeast. J Basic Microbiol. 1980;21:63.

257. Yukawa M, Maki T. Regarding the new fission yeast *Schizosaccharomyces japonicus*. Kyushu Daigaku Kiyou. 1931;4:218–26.

258. Wickerham LJ, Duprat E. A remarkable fission yeast, *Schizosaccharomyces versatilis nov. sp.* J Bacteriol. 1945;50:597–607.

259. Domizio P, Lencioni L, Calamai L, Portaro L, Bisson LF. Evaluation of the yeast *Schizosaccharomyces japonicus* for use in wine production. Am J Enol Vitic. 2018;69:266–77.

260. Benito S. The impacts of *Schizosaccharomyces* on winemaking. Appl Microbiol Biotechnol. Applied Microbiology and Biotechnology; 2019;103:4291–312.

261. Rhind N, Chen Z, Yassour M, Thompson DA, Haas BJ, Habib N, et al. Comparative functional genomics of the fission yeasts. Science (80-). 2011;332:930–6.

262. Flagfeldt DB, Siewers V, Huang L, Nielsen J. *Schizosaccharomyces japonicus*: the fission yeast is a fusion of yeast and hyphae. Yeast. 2009;26:545–51.

263. Kinnaer C, Dudin O, Martin SG. Yeast-to-hypha transition of *Schizosaccharomyces japonicus* in response to environmental stimuli. Mol Biol Cell. 2019;30:975–91.

264. Klar AJS. *Schizosaccharomyces japonicus* yeast poised to become a favorite experimental organism for eukaryotic research. G3 Genes, Genomes, Genet. 2013;3:1869–73.

265. Alfa CE, Hyams JS. Distribution of tubulin and actin through the cell division cycle of the fission yeast *Schizosaccharomyces japonicus var. versatilis:* A comparison with Schizosaccharomyces pombe. J Cell Sci. 1990;96:71–7.

266. Kaino T, Tonoko K, Mochizuki S, Takashima Y, Kawamukai M. *Schizosaccharomyces japonicus* has low levels of CoQ10 synthesis, respiration deficiency, and efficient ethanol production. Biosci Biotechnol Biochem. Taylor & Francis; 2018;82:1031–42.

267. Bulder CJEA, Weijers C. Absence of cyanide-insensitive respiration in *Schizosaccharomyces japonicus*. FEMS Microbiol Lett. 1982;15:145–7.

268. Makarova M, Peter M, Balogh G, Glatz A, MacRae JI, Lopez Mora N, Booth P, Makeyev E, Vigh L, Oliferenko S. Delineating the rules for structural adaptation of membrane-associated proteins to

evolutionary changes in membrane lipidome. Curr Biol. 2020;30:367-380.e8.

269. Kirschvink JL, Kopp RE. Palaeoproterozoic ice houses and the evolution of oxygen-mediating enzymes: The case for a late origin of photosystem II. Philos Trans R Soc B Biol Sci. 2008;363:2755–65.

270. David MH, Kirsop BH. Yeast growth in relation to the dissolved oxygen and sterol content of wort. J Inst Brew. 1973;79:20–5.

271. Varela C, Torrea D, Schmidt SA, Ancin-Azpilicueta C, Henschke PA. Effect of oxygen and lipid supplementation on the volatile composition of chemically defined medium and chardonnay wine fermented with *Saccharomyces cerevisiae*. Food Chem. Elsevier; 2012;135:2863–71.

272. Shiojima K, Arai Y, Masuda K, Takase Y, Ageta T, Ageta H. Mass spectra of pentacyclic triterpenoids. Chem Pharm Bull. 2002;2091.

273. Mallory FB, Gordon JT, Conner RL. The isolation of a pentacyclic triterpenoid alcohol from a protozoan. J Am Chem Soc. 1963;85:1362–3.

274. Takishita K, Chikaraishi Y, Tanifuji G, Ohkouchi N, Hashimoto T, Fujikura K, Roger AJ. Microbial eukaryotes that lack sterols. J Eukaryot Microbiol. 2017;64:897–900.

275. Giera M, Plössl F, Bracher F. Fast and easy *in vitro* screening assay for cholesterol biosynthesis inhibitors in the post-squalene pathway. Steroids. 2007;72:633–42.

276. Sessions AL, Zhang L, Welander P V, Doughty D, Summons RE, Newman DK. Identification and quantification of polyfunctionalized hopanoids by high temperature gas chromatography-mass spectrometry. 2013.

277. Hoshino T, Sato T. Squalene–hopene cyclase: catalytic mechanism and substrate recognition. Chem commun. 2002;290–301.

278. Müller C, Binder U, Bracher F, Giera M. Antifungal drug testing by combining minimal inhibitory concentration testing with target identification by gas chromatography-mass spectrometry. Nat Protoc. 2017;12:947–63.

279. Giera M, Müller C, Bracher F. Analysis and experimental inhibition of distal cholesterol biosynthesis. Chromatographia. 2014;78:343–58.

280. Corey EJ, Matsuda SPT, Baker CH, Ting AY, Cheng H. Molecular cloning of a *Schizosaccharomyces pombe* cDNA encoding lanosterol synthase and investigation of conserved tryptophan residues. Biochem Biophys Res Commun. 1996;219:327–31.

281. Ochs D, Kaletta C, Entian KD, Beck-Sickinger A, Poralla K. Cloning, expression, and sequencing of squalene-hopene cyclase, a key enzyme in triterpenoid metabolism. J Bacteriol. 1992;174:298–302.

282. Mistry J, Finn RD, Eddy SR, Bateman A, Punta M. Challenges in homology search: HMMER3 and convergent evolution of coiled-coil regions. Nucleic Acids Res. 2013;41.

283. Sievers F, Higgins DG. Clustal Omega for making accurate alignments of many protein sequences. Protein Sci. 2018;27:135–45.

284. Kannenberg EL, Poralla K. Hopanoid biosynthesis and function in bacteria. Naturwissenschaften. 1999;86:168–76.

285. Belin BJ, Busset N, Giraud E, Molinaro A, Silipo A, Newman DK. Hopanoid lipids: from membranes

to plant–bacteria interactions. 2018;

286. Gerts EM, Yu YK, Agarwala R, Schäffer AA, Altschul SF. Composition-based statistics and translated nucleotide searches: Improving the TBLASTN module of BLAST. BMC Biol. 2006;4:1–14.

287. Mikkelsen MD, Buron LD, Salomonsen B, Olsen CE, Hansen BG, Mortensen UH, Halkier BA. Microbial production of indolylglucosinolate through engineering of a multi-gene pathway in a versatile yeast expression platform. Metab Eng. 2012;14:104–11.

288. Conner RL, Mellory FB, Landrey JR, Ferguson KA, Kaneshiro ES, Ray E. Ergosterol replacement of tetrahymanol in Tetrahymena membranes. Bioch Biophys Res Commun. 1971;44:995–1000.

289. Youssef NH, Couger MB, Struchtemeyer CG, Liggenstoffer AS, Prade RA, Najar FZ, Atiyeh HK, Wilkins MR, Elshahed MS. The genome of the anaerobic fungus *Orpinomyces* sp. strain C1A reveals the unique evolutionary history of a remarkable plant biomass degrader. Appl Environ Microbiol. American Society for Microbiology; 2013;79:4620–34.

290. Furuya K, Niki H. Isolation of heterothallic haploid and auxotrophic mutants in *Schizosaccharomyces japonicus*. Yeast. 2009;26:221–3.

291. Shinozaki J, Shibuya M, Masuda K, Ebizuka Y. Squalene cyclase and oxidosqualene cyclase from a fern. FEBS Lett. 2008;582:310–8.

292. Shinozaki J, Nakene T, Takano A. Squalene cyclases and cycloartenol synthases from polystichum polyblepharum and six allied ferns. Molecules. 2018;23.

293. Frickey T, Kannenberg E. Phylogenetic analysis of the triterpene cyclase protein family in prokaryotes and eukaryotes suggests bidirectional lateral gene transfer. Environ Microbiol. 2009;11:1224–41.

294. Racolta S, Juhl PB, Sirim D, Pleiss J. The triterpene cyclase protein family: A systematic analysis. Proteins Struct Funct Bioinforma. 2012;80:2009–19.

295. Pale-Grosdemange C, Feil C, Rohmer M, Poralla K. Occurrence of cationic intermediates and deficient control during the enzymatic cyclization of squalene to hopanoids. Angew Chemie - Int Ed. 1998;37:2237–40.

296. Syrén PO, Henche S, Eichler A, Nestl BM, Hauer B. Squalene-hopene cyclases - evolution, dynamics and catalytic scope. Curr Opin Struct Biol. 2016;41:73–82.

297. Howard DL, Simoneit BRT, Chapman DJ. Triterpenoids from lipids of *Rhodomicrobium vannielliі*. Arch Microbiol. 1984;137:200–4.

298. Douka E, Koukkou AI, Drainas C, Grosdemange-Billiard C, Rohmer M. Structural diversity of the triterpenic hydrocarbons from the bacterium *Zymomonas mobilis*: The signature of defective squalene cyclization by the squalene/hopene cyclase. FEMS Microbiol Lett. 2001;199:247–51.

299. Poger D, Mark AE. The relative effect of sterols and hopanoids on lipid bilayers: When comparable is not identical. J Phys Chem B. 2013;

300. Sáenz JP, Sezgin E, Schwille P, Simons K. Functional convergence of hopanoids and sterols in membrane ordering. Proc Natl Acad Sci U S A. 2012;109:14236–40.

301. Bradley AS, Pearson A, Sáenz JP, Marx CJ. Adenosylhopane: The first intermediate in hopanoid side chain biosynthesis. Org Geochem. 2010;41:1075–81.

302. Koch B, Schmidt C, Daum G. Storage lipids of yeasts: A survey of nonpolar lipid metabolism in *Saccharomyces cerevisiae*, *Pichia pastoris*, and *Yarrowia lipolytica*. FEMS Microbiol Rev. 2014;38:892–915.

303. Csáky Z, Garaiová M, Kodedová M, Valachovič M, Sychrová H, Hapala I. Squalene lipotoxicity in a lipid dropletless yeast mutant is linked to plasma membrane dysfunction. Yeast. 2020;37:45–62.

304. Schmerk CL, Bernards MA, Valvano MA. Hopanoid production is required for low-pH tolerance, antimicrobial resistance, and motility in *Burkholderia cenocepacia.* J Bacteriol. 2011;193:6712–23.

305. Welander P V., Hunter RC, Zhang L, Sessions AL, Summons RE, Newman DK. Hopanoids play a role in membrane integrity and pH homeostasis in *Rhodopseudomonas palustris* TIE-1. J Bacteriol. 2009;191:6145–56.

306. Brenac L, Baidoo EEK, Keasling JD, Budin I. Distinct functional roles for hopanoid composition in the chemical tolerance of *Zymomonas mobilis*. Mol Microbiol. 2019;112:1564–75.

307. Entian KD, Kötter P. 25 Yeast genetic strain and plasmid collections. Methods Microbiol. 2007;36:629–66.

308. Nijkamp JF, van den Broek M, Datema E, de Kok S, Bosman L, Luttik MA, et al. *De novo* sequencing, assembly and analysis of the genome of the laboratory strain *Saccharomyces cerevisiae* CEN.PK113-7D, a model for modern industrial biotechnology. Microb Cell Fact. BioMed Central Ltd; 2012;11:36:1-16.

309. Miyata M, Doi H, Miyata H, Johnson BF. Sexual co-flocculation by heterothallic cells of the fission yeast *Schizosaccharomyces pombe* modulated by medium constituents. Antonie Van Leeuwenhoek. 1997;71:207–15.

310. Jensen NB, Strucko T, Kildegaard KR, David F, Maury J, Mortensen UH, Forster J, Nielsen J, Borodina I. EasyClone: Method for iterative chromosomal integration of multiple genes in *Saccharomyces cerevisiae*. FEMS Yeast Res. 2013;14:238–48.

311. Solis-Escalante D, Kuijpers NGA, Bongaerts N, Bolat I, Bosman L, Pronk JT, Daran JM, Daran-Lapujade P. *amdSYM*, A new dominant recyclable marker cassette for *Saccharomyces cerevisiae*. FEMS Yeast Res. 2013;13:126–39.

312. Raab D, Graf M, Notka F, Schödl T, Wagner R. The GeneOptimizer Algorithm: Using a sliding window approach to cope with the vast sequence space in multiparameter DNA sequence optimization. Syst Synth Biol. 2010;4:215–25.

313. Itoh S, Takahashi S, Tsuboi M, Shimoda C, Hayashibe M. Effect of light on sexual flocculation in *Schizosaccharomyces japonicus*. Plant Cell Physiol. 1976;17:1355–8.

314. Okamoto S, Furuya K, Nozaki S, Aoki K, Niki H. Synchronous activation of cell division by light or temperature stimuli in the dimorphic yeast *Schizosaccharomyces japonicus*. Eukaryot Cell. 2013;12:1235–43.

315. Verhoeven MD, Lee M, Kamoen L, van den Broek M, Janssen DB, Daran J-MG, van Maris AJA, Pronk JT. Mutations in *PMR1* stimulate xylose isomerase activity and anaerobic growth on xylose of engineered *Saccharomyces cerevisiae* by influencing manganese homeostasis. Sci Rep. Nature Publishing Group;

2017;7:46155.

316. Kolmogorov M, Yuan J, Lin Y, Pevzner PA. Assembly of long, error-prone reads using repeat graphs. Nat Biotechnol. Springer US; 2019;37:540–6.

317. Walker BJ, Abeel T, Shea T, Priest M, Abouelliel A, Sakthikumar S, Cuomo CA, Zeng Q, Wortman J, Young SK, Earl AM. Pilon: An integrated tool for comprehensive microbial variant detection and genome assembly improvement. PLoS One. 2014;9.

318. Love J, Palmer J, Stajich J, Esser T, Kastman E, Bogema D. Funannotate v1.7.1. Zenodo. 2019.

319. Jones P, Binns D, Chang H, Fraser M, Li W, McAnulla C, McWilliam H, Maslen J, Mitchell A, Nuka G, Pesseat S, Quinn A, Sangrador-Vegas A, Scheremetjew M, Yong S, Lopez R, Hunter S. InterProScan 5: Genome-scale protein function classification. Bioinformatics. 2014;30:1236–40.

320. Katoh K, Standley DM. MAFFT multiple sequence alignment software version 7: Improvements in performance and usability. Mol Biol Evol. 2013;30:772–80.

321. Capella-Gutiérrez S, Silla-Martínez JM, Gabaldón T. trimAl: A tool for automated alignment trimming in large-scale phylogenetic analyses. Bioinformatics. 2009;25:1972–3.

322. Kozlov AM, Darriba D, Flouri T, Morel B, Stamatakis A. RAxML-NG: A fast, scalable and user-friendly tool for maximum likelihood phylogenetic inference. Bioinformatics. 2019;35:4453–5.

323. Letunic I, Bork P. Interactive tree of life (iTOL) v3: an online tool for the display and annotation of phylogenetic and other trees. Nucleic Acids Res. 2016;44:W242–5.

324. Rowland P, Björnberg O, Nielsen FS, Jensen KF, Larsen S. The crystal structure of *Lactococcus lactis* dihydroorotate dehydrogenase A complexed with the enzyme reaction product throws light on its enzymatic function. Protein Sci. 1998;7:1269–79.

325. Rowland P, Nielsen FS, Jensen KF, Larsen S. The crystal structure of the flavin containing enzyme dihydroorotate dehydrogenase A from *Lactococcus lactis.* Structure. 1997;5:239–52.

326. Björnberg O, Grüner AC, Roepstorff P, Jensen KF. The activity of *Escherichia coli* dihydroorotate dehydrogenase is dependent on a conserved loop identified by sequence homology, mutagenesis, and limited proteolysis. Biochemistry. 1999;38:2899–908.

327. Jordan DB, Bisaha JJ, Picollelli MA. Catalytic properties of dihydroorotate dehydrogenase from *Saccharomyces cerevisiae*: Studies on pH, alternate substrates, and inhibitors. Arch Biochem Biophys. 2000;378:84–92.

328. Fagan RL, Nelson MN, Pagano PM, Palfey BA. Mechanism of flavin reduction in class 2 dihydroorotate dehydrogenases. Biochemistry. 2006;45:14926–32.

329. Fagan RL, Jensen KF, Björnberg O, Palfey BA. Mechanism of flavin reduction in the class 1A dihydroorotate dehydrogenase from *Lactococcus lactis*. Biochemistry. 2007;46:4028–36.

330. Björnberg O, Jordan DB, Palfey BA, Jensen KF. Dihydrooxonate is a substrate of dihydroorotate dehydrogenase (DHOD) providing evidence for involvement of cysteine and serine residues in base catalysis. Arch Biochem Biophys. 2001;391:286–94.

331. Armenta-Medina D, Segovia L, Perez-Rueda E. Comparative genomics of nucleotide metabolism:

A tour to the past of the three cellular domains of life. BMC Genomics. 2014;15:1–16.

332. Hagman A, Sall T, Compagno C, Piskur J. Yeast " Make-Accumulate-Consume " Life Strategy Evolved as a Multi-Step Process That Predates the Whole Genome Duplication Yeast. PLoS One. 2013;8.

333. Annoura T, Nara T, Makiuchi T, Hashimoto T, Aoki T. The origin of dihydroorotate dehydrogenase genes of kinetoplastids, with special reference to their biological significance and adaptation to anaerobic, parasitic conditions. J Mol Evol. 2005;60:113–27.

334. Blomqvist J, Eberhard T, Schnürer J, Passoth V. Fermentation characteristics of *Dekkera bruxellensis* strains. Appl Microbiol Biotechnol. 2010;87:1487–97.

335. UniProt Consortium. Universal Protein Resource [Internet]. 2002 [cited 2019 Nov 28]. Available from: https://www.uniprot.org/

336. Pronk JT. Auxotrophic yeast strains in fundamental and applied research. Appl Environ Microbiol. 2002;68:2095–100.

337. Haitjema CH, Solomon K V., Henske JK, Theodorou MK, O'Malley MA. Anaerobic gut fungi: Advances in isolation, culture, and cellulolytic enzyme discovery for biofuel production. Biotechnol Bioeng. 2014;111:1471–82.

338. Zameitat E, Gojković Z, Knecht W, Piškur J, Löffler M. Biochemical characterization of recombinant dihydroorotate dehydrogenase from the opportunistic pathogenic yeast *Candida albicans*. FEBS J. 2006;273:3183–91.

339. Löffler M, Knecht W, Rawls J, Ullrich A, Dietz C. *Drosophila melanogaster* dihydroorotate dehydrogenase: The N-terminus is important for biological function *in vivo* but not for catalytic properties *in vitro*. Insect Biochem Mol Biol. 2002;32:1159–69.

340. Liu S, Neidhardt EA, Grossman TH, Ocain T, Clardy J. Structures of human dihydroorotate dehydrogenase in complex with antiproliferative agents. Structure. 2000;8:25–33.

341. Hansen M. Inhibitor binding in a class 2 dihydroorotate dehydrogenase causes variations in the membrane-associated N-terminal domain. Protein Sci. 2004;13:1031–42.

342. Fagan RL, Palfey BA. Roles in binding and chemistry for conserved active site residues in the class 2 dihydroorotate dehydrogenase from *Escherichia coli*. Biochemistry. 2009;48:7169–78.

343. Vowinckel J, Hartl J, Butler R, Ralser M. MitoLoc: A method for the simultaneous quantification of mitochondrial network morphology and membrane potential in single cells. Mitochondrion. 2015;24:77–86.

344. Visser W, van Spronsen EA, Nanninga N, Pronk JT, Kuenen JG, van Dijken JP. Effects of growth conditions on mitochondrial morphology in *Saccharomyces cerevisiae*. Antonie Van Leeuwenhoek. 1995;67:243–53.

345. Kováč L, Varečka Ľ. Membrane potentials in respiring and respiration-deficient yeasts monitored by a fluorescent dye. Biochim Biophys Acta- Bioenerg. 1981;637:209–16.

346. Kapuscinski J. DAPI: A DNA-Specific fluorescent probe. Biotech Histochem. 1995;70:220–33.

347. Perez-Samper G, Cerulus B, Jariani A, Vermeersch L, Simancas NB, Bisschops MMM, van den Brink J, Solis-Escalante D, Gallone B, De Maeyer D, van Bael E, Wenseleers T, Michiels J, Marchal K, Daran-Lapujade P, Verstrepen KJ. The crabtree effect shapes the *Saccharomyces cerevisiae* lag phase during

the switch between different carbon sources. MBio. 2018;9:1–18.

348. Bullerwell CE, Leigh J, Forget L, Lang BF. A comparison of three fission yeast mitochondrial genomes. Nucleic Acids Res. 2003;31:759–68.

349. Andersen PS, Jansen PJG, Hammer K. Two different dihydroorotate dehydrogenases in *Lactococcus lactis*. J Bacteriol. 1994;176:3975–82.

350. Hey-Mogensen M, Goncalves RLS, Orr AL, Brand MD. Production of superoxide/H_2O_2 by dihydroorotate dehydrogenase in rat skeletal muscle mitochondria. Free Radic Biol Med. Elsevier; 2014;72:149–55.

351. Arakaki TL, Buckner FS, Gillespie JR, Malmquist NA, Phillips MA, Kalyuzhniy O, Luft JR, Detitta GT, Verlinde CLMJ, Voorhis WC Van, Hol WGJ, Ethan A. Characterization of *Trypanosoma brucei* dihydroorotate dehydrogenase as a possible drug target; structural, kinetic and RNAi studies. Mol Microbiol. 2008;68:37–50.

352. Zameitat E, Pierik AJ, Zocher K, Löffler M. Dihydroorotate dehydrogenase from *Saccharomyces cerevisiae*: Spectroscopic investigations with the recombinant enzyme throw light on catalytic properties and metabolism of fumarate analogues. FEMS Yeast Res. 2007;7:897–904.

353. Mohsen AWA, Rigby SEJ, Jensen KF, Munro AW, Scrutton NS. Thermodynamic basis of electron transfer in dihydroorotate dehydrogenase B from *Lactococcus lactis*: Analysis by potentiometry, EPR spectroscopy, and ENDOR spectroscopy. Biochemistry. 2004;43:6498–510.

354. Palfey BA, Björnberg O, Jensen KF. Insight into the chemistry of flavin reduction and oxidation in *Escherichia coli* dihydroorotate dehydrogenase obtained by rapid reaction studies. Biochemistry. 2001;40:4381–90.

355. Schafer FQ, Buettner GR. Redox state and redox environment in biology. In: Forman HJ, Fukuto J, Torres M, editors. Signal transduction by reactive oxygen and nitrogen species: pathways and chemical principles. Dordrecht: Springer Netherlands; 2003. p. 1–14.

356. Tiegh. S, le Monn G. Coemansia reversa. Ann Sci Nat, Bot. 1873;17:392.

357. Lastra CCL. Primera cita de *Smittium culisetae* y *S. culicis* (Trichomycetes:Harpellales) en larvas de mosquitos (Diptera:culicidae) de la republica Argentina. Bol Soc Argent Bot. 1997;33:43–6.

358. Fuller MS, Clay RP. Observations of *Gonapodya* in pure culture: Growth, development and cell wall characterization. Mycologia. 1993;85:38–45.

359. Draper RD, Ingraham LL. A potentiometric study of the flavin semiquinone equilibrium. Arch Biochem Biophys. 1968;125:802–8.

360. Kim S, Kim CM, Son YJ, Choi JY, Siegenthaler RK, Lee Y, Jang TH, Song J, Kang H, Kaiser CA, Park HH. Molecular basis of maintaining an oxidizing environment under anaerobiosis by soluble fumarate reductase. Nat Commun. Springer US; 2018;9:1–12.

361. Arikawa Y, Enomoto K, Muratsubaki H, Okazaki M. Soluble fumarate reductase isoenzymes from *Saccharomyces cerevisiae* are required for anaerobic growth. FEMS Microbiol Lett. 1998;165:111–6.

362. Ullrich A, Knecht W, Fries M, Löffler M. Recombinant expression of N-terminal truncated mutants

of the membrane bound mouse, rat and human flavoenzyme dihydroorotate dehydrogenase: A versatile tool to rate inhibitor effects? Eur J Biochem. 2001;268:1861–8.

363. Linehan WM, Rouault TA. Molecular pathways: Fumarate Hydratase-deficient kindey cancer - targeting the Warburg effect in cancer. Clin Cancer Res. 2013;19:3346–52.

364. Pithukpakorn M, Wei MH, Toure O, Steinbach PJ, Glenn GM, Zbar B, Linehan WM, Toro JR. Fumarate hydratase enzyme activity in lymphoblastoid cells and fibroblasts of individuals in families with hereditary leiomyomatosis and renal cell cancer. J Med Genet. 2006;43:755–62.

365. Marque M, Gardie B, Bressac De Paillerets B, Rustin P, Guillot B, Richard S, Bessis D. Novel FH mutation in a patient with cutaneous leiomyomatosis associated with cutis verticis gyrata, eruptive collagenoma and Charcot-Marie-Tooth disease. Br J Dermatol. 2010;163:1337–9.

366. Picaud S, Kavanagh KL, Yue WW, Lee WH, Muller-Knapp S, Gileadi O, Sacchettini J, Oppermann U. Structural basis of fumarate hydratase deficiency. J Inherit Metab Dis. 2011;34:671–6.

367. Ylisaukko-oja SK, Cybulski C, Lehtonen R, Kiuru M, Matyjasik J, Szymańska A, Szymańska-Pasternak J, Dyrskjot L, Butzow R, Orntoft TF, Launonen V, Lubiński J, Aaltonen LA. Germline fumarate hydratase mutations in patients with ovarian mucinous cystadenoma. Eur J Hum Genet. 2006;14:880–3.

368. Doudican NA, Song B, Shadel GS, Doetsch PW. Oxidative DNA damage causes mitochondrial genomic instability in *Saccharomyces cerevisiae* . Mol Cell Biol. 2005;25:5196–204.

369. Sipiczki M, Kucsera J, Ulaszewski S, Zsolt J. Hybridization studies by crossing and protoplast fusion within the genus *Schizosaccharomyces Lindner.* J Gen Microbiol. 1982;128:1989–2000.

370. Bulder CJEA. On respiratory defiency in yeasts. Delft University of Technology; 1963.

371. Salazar AN, de Vries ARG, van den Broek M, Wijsman M, Cortés P de la T, Brickwedde A, Brouwers N, Daran JMG, Abeel T. Nanopore sequencing enables near-complete *de novo* assembly of *Saccharomyces cerevisiae* reference strain CEN.PK113-7D. FEMS Yeast Res. 2017;17:1–11.

372. Bertani G. Studies on lysogenesis. I. The mode of phage liberation by lysogenic *Escherichia coli.* J Bacteriol. 1951;62:293–300.

373. Lee ME, DeLoache WC, Cervantes B, Dueber JE. A highly characterized yeast toolkit for modular, multipart assembly. ACS Synth Biol. 2015;4:975–86.

374. Gietz RD, Woods RA. Transformation of yeast by lithium acetate/single-stranded carrier DNA/ polyethylene glycol method. Methods Enzymol. 2002;350:87–96.

375. Robinson JT, Thorvaldsdóttir H, Winckler W, Guttman M, Lander ES, Getz G, Mesirov JP. Integrative Genome Viewer. Nat Biotechnol. 2011;29:24–6.

376. Roach MJ, Borneman AR. New genome assemblies reveal patterns of domestication and adaptation across *Brettanomyces (Dekkera*) species. BMC Genomics; 2020;21:1–14.

377. Altschul SF, Wootton JC, Gertz ME, Agarwala R, Morgulis A, Schäffer AA, Yu Y-K. Protein database searches using compositionally adjusted substitution matrices. FEBS J. 2005;270:5101–9.

378. Horton P, Park KJ, Obayashi T, Fujita N, Harada H, Adams-Collier CJ, Nakai K. WoLF PSORT: Protein localization predictor. Nucleic Acids Res. 2007;35:585–7.

379. The UniProt Consortium. UniProt: A worldwide hub of protein knowledge. Nucleic Acids Res.

Oxford University Press; 2019;47:D506–15.

380. Lechner M, Findeiß S, Steiner L, Marz M, Stadler PF, Prohaska SJ. Proteinortho : Detection of (Co-) orthologs in large-scale analysis. BMC Bioinformatics. 2011;12:1–9.

381. Buchfink B, Reuter K, Drost HG. Sensitive protein alignments at tree-of-life scale using DIAMOND. Nat Methods. Springer US; 2021;18:366–8.

382. Sievers F, Wilm A, Dineen D, Gibson TJ, Karplus K, Li W, Lopez R, McWilliam H, Remmert M, Söding J, Thompson JD, Higgins DG. Fast, scalable generation of high-quality protein multiple sequence alignments using Clustal Omega. Mol Syst Biol. 2011;7.

383. Schindelin J, Arganda-Carreras I, Frise E, Kaynig V, Longair M, Pietzsch T, Preibisch S, Rueden C, Saalfeld S, Schmid B, Tinevez J-Y, White DJ, Hartenstein V, Eliceiri K, Tomancak P, Cardona A. Fiji - an Open platform for biological image analysis. Nat Methods. 2012;9:676–82.

384. Vuralhan Z, Luttik MAH, Tai SL, Boer VM, Morais MA, Schipper D, Almering MJH, Kötter P, Dickinson JR, Daran JM, Pronk JT. Physiological characterization of the *ARO10*-dependent, broad-substrate-specificity 2-oxo acid decarboxylase activity of *Saccharomyces cerevisiae*. Appl Environ Microbiol. 2005;71:3276–84.

385. Lowry OH, Rosebrough NJ, Farr AL, Randall RJ. Protein determination with the folin phenol reagent. J Biol Chem. 1951;193:265–76.

386. Bernofsky C, Wanda SY. Formation of reduced nicotinamide adenine dinucleotide peroxide. J Biol Chem. 1982;257:6809–17.

387. O'Donovan GA, Neuhard J. Pyrimidine metabolism in microorganisms. Bacteriol Rev. 1970;34:278–343.

388. di Carlo FJ, Schultz AS, Kent AM. Cytosine antagonism in yeast by diazobarbituric anhydride. J Biol Chem. 1952;194:769–74.

389. Vogels GD, van der Drift C. Degradation of purines and pyrimidines by microorganisms. Bacteriol Rev. 1976;40:403–68.

390. Hayaishi O, Kornberg A. Metabolism of cytosine, thymine, uracil, and barbituric acid by bacterial enzymes. J Biol Chem. 1952;197:717–32.

391. Andersen G, Björnberg O, Polakova S, Pynyaha Y, Rasmussen A, Møller K, Hofer A, Moritz T, Sandrini MPB, Merico AM, Compagno C, Åkerlund HE, Gojković Z, Piškur J. A second pathway to degrade pyrimidine nucleic acid precursors in eukaryotes. J Mol Biol. 2008;380:656–66.

392. Loh KDI, Gyaneshwar P, Markenscoff Papadimitriou E, Fong R, Kim KS, Parales R, Zhou Z, Inwood W, Kustu S. A previously underscribed pathway for pyrimidine catabolism. Proc Natl Acad Sci U S A. 2006;103:5114–9.

393. Zrenner R, Stitt M, Sonnewald U, Boldt R. Pyrimidine and purine biosynthesis and degradation in plants. Annu Rev Plant Biol. 2006;57:805–36.

394. Dobritzsch D, Schneider G, Schnackerz KD, Lindqvist Y. Crystal structure of dihydropyrimidine dehydrogenase, a major determinant of the pharmacokinetics of the anti-cancer drug 5-fluorouracil.

EMBO J. 2001;20:650–60.

395. Berger R, Stoker-de Vries SA, Wadman SK, Duran M, Beemer FA, de Bree PK, Weits-Binnerts JJ, Penders TJ, van der Woude JK. Dihydropyrimidine dehydrogenase deficiency leading to thymine-uraciluria. An inborn error of pyrimidine metabolism. Clin Chim Acta. 1984;141:227–34.

396. van Kuilenburg ABP, van Vreken P, Abeling NGGM, Bakker HD, Meinsma R, van Lenthe H, *et al*. Genotype and phenotype in patients with dihydropyrimidine dehydrogenase deficiency. Hum Genet. 1999;104:1–9.

397. Heggie GD, Sommadossi JP, Cross DS, Huster WJ. Clinical pharmacokinetics of 5-fluorouracil and its metabolites in plasma, urine, and bile. Cancer Res. 1987;47:2203–6.

398. Hull WE, Port RE, Herrmann R, Britsch B, Kunz W. Metabolites of 5-fluorouracil in plasma and urine, as monitored by 19F nuclear magnetic resonance spectroscopy, for patients receiving chemotherapy with or without methotrexate pretreatment. Cancer Res. 1988;48:1680–8.

399. Van Gennip AH, Abeling NGGM, Vreken P, Van Kuilenburg ABP. Inborn errors of pyrimidine degradation: clinical, biochemical and molecular aspects. J Inherit Metab Dis. 1997;20:203–13.

400. Smith A, Yamada E. Dihydrouracil dehydrogenase of rat liver. J Biol Chem. 1971;246:3610–7.

401. Podschun B, Wahler G, Schnackerz KD. Purification and characterization of dihydropyrimdine dehydrogenase from pig liver. Eur J Biochem. 1989;185:219–24.

402. Zrenner R, Riegler H, Marquard CR, Lange PR, Geserick C, Bartosz CE, Chen CT, Slocum RD. A functional analysis of the pyrimidine catabolic pathway in Arabidopsis. New Phytol. 2009;183:117–32.

403. Lu ZH, Zhang R, Diasio RB. Purification and characterization of dihydropyrimidine dehydrogenase from human liver. J Biol Chem. 1992;267:17102–9.

404. Podschun B, Cook PF, Schnackerz KD. Kinetic mechanism of dihydropyrimidine dehydrogenase from pig liver. J Biol Chem. 1990;265:12966–72.

405. Davis CH, Putnam MD, Thwaites WM. Metabolism of dihydrouracil in *Rhodosporidium toruloides*. J Bacteriol. 1984;158:347–50.

406. Owaki J, Uzura K, Minami Z, Kusai K. Partial purification and characterization of dihydrouracil oxidase, a flavoprotein from *Rhodotorula glutinis*. J Ferment Technol. 1986;64:205–10.

407. Andersen G, Merico A, Björnberg O, Andersen B, Schnackerz KD, Dobritzsch D, Piškur J, Compagno C. Catabolism of pyrimidines in yeast: A tool to understand degradation of anticancer drugs. Nucleosides, Nucleotides and Nucleic Acids. 2006;25:991–6.

408. Bartnicki-Garcia S, Nickerson WJ. Nutrition, growth and morphogenesis of Mucor rouxii. J Bacteriol. 1962;84:841–58.

409. Jeennor S, Laoteng K, Tanticharoen M, Cheevadhanarak S. Comparative fatty acid profiling of *Mucor rouxii* under different stress conditions. FEMS Microbiol Lett. 2006;259:60–6.

410. Shiotani T, Weber G. Purification and properties of dihydrothymine dehydrogenase from rat liver. J Biol Chem. 1981;256:219–24.

411. Oliver JD, Sibley GEM, Beckmann N, Dobb KS, Slater MJ, McEntee L, Du Pré S, Livermore J, Bromley MJ, Wiederhold NP, Hope WW, Kennedy AJ, Law D, Birch M. F901318 represents a novel class of antifungal

drug that inhibits dihydroorotate dehydrogenase. Proc Natl Acad Sci U S A. 2016;113:12809–14.

412. Cambell LL. Reductive degradation of pyrimidines. II. Mechanism of uracil degredation by *Clostridium uracilicum*. J Bacteriol. 1956;73:225–9.

413. Yakovlev DY, Skuridin SG, Khomutov AR, Yevdokimov YM, Khomutov RM. The reduction of thymine residues in DNA by the combined action of UV light and hypophosphite. J Photochem Photobiol B Biol. 1995;29:119–23.

414. Wierzchowski KL, Schugar D. Photochemistry of cytosine nucleosides and nucleotides. Biochim Biophys Acta. 1957;25:355–64.

415. Venkhataraman R, Donald CD, Roy R, You HJ, Doetsch PW, Kow YW. Enzymatic processing of DNA containing tandem dihydrouracil by endonucleases III and VIII. Nucleic Acids Res. 2001;29:407–14.

416. Basbous J, Aze A, Chaloin L, Lebdy R, Hodroj D, Ribeyre C, Larroque M, Shepard C, Kim B, Pruvost A, Moreaux J, Maiorano D, Mechali M, Constantinou A. Dihydropyrimidinase protects from DNA replication stress caused by cytotoxic metabolites. Nucleic Acids Res. 2020;48:1886–904.

417. Kikugawa M, Kaneko M, Fujimoto-Sakata S, Maeda M, Kawasaki K, Takagi T, Tamaki N. Purification characterization and inhibition of dihydropyrimidinase from rat liver. Eur J Biochem. 1994;219:393–9.

418. Brooks KP, Dong Kim B, Sander EG. Dihydropyrimidine amidohydrolase is a zinc metalloenzyme. Biochim Biophys Acta. 1979;570:213–4.

419. Dobritzsch D, Andersen B, Piškur J. Crystallization and X-ray diffraction analysis of dihydropyrimidinase from *Saccharomyces kluyveri*. Acta Crystallogr Sect F Struct Biol Cryst Commun. 2005;61:359–62.

420. Andersen B, Lundgren S, Dobritzsch D, Piškur J. A recruited protease is involved in catabolism of pyrimidines. J Mol Biol. 2008;379:243–50.

421. Brouwers N, Gorter de Vries AR, van den Broek M, Weening SM, Elink Schuurman TD, Kuijpers NGA, Pronk JT, Daran JMG. *In vivo* recombination of *Saccharomyces eubayanus* maltose-transporter genes yields a chimeric transporter that enables maltotriose fermentation. PLoS Genet. 2019;15:1–30.

422. Entian KD, Kötter P. Yeast genetic strain and plasmid collections. In: Stansfield, I. , and Stark MJR, editor. Methods in microbiology: Yeast gene analysis. Amsterdam: Academic Press; 2007. p. 629–66.

423. Gibson DG, Young L, Chuang RY, Venter JC, Hutchison CA, Smith HO. Enzymatic assembly of DNA molecules up to several hundred kilobases. Nat Methods. 2009;6:343–5.

424. de Kok S, Yilmaz D, Suir E, Pronk JT, Daran JM, van Maris AJA. Increasing free-energy (ATP) conservation in maltose-grown *Saccharomyces cerevisiae* by expression of a heterologous maltose phosphorylase. Metab Eng. 2011;13:518–26.

425. Camacho C, Coulouris G, Avagyan V, Ma N, Papadopoulos J, Bealer K, Madden TL. BLAST+: Architecture and applications. BMC Bioinformatics. 2009;10:1–9.

426. Gorter de Vries AR, Koster CC, Weening SM, Luttik MAH, Kuijpers NGA, Geertman JMA, Pronk JT, Daran JMG. Phenotype-independent isolation of interspecies *Saccharomyces* hybrids by dual-dye fluorescent staining and fluorescence-activated cell sorting. Front Microbiol. 2019;10:1–12.

Curriculum Vitae

Jonna Bouwknegt was born in Amsterdam on September 19, 1989. In 2001 she went to the Spinoza Lyceum in Amsterdam for senior general secondary education (HAVO), followed by pre-university education (VWO) at Caland Lyceum Amsterdam from 2007 to 2009. Jonna was already intrigued by sciences, but the last two years of high school triggered a particular interest in DNA. She therefore entered the joint BSc programme in Life Science and Technology of Delft University of Technology and Leiden University. Jonna finished the BSc programme with an internship at the Industrial Microbiology Section (Department of Biotechnology) of TU Delft under the supervision of dr.ir. Robert Mans. In this project, she studied energy conservation in *Saccharomyces cerevisiae* and directly fell in love with yeast and its potential for industrial applications. Instead of directly continuing with an MSc study, Jonna decided to pause her studies for a year to join the Board of Study Association LIFE. In 2015, she enrolled for the MSc programme Life Science and Technology at TU Delft. The last year of the MSc programme encompassed a research project and an industrial internship. Still excited about yeast, she chose to also do her MSc research internship at the group of Industrial Microbiology. Under the supervision of dr.ir. Maarten Verhoeven, she worked on improving L-arabinose utilisation in *S. cerevisiae* for cost-effective second-generation bioethanol production. Her industrial internship with HEINEKEN in Zoeterwoude focused on the aroma profile of beer. In 2017, Jonna returned to the Industrial Microbiology group at TU Delft for a PhD project under the supervision of prof.dr. Jack T. Pronk. During her PhD she enthusiastically supervised five BSc students and five MSc students during their final research assignments. Jonna was a member of the PhD Council of the faculty of Applied Sciences and, always eager to learn, participated in the start-up competition Rotterdam 100 and also in the THRIVE PhD Academy, where her team of five designed a business plan for De Mobiele Fabriek. After finishing her PhD, she decided to switch career from science to strategy consulting, and in 2022 Jonna started as associate at Strategy&. The results of the PhD research are presented in this thesis.

Acknowlegdements

This dissertation would not have been here without the inspiration and support of so many people. I will try to express my gratitude in words, in random order, but this will never cover the gratefulness I feel towards all of you.

It all started during the first lecture of microbial physiology, somewhere in the summer of 2012. I had always enjoyed the BSc Life Science and Technology, but up until that moment, I was not exactly sure in which direction I wanted to go. I never forget the amazing harmony between Jack and Ton, the enthusiasm with which they talked about microbiology, their research and the industrial applications, just hit me. I think it only took me five minutes in their class to decide I wanted to do my bachelor internship in their group. **Jack** and **Ton** I want to thank both of you for your amazing teaching capabilities, without the two of you and the microbial physiology class, I would have never gotten enthusiastic about IMB, and I would not have ended up doing a PhD.

They did not disappoint me, I was coupled to Robert, who had just finished his master, and had the pleasure to be his first student. As enthusiastic as Ton and Jack made me about microbiology, Robert made me excited about research in general. I do not think I could have gotten any supervisor better than Robert. **Robert** I want to thank you for investing so many hours in me, teaching me how to do research, how to write and more importantly for inspiring me. I enjoyed this time so much, that I knew right away I wanted to do my master thesis in this group as well.

Which I did, two years later I returned to do my master thesis under the supervision of Maarten. I chose this project because I wanted to do fermentations, and for that I could not have had a better teacher (even though we all had to start learning how to build up fermenters by cleaning Maarten's). **Maarten**, besides your extreme bioreactor setup skills, you really taught me how to be an independent researcher. You always encouraged me to dig into literature, come up with hypotheses and design my own experiments, basically all skills I needed to do a PhD. I really enjoyed the little brainstorm sessions we had, and you inspired me to do a PhD.

But, before I could, I first had to do an industrial internship, which I did at HEINEKEN. Again, I had a great supervisor, **Niels**, although my time at HEINEKEN was short, also you have been one of my inspirations. You were still so excited about research, and extremely engaged with all your students. The enthusiasm, pep-talks and coffee breaks have made my time at HEINEKEN a great pleasure, and most of all I want to thank you for making me believe in myself.

I am glad to have had the pleasure to be supervised and inspired by all three of you, and that you all have formed me into the researcher I am today.

I couldn't be more happy than to start a PhD in the group that had raised me to be a researcher, in which I felt at home, where I made friends, under the supervision of one of my first inspirations. **Jack**, I am so happy that you decided to write a project proposal to directly supervise PhD students again, and I feel honoured that together with Wijb and Sanne we could take on the role of your new PhD students. Together with the ELOXY team we started on this great adventure, that has not only resulted in this book but in two other, beautiful theses. Your never-ending enthusiasm, has always be a great motivation, up until the end where we unfortunately had to let go of some dreams. Although your new position as head of department has taken up a lot of time, you always gave priority to ELOXY. Every time I panicked, which I did a lot, you would give me a call within a day to cool me down, calmly going through the new results, showing me it was all as bad as I thought. Especially in the end of my project you have been essential, I think I would still have been writing, deleting and rewriting the first paragraph of my introduction if it wasn't for you. It doesn't matter how busy you are, you ensured to check everything within a couple of days, for which I am still very grateful.

Sanne I will never forget our first day in the lab, definitely Jut en Jul, and unfortunately for most people, I do not think we ever stopped being that. You have supported me throughout the 4.5 years, listened to all my complaining, danced with me in the middle of the night because FINALLY our wappie sjappie listened to us. You have not only been a great colleague, but our close collaborations and mental support to one another, have for me evolved into a friendship, and I hope that wherever you and Xavier go, we will keep in touch.

Aurin, I think our personalities might have clashed a bit sometimes like the typical "yellow" and "blue" personalities, but luckily you don't get scared off that fast. You have taught me about myself and have taken on a mentor role on the level of personal development. Moreover, you have been actively involved in most of my research, and sometimes were even more enthusiastic about the results than I was. I am still sad that we're not colleagues anymore, but I want to thank you for the nice time when we were.

I also want to thank the rest of the ELOXY team Christiaan, Wijb and Raúl. All of you have contributed to my research, **Wijb** with all your extremely complex hypotheses and explanations, **Christiaan** with translating these for the bioreactor setups to 'Jip-en-Janneke taal' and **Raúl** with making a LOT of trees. All of you have been an inspiration and a pleasure to work with, and I am happy that we had the opportunity to work together.

IMB would not be IMB if it wasn't for the PI's, **Jean-Marc**, **Pascale**, **Robert** and now also **Rinke**. You all hire the smartest people, that together form the group as it is. The work discussions would not be the same if it wasn't for all of you, you have asked critical questions or came up with suggestions, which is essential for our, and also has been for my, research. **Jean-Marc**, I also want to thank you for being promotor together with Jack and mostly for your support during the yearly progress meetings and supporting me in getting an extension.

As IMB would not function without the supervision of the PI's, it would not function without the supporting staff; **Marcel**, **Marijke**, **Erik**, **Susan**, and up until last year **Pilar**, all of you keep the labs and the group running.

Marcel, you are always extremely patient with all of us, taking the time to take us through every step of anything related to bioinformatics. I have always felt comfortable asking stupid questions, and I believe that giving students this feeling, is extremely powerful.

Erik, you always try to help everyone as much as you can and I do not think I have ever walked in a room without you asking me how I am doing. Thank you for keep on reminding me not to use my phone in the lab (sorry!) and for always stepping up when help was required for the anaerobic chambers.

Marijke, you have such an essential role in IMB, you really guide all the PhD students trough rough times, keep them motivated and sane. I hope you will continue to do this because it has been so valuable to me, and we need someone like you in our group. You are one of a kind, and I want to thank you for all mental support from my master thesis up until now.

Apilena, **Jannie** en **Astrid**, jullie zorgen/hebben gezorgd dat de keuken blijft draaien, en belangrijker nog voor mijn onderzoek, de anaerobe kamers. Hoe vaak ik wel weer niet voor jullie deur heb gestaan om te vragen of de droogstoof weer op een andere tijd aan kon, omdat we de katalysatoren op een andere dag nodig hadden. Jullie hebben nooit ergens moeilijk over gedaan, en passen jullie altijd snel aan. Dit is zo ongelofelijk waardevol en BT mag blij zijn met jullie, en zo ook met de nieuwe rol van Astrid.

One of the things I enjoyed most during my PhD was teaching, especially my bachelor and master students. **Daphne**, **Petrik**, **Jisk**, **Sabina**, **Eline**, **Remon**, **Magdalena**, **Elisabeth**, **Mats** and **Matthijs**, you have not only contributed to my research, but more importantly, to my personal development. I have learned so much by supervising so many different and smart students. Thank you all, for your contribution to my projects, the scientific discussions and mostly for a great time.

During my PhD I had the opportunity to work together with so many people, and got help of so many. Thanks to **Martin** from Leiden University, **Christoph** from Ludwig Maximilian University of Munich and **Peter-Leon** and **Marc** from the Biocatalysis section, it was a great pleasure to learn from experts in other groups.

Marijke for helping me with enzyme assays and performing BOM experiments, **Marcel** for all the fast processing of sequencing data and **Charlotte** for all your help with the FACS, sequencing, microscopy and scientific brainstorm sessions and **Thomas** for the collaboration on the PaNic project. **Erik**, you have started the Eloxy project before we were even in, thank you for all the preparations.

Aafke and **Sophie**, both of you have been my go-to persons when I needed something in the anaerobic chambers, thanks for that. **Nicole** and **Sanne**, thank you so much for helping me out with the growth experiment, it was way more fun doing it together with you then alone and I couldn't have sampled all these flasks without you.

My PhD would have not been the same without the nice people in IMB making my time fun.

Michał, sletjeeeeh, it was superlekker being your colleague, albeit it very short. The parties, adventures (Den Haag central station is a night station right?), trips to Wrocław, but mostly just your crazy, fun personality have made IMB the best place start a PhD.

Jasmijn, our adventure already started during our master thesis, and I was so happy to hear that you would also start a project at IMB. You are one of the most social persons I know, always getting everyone to join any activity and making sure everyone feels comfortable. You have been a great support and a great friend. And with that I obviously also have to thank you partner in crime, Anna. **Anna**, also you, thank you for the amazing four years. I can't imagine that I would not have met you if you didn't chose to do your PhD in our group. You are so invested in everyone, even moving to Zwolle is not holding you back from coming to Delft or Amsterdam. Your presence on an event always equals fun and I enjoyed our trip to Michał, our short time together in the office, but mostly simply the dinners and borrels.

Arthur, **Xavier** and **Laura**, I have to thank all three of your for your pep-talks. **Laura**, I think that just like me you are sometimes too insecure as scientist. You always tried to make me feel better, compliment my work and I enjoyed it a lot when you joined the anaerobics meetings. **Xavier**, we met when you started the board and became QQ of the BuLaCo, the mentor-like role you had at that point, you kept during my masters and my PhD. You were always invested in how I was coping with everything and I still enjoy our sporadic calls. **Arthur**, also you have been one of the persons that has always made me believe more in myself. I enjoyed our coffee breaks, but also the borrels and dinners and I hope that your work will allow for occasional meet-ups in the future as well.

Sam en **Charlotte**, ik ben blij dat jullie er zijn en me echt door deze laatste periode heen hebben gesleept. **Sam**, je bent zo ongelofelijk goed bezig bij BOC/EBT, je bent altijd super enthousiast over al je eigen onderzoek en dat van mij, en ik ben nu al trots op je. **Carlo**, je bent één van de slimste mensen die ik ken en dat in combinatie met je fantastische persoonlijkheid gaat je heel ver brengen, ook op jou ben ik heel trots.

Afegelopen 2 jaar zijn ook voor jullie zeker niet makkelijk geweest, maar ondanks dat stonden jullie altijd voor me klaar, daarvoor kan ik jullie nooit genoeg bedanken. Sinds ik jullie ken zijn jullie goede vrienden/ bestuursgenoot/huisgenoot en geweldige steun geweest, ik ben blij en trots dat ik jullie aan mijn zijde mag hebben als paranimfen.

During my PhD I had joined the PhD Academy of THRIVE Institute, in which I had the pleasure to work with amazing people. They have contributed significantly to my personal development, but more importantly I enjoyed spending a year with such inspiring personalities. **Han**, **Maud**, **Daphne** and **Juliëtte**, I want to thank all of you for giving me the opportunity to participate in the project, for the great supervision and for the continuous support. **Andrea**, **Christine** and **Jennifer** I think all of us are very different and that's what made us a great team, thank you for all the fun times and for coping up with all PhD complaints.

I would have never been able to finish the last two years, if it wasn't for four amazing physical therapists.

Hayo, jij hebt me niet alleen fysiek door het eerste jaar van de revalidatie geholpen, maar voornamelijk mentaal. De omschakeling van volledige revalidatie naar het combineren van werk met revalidatie was lastig en ik heb veel last minute moeten afzeggen. Jij hebt altijd begrip getoond voor de misschien niet zo straightforward werkuren, en geprobeerd om samen met mij hier omheen te werken. Ik ging met ongelofelijk veel tegenzin weg bij Fysio Concept, maar ik ben blij dat Mirthe, Kim en Stefan van Fysio de Meer dit hebben opgevangen. **Stefan**, ik kom nu alleen nog langs om mij lek te laten prikken, nog steeds met tegenzin maar wel dankbaarheid achteraf. **Kim**, jij hebt altijd veel te goed door wanneer er een stapje terug gedaan moet worden, en ondanks dat ik hier absoluut niet op zat te wachten, waren de stappen terug de laatste paar maanden van mijn PhD de enige oplossing om zowel mijn knie als mijn werk er doorheen te slepen. **Mirthe**, bedankt voor het laatste jaar, je weet altijd het schema precies aan te passen op de grens van wat ik kan (zowel mentaal als fysiek) en waar ik nog enigszins gelukkig van wordt. Je houdt altijd rekening met alles wat er omheen speelt en dit is waardoor ik dit laatste jaar geen andere fysio had gewenst.

Besides being supported throughout my PhD, and revalidation, the greatest support for me have been my family and friends. They have not only supported me in all the steps I have taken, but they have always been able to take my mind off work, which has also been an essential component in finishing.

Lieve **Amber**, **Joris**, **Lotte**, **Tom** en **Joëlle**, ik ben zo blij dat ik jullie gratis bij Steijn kreeg, en daarnaast dat ik bij Joëlle een gratis **Tjalling** kreeg. Ik kan me bijna niet meer voorstellen hoe het was geweest als ik jullie niet had ontmoet. Alle leuke feestjes, fysio sessies, jullie lieve berichtjes, geduld en steun ben ik jullie eeuwig dankbaar.

Linda, **Jinke** en **Ashley**, wellicht dat jullie na het zien van dit boekje eindelijk weten wat ik heb gedaan sinds de middelbare school. Ik weet dat ik jullie voornamelijk in het laatste jaar heel weinig heb gezien, maar het feit dat ik hoe lang het ook geleden is nog steeds bij jullie kan aankloppen, maar het voor mij een waardevolle vriendschap. Jullie zijn mijn oudste vriendinnen, ik hoop dat we dit altijd blijven en dat ik ooit zo ver kom onze "Las Vegas pact" te kunnen nakomen.

Lieve ViMaJoJo, **Vicky**, **Marissa** en **Jolanda**, ik heb aan jullie als vriendinnengroepje, maar ook allemaal los op jullie eigen manier veel steun gehad. **Jojo** ik denk dat we heel wat mensen gek hebben gemaakt met onze drukte tijdens de master en ik ben blij dat je ook nog een half jaartje onderdeel van ons team hebt kunnen zijn, want 1 ding is zeker en dat is dat ik met jou altijd lol kan hebben. **Marips**, toen ik begon, was jij alweer bijna klaar met jouw PhD, onze koffietjes in het gebouw waren altijd een fijn moment en het is nog steeds heel raar dat ik zowel jou als jo opeens minder zie. Lieve **Vick**, ik vind het superleuk dat je in Amsterdam bent komen wonen en dat we af en toe een door de weeks etentje kunnen doen. Jij hebt mij vooral heel erg geholpen in de stappen die na mijn PhD komen en bent een grote bron van inspiratie geweest hiervoor. Onze momenten met zijn vieren zijn altijd weer leuk en op het moment van schrijven zijn we ons aan het voorbereiden op het volgende ViMaJoJo avontuur.

Wienie, **Isa**, **Rabo** en **Ce**, met jullie is het altijd leuk, met zijn vijven, vieren, drieën of tweeën, het is altijd weer genieten. De uit de hand lopende avonden bij Wildschut, zijn altijd goed geweest om even mijn hoofd van werk af te zetten. Maar jullie hebben me ook in alle stappen van mijn PhD ondersteund met juist hele serieuze gesprekken en deze combinatie is goud. **Ce**, met jou samen werken is hilarisch, alhoewel ik misschien niet altijd even hard aan werken toekom. **Wien**, de dagen knallen met jou waren echt het lichtpuntje van de hele corona-tijd. Samen keihard werken, even naar de markt voor een pauze en wellicht af en toe een vrijmibo hebben mijn productiviteit, maar ook plezier in werk enorm verhoogd.

Lieve **Jelle**, **Joeri** en **Roel**, sinds het begin van de studie zijn jullie altijd mijn buddies geweest. **Roel**, ondanks dat je zelf een hele zware tijd doormaakt, ben je altijd een steun geweest voor mij. Je checkt altijd of alles nog goed gaat en als we even geen tijd hebben om af te spreken, dan lossen we dat op met videobellen. Ik hoop dat we snel weer verder kunnen zoals het vroeger was. **Haaker**, mijn partybuddy, jij doet je altijd veel vervelender voor dan je eigenlijk bent, want stiekem ben je gewoon een lieve jongen. Ook al verwoord je het als "ben je nou al klaar?" ik weet dat je stiekem van binnen vraagt of het nog goed gaat. Ik hou van onze gesprekken waarin we continue door elkaar heen praten, en van de feestjes **Jelle**, ik denk niet dat ik iemand ken die zo'n grote idioot is als jij, en daarom ben je nog steeds stiekem mijn beste vriend. Ik weet dat je denkt dat je altijd gelijk hebt, maar gelukkig heb ik straks eindelijk een hogere titel dan jij en kan ik eindelijk ook doen alsof ik gelijk heb. Ik vind het heerlijk dat we over onzin kunnen praten, discussiëren tot je het bloed onder mijn nagels vandaan haalt en praten over serieuze dingen. Jouw oplossing voor dat ik het druk heb of moe ben door werk is helaas wel altijd dat er meer bier gedronken moet worden, maar misschien is dat ook af en toe wel goed.

Lieve familie, **Papa**, **Mama**, **Maaike**, **Rik** en **Omi**, zonder jullie had ik het allemaal niet kunnen of willen doen. De barbecues, etentjes, biertjes, het samen klussen of aan de tuin werken, alle kleine dingen tussendoor waarbij we gewoon even samen zijn en ik jullie de oren van de kop af klets, zijn de dingen die mijn steun hebben gegeven door de hele periode heen. **Mam**, bedankt voor het inscannen van alle figuren, het maken van al mijn kleren en het altijd paraat staan als er iets moet gebeuren. Ik vind het altijd gezellig als je weer langskomt en we met zijn tweeën een klus afmaken. **Pap**, ik denk dat weinig mensen zo'n gestoorde vader hebben als ik, en ik vind het fantastisch. De dagen samen werken in het nieuwe kantoortje, de duizend koffie die ik daarbij te drinken krijg en de vreselijke muziek op de achtergrond waren ook een genot, en ik ben blij dat je een onderdeel bent geweest van de laatste paar maanden bikkelen. Lief/gek **broertje** en **zusje**, met jullie erbij weet ik 1 ding zeker, en dat is dat het een drukke, gekke, grappige boel is. Er zijn weinig mensen zo gestoord als jou **Maaike** (Behalve misschien Bram, ook al is het een close call) en samen met de droge humor van **Rik**, is het altijd genieten. Ook al kunnen we dikke ruzie maken zoals echte broer en zussen, we kunnen ook samen borrelen, schilderen, gek doen of zelfs feesten en ik geniet van alle tijd die ik samen met jullie doorbreng. Lieve **Omi**, ik ben altijd blij als je weer even belt om te vragen of ik nog leef en of alles wel goed met me gaat, de tijd gaat te snel en dan word ik er weer even aan herinnerd dat het veel te lang geleden

is. Als ik langskom bij jou is het altijd gezellig en vertel je verhalen van vroeger. Ik ben er van overtuigd dat niemand zo'n lieve oma heeft als dat wij hebben. **Papa**, **Mama**, **Rik**, **Maaike** en **Omi**, ik hou van jullie en mede dankzij jullie liefde en steun heb ik het voor elkaar gekregen dit af te maken.

Lieve **Steijn**, ik denk niet dat er iemand op de wereld bestaat die beter mij me past dan jij, juist omdat je zo anders bent. Tot ik jou leerde kennen, heeft niemand mijn temperament weten te temmen of tolereren. Als jij me niet altijd rustig had weten te krijgen, me troosten als alles weer tegen zat, of wanneer ik gewoon op was door de doorgehaalde nachten, denk ik niet dat ik het zonder burn-out tot de eindstreep had gehaald. Het feit dat jij naast me staat, heeft alles makkelijker gemaakt dan het was, ik hou van je, en ik heb nu al zin in wat ons nog te wachten staat.

List of publications

6. **J. Bouwknegt**, C.C. Koster, A.M. Vos, R.A. Ortiz-Merino, M. Wassink, M.A.H. Luttik, M. van den Broek, P.L. Hagedoorn, J.T. Pronk. Class-II dihydroorotate dehydrogenases from three phylogenetically distant fungi support anaerobic pyrimidine biosynthesis. Fungal Biol Biotechnol 8, 10 (2021).

5. **J. Bouwknegt**[1], S.J. Wiersma[1], R.A. Ortiz-Merino, E.S.R. Doornenbal, P. Buitenhuis, M. Giera, C. Müller, J.T. Pronk. A squalene–hopene cyclase in *Schizosaccharomyces japonicus* represents a eukaryotic adaptation to sterol-limited anaerobic environments. Proc Natl Acad Sci. 118, e2105225118 (2021).

4. T. Perli[1], A.M. Vos[1], **J. Bouwknegt**, W.J.C. Dekker, S.J. Wiersma, C. Mooiman, R.A. Ortiz-Merino, J.-M. Daran, J.T. Pronk, Identification of oxygen-independent pathways for pyridine nucleotide and Coenzyme A synthesis in anaerobic fungi by expression of candidate genes in yeast. MBio. 12(3), e00967-21 (2021).

3. C. Mooiman[1], **J. Bouwknegt**[1], W.J.C. Dekker[1], S.J. Wiersma[1], R.A. Ortiz-Merino, E.A.F. de Hulster, J.T. Pronk, Critical parameters and procedures for anaerobic cultivation of yeasts in bioreactors and anaerobic chambers. FEMS Yeast Res., foab035 (2021).

2. W.J.C. Dekker[1], S.J. Wiersma[1], **J. Bouwknegt**, C. Mooiman, J.T. Pronk, Anaerobic growth of *Saccharomyces cerevisiae* CEN.PK113-7D does not depend on synthesis or supplementation of unsaturated fatty acids. FEMS Yeast Res. 19(6) (2019).

1. M.D. Verhoeven, J.M. Bracher, J.G. Nijland, **J. Bouwknegt**, J.M.G. Daran, A.J.M. Driessen, A.J.A. Van Maris, J.T. Pronk, Laboratory evolution of a glucose-phosphorylation-deficient, arabinose-fermenting *S. cerevisiae* strain reveals mutations in *GAL2* that enable glucose-insensitive L-arabinose uptake. FEMS Yeast Res. 18(6), 1–15 (2018).

ISBN 978-94-6384-288-4